University College London.

CHARACTERISATION OF HUMAN PROSTATE EPITHELIUM COLONY FORMING CELLS

Thesis for the degree of Doctor of Medicine (Research)
University of London, 2007

Charlotte Louise FOLEY

ProQuest LLC
789 East Eisenhower Parkway
P.O. Box 1346
Ann Arbor, MI 48106-1346

DECLARATION OF ORIGINALITY

I hereby declare that this thesis and the work reported herein was composed and originated entirely by myself, and that the dissertation does not contain material that has already been used to any substantial extent for a comparable purpose.

Charlotte L. Foley

25th September 2007

ABSTRACT

Objectives: Rare prostate epithelial stem cells have been implicated in the aetiology of prostate disease, yet are overlooked in studies on the whole tissue. When prostate epithelial cells are cultured at low density, two distinct colony types arise, postulated to represent the progeny of stem cells (type II colonies) and committed 'transit amplifying' cells (type I). This project aimed to further characterize these rare colonies and confirm their position in the prostate epithelial cell hierarchy, in benign, and for the first time, malignant tissue.

Methods: Colonies derived from transurethral resection tissue were compared for proliferation, differentiation, colony self-renewal and gene expression. Paired benign and malignant radical prostatectomy samples were cultured. To confirm the benign / malignant nature of individual colonies, loss of heterozygosity and expression of known prostate cancer markers were assessed.

Results: There was a trend to greater type II colony proliferation, but no difference in ability to differentiate into multi-layered acinus-like structures expressing early and late epithelial markers. When passaged, type II colonies never re-created themselves, but resembled type I colonies. Using cDNA microarrays, comparison of gene expression in the two colony types showed a limited magnitude of differences, most notably in differentiation markers. Malignant tissue yielded both colony types, which were indistinguishable from their benign counterparts. Neither loss of heterozygosity analysis nor prostate cancer marker expression distinguished benign from malignant colonies.

Conclusions: These colonies behave like differently-aged populations of transit amplifying cells – the committed offspring of the stem cell. If a stem cell does generate type II colonies, it appears to lose self-renewal ability and differentiate in culture. Colonies derived from cancer tissue show neither a malignant genotype nor phenotype suggesting that malignant cells are not cultured in these conditions. This highlights the need to confirm malignancy in primary prostate cancer cultures, hitherto assumed by many authors.

[300 words]

ACKNOWLEDGEMENTS

I would like to thank the following people for providing support, inspiration and guidance in the generation of this thesis.

Professor Roger Kirby, Professor of Urology, St George's Hospital, London.
Dr Cathy Corbishley, Consultant Histopathologist, St George's Hospital Medical School, London.
Dr M Constance Parkinson, Consultant Histopathologist, UCL Hospitals Trust, London.
Ms Nipurna Jina, Manager, ICH Gene Microarray Centre, UCL Institute of Child Health, London.
Dr Charles Mein, Laboratory Manager, The Genome Centre, William Harvey Research Institute, Queen Mary's School of Medicine, London.
Dr Isabelle Bisson, Post-doctoral Research Scientist, Prostate Cancer Research Centre, London.
Dr David Hudson, Lead Scientist, Prostate Stem Cell Laboratory, Institute of Cancer Research, Surrey.
Dr Aamir Ahmed, Senior Lecturer, Prostate Cancer Research Centre, London.
Professor John Masters, Professor of Cellular Pathology, Prostate Cancer Research Centre, London.

And thanks also for their financial support for this project.

Royal College of Surgeons of England
Cancer Research UK
The Prostate Research Campaign UK.
The Prostate Cancer Research Centre

CONTENTS

Chapter 1: INTRODUCTION

1.1 The clinical entity of prostate disease

1.2 The normal prostate

- 1.2.1 The function of the prostate
- 1.2.2 Human prostatic development
- 1.2.3 The anatomy of the prostate
  - 1.2.3.1 The Transition zone
  - 1.2.3.2 The Central zone
  - 1.2.3.3 Peripheral Zone
  - 1.2.3.4 Anterior Fibromuscular Stroma
- 1.2.4 Zonal variation within the prostate
- 1.2.5 The histology of the normal prostate
- 1.2.6 Stromal-epithelial interactions
- 1.2.7 Androgens and the prostate

1.3 Epithelial cellular hierarchies

- 1.3.1 Stem cell characteristics

1.4 Models of prostate epithelial cell lineages

- 1.4.1 Basal, intermediate and luminal epithelial cell markers

1.5 Defining the prostate stem cell

1.6 Characterizing prostate stem cells

1.7 Summary of prostate epithelial markers

1.8 The prostate in disease

- 1.8.1 Benign prostatic hyperplasia (BPH)
- 1.8.2 Prostate Adenocarcinoma
  - 1.8.2.1 The natural history of prostate cancer
  - 1.8.2.2 Histological changes in prostate cancer

1.9 Cancer stem cells and the stem cell model of cancer

- 1.9.1 Stem cells as targets for malignant transformation

1.10 Evidence for the prostate cancer stem cell

- 1.10.1 The origin of the cancer stem cell

1.11 The aims of this project

Chapter 2: MATERIALS AND METHODS

2.1 Culture media

- 2.1.1 Prostate Epithelial Growth Medium (PrEGM)
- 2.1.2 Dulbecco's Modified Eagle's medium (DMEM)
- 2.1.3 Tissue Collecting Medium
- 2.1.4 Conditioned medium
- 2.1.5 Collagenase solution

2.2 Tissue Culture

2.3 Preparation of mouse 3T6 fibroblast feeder cell layer

2.4 Acquisition of prostate tissue

- 2.4.1 Acquisition of benign hyperplastic prostate tissue
- 2.4.2 Acquisition of paired malignant and benign prostate tissue samples

2.5 Processing Prostate Tissue

2.6 Sampling Type I or Type II prostate epithelial colonies

- 2.6.1 Ring cloning of colonies
- 2.6.2 Harvesting of passaged colonies for RNA extraction
- 2.6.3 Harvesting of single or multiple colonies for RNA extraction

2.7 Three dimensional culture in Matrigel™

2.8 Preparation of histological sections

2.9 Immunohistochemistry

2.10 Genomic DNA extraction from large and small tissue samples

2.11 Polymerase Chain Reaction (PCR)

2.12 Semi-quantitive reverse transcription PCR (RT-PCR)

2.13 Loss of Heterozygosity (LOH) Analysis

2.14 RNA extraction

2.15 Quantification and quality assessment of RNA samples

2.16 Concentration of RNA samples

2.17 Agarose gel electrophoresis

2.18 Total RNA processing, amplification and application onto oligoarrays to obtain raw gene expression data.
2.18.1 Transcription of total RNA and hybridisation onto the Affymetrix GeneChip® array
2.18.2 Selectively amplifying mRNA
2.18.3 Amplification of small target RNA samples: First cycle of cDNA synthesis
2.18.4 Second cycle of cDNA synthesis to produce biotin-labelled cRNA
2.18.5 Fragmentation, hybridisation, array processing and scanning
2.19 Built in controls for GeneChip expression analysis
2.19.1 Visual array inspection
2.19.2 B2 Oligo Performance
2.19.3 Average Background and Noise Values
2.19.4 Poly-A Controls
2.19.5 Hybridisation Controls
2.19.6 Internal Control Genes
2.19.7 Percent Present calls
2.19.8 Scaling Factors
2.20 Analysis of GeneChip expression data
2.21 Statistical analysis

Chapter 3: ACQUISITION AND ANALYSIS OF EPITHELIAL COLONIES FROM BENIGN PROSTATIC HYPERPLASIA TISSUE

3.1 Morphological characteristics of primary prostate epithelial colonies
3.2 Growth characteristics of type I and type II colonies
3.3 Three-dimensional culture of type I and type II colonies
3.4 Comparison of gene expression profiles of type I and type II prostate epithelial colonies.
3.4.1 Optimising samples for gene expression analysis
3.4.1.1 Use of a single representative colony per patient versus pooling of cells from several colonies

3.4.1.2 Culture of prostate epithelial cells in the absence of a feeder layer
3.4.2 Acquisition of total RNA from pooled type I and type II prostate epithelial colonies
3.4.3 Concentration of dilute total RNA samples
3.4.4 Choice of RNA samples for gene chip analysis
3.5 GeneChip Quality control parameters
3.6 Validation of cDNA microarrays using RT-PCR
3.7 Identification of differential gene expression between type I and type II colonies using cDNA microarrays
3.8 Identifying the biological significance underlying statistically significantly differently expressed genes in type I and II colonies
3.8.1 Genes upregulated in type I colonies
3.8.2 Genes upregulated in type II colonies
3.8.3 Apparent biological differences in gene expression between type I and type II colonies
3.9 Discussion
3.10 Future directions

Chapter 4: ACQUISITION AND ANALYSIS OF EPITHELIAL COLONIES FROM RADICAL PROSTATECTOMY TISSUE

4.1 Introduction
4.2 Acquisition of paired benign and malignant prostate tissue samples from radical prostatectomy specimens
4.3 Outcomes of culture of paired benign and malignant radical prostatectomy tissue samples
4.4 Morphological characteristics of primary prostate epithelial colonies derived from presumed benign and malignant colonies
4.5 Differentiating between benign and malignant colonies using LOH analysis
4.5.1 Establishing LOH control samples using early prostate cancer cell lines with LOH at known loci

4.5.2 LOH analysis of original tumour / benign prostate tissue sampled for culture of colonies

4.5.3 LOH analysis of presumed benign and malignant colonies at loci demonstrating LOH in the primary tumour

4.6 Differentiating between benign and malignant colonies using expression levels of genes upregulated in prostate cancer

4.7 Discussion

4.8 Future directions

Chapter 5: CONCLUSIONS

Published Work

References

Appendices

Appendix A: Patient consent forms and information sheets

Appendix B: Sequences of primers for PCR for LOH and RT-PCR.

TABLES

Table 1.1: Intermediate cytokeratin phenotypes of cells in the basal or luminal prostate epithelium.

Table 1.2: Summary of cell marker expression by the different cell populations in normal human prostate epithelium.

Table 2.1: Characteristics of BPH derived type I and type II prostate epithelial colonies after two weeks in culture.

Table 2.2: Antibody Reagents

Table 3.1: Colony forming efficiencies of primary prostate epithelial cell cultures.

Table 3.2: Characteristics of the two colony types obtained from primary prostate epithelial cell culture by Hudson *et al*, (2000) and in the present study.

Table 3.3: Outcome of ring cloning and passaging of individual type I and type II colonies.

Table 3.4: Total RNA yield from pooled type I or type II primary colonies.

Table 3.5: Colony yield in alternative feeder-layer free culture conditions.

Table 3.6: Culture of primary prostate epithelial cells: patient characteristics, histology, and colony and total RNA yields.

Table 3.7: Concentration of RNA samples by nitrogen evaporation.

Table 3.8: Characteristics of paired colony total RNA samples.

Table 3.9: Quality control parameter outcomes for each GeneChip.

Table 3.10. Logistic regression values of R when type I or type II sample raw signal intensity data is compared.

Table 3.11: The most significant and differentially expressed genes between type I and II colonies.

Table 4.1: Patient characteristics and histopathology of prostates sampled for benign and malignant tissue.

Table 4.2: Outcome of culture of benign and malignant prostate tissue.

Table 4.3: CFEs of presumed primary benign / malignant prostate epithelial cell cultures.

Table 4.4: Characteristics of the two colony types obtained from primary prostate epithelial cell culture by Hudson *et al*, (2000) and in the present study from peripheral benign and malignant and transitional zone tissue.

Table 4.5: LOH analysis of three paired cell lines for the eight loci assessed by Bright *et al* and for 29 loci assessed in the present study.

Table 4.6: DNA derived from histologically confirmed benign / malignant areas of six paraffin embedded prostates that had been sampled for colonies was analysed at 55 loci for LOH.

Table 4.7: Outcome of LOH analysis of presumed benign and malignant colony DNA at loci identified as missing in the original prostate sample.

Table 4.8: Summary of findings of colony LOH analysis, using a cut-off of 70%.

FIGURES

Figure 1.1: Zonal anatomy of the prostate as described by J. E. McNeal (Am J Surg Pathol 1988; 12:619–33).

Figure 1.2: Haematoxylin and eosin (H&E) stained view of a normal prostate acinus surrounded by fibro-muscular stroma.

Figure 1.3: Diagrammatic representation of the cell populations within the prostate epithelium.

Figure 1.4: Colony types formed two weeks after plating 1000 freshly isolated epithelial cells from prostate tissue in a 5cm dish.

Figure 2.1: Apparatus for selective harvesting of type I or type II colonies for total RNA extraction.

Figure 2.2: Sourcing DNA from the prostate blocks.

Figure 2.3: The underlying genetic differences in microsatellite instability and LOH.

Figure 2.4: Electropherogram pairs demonstrating A) a homozygous, non-informative locus and B) LOH with 81% loss of the shorter allele in the upper specimen.

Figure 2.5: Concentration of RNA samples using N_2 gas.

Figure 2.6: Human prostate epithelial target amplification and labelling for Affymetrix GeneChips from the GeneChip Expression Analysis Technical Manual.

Figure 3.1: Distribution of prostate epithelial cell colony size by type.

Figure 3.2: A Representative collagen coated dish seeded with 1000 primary prostate epithelial cells, cultured for 14 days then stained for K 5/6/18. **B&C** The 2 colony types are distinguishable by eye. 'Stranded' feeder cells (*) are visible within the colonies.

Figure 3.3: Proliferation of type I and II colonies. After 14 days in culture, 10,000 pooled type I or type II colony cells were cultured in 25cm^2 collagen coated flasks for 28 days.

Figure 3.4: Appearances of acini and ducts obtained from pooled type I (A, C & E) or type II (B, D & F) colonies in Matrigel culture at 4 (A & B) and 14 days (C to F).

Figure 3.5: All scale bars are 100μm. Expression of prostate epithelial basal markers K14 and CD133, and luminal markers K8 and AR in monolayer primary and three-dimensional Matrigel secondary culture.

Figure 3.6: Two colonies from prostate 2 in table 3.3 were photographed before ring cloning and at intervals during their secondary culture on a feeder layer.

Figure 3.7: Agarose gel electrophoresis of total RNA samples before and after nitrogen gas concentration.

Figure 3.8: Agilent bioanalyser electropherograms and gel images for two total RNA samples for GeneChip analysis.

Figure 3.9: Graph of Prostate 1 type I colony raw signal intensity data plotted against Prostate 4 type I raw data.

Figure 3.10: Validation of expression levels on GeneChip using RT-PCR for five genes with GAPDH control.

Figure 3.11: Normalised dye intensities for 874 genes significantly ($p \leq 0.05$) differentially expressed between type I and type II colonies.

Figure 3.12: Volcano plot of all 874 selected genes showing their degree of differential expression (fold change or ratio of type I to type II) and their significance (as the p value derived from the ANOVA).

Figure 3.13: Flow diagram showing selection of the most significant and differentially expressed genes from the original normalised GeneChip data.

Figure 3.14: Scatter diagram showing the relationship of genes between clusters.

Figure 4.1: A&B Representative dishes after 14 days of low density culture of 1000 primary prostate epithelial cells from presumed benign or malignant radical prostatectomy tissue; stained for cytokeratins 5,6 and 18. Type I colonies from benign (**C**) and malignant (**D**) cells, and type II colonies from benign (**E**) and malignant (**F**) cells looked similar.

Figure 4.2: Distribution of presumed benign and malignant prostate epithelial cell colonies by total colony cell number (binned by cell doublings) and type.

Figure 4.3: Distribution of presumed benign and malignant prostate epithelial cell colonies by cell density per millimetre.

Figure 4.4: LOH analysis of original benign/malignant tissue from prostate #1 and corresponding colonies.

Figure 4.5: RT-PCR of total RNA from presumed benign and malignant colonies from three prostates was performed for 3 genes AMACR, EZH2 and PIM1 reported as being upregulated in prostate cancer, and for GAPDH.

CHAPTER 1: INTRODUCTION

When freshly isolated prostate epithelial cells are cultured at low-density in serum-free medium, two distinct types of colonies clonally expanded from single cells are obtained. It has been postulated that these colonies derive from stem cells or their progeny, transit amplifying (TA) cells. This thesis aimed to characterise these two colony types from both benign and malignant prostate tissue, and establish what differences in gene expression lay behind their different phenotypes, and behind the malignant or benign nature of the prostate tissue that they derive from.

1.1 The clinical entity of prostate disease

The prostate gland is situated below the bladder in the male urogenital tract, enclosing the urethra and ejaculatory ducts. Though small, it is responsible for a disproportionate amount of morbidity and mortality. Adenocarcinoma of the prostate is the commonest non-cutaneous cancer of Western males, with an annual UK incidence of 93 men per 100,000 and a UK morbidity of 27 men per 100,000 (http://www.statistics.gov.uk). In 2004, this equated to 9,163 men, or 3.7% of all male deaths. Additionally, it has been estimated that 50% of males will develop symptomatic benign prostatic hyperplasia (BPH) in their lifetime and 50% will experience prostatitis (Partin and Rogriguez, 2002).

Both BPH and prostate cancer are diseases of the prostate epithelium, albeit influenced by adjacent stroma. Elucidating the processes that govern the growth and turnover of the normal and pathological prostate epithelium is therefore key to understanding and manipulating these diseases.

1.2 The normal prostate

1.2.1 The function of the prostate

The prostate gland contributes 0.5-1ml of secretions to seminal fluid, with the remaining 80% of the ejaculate deriving from the seminal vesicles, Cowper's and

Littré's glands and the testes. The constituents of semen have been widely studied, though the physiologic function of many of them is poorly understood (Aumüller and Seitz, 1990). Seminal plasma contains high concentrations of fructose, zinc, citrate, spermine, prostaglandins as well as potassium, immunoglobulins, amino acids, seminogelin and enzymes such as prostatic acid phosphatase (PAP), proteases, esterases, α-amylase, β-glucuronidase and prostatic specific antigen (PSA) – a serine protease. Together they optimise conditions for fertilization by providing a buffered environment for the sperm, improving sperm motility and extending viability. Seminogelin promotes coagulation of the ejaculate, which subsequently liquifies, possibly due to the action of PSA (Lilja *et al*, 1987). Prostaglandins suppress the female immune response to foreign sperm antigens; and spermine, spermidine and zinc have antibacterial properties (Aumüller and Seitz, 1990).

During ejaculation, the seminal vesicles, prostate and bladder neck contract forcing semen into the prostatic urethra. Subsequent relaxation of the distal prostatic sphincter and rhythmic bulbocavernosal muscle contractions then expel the semen.

1.2.2 Human prostatic development

For the first six weeks of gestation both sexes have a bipotential gonad. Under the influence of the SRY gene on the Y chromosome, Sertoli cells within the primitive gonads secrete Müllerian Inhibitory Substance that causes regression of the female genital precursors and stimulates testicular Leydig cells to produce testosterone (Thomas, 2002).

The male genitalia derive from the mesodermal Wolffian ducts (seminal vesicles, epididymes, vas deferens and ejaculatory ducts) and the endodermal urogenital sinus, (prostate, urethra, bulbourethral and periurethral glands, penis and scrotum). The prostate develops in the uppermost part of the urogenital sinus where the Wolffian ducts open into the developing urethra, though the exact contributions of each tissue type are not fully elucidated (Aumüller *et al*, 1998). Testosterone enables Wolffian duct differentiation, however urogenital sinus

differentiation is dependent on dihydrotestosterone (DHT) produced from testosterone by 5α-reductase enzyme in the urogenital sinus (Gilbert, 2000). The urogenital sinus mesenchyme is vital for the development of the prostate and there is a complex interplay of signals between the stroma, basement membrane and epithelium (see section 1.2.6).

The prostate develops between weeks ten and 22. Paired urethral epithelial buds invade surrounding urogenital sinus mesenchyme, radiating out in different directions to form the various zones of the prostate. The buds branch out from their tips and cannulate to form ducts and acini. The surrounding mesenchyme develops into myoblasts and fibroblasts.

The prostate further matures due to the influence of androgens at puberty until age 20. An increase in the number and complexity of glands is seen, with increased secretory function (Aumüller, 1983). Thereafter it remains dependent on dihydrotestosterone throughout life.

1.2.3 The anatomy of the prostate.

The normal adult prostate volume is 20 ± 6ml (Berry *et al*, 1984). It is described as an inverted pyramid, with the base abutting the bladder and the urethra emerging just anterior and proximal to the apex. The prostate is surrounded by a thin capsule of smooth muscle, collagen and elastin fibres, which blends internally with prostatic stroma and externally with pelvic fascia (Brooks, 2002, McNeal, 1998). The capsule is deficient where the prostate abuts the bladder and anterolaterally at the apex, where glands merge into the striated muscle of the urethral sphincter. This is relevant in the histopathological assessment of surgically removed prostates when determining whether cancer has grown beyond the gland, and whether the prostate has been removed intact.

At the midpoint of the prostatic urethra is the veru montanum, a protrusion of tissue where the ejaculatory ducts from the seminal vesicles and vas deferens drain into the urethra alongside the prostatic ducts.

The prostate tissue itself is comprised of a branching arrangement of glandular epithelial structures supported by contractile fibromuscular stroma that assists duct emptying during ejaculation. The internal anatomy of the prostate was a subject of debate for many years (McNeal, 1980). In 1968, after studying hundreds of post-pubertal prostates sectioned in multiple planes, McNeal proposed four zones within the prostate, a model that remains widely accepted (McNeal, 1968). Zones were distinguished by differences in histology, duct architecture and sites of urethral drainage; all thought to reflect different biological functions and account for different predilections to pathology (McNeal, 1988, McNeal *et al*, 1988). Figure 1.1 demonstrates how the separate zones fit together as a whole.

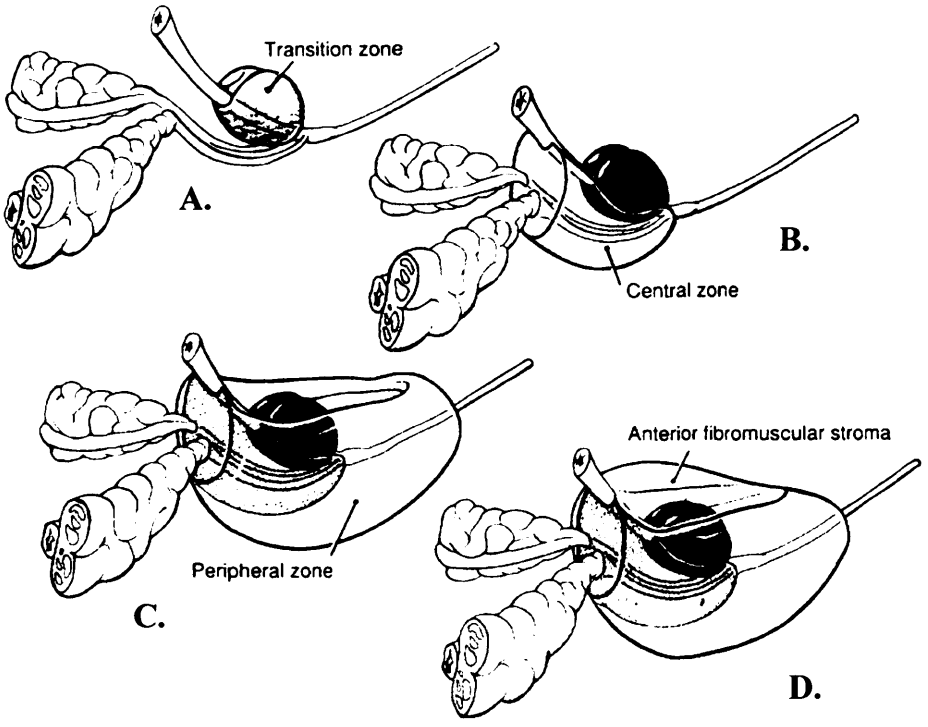

Figure 1.1: Zonal anatomy of the prostate as described by J. E. McNeal (Am J Surg Pathol 1988; 12:619–33). A: Transition zone, B: Central zone, C: Peripheral zone, D: Anterior fibromuscular stroma.

1.2.3.1 The Transition zone

The transition zone in health represents 5% by volume of the glandular prostate, but as the sole site of BPH can grow to become the largest zone. It surrounds the

urethra proximal to the ejaculatory ducts and veru montanum, while its ducts radiate proximally from this level with the zone defined by a discrete fibromuscular margin. Histologically the acini and ducts are small, round, regular and smooth walled made up of a simple columnar epithelium of pale cells with basal nuclei (McNeal, 1988). Approximately 20% of prostate adenocarcinoma arises here (McNeal *et al*, 1988).

1.2.3.2 The Central zone

Most of the base of the prostate is comprised of this zone. Central zone ducts arise close to the ejaculatory duct openings and lead proximally. The ducts are typically large and irregular with septae projecting into the lumen. Cells are variable in length and extent of luminal border and nuclei are larger, paler and positioned throughout the cells. These histological appearances are reminiscent of the seminal vesicles, suggesting a possible common derivation from the Wolffian ducts, supported by the fact that only up to 5% of cancers arise here (Tisell and Salander, 1975).

1.2.3.3 Peripheral Zone

The peripheral zone represents around seventy percent by volume of the glandular post-pubertal prostate constituting the bulk of the posterior, apical and lateral prostate. Ducts radiate laterally and distally from the urethra distal to the veru montanum. Histologically, they are similar to transition zone ducts (McNeal, 1988). Seventy percent of cancers arise in this zone and it is most commonly affected by chronic prostatitis (McNeal *et al*, 1988).

1.2.3.4 Anterior Fibromuscular Stroma

The anterior surface of the gland is covered by stromal tissue extending from the bladder neck to the striated urethral sphincter, which contains no glandular tissue.

1.2.4 Zonal variation within the prostate.

While the zones can be distinguished histologically and by their susceptibility to disease, their precise embryological, molecular and biological differences are less well established. Laczkó *et al* (2005) compared the morphology, cell kinetics and immunohistochemistry of the three glandular zones. The peripheral zone and transition zone were comparable in appearance and rates of proliferation and apoptosis while the central zone was distinct histologically, had half as many neuroendocrine (NE) cells and lower rates of cell turnover. They found no differences in cytokeratin or androgen receptor (AR) expression, though lactoferrin was more frequent in the central zone and the stromal cells here expressed significantly more smooth muscle actin. Others have reported segregation of oestrogen receptor α to peripheral zone stroma and greater expression of stromal α1-adrenoreceptors in the central and transition zones compared to the peripheral zone (Tsurusaki *et al*, 2003; Kobayashi *et al*, 1991).

The protein expression of all three zones was compared by Lexander *et al* (2005) who found the peripheral and transition zones to have highly similar major protein expression profiles, but identified ten proteins differentially expressed by the central zone.

Van der Heul-Nieuwenhuijsen and colleagues explored peripheral and transition zone differences and their possible implications using DNA microarrays (2006). In all, 147 genes were more highly expressed in the transition zone, and these tended to overlap with those over-expressed in BPH and under-expressed in prostate cancer, while 199 genes more highly expressed in the peripheral zone were almost all known to be over-expressed in prostate cancer. As several of the latter genes had been previously implicated in the origin and progression of cancer, while some over-expressed in the transition zone are known to have anti-tumour properties, the authors proposed that the zone-specific microenvironment of the peripheral zone might support malignant transformation, while that of the transition zone might be protective. As several of the highly expressed transition zone genes are stroma specific it is possible that stromal-epithelial interactions help establish these different milieu.

1.2.5 The histology of the normal prostate

The prostate may be described as 'normal' for only a brief time window during life as prostate development is only complete after puberty, and prostate disease may commence as early as the 4th decade (Berry, 1984).

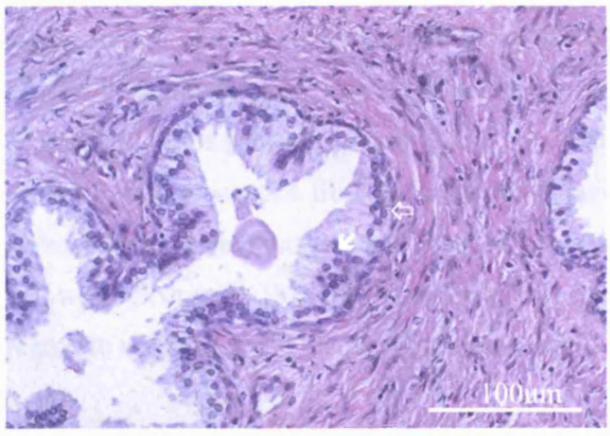

Figure 1.2: Haematoxylin and eosin (H&E) stained view of a normal prostate acinus surrounded by fibro-muscular stroma. ⇦ indicates a cell in the basal layer, and ↙ a luminal cell.

The normal prostate is comprised of epithelial ducts and acini surrounded by stroma (see figure 1.2). The epithelial compartment is believed to comprise stem cells, TA cells, terminally differentiated secretory cells and NE cells arranged as luminal and basal layers of epithelium (De Marzo *et al*, 1998a). The relationship between these various epithelial cell types is discussed in more detail in section 1.3 below.

The luminal epithelial cells outnumber the basal epithelial cells by 2.7:1.0 (Hudson *et al*, 2001). These terminally differentiated, functional cells form a continuous layer as tall, columnar cells with their apical borders defining the lumens of the prostate acini and ducts and their bases separated from the basement membrane by the basal layer (De Marzo *et al*, 1998a). Their cytoplasm is rich in secretory granules containing enzymes such as PSA and PAP. Secretions produced within the cells are secreted into the prostatic acini and ducts and ultimately drain into the urethra.

Small flattened basal cells with minimal cytoplasm rest on the basement membrane (Bonkhoff and Remberger, 1996; Rizzo *et al*, 2005). They may not be

easily visible but can be demonstrated as a discrete layer by staining with the basal cell specific antibody 34β-E12 that binds to high molecular weight cytokeratins 1, 5, 10 and 14 (Wojno and Epstein, 1995). TA cells and possibly prostate stem cells are thought to reside in this layer (Bonkhoff, 1998).

It has long been known that castration results in an almost complete involution of the prostate epithelium, a fact utilised today in the treatment of BPH and prostate cancer. Withdrawal of androgens (either by castration or drugs) results in loss of nearly 90% of the prostate epithelial cells (Staack *et al*, 2003). This cell loss occurs through apoptosis from the androgen dependent luminal cell layer, leaving the androgen independent basal layer and stroma intact (see section 1.3.1 below, English *et al*, 1989). Restoration of androgens results in epithelial regrowth until the gland reaches its previous size.

Terminally differentiated NE cells are scattered throughout the epithelium, again resting on the basement membrane. There are two types, 'open' NE cells which protrude apical microvilli into the lumen, and 'closed' ones that send long processes to adjacent cells (diSant-Agnese and deMesy-Jensen, 1984; diSant-Agnese *et al*, 1985). Also inconspicuous, they are best demonstrated using stains for serotonin, synaptophysin or chromogranin A, but lack AR or PSA. Their nuclei are also negatively staining for Ki67, a proliferation associated antigen so they are thought to be terminally differentiated, post-mitotic cells (Bonkhoff and Remberger, 1996; Bonkhoff *et al*, 1995). NE cells are thought to help regulate prostate growth, differentiation and secretion through the paracrine and autocrine secretion of neurotransmitters, hormones and bioactive molecules for which receptors have been demonstrated in the prostate (Vashchenko and Abrahamsson, 2005)

The surrounding stromal tissue is comprised of smooth muscle cells, fibroblasts, myofibroblasts, nerves, capillaries and lymphatics. It supports the ducts, contracts to assist duct emptying during ejaculation and is important in directing epithelial function and growth (McNeal, 1998). An extracellular matrix of collagens, elastin, fibronectin, laminin and glycosoaminoglycans, complex

polysaccharide and glycolipids exists between the cells and forms the basement membrane (Aumüller, 1983).

1.2.6 Stromal-epithelial interactions

A complex interplay of signals between the epithelium and the stroma across the basement membrane starts as early as the prostate itself and continues throughout life. The prostate develops under the permissive influence of DHT. This activates mesenchymal AR resulting in the induction of epithelial differentiation in the adjacent endoderm, through an unknown mechanism, which might involve the paracrine effects of a diffusible growth factor, or alterations in the configuration of insoluble extracellular matrix proteins (Cunha *et al*, 2002). The primitive epithelium lacks AR at this stage so must be influenced indirectly by DHT (Takeda and Chang, 1991).

The inductive ability of mesenchyme was elegantly demonstrated by Cunha and colleagues (1983) using an assay system whereby embryonic tissue can be slipped under the renal capsule of male nude mice, thereby providing an angiogenic and androgenic environment that supports further development. They demonstrated the ability of rodent urogenital sinus mesenchyme to induce prostate development in various embryonic epithelia and even the non-glandular, AR negative adult urinary bladder.

In turn, prostate epithelium induces urogenital sinus mesenchyme to undergo smooth muscle differentiation. Co-culture of urogenital sinus mesenchyme with adult prostate or bladder epithelium in male mice produces prostatic ducts surrounded by α-actin positive smooth muscle cells (Cunha *et al*, 1992).

Overall, it appears that stromal androgen sensitivity is essential for prostate proliferation and development, orchestrated via paracrine mechanisms, but subsequent differentiation into functional secretory epithelium requires epithelial expression of AR and direct androgen effects (Cunha and Young, 1991). The situation is similar in adulthood, with stromal smooth muscle ARs maintaining a

fully differentiated, growth quiescent gland, while epithelial ARs ensure secretory function (Cunha and Young, 1991).

1.2.7 Androgens and the prostate

Prostate growth, maintenance and function throughout life are dependent on the continued presence of androgens. The testes produce >95% of circulating androgens in the form of testosterone with the remainder arising from adrenal secretion of the weaker androstenedione, though only testosterone is biologically significant to the prostate. Only 2% of circulating testosterone is unbound to plasma proteins and thus available for conversion to DHT. This free testosterone is taken up by prostate cells and converted to DHT by cytoplasmic 5α-reductase enzyme. Within the prostate therefore DHT is present in five-fold greater concentrations and is 1.5 to 2.5 times as potent as testosterone (Veltri and Rodriguez, 2007a).

Inside the prostate cell, DHT binds to cytoplasmic ARs, activating them and causing their transport in pairs into the nucleus. Following the binding of other co-factors, the protein complex acts as a transcription factor at androgen response elements within the promoters of various genes. A cell specific cascade of gene and protein expression ensues (Veltri and Rodriguez, 2007b).

Castration results in a 90% decrease in total epithelial cell number and a slower 40% decrease in stromal cell number (DeKlerk *et al*, 1976; Staack *et al*, 2003). Hours after withdrawal of testosterone, the active and irreversible process of apoptosis commences in the luminal cells, leaving only androgen independent cells surviving (Isaacs, 1984). In the rat ventral prostate this amounts to a subpopulation of cuboidal cells in the luminal layer adjacent to an intact layer of basal cells (English *et al*, 1987). Gerald Cunha and colleagues have again studied whether apoptosis is triggered by epithelial or stromal events and implicated the latter (Prins *et al*, 1991; Cunha *et al*, 2004).

When castrated rats are treated with androgens, there is an initial delay of one day before the onset of DNA synthesis, which peaks at two to three days then

subsides to normal once the gland is restored to its normal size and function (Suffrin and Coffey, 1973). This cycle of withdrawal and replacement can be repeated over 30 times, or over three years after castration suggesting the existence of a long-lived, androgen-independent population of stem cells in the basal layer (Isaacs and Coffey, 1989).

1.3 Epithelial cellular hierarchies.

All epithelial tissues within the human body are maintained throughout life by a constant process of cell turnover. The loss of terminally differentiated cells must be balanced by the generation of new cells. For some tissues, this requires a very high rate of cell turnover throughout life, for instance in man, the entire outer layer of the skin is shed each day (Dexter, 1987). This challenge is met by a tiny population of epithelial stem cells responsible for tissue homeostasis and regeneration after tissue loss.

Epithelial stem cells, be they in gut, skin or breast tissues are rare, long-lived, infrequently dividing yet infinitely proliferative, tissue specific cells (Potten and Loeffler, 1990). They possess two defining characteristics – pluripotency with the ability to generate differentiated progeny in a number of different tissue-specific cell lineages, and the ability to self-renew such that stem cell mitosis results in one new stem cell and one daughter or TA cell.

TA cells have limited though significant proliferative potential, are committed to a certain cell lineage or subset of lineages, and divide frequently to ensure the clonal amplification of the initial TA cell into the differentiated cells that comprise the bulk of the tissue. The TA cells divide until their proliferative potential is exhausted and they become post-mitotic, terminally differentiated cells. These specialised cells perform the function of the tissues.
The traditional stem cell model therefore describes a linear and irreversible process of differentiation (Morrison *et al*, 1997). There is an inverse relationship between proliferative potential (greatest in the stem cell) and differentiation (greatest in the terminally differentiated cells). Successive generations of TA cells progressively lose the former and gain the latter. In some tissues, full

function is clearly incompatible with mitosis (mature erythrocytes and cornified epithelial cells lose their nucleus, muscle filaments preclude cell cleavage) so the separation of proliferation and terminal differentiation are essential.

1.3.1 Stem cell characteristics

Our understanding of stem cells originated from studies on high turnover tissues such as the haematopoietic system, epidermis and intestinal mucosa. More recently stem cells have been recognised in other organs, such as liver, olfactory epithelium, breast and brain, and the prostate stem cell phenotype is now being approached (Houghton *et al*, 2007). Stem cells are typically classified by their specific pattern of cell markers. However, their initial identification requires behavioural assays, most importantly of the fundamental characteristics of self-renewal and pluripotency.

Pluripotency is defined as the ability of the undifferentiated stem cell to produce differentiated progeny for the full range of cell types in a specific tissue. Embryonic stem cells are described as totipotent, i.e., given the necessary signals they can give rise to any cell lineage within the organism. During development, these cells are progressively committed to an increasingly narrow repertoire of cells until as adult stem cells they are ordinarily restricted to tissue specific lineages. Some stem cells such as muscle satellite cells are in reality unipotent, as only one lineage arises (Marshak *et al*, 2001). However bone marrow haematopoietic stem cells (HSC) produce all blood cell types: red blood cells, B and T lymphocytes, natural killer cells, neutrophils, basophils, eosinophils, monocytes, macrophages and platelets (Kondo *et al*, 2003). Isolated human bone marrow stem cells will repopulate the bone marrow of a lethally irradiated mouse for all lineages for its life span and successful serial transfer into secondary recipients has demonstrated self-renewal properties (Larochelle *et al*, 1996). Self-renewal implies the generation of at least one pluripotent new stem cell at mitosis. The lineage potential and properties of a stem cell are determined by dynamic intracellular properties and/or cues from its microenvironment (Morrison *et al*, 1997). Following mitosis, the exact mechanisms whereby stem cells decide whether to self renew or differentiate are unknown (Sherley, 2002).

Stem cells characteristically reside in specific niches within the tissue, surrounded by supporting cells that help maintain a stable microenvironment (Potten and Loeffler, 1990). In gastrointestinal mucosa, it has been proposed that daughter cells that migrate outside of the limited space of the mucosal crypt are released from the restraints of the niche microenvironment and differentiate (Yen and Wright, 2006).

Control of stem cell fate is critical to ensure a balance of cell proliferation and loss. Division of a stem cell may be asymmetric, resulting in one TA cell and one stem cell or symmetric, producing either two TA cells or two more stem cells (Morrison *et al*, 1997). These situations result in tissue maintenance, tissue depletion or tissue growth respectively. Tissue growth may be intentional after tissue loss, or represent unrestrained self-renewal as seen in cancer.

Controversially, it has been proposed that the same chromatids are retained by the new stem cell at each asymmetric division with the new chromatid copies inherited by the daughter cell (Cairns, 2002; Potten *et al*, 2002). This prevents the retention in the stem cell pool of mutations caused by inaccurate DNA replication, which instead are inherited by cells committed to maturation and death. Additionally stem cells are deficient in some DNA repair mechanisms, so that damaged DNA is not subject to error prone repair, but results in sacrifice of the stem cell by apoptosis. This could account for the sensitivity of stem cells to DNA damaging agents (Cairns, 2002).

Intimately associated with self-renewal is the longevity of stem cells. They divide rarely being predominately found in the G0/G1 phase at cell-cycle analysis, thereby minimising DNA replication related mutations though this alone does not confer immortality (Li *et al*, 1998). Every chromosome has telomeric DNA at its ends, some of which is lost at every cell division. Most cells therefore, can only undergo about 50 cell divisions before their chromosomes are critically shortened, and they undergo apoptosis (Hayflick, 1961). Telomerase is a riboprotein enzyme complex with reverse transcriptase activity that replaces lost telomere sequences after mitosis, thereby allowing indefinite cell division (Campisi, 2005). Telomerase has been reported to be

expressed in longer living or immortalised cells (Kim *et al*, 1994). Other epigenetic processes are also thought to help prevent senescence. Genes such as Bmi1, which are involved in chromatin remodelling, are highly expressed in haematopoietic and neural stem cells (Lessard *et al*, 2003; Molofsky *et al*, 2003).

There has been much interest in assigning the cells in the prostate epithelium to this model, with particular reference to the location and phenotype of the prostate stem cell, which has the potential to be the key focus of intervention for the treatment of prostate diseases.

1.4 Models of prostate epithelial cell lineages

The different cell populations within the prostate epithelium have long been studied in terms of their behaviour, phenotype and ultrastructural appearances, and more recently their intracellular and cell surface marker expression. In the 1980's and 1990's, three models of prostate epithelial maintenance were proposed to account for the three histologically distinct cell types (basal, luminal and NE cells) present in the two-layered prostate epithelium.

1. The luminal and basal layers represent discrete cell lineages with discrete stem cells, that divide when necessary to self renew and maintain the relevant cell layer. NE cells represent an entirely separate third lineage (Aumüller, 1983; Evans and Chandler, 1987).
2. A basally located stem cell divides rarely, generating a stem cell and a basal TA cell. This TA cell can differentiate into two distinct lineages producing terminally differentiated luminal secretory cells after many divisions or rarer NE cells after fewer (Isaacs, 1987).
3. The progeny of the stem cells in an intermediate location become committed to one of two separate lineages, producing either basal cells or luminal cells (Wang *et al*, 2001).

In the 1980's, from work in rat seminal vesicles and prostates, Aumüller (1983) proposed the 'homeostatic constraint mechanism of accessory gland cell growth', which stated that prostate secretory (luminal) cells in the normal prostate divide

when the amount of secretory product within them falls below a critical level. This mechanism depends upon the presence of androgens, and stromal growth factors reaching the secretory cells via the basal cells (Aumüller, 1983). In the absence of the appropriate hormones, the basal cells are stimulated to proliferate, though their capability to differentiate is low.

In this model, NE cells represent a distinct lineage, derived from neural crest cells in periprostatic paraganglia (Aumüller *et al*, 1999; 2001). During gestation, these invade into the developing prostate and distribute themselves throughout the gland. Accordingly there are fewer NE cells at the periphery, the number of NE cells is stable throughout development and they reach maturity 15 years before the epithelial cells.

Evans and Chandler (1987) in agreement with Aumüller, further proposed that basal and luminal layer cells were individually self-replicating cell types with discrete functions. During their study of post-natal rat prostate development, they observed basal cells as small solid cords of cells with a lumen and secretory cells appearing a few days later. Mitotic figures were seen in both cell layers even after they had acquired their characteristic luminal and basal ultrastructural features. Mitoses were seen more frequently in the luminal layer and the rate of increase of luminal cell number appeared more related to their own proliferative activity than the slower basal cell rate. No cells with intermediate ultrastructural characteristics were seen. However this work in the 1980's distinguished cells only by their appearance and little corroborating evidence has emerged to support this model since its proposition.

An alternative stem cell organisation of the prostate was proposed by Isaacs (1987), based on the kinetics of prostate growth. In this model, a small population of androgen independent, basal stem cells generate TA cells which are committed to become either prostate luminal cells or more rarely NE cells. Basal TA cells are androgen independent for survival yet will proliferate in response to androgen to amplify the cell numbers derived from the slowly proliferating stem cell. During progressive divisions the TA cells migrate into the luminal layer where they become dependent on androgens for survival and

undergo fewer divisions. Ultimately terminally differentiated secretory cells arise within the luminal compartment (see figure 1.3).

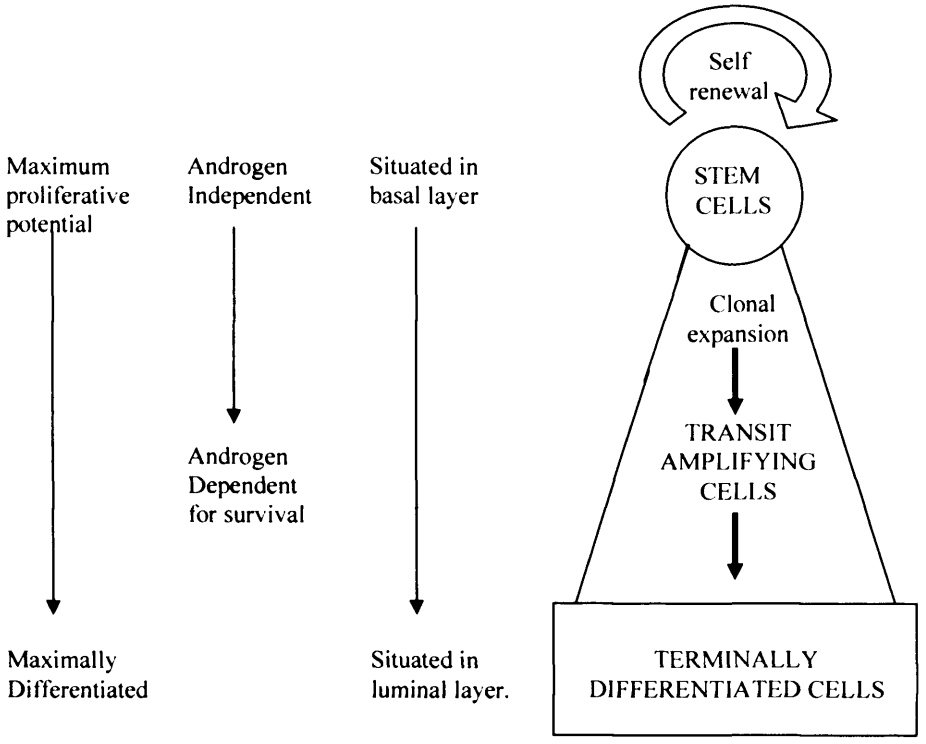

Figure 1.3: Diagrammatic representation of the cell populations within the prostate epithelium (Isaacs, 1987; Bonkhoff and Remberger 1996).

Evidence for this model derives from several sources. The prostate's ability to reconstitute itself with androgen reintroduction after castration suggests the presence of androgen independent stem cells in the basal layer (Isaacs and Coffey, 1989). Additionally, the identification of cells with an intermediate phenotype between the basal and luminal cells allowed the definition of the TA cell population. Thus the markers expressed by epithelial cells at different locations in the epithelium show a progression that fits with their postulated process of differentiation.

1.4.1 Basal, intermediate and luminal epithelial cell markers

Since the 1970's, cells sharing microscopic features of both basal and secretory cell have been reported (Dermer, 1978). Immunohistochemistry and immunofluorescence of many other markers have better characterised the phenotypes of the basal, TA and luminal cells. More recently the phenotype of the stem cell population has become more established (discussed in section 1.5 below).

Cytokeratin expression varies between the epithelial layers. Keratins are one of the five classes of intermediate filament proteins within the eukaryote cytoskeleton in all epithelial cells. Twenty keratins (K) have been documented but K1, 4, 6, 10 and 11 are not expressed in prostate epithelium (Moll, 1994).

Basal cells express K15, 5 and 14. Luminal cells express high levels of K8 and K18 (Sherwood *et al*, 1991; Nagle *et al*, 1991; Yang *et al*, 1997; van Leenders *et al*, 2000; Schmelz *et al*, 2005). Cells expressing combinations of these and other keratins are believed to be TA cells in transition between the two phenotypes. Numerous studies have identified intermediate cell phenotypes, listed in table 1.1 using a range of antibodies with different specificities for the keratin family.

Epithelial layer	Phenotype	Reference
Basal	$K14^-K5^+K18^-$, $K14^+K5^+K18^+$	Verhagen *et al*, 1992; van Leenders *et al*, 2000; Hudson *et al*, 2001
	$K14^-K15^+$, $K14^+K15^+$, $K14^+K17^+$, $K14^-K17^+$, $K15^+K19^+$, $K15^+K19^-$	Hudson *et al*, 2001
	$K14^-K5^+K19^+$, $K14^+K19^+$	Verhagen *et al*, 1992; Hudson *et al*, 2001
	$K5^+$ $K6a^+$, $K6a^+K19^-$	Schmelz *et al*, 2005
	$K8^+K18^+$	Nagle *et al*, 1991; Yang *et al*, 1997
Luminal	$K5^+K18^+$	Verhagen *et al*, 1992; van Leenders *et al*, 2000
	$K19^+K8^-$, $K19^+K8^+$	Verhagen *et al*, 1992; Hudson *et al*, 2001
	$K6a^+K19^+$, $K6a^-K19^+$	Schmelz *et al*, 2005
	$K19^+K7^+$	Hudson *et al*, 2001

Table 1.1: Intermediate cytokeratin phenotypes of cells in the basal or luminal prostate epithelium.

So in summary, while K14 is only expressed in the basal layer, TA cells express a number of keratins as they migrate from the basal to the luminal layer, ultimately retaining only K8 and K18. Early TA cells within the basal layer lose K14 expression and retain K15, K17, K19 and K5, later luminal TA cells continue to express K19 and K5 and gain K8 and K18 expression. After androgen ablation, $K5^+$ and $K5^-$ cells exist in the subpopulation of remaining prostate cells suggesting that late intermediate $K5^-$ cells within the luminal layer are still androgen independent (van Leenders and Schalken, 2003).

A number of other differentially expressed markers have also been reported. Prostate stem cell antigen (PSCA) despite its title is thought to be a marker of late TA cells in the basal layer that co-express K5/K14/K18 (Tran *et al*, 2002). De Marzo *et al* (1988a) studied expression of a cyclin-dependent kinase inhibitor $p27^{Kipl}$, which is thought to prevent cell division and may signal exit from the cell cycle. Luminal cell nuclei stained strongly for $p27^{Kipl}$, but this was strong to absent in basal cells. There was also an intermediate layer of $p27^{Kipl}$ negative cells that were positive for the 34ßE12 basal keratin marker (that binds K5 and K14). The authors postulated that absence of $p27^{Kipl}$ correlated with rapid cell division such that slowly cycling $p27^{Kipl}$ positive stem cells produced $p27^{Kipl}$ negative TA cells that proliferate to amplify the epithelium prior to terminal differentiation and re-expression of $p27^{Kipl}$.

Other basal cell markers include p63, CD44, the transcription factor ETS-2 and EGFR (epithelial growth factor receptor) (Liu *et al*, 1997; Kellogg Parsons *et al*, 2001; van Leenders and Schalken, 2003). The nuclear phosphoprotein pp32, found in self-renewing and long-lived cell populations is moderately expressed only in basal cells (Kadkol *et al*, 1998). The luminal layer also secretes PSA and PAP and expresses CD57 and greater quantities of nuclear AR than basal cells (Ruizeweld de Winter *et al*, 1991; Liu *et al*, 1997).

As would be expected with Isaacs' model, the distribution of Ki67 suggests that 80% of proliferating epithelial cells are in the basal layer (Hudson *et al*, 2001). The antiapoptotic oncogene Bcl-2, expressed in stem cells and proliferation zones in the skin and gut, is also expressed in the basal cell layer, but

downregulated in the luminal cells, while the pro-apoptotic protein CPP32 (a caspase protein that acts as an apoptosis effector molecule) is more highly expressed luminally (Bonkhoff and Remberger, 1996; Krajewska *et al*, 1997). *In situ* hybridisation has demonstrated telomerase exclusively in basal cells (Paradis *et al*, 1999). GST-π, a member of the π class of glutathione S-transferases that protect against electrophilic carcinogens is also only basally expressed, perhaps implying greater protection of the genome in the longer-lived stem cells (DeMarzo *et al*, 1998b).

In Isaacs' stem cell model, the NE cells derive from division of the same population of stem cells, but the daughter cells differentiate into an alternative lineage. Cells have been reported that share epithelial cell and NE characteristics, which may represent the differentiating, proliferating cells of the NE lineage. Cells co-expressing chromogranin A and PSA have been identified in hyperplastic prostates and adenocarcinomas, while occasional 'closed' NE cells positive for chromogranin A and basal cytokeratins have been seen in normal and hyperplastic glands (Bonkhoff *et al*, 1994a). Rumpold *et al*, (2002) reported the appearance of K5/K14 and chromogranin A expressing 'NE-like' cells appearing *de novo* in cultures of basal (positive for K5/14 and CD44) epithelial cells after three days. These cells were not however seen in the studies by Aumüller *et al* (2001).

Cunha and colleagues however argued against this hierarchy based on their studies of embryological cell characteristics (Wang *et al*, 2001). They reported that the cells of the urogenital sinus epithelium, (that might be expected to be rich in prostate progenitor/stem cells) in mice, rats and humans all co-express luminal and basal cell markers. Exclusively luminal markers are seen only once prostate buds and ducts form at 10 weeks of gestation and purely basal cells are first seen even later at week 18. They therefore proposed that basally located $K8^+/18^+/14^+/5^+/19^+$, $p63^+$, GST-π^+ cells represented the true stem cells. The frequency of these cells decreases steadily through development, and represent only 0.59% of basal cells in the adult human prostate. Thus progeny from these stem cells differentiates into two separate lineages of luminal or basal cells.

Subsequent work by the same group addressed the origins of NE cells and again supported this model (Kurita *et al*, 2004). In 2000, Signoretti *et al* reported that $p63^{-/-}$ knockout mice (lacking the gene for the exclusively basal marker p63) failed to develop prostates suggesting that the $p63^{+}$ basal cell population is critical for prostate development, and might contain stem cells, although it is difficult to identify the undeveloped prostate perinatally when $p63^{-/-}$ mice die. Kurita *et al* (2004) found that transplanting urogenital sinus tissue (mesenchyme and epithelium together) from $p63^{-/-}$ mice under the renal capsules of male nude mice produced prostate tissue with grossly normal ductal morphology surrounded by normal prostate smooth muscle. The ducts were lined by AR^{+} luminal cells, but no definable $p63^{+}/K14^{+}/K19^{+}$ basal layer was present. Both $p63^{-/-}$ and $p63^{+/+}$ prostates contained equal numbers and distributions of rare $synaptophysin^{+}$ NE cells. Castration caused the entire $p63^{-/-}$ graft to lose almost all luminal cells and duct complexity but they regenerated with reintroduction of testosterone.

The authors concluded that p63 is essential for development of the basal layer, branched ducts and secretory luminal cells, but not for differentiation of NE and smooth muscle cells. The basal layer does seem to play a role in normal luminal cell differentiation and secretion, perhaps by mediating interactions with the basement membrane.

While, Kurita *et al* (2004) concurred with Cunha's model and suggested the presence of a single $p63^{-}$ stem cell that chooses between luminal, basal or NE lineages, it is equally possible that three separate stem cells ($p63^{-}$ for luminal and NE, $p63^{+}$ for basal cells) exist in step with Aumüller's model. It is also still possible that in the normal adult $p63^{+/+}$ prostate, basal cells do develop into luminal cells as in Isaacs' model. The debate over the developmental cell-linage relationships between luminal, basal and NE cells is as yet unresolved. However since 2000, a number of studies have progressively defined a population of prostate epithelial cells that possess stem cell properties (though not all have been tested). Study of these stem cells promises to provide the answer.

1.5 Defining the prostate stem cell

Recent work suggests that the prostate stem cell can be identified by its unique molecular expression profile: $CD133^{+}/ABCG2^{+}/\alpha2\beta1^{Hi}/p63^{-}/PSCA^{-}/AR^{-}/PSA^{-}$ (Litvinov *et al*, 2006) though its location and relationship to basal and luminal cells remains uncertain. Identification lagged behind that of other tissues due to inherent technical difficulties. As a solid tissue, extraction of cells requires mechanical disruption and enzymatic digestion, which risks the very cell surface markers used to define them and adult stem cells are refractory to traditional methods of cell culture as they tend to differentiate and senesce (Sherley, 2002; Dontu *et al*, 2003). A number of extraction and isolation techniques used in other tissues have been applied with success to prostate tissue. Equally the search for specific markers has been guided by those found in other tissues suggesting that some determine the stem cell phenotype, while others determine tissue specificity (Gu *et al*, 2007).

Several studies have isolated populations of primary epithelial cells that demonstrate some stem cell features. Primary culture of prostate epithelial cells from explants and partially and entirely digested tissue yields tightly-packed cobblestone-like cells expressing mostly intermediate and some basal keratins, that form a monolayer (Merchant *et al*, 1987). Subsequently the cultures become multilayered with overlying luminal cytokeratin expressing cells containing secretory granules. Isolation and culture of the upper layer of cells demonstrates these cells to be viable, but have no mitotic activity (Merchant *et al*, 1987). This spontaneous differentiation *in vitro* in the absence of androgens, serum and stroma has been taken as evidence that basal cells give rise to luminal cells (Robinson *et al*, 1998).

Hudson *et al* (2000) confirmed the proliferative heterogeneity of primary prostate cells in low calcium, serum and androgen free culture of dissociated epithelial cells and retrospectively isolated colonies from putative prostate stem cells. Two colony types were identified after two weeks culture of prostate epithelial cells with an overall colony forming efficiency of 5.8% ±1.8 (see figure 1.4).

Type I colonies were up to 4mm across, and loosely packed with <30 cells per linear millimetre, they had irregular outlines, represented 89.5% of all colonies or 6.2% of all plated cells and expressed either K8 and K14 or just K8 in the smallest colonies. Type II colonies were large, dense, round colonies, 3mm or more across, with 30-50 cells per millimetre. They formed 10.5% of all colonies or 0.6% of all plated cells, and almost exclusively expressed K14 only.

These type II colonies were proposed to be the progeny of basal layer stem cells, while type I cells derived from TA cells. Furthermore, selection of cells rich in integrins that adhered to type 1 collagen-coated dishes for five or twenty minutes, enriched five-fold for colony forming cells, but not for colony type. This suggests that both stem cell and TA cells are adherent, while later androgen dependent TA and terminally differentiated cells within the primary epithelial cell suspension were not.

Type II colonies were also grown in three-dimensional Matrigel™ culture (an artificial basement membrane) and formed spherical structures connected by ducts reminiscent of the two-layered architecture of the prostate *in vivo*. The spheres consisted of a basal layer of cells expressing K5 and K14 and one or more luminal layers of larger, flatter cells expressing weak K5 and K14 and strong K17, K19 and K8 arranged around a lumen. Shed cells within the lumen expressed AR, but no staining for PSA or PAP was seen in this androgen free culture.

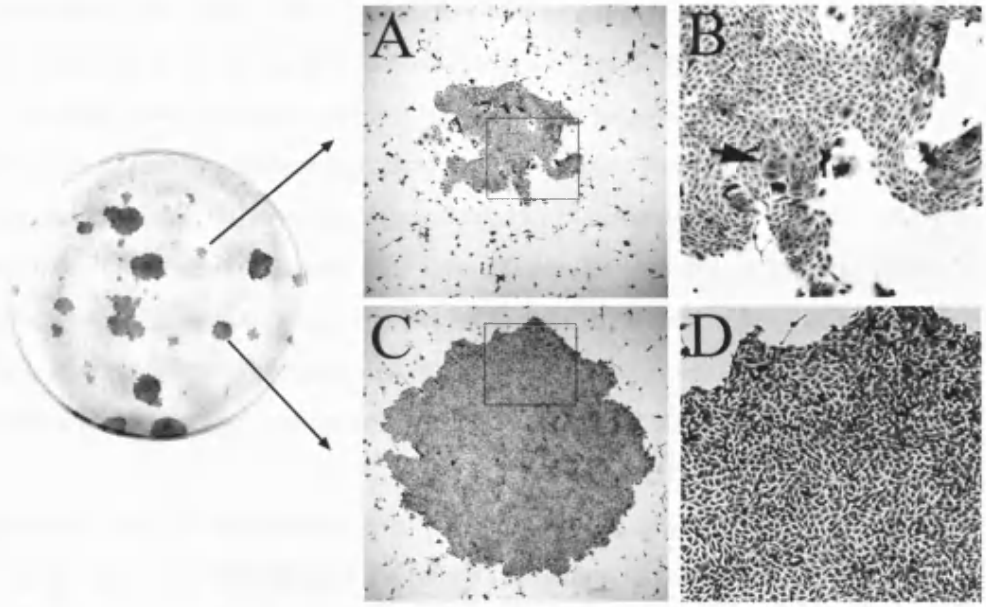

Figure 1.4: Colony types formed two weeks after plating 1000 freshly isolated epithelial cells from prostate tissue in a 5cm dish. Type I colonies (A and B) are relatively small, irregular and contain a mixture of differentiated and undifferentiated cells, type II colonies (C and D) are large, regular and consist almost entirely of small undifferentiated cells (Hudson *et al*, 2000).

Collins *et al* (2001) demonstrated that rapid type 1 collagen adherence is due to the high level expression of $\alpha_2\beta_1$-integrins. They suspected that as integrin expression enriches for epidermal stem cells, it might do so for prostate stem cells that also rest on an integrin-rich basement membrane. Basal prostate cells (selected by their expression of CD44) were plated onto type 1 collagen for five minutes. Adherent cells were $\alpha_2\beta_1$ integrin bright and showed 3.8-fold greater colony forming efficiency compared to non-selected basal cells. *In vitro* 15% of basal cells showed strong $\alpha_2\beta_1$-integrin expression and high levels of α_2-integrin staining were also seen in 1.07% of human basal cells *in vivo* (Collins *et al*, 2001).

In agreement with Hudson *et al* (2000), different colony types were noted, however Collins *et al* (2001) reported three different morphologies after three weeks in culture. Collins' type 1 (probably akin to Hudson and colleagues' type II colonies after longer in culture) are large, circular, smooth edged colonies

made up of small cells with larger differentiating cells overlying them. Cells divided after an initial lag period of seven days. Type 2 colonies (probably akin to Hudson type I) grew more rapidly and could be larger than type 1 with an irregular perimeter and heterogeneous cell sizes. Type 3 colonies were <32 cells big and terminally differentiated (not scored by Hudson *et al*, (2000)). Selection for integrins could not influence the type of colonies obtained. When implanted subcutaneously with stromal cells into male nude mice these rapidly adherent cells formed fully differentiated prostate tissue after six weeks. Acini were visible with basal and luminal cells that expressed PSA and AR.

Together these studies confirm that basal, androgen independent, $\alpha_2\beta_1^{Hi}$ integrin prostate epithelial cells comprise a mixed population of highly clonogenic cells with variable proliferative abilities that can reconstitute both layers of prostate epithelium (Hudson *et al*, 2000; Collins *et al*, 2001). These are likely to equate to stem and early TA cells but stem cell properties have not been demonstrated. Self-renewal was not tested and pluripotency was shown inasmuch as the Matrigel™ and mouse xenograft assays demonstrated differentiation, but generation of the NE lineage was not achieved. The type II colonies appeared to differentiate between the second and third weeks in culture, suggesting that while stem cells may establish the colony, at an undefined point or number of cells some progeny commence differentiation as TA cells.

Selecting prostate epithelial $\alpha2\beta1^{Hi}$ basal cells for CD133 expression further enriches for stem cells (Richardson *et al*, 2004). In the haematopoietic, endothelial and central nervous systems, CD133, a five-transmembrane glycoprotein of no known function has been used to isolate stem cells (Yin *et al*, 1997; Peichev M *et al*, 2000; Uchida *et al*, 2000). It is expressed by developing epithelial cells, and is rapidly down regulated upon differentiation (Corbeil *et al*, 2000). Amongst isolated prostate epithelial cells, 25% of $\alpha2\beta1^{Hi}$ cells also express CD133. The majority (75%) of these $\alpha2\beta1^{Hi}$ $CD133^+$ cells express basal cytokeratins (K14 and K5) but given that a minority (11%) express intermediate cytokeratins instead, CD133 may also be a marker of early TA cells. No $CD133^+$ cells express AR, PSA or PAP and they tend to be quiescent, expressing less

Ki67 than $CD133^-$ cells. Immunohistochemistry localized CD133 expressing cells to clusters of 1 to 5 basal layer cells.

When passaged to exhaustion, the $CD133^+$ population generated over two-fold more cells than the $CD133^-$ population. Equally, $\alpha2\beta1^{Hi}CD133^+$ cells showed a 10.6-fold greater colony forming ability, and the $\alpha2\beta1^{Hi}CD133^-$ cells a 4.5-fold one than unsorted basal cells. This suggests the former are stem cell derived, while the latter are TA cell derived and the remaining non-adherent basal cells are TA cells nearing terminal differentiation. $\alpha2\beta1^{Hi}CD133^+$ derived colonies are also larger, and appear five days later, possibly due to the slow cell cycle time of stem cells *in vivo*.

In vivo studies obtained two layer epithelial structures, with a K5 and K14 expressing basal layer and a K18, PAP and AR expressing luminal layer when $\alpha2\beta1^{Hi}CD133^+$ cells were injected subcutaneously with human stromal cells into male mice.

Richardson *et al* (2004) managed to demonstrate many features that would be expected of stem cells in their $\alpha2\beta1^{Hi}CD133^+$ cell fraction. These cells are indeed quiescent, undifferentiated and rare - found in 0.75% of the total basal cell population. However their niche environment is not apparent immunohistologically and far from showing indefinite proliferative potential, all cells senesced in culture after 55-75 days. Above all, neither true pluripotency nor self-renewal was demonstrated, though the former might have been had they stained the xenografts for NE cell markers. In effect these cells have not distinguished themselves from a population of early, committed TA cells. When 10,000 to 50,000 such cells are grafted it is possible that their residual proliferative activity is sufficient to generate the prostate epithelium seen here eight weeks later. Finally, these cells are still heterogeneous for cytokeratin expression, so these markers enrich for stem cells rather than isolate a pure population.

Breast cancer resistance protein (BCRP) also known as the G2 isotype of the ATP-binding cassette (ABC) transporter family (ABCG2) is consistently expressed by adult bone marrow, skeletal muscle and neural stem cells (Bunting,

2002). It transports from the cell chemotherapeutic drugs (thereby conferring resistance), steroids including androgens and experimentally the nucleic acid binding dye Hoechst 33342. Huss *et al* (2005) investigated the location, number and cell marker expression of BCRP/ABCG2$^+$ cells in benign prostate tissue, and a human prostate mouse xenograft model. In prostate tissue, 1% of all epithelial cells were ABCG2$^+$ and these appeared to be neither basal or luminal, being seen under the basal layer. Though close to basal cells expressing p63 and basal cytokeratins, NE cells expressing synaptophysin, AR$^+$ luminal cells and α-actin expressing smooth muscle, they were negative for all these markers. Castration made no difference to the number of ducts containing these ABCG2$^+$p63$^-$AR$^-$ cells in xenografts but a small proportion of the immediate progeny of these putative stem cells differentiated preferentially along a NE lineage (Huss *et al*, 2004). Reintroduction of androgens resulted in focal proliferative activity in the xenograft epithelial compartment with a cluster of ABCG2$^-$Ki67$^+$ cells appearing around ABCG2$^+$ cells, which themselves remained Ki67$^-$. These proliferating cells were proposed to represent TA cells that had exited the ABCG2$^+$ stem cell compartment.

Huss and colleagues' ABCG2$^+$p63$^-$AR$^-$synaptophysin$^-$α-actin$^-$ stem cells are pluripotent, quiescent, undifferentiated and rare. Their lack of p63 fits with the p63$^{-/-}$ work of Kurita *et al* (2004). They also appear to be a pure population as all ABCG2$^+$ cells are homogeneously negative for other markers. Though self-renewal was not demonstrated in this study, this phenotype has been further expanded upon since (Litvinov *et al*, 2006).

Bhatt *et al* (2003) also studied Hoechst 33342 dye exclusion by primary prostate epithelial cells but did not relate this to ABCG2 transporter expression. They identified two separate cell populations that together amounted to 1% of all cells and 10% of all α_2 integrin expressing cells. They differed in cell cycle position with the slightly more K14 rich population in G0 and the slightly more K8 expressing one in G1. Bhatt *et al* (2003) postulated that the former were stem cells and the latter TA. However further characterisation of these cell populations was not reported, so it is difficult to relate them to the cells described by Huss *et al*, (2005). The ABCG2 transporter is expressed in several other cell types,

including inflammatory cells and venous and capillary endothelium (Huss *et al*, 2005). Though a number of extraction steps were taken, contamination might account for the difference.

Though Huss *et al* (2005) demonstrated the immunohistochemical location of their prostate stem cell to be adjacent to but not within either the basal or luminal layer in human tissue, Tsujimura *et al* (2002) reported a small population of slowly proliferating cells in both basal and luminal compartments of proximal ducts in the mouse dorsal prostate. These putative stem cells retained bromodeoxyuridine when androgen was reintroduced after castration, could generate branching structures in collagen gels and were highly proliferative *in vitro*. When this cell population was dissected out and compared using a cDNA microarray to similar cells sourced from other regions of the dorsal prostate. CD133 emerged as one of the seven most upregulated genes, and $CD133^+$ cells also stained for telomerase (Tsujimura *et al*, 2007).

These same dissected out proximal murine prostate cells, were then investigated using fluorescent activated cell sorting (FACS) for expression of stem cell antigen-1 (Sca-1), a stem cell marker established in bone marrow and mammary tissue (Burger *et al*, 2005). Sca-1 was expressed more proximally and proximal $Sca\text{-}1^+$ cells produced greater weights of typical basal $p63^+$, luminal AR^+ prostate tissue than $Sca\text{-}1^-$ or distal $Sca\text{-}1^+$ cells when grown with urogenital sinus mesenchyme under mouse renal capsules. Though Sca-1 expression did enrich for prostate regeneration, some occurred in its absence, and with $Sca\text{-}1^+$ noted distally it did not segregate for the proximal prostate only. Thus, alone it does not appear to define the murine stem cell. As with all murine studies, it is as yet unknown how this work correlates with the human prostate.

1.6 Characterising prostate stem cells

Bringing this work together, Litvinov *et al*, (2006) studied the prostate epithelial stem cell population *in vitro* that they defined as $CD133^+/ABCG2^+/\alpha2\beta1^{Hi}/p63^-/PSCA^-/AR^-/PSA^-$. Their working model describes a prostate epithelial differentiation process that sees cells proceed down

a NE or luminal lineage. Cells destined for the luminal epithelium become TA cells with the phenotype $CD133^-$ /$ABCG2^-$ /$\alpha2\beta1^{Hi}$ /$p63^+$ /$PSCA^-$ /AR^- /PSA^- as well as expressing K5 and K14 and amplify through a number of divisions. At some point these cells acquire the 'intermediate' (TA) cell phenotype of $CD133^-$ /$ABCG2^-$ /$\alpha2\beta1^{Lo}$ /$p63^-$ /$PSCA^+$ /AR^- /PSA^- expressing K8 and K18 also. This transition was also noted by Tran *et al* (2002) studying PSCA who called these 'late' TA cells. Finally the cells migrate into the luminal layer and complete their differentiation becoming post-mitotic, androgen sensitive, secretory $CD133^-$/$ABCG2^-$/$\alpha2\beta1^{Lo}$/$p63^-$/$PSCA^-$/AR^+/PSA^+ cells. Table 1.2 summarises the locations of these markers.

A commercially available source of non-immortalized second passage normal human
prostatic epithelial cells (PrEC) was cultured in low calcium, serum-free defined medium and the phenotype of the constituent cells assessed. These cells will undergo ten passages before becoming quiescent. Almost all (98.9%) cells expressed $\alpha2\beta1$ integrins, and 1.3% of cells expressed all three stem cell markers ($CD133^+$ /$ABCG2^+$ /$\alpha2\beta1^{Hi}$). Over 80% of these latter cells were negative for p63 with some positives appearing to arise from cells in mitotic telophase where one cell was negative and one was positive.

After less than six passages, p63 expression was apparent in a majority (90%) of cells. Of the 10% negative cells, 1% were small and expressed stem cell markers, 1% expressed chromogranin with NE cell morphology and the remaining 8% were larger cells and $PSCA^+$ confirming their intermediate TA cell phenotype. When $CD133^+$ cells alone were cultured at low density, amplification yielded predominantly small TA cells with no more than 20% progressing to become (as seen on time lapse photography) larger intermediate $PSCA^+$ cells and none completing differentiation to AR^+ PSA^+ cells. NE cells also arose 1-3% of the time. Addition of androgens to the culture media was not sufficient to assist the intermediate cells to full differentiation. This inability was correlated with the low calcium content in the medium, which activates the notch signaling pathway that inactivates AR and PSA expression. The down-regulation of the notch-1

receptor has been associated with the up-regulation of AR and PSA and progression to a more differentiated state (Tran *et al*, 2002).

This study on a heterogeneous cell line *in vitro* has not demonstrated the two critical stem cell characteristics. Though self-renewal has not been convincingly displayed, asymmetric cell division was demonstrated immunohistochemically with a $p63^+$ TA cell separating from a $p63^-$ stem cell. Pluripotency was suggested by the two lineages generated by the $CD133^+$ cells, however, the cells were only sorted for this single stem cell marker, and as Richardson *et al* (2004) acknowledged, CD133 may also be a marker of early TA cells. Hence it would be interesting to see the outcome of a truly pure population of $CD133^+$ /$ABCG2^+$ /$\alpha2\beta1^{Hi}$ cells grown in a stromal / epithelial xenograft assay to determine whether one or more stem cells is required to obtain all three prostate epithelial lineages. Serial transplantation of cell fractions from the xenografts with the generation of a second generation prostate would also convincingly demonstrate self-renewal and though ideally this should be achieved from a single cell, mixtures of marked cells might also show clonally derived tissue (Houghton *et al*, 2007; Collins and Maitland, 2006; Lawson *et al*, 2007).

Currently, the prostate stem cell phenotype remains unconfirmed. Identification of neural stem cells has been advanced by neurosphere culture (Rietze *et al*, 2001). When cultured in ultra-low adhesion dishes, neural stem cells will form nestin and $CD133^+$ neurospheres. However plating onto poly-L-ornithine coated glass coverslips causes differentiation into one of three lineages – neurons recognisable by β tubulin type III expression, astrocytes expressing glial fibrillary acidic protein or oligodendrocytes expressing platelet derived growth factor receptor-α. Secondary neurospheres can be derived from a proportion of single dissociated primary neurosphere cells, and this can be repeated through further generations (Gritti *et al*, 1996). Though 'sphere' formation is increasingly being reported, a distinction should be made between low-adherence culture that attempts to maintain cells in an undifferentiated state, and substances such as Matrigel™ that promote differentiation. There is evidence that human prostate epithelial cells will form spheres too in low-adherence culture, but none have been passaged as yet to confirm self-renewal (Gu *et al*, 2007; Miki *et al*, 2007;

Tokar *et al*, 2005). Using a differentiation assay, Lawson *et al* (2007) have shown that mouse prostate basal cells will form sphere-like structures when co-cultured with urogenital sinus mesenchyme in Matrigel™ and these can be passaged for six generations.

1.7 Summary of prostate epithelial markers.

Table 1.2 lists many of the markers discussed above. New markers for the epithelial components of the prostate are being identified continually.

Histological Location	Basal / sub-basal / intermediate	Basal epithelial		Luminal epithelial
Cell type	Stem cell	Transit Amplifying		Secretory luminal
Marker	$CD133^+$ $ABCG2^+$ $\alpha2\beta1^{Hi}$	$K14^+$ $K5^+$ $K15^+$ $K17^+$ $K19^+$ $p63^+$ $\alpha2\beta1^{Hi}$ $CD44^+$ $Bcl\text{-}2^+$ $ETS\text{-}2^+$ $pp32^+$, $Telomerase^+$ $GSTP1^+$ $Ki67^+$	$K8^+$ $K18^+$ $K5^+$ $K15^+$ $K17^+$ $K19^+$ $K7^+$ $CD44^+$ $PSCA^+$ $p63^+$	AR^+ PSA^+ $K8^+$ $K18^+$ PAP^+ PSA^+ $CPP32^+$ $CD57^+$ $p21^{Kip1+}$
	$p63^-$ $PSCA^-$ AR^- PSA^-	$CD133^-$ $ABCG2^-$ $PSCA^-$ AR^- PSA^- $p21^{Kip1-}$ $K8^-$ $K18^-$	$CD133^-$ $ABCG2^-$ $\alpha2\beta1^{Lo}$ $p63^-$ AR^- PSA^- $p21^{Kip1-}$	$CD133^-$ $ABCG2^-$ $\alpha2\beta1^{Lo}$ $p63^-$ $PSCA^-$ $K5^-$ $K14^-$

Table 1.2: Summary of cell marker expression by the different cell populations in normal human prostate epithelium.

1.8 The prostate in disease

1.8.1 Benign prostatic hyperplasia (BPH)

The prostate epithelium is prone to pathology. BPH is a histological diagnosis, and is detected at autopsy in 25% of men in their 40's rising to 85% of 80-year olds (Berry *et al*, 1984). Risk factors are aging, the presence of androgens and a positive family history (Lepor, 2004). The hyperplastic process occurs in both the stromal and epithelial compartments in the transition zone so tissue architecture remains largely normal. Enlargement may be diffuse or comprise of nodules of predominantly stromal or epithelial tissue or a mixture of both. Nodules in smaller prostates under 50g tend to be stromal suggesting that increased stromal activity secondarily triggers epithelial growth while epithelial nodules predominate in larger glands due to new budding and branching of ducts (McNeal, 1990).

BPH is associated with a mechanical bladder outflow obstruction and/or lower urinary tract symptoms such as reduced flow, incomplete bladder emptying and voiding at night. However it can be asymptomatic, and the link between prostate enlargement and morbidity is a complex one. On average symptoms gradually worsen over time, though the experiences of individual patients can vary and some men notice an improvement (Barry *et al*, 1997). Treatment amounts to lifestyle modification, α-adrenergic blocking drugs to relax bladder neck smooth muscle and 5α-reductase inhibitors to reduce intra-prostatic DHT levels and shrink the gland by 20-25%. Where medical therapy is insufficient, obstructing prostate tissue can be surgically removed by open, endoscopic or minimally invasive techniques (Desgrandchamps *et al*, 2006). Complications include urinary infections, bladder stones, acute urinary retention, haematuria and urinary incontinence. However these are rare events affecting about 5% of men (McConnell *et al*, 2003).

It has been proposed that BPH arises when stem cells within the adult prostate are somehow reawoken, resulting in the growth of new ducts to form an epithelial nodule (McNeal, 1978; Isaacs and Coffey, 1989). Alterations in the

normal homeostatic stromal–epithelial interactions seem likely to play a role. In the normal adult prostate, the stroma and epithelium are essentially growth-quiescent with rates of proliferation and cell death low and in balance. It appears that each tissue compartment keeps the other in check, as when both are cultured in isolation, their proliferative activity increases dramatically (Hayward and Cunha, 2000; Cunha *et al*, 2002). However, in dogs, androgen and oestrogen induced BPH is associated with reduced DNA synthesis suggesting that gland enlargement is due to decreased cell death rather than increased proliferation (Barrack and Berry, 1987). A number of growth factors are emerging that may alter the balance between cell proliferation and death, with the most likely candidate being keratinocyte growth factor (Lee and Peehl, 2004).

1.8.2 Prostate Adenocarcinoma

1.8.2.1 The natural history of prostate cancer

The aetiology of prostate cancer is not well understood, though a number of risk factors are recognised, such as increasing age, a positive family history, African-American ethnicity, and consumption of a Western diet (Grönberg, 2003). Incidence is highest in the US, Canada and Scandinavia and lowest in China and Asia, likely reflecting the above factors and also variations in healthcare availability and cancer registration (Quinn and Babb, 2002). There is also a significant amount of subclinical disease: the risk of having pathological evidence of prostate cancer in a 50 year old man is 42%, the risk of symptoms is 9.5%, and the risk of mortality 2.9% (Scher *et al*, 2004).

Prostate cancer usually grows slowly, progressing from localised and asymptomatic disease, to locally advanced and/or metastatic cancer following lymphatic and haematogenous spread. Locally advanced cancer may invade the urethra, bladder, pelvic nerves or pelvic lymph nodes. Metastatic cancer spreads to the axial skeleton or long bones, and soft tissues such as lung or liver (Kirby, 2000).

Current clinical practice is to observe men with low grade, low stage disease and an estimated life expectancy of less than 10 years. Others with clinically organ-confined disease may be offered active surveillance or radical prostatectomy, brachytherapy or external beam conformal radiotherapy with curative intent (Peschel and Colberg, 2003). For locally advanced or metastatic cancer, androgen withdrawal therapy offers symptomatic control, a delay in clinical progression (for a median of 18 months in metastatic disease) and possibly increased survival (Robinson *et al*, 1995). Ultimately, hormone independent cancer emerges and though second line therapies such as oestrogens or chemotherapy are used, at this stage the disease is usually fatal.

1.8.2.2 Histological changes in prostate cancer.

There is a continuum of histological changes seen within the prostate between benign and malignant states, and distinguishing some atypical lesions from early low-grade cancer is difficult. The identification of pre-malignant lesions within the prostate is hampered by the fact that abnormal areas cannot be followed over time as it is impossible to reliably rebiopsy them. High grade Prostatic Intraepithelial Neoplasia (PIN) is the most likely precursor of prostate carcinoma and is strongly predictive of coexistent carcinoma. Like cancer, it is multifocal, commonest in the peripheral zone and its incidence increases with age though epidemiologically it predates cancer by over five years, (Bostwick *et al*, 1995). Low grade PIN cannot be reproducibly recognised and no clinical significance is attached to it. High grade PIN is architecturally benign with normal duct morphology but cytologically atypical. The basement membrane is intact, though the basal cell layer may show some disruption while the luminal cells demonstrate cytologic features that mimic cancer such as nuclear and nucleolar enlargement, variable nuclear size, hyperchromasia, mitotic figures and multiple nucleoli.

More than 95% of prostate cancers are acinar adenocarcinoma and most are multifocal (DeMarzo *et al*, 2003). Architecturally cancer is defined by variable acinus sizes, haphazard directions of infiltration with displacement of stroma, back-to-back glands that share a basement membrane and increased cellularity.

Perineural invasion is also diagnostic. The basal cell layer is absent in prostate adenocarcinoma, such that negative staining for basal cell-specific cytokeratins using antibody, 34β-E12 is used to help confirm a suspected diagnosis of cancer (Allsbrook and Pfeifer, 1998).

The low-power architectural appearance also forms the basis of the grading of prostate cancer from 1 (least abnormal) to 5 (Gleason and Mellinger, 1974). Gleason grading accounts for the heterogeneity of prostate cancer by noting the two most common patterns by area, and is now widely accepted due to its simplicity, reproducibility and prognostic accuracy (Allsbrook *et al*, 2001).

Small cell carcinomas of the prostate make up 1–2% of all prostate malignancies and are thought to arise from the malignant transformation of NE cells. These tumours are negative for PAP and PSA and may arise *de novo* but more often do so after hormonal treatment of adenocarcinoma. They do not respond to hormonal withdrawal therapy and behave aggressively. Additionally most adenocarcinomas demonstrate some degree of focal NE differentiation (diSant'Agnese, 1992). It has been postulated that NE secretions promote carcinogenesis in adjacent cells. Also, being androgen independent they might be expected to persist despite androgen withdrawal, and their numbers do increase in hormonally treated and hormone-refractory prostate cancer. In such cancers, treatments directed at the NE cells may have a role in the future (Huang *et al*, 2007).

Stroma contains predominately smooth muscle cells and extracellular matrix, but stroma associated with prostate cancer is typically fibroblastic or myofibroblastic. Experimentally, such carcinoma-associated stroma induces cancers in the immortalized human prostatic epithelial cell line BPH-1, though not in normal epithelial cells. (Olumi *et al*, 1999). Thus it has been proposed that cancer initiating events within the epithelium result in altered stromal-epithelial signaling converting the normally repressive stroma into tissue that stimulates proliferation and carcinogenesis through paracrine means (Cunha *et al*, 2002). There is also evidence that unlike benign tissue, malignant prostate epithelium

becomes stimulated directly by androgens through autocrine mechanisms (Gao *et al*, 2001).

Despite these histological changes, prostate cancers in their early stages at least show a cellular and structural organization reminiscent of benign tissue. While stem cells maintain tissue growth in health, the concept of cancer stem cells that perform this role in tumours has long been suggested (McCulloch and Till, 1964).

1.9 Cancer stem cells and the stem cell model of cancer

There is good evidence for the existence of cancer stem cells, or tumour initiating cells in some cancers. Tumours have long been recognised as heterogeneous in terms of the differentiation of their constituent cells and their proliferative ability. For instance, no more than 0.01 to 1% of mouse myeloma cells will form colonies *in vitro* of which a small proportion showed 'self-renewal', in that they had the ability to be disaggregated and replated (Buick and Pollack, 1984). The reason for this may be that all tumour cells have equal but low proliferative abilities, or that a small subset of tumour cells possess all the proliferative ability (Houghton *et al*, 2007).

The latter has been shown to be true for acute myeloid leukaemia (AML) and for an increasing number of solid tumours. HSC are $CD34^{+}CD38^{-}$, while committed lymphoid precursors are $CD34^{+}CD38^{+}$. In acute myeloid leukaemia (AML), the only cells capable of inducing human AML in mice was a small population with the HSC phenotype, while the more differentiated $CD34^{+}CD38^{+}$ cells that looked cancerous, could not in most cases (Bonnet and Dick, 1997). Furthermore, these cells could be passed from animal to animal and maintain the AML phenotype confirming the property of self-renewal (Dick, 1996). In solid cancers, self-renewing tumourigenic human breast cancer cells have been sufficiently enriched so that as few as 200 $CD44^{+}/CD24^{-/low}$ tumour cells will consistently form tumours when injected into mouse mammary fat pads while 100,000 cells of other lineages do not. Such tumours have been harvested and passaged into

subsequent mice four times with no decrease in tumourigenicity (Al-Hajj *et al*, 2003). Using similar assays, the colorectal cancer stem cell is emerging as $CD44^{+}$/epithelial cell adhesion molecule $(EpCAM)^{high}$/$CD166^{+}$, the pancreatic cancer cell has been defined as $CD44^{+}$/$CD24^{+}$/epithelial-specific antigen $(ESA)^{+}$, human brain tumour stem cells are $CD133^{+}$/$nestin^{+}$ and CD44 defines a tumourigenic self-renewing population in head and neck cancers (Dalerba *et al*, 2007; Li *et al*, 2007; Singh *et al*, 2004; Prince *et al*, 2007).

Both cancer cells and stem cells have similar cellular properties. They possess limitless proliferative activity, can self-renew and are resistant to senescence and apoptosis (Hanahan and Weinberg, 2000). Tumour cells and tissue stem cells exploit many of the same pathways, such as Wnt, Notch and Sonic hedgehog, to give them the capacity for and self-renewal (Reya *et al*, 2001). The classic tumour suppressor gene p53, lost in >50% of human cancers, induces cell cycle arrest in the presence of DNA damage to allow repair or apoptosis but has also been implicated in the regulation of asymmetric stem cell divisions (Rambhatla *et al*, 2001). The transformation of a cell must therefore involve the acquisition (if not already possessed) and deregulation of stem cell properties.

As in epithelium, the bulk of the tumour is comprised of terminally differentiated cancer cells upon which histological diagnosis and prognostication is based. However the stem cell model of cancer states that tumour maintenance and expansion is driven by a few anonymous cancer stem cells. Frequently dividing cancer stem cells that favour self-renewal over generation of a TA cell will produce a rapidly growing tumour. As cancers progress, they tend to lose their normal tissue specific appearance and become 'less differentiated'. This may in reality reflect the expansion of the undifferentiated stem cell compartment (Mackillop *et al*, 1983, Mackillop *et al*, 1985). In addition, the differentiating daughter cancer stem cells may follow aberrant pathways to different lineages, resulting in heterogeneous phenotypes such as NE differentiation in prostate cancer, or squamous differentiation in bladder cancer.

This concept has far reaching implications. Studies of whole tumour tissues will identify the characteristics of the most predominant, terminally differentiated cells that are destined to die anyway, and shed no light on the most critical cells. A successful cancer treatment is judged on its ability to reduce the bulk of a tumour, however only a few cancer stem cells need survive for recurrence to be inevitable (Mackillop *et al*, 1983). This may also explain why small numbers of disseminated cancer cells can be detected throughout the body in patients who never develop metastases. The aim of treatment must be to identify and destroy the cancer stem cells. This will require isolation of cancer stem cells from the bulk of the tumour to allow prognostic markers and therapeutic targets to be found.

1.9.1 Stem cells as targets for malignant transformation.

The stem cell theory of cancer states that the carcinogenic process probably starts in a stem cell. Theoretically, the exact target for transformation into a cancer stem cell could be a stem, TA or terminally differentiated cell. Stem cells are thought to be the most likely candidates. They already have the machinery for self-renewal activated, so maintaining and deregulating this activation may require fewer mutations that turning it on *de novo* within a more differentiated cell (so called 'dedifferentiation', Buick and Pollack, 1984). In addition, carcinogenesis is a slow process that may take years or decades, and it is the stem cells within a tissue that persist long enough to accumulate the necessary mutations (Fearon and Vogelstein, 1990; Hanahan *et al*, 2000). The commonest five human cancers (skin, lung, colon, breast and prostate) all develop in stem cell derived tissues. Radiotherapy of skin cancers is successful with surprisingly low doses of radiation, but this is understandable if the stem cells are preferentially destroyed (Mackillop et al, 1983). There is also evidence that leukaemias arise from mutations harboured by HSC. In addition to the $CD34^{+}CD38^{-}$ AML cancer stem cell phenotype described above, other clonal markers such as the Philadelphia chromosome (9;22 chromosomal translocation) and isoenzymes of glucose-6-phosphate dehydrogenase have been found in multiple cell lineages in patients with AML (Reya *et al*, 2001).

Alternatively, since every mutation that occurs within the stem cell is passed onto its progeny. It is possible that a TA cell that has inherited several mutations, could accrue one more that allows it to self renew in its own right and make the final step towards transformation. An example of this mechanism occurring is again found in haematological cancers. The progeny of HSC include common myeloid progenitors, granulocyte-macrophage progenitors, and megakaryocyte-erythroid progenitors. In patients with chronic myeloid leukaemia, granulocyte-macrophage progenitors have been found to have higher expression levels of HSC self-renewal genes (β-catenin and LEF-1) than normal granulocyte-macrophage progenitors. Unlike these normal cells, CML granulocyte-macrophage progenitors also formed self-renewing, replatable myeloid colonies *in vitro*, behaviour suggestive of leukaemic stem cells (Jamieson *et al*, 2004).

The answer may be that all cells have the potential to transform, but will require different mutations to do so and the cell of origin will differ from case to case (Signoretti and Loda, 2007). It is also possible that malignant transformation alters gene expression sufficiently to distort lineage relationships entirely and that disordered stromal architecture alters the actions of the stem cell niche (MacKenzie, 2006). There is much that is unknown in this area, but it is likely that studies on cancer and on stem cells will increasingly share common ground.

1.10 Evidence for the prostate cancer stem cell.

It seems likely that in malignancy, the prostate tumour is still maintained as a stem cell structure. Like its benign counterpart, it remains heterogeneous in terms of keratin marker expression, differentiation and hormone responsiveness suggesting the presence of different cell populations. However the cancer stem cell model is most convincingly demonstrated by its response to treatment. Therapeutic androgen withdrawal causes luminal cell apoptosis, serum PSA reduction and shrinkage of the tumour mass. However some androgen independent epithelial and NE cells survive. Eventually, having acquired further mutations allowing them to recruit androgen independent growth pathways, the cancer stem cells proliferate in the absence of androgen, repopulate the tumour and PSA rises again.

1.10.1 The origin of the cancer stem cell

As in benign tissue, the origin, location and phenotype of the prostate cancer stem cell has been long sought, and remains equally unresolved. Several authors have nominated luminal cells (expressing K8, K18, PSA and AR), TA cells expressing intermediate keratins (K5 and K18) or as yet undefined normal stem cells. Their conclusions are based on the expression of markers seen in prostate cancer, although of course the phenotype of a few cancer stem cells may be difficult to discern amongst their massively more represented progeny.

The histological appearance of prostate cancer varies dramatically from that of normal prostate epithelium, most markedly due to the loss of the basal layer. PIN is widely accepted as a precursor to cancer, and the degree of basal layer disruption increases from low grade to high grade PIN (Bostwick and Brawer, 1987). Within PIN, proliferation of luminal cells increases dramatically, such that whereas in normal prostate 70% of proliferating cells are in the basal layer, in high grade PIN 90% of proliferation occurs in the luminal cells (Bonkhoff *et al*, 1994b). Expression of the apoptosis suppressing Bcl-2 oncoprotein mirrors the region of proliferation in high grade PIN which may extend the lifespan of these cells exposing them to further mutations. Telomerase expression is also seen (Paradis *et al*, 1999). The fact that the vast majority of prostate cancer cells demonstrate a luminal phenotype with PSA, AR, K8 and K18 has lead to the proposition that luminal cells transform into cancers (Bostwick and Brawer 1987).

In fact, *in vitro*, prostate cancer epithelial cells will express K5 and K14, and while basal cells are histologically absent, basal markers are expressed in cancer cells (Peehl, 2005). Based on cytokeratin expression, others contend that basally located, androgen independent, intermediate cells undergo carcinogenesis (Isaacs and Coffey, 1989; Bui and Reiter, 1999; van Leenders *et al*, 2001; van Leenders and Schalken, 2001; Schalken and van Leenders, 2003; Kellogg-Parsons *et al*, 2001, Nagle *et al*, 1987). De Marzo *et al* (1998b) alternatively suggest that the intermediate cells in question reside in the luminal layer. Verhagen *et al* (1992) failed to identify any K14 expressing cells in primary and hormone independent

cancers but did identify $K5^+$ cells in 25-35% of primary cancers and 10-15% of hormone independent cancers, while K19 was commoner in 50-75% and 25-90% of cells respectively, and all cancers stained for K18. Another analysis confirmed co-expression of both keratins in androgen treated cancers, but found a reversed trend, towards a more basal K5 phenotype in more advanced cancers (Gil-Diez de Medina *et al*, 1998). A similar trend was noted by Lui and colleagues (1999, 2002) who found that while primary cancers predominately expressed a luminal cell marker CD57, advanced cancers and metastases expressed more CD44. Nagle *et al* (1987) also reported a luminal phenotype in localised prostate cancer, but found this persisted in metastatic prostate cancer cell lines. A study of 56 prostate cancer metastases identified K18 in 100% and K5 expression that ranged from 29% in untreated cancers, to 75% after androgen withdrawal, and 57% of hormone escaped cancers (van Leenders *et al*, 2001).

The normal stem cell was implicated by Bonkhoff on the basis of androgen insensitivity and that the increased prevalence of post-mitotic NE cells in advancing cancers are derived from the pluripotent stem cell (1996, 1994a). Additionally, basal cell markers such as Bcl-2 and telomerase are increasingly overexpressed in PIN and prostate cancer (McDonnell *et al*, 1992; Paradis *et al*, 1999). Overall, it seems that categorizing prostate cancer cells as basal or secretory is too simplistic, and other markers will identify the cancer stem cell.

As increasing numbers of stem cell markers are identified in other tissues, more recent research has hypothesised that these might equally apply to the malignant prostate stem cell. Experience in malignant and benign stem cells from skin has shown the expression of similar markers, while malignant and benign breast and neural stem cells will both grow in suspension culture, suggesting similarities are retained despite transformation (Mackenzie, 2006). However, studies so far have shown disagreement with the benign prostate stem cell phenotype as it is understood currently.

Sca-1 has been proposed as a stem cell marker in the murine prostate. Xin *et al* (2005) managed to make Sca-1^+ cells tumourigenic using transfection of a lentiviral vector to activate their PTEN/AKT1 signalling pathway, which has

been strongly correlated with prostate carcinogenesis. When cultured with urogenital sinus mesenchyme under mouse renal capsules, such cells produced cancerous glands expressing intermediate cytokeratin. However histology alone was the determinant of malignancy and no self-renewal was studied in the structures. Ultimately, though it may be possible to transform such a cell with a viral vector, this does not mean that this is the mechanism whereby cancer arises *in vivo*. p63 is not expressed in human prostate cancer, so might be expected to be absent in these 'cancers' though its expression in murine prostate cancer is unknown (Kellogg Parsons *et al*, 2001; Wang *et al*, 2006). In benign mouse prostates, p63 is a basal cell (but not stem cell) marker (Kurita *et al* 2004).

The same group subsequently studied cytokeratin and stem cell marker expression in the Pten-null prostate cancer model (Wang *et al*, 2006). These mice progress from prostate hyperplasia at four weeks, through PIN and cancer to metastases at twelve weeks. During this process, an increase in basal layer $K5^+p63^+$ cells was seen and there was an even greater proliferation of intermediate K5 and K8 expressing cells. Sca-1 seemed to segregate to the basal cells, while Bcl-2 was expressed by the more proliferative intermediate cells. Both these populations were proposed as candidates for the tumour initiating cells, but again this work in genetically manipulated mice may not translate well to human prostate carcinogenesis.

Patrawala *et al* (2005) isolated the Hoechst 33342 excluding side population of cells derived from a human prostate tumour xenograft (Klein *et al*, 1997). Comprising 0.07% of the total cells, side population cells were 100-fold more tumourigenic *in vivo*, than non-side population cells. ABCG2 was more expressed in the side population, however when all cells were sorted for ABCG2 expression, there was no difference in tumourigenicity between positive and negative cells. When injected into mice, $ABCG2^-$ cells produced tumours predominantly containing $ABCG2^+$ cells suggesting differentiation from a stem cell to TA phenotype, and $ABCG2^+$ derived tumours were also predominantly $ABCG2^+$ though these cells could also generate a few $ABCG2^-$ cells. $ABCG2^-$ cells also expressed higher levels of 'stemness' genes Notch-1, β-catenin and Oct-4 (an embryonic and adult stem cell transcription factor).

The heterogeneity of the side population has been recognised before, and side population cells may express other ABC transporters than the G2 isotype accounting for the $ABCG2^-$ cells within it. However, in benign tissue $ABCG2^+$ cells have been proposed as stem cells, whereas $ABCG2^-$ cells behave more like cancer stem cells in this study. The differing findings of Huss *et al*, (2005) and Bhatt *et al* (2003) suggest that these markers have more complex associations in benign tissue, and this seems no less true in malignancy.

The same group then performed very similar assays on $CD44^+$ cells with more straightforward results (Patrawala *et al*, 2006). The $CD44^+$ fraction of prostate cancer cell lines and human prostate cancer xenografts exceeded the $CD44^-$ cells in terms of clonogenicity, tumourigenicity and local tumour invasion. They also expressed higher levels of stem cell genes Notch-1, β-catenin, Oct-4 and Bmi1. Finally *in vitro* and *in vivo*, they differentiated into $CD44^-$ cells and expressed AR. Thus while not a pure population, CD44 does seem to enrich for prostate cancer stem cells.

Next they turned their attention to α2β1 integrin expression in the same cells (Patrawala *et al*, 2007). *In vitro* $\alpha2\beta1^{+/Hi}$ cells were more clonogenic than negative cells, however when cells were injected orthotopically into mouse dorsal prostate, no greater tumourigenicity – the gold standard test for the cancer stem cell – was seen between the two fractions. Co-localization immunohistochemistry showed that 70-80% of cells expressed both α2β1 and CD44, and all ABCG2 cells stained for these two markers. They devised a tumourigenic hierarchy with $CD44^+\alpha2\beta1^{+/Hi}$ and $CD44^+$ $\alpha2\beta1^{-/Lo}$ fractions being most tumourigenic, and $CD44^-$ $\alpha2\beta1^{-/Lo}$ cells the least.

Proof of principle of the prostate cancer stem cell has been demonstrated using human telomerase reverse transcriptase (hTERT)-immortalized primary prostate epithelial cells from radical prostatectomy specimens (Gu *et al*, 2007). A single transformed cell was able to establish an indefinitely proliferative cell line, which expressed stem cell (Oct4) and early progenitor cell markers (CD133, CD44). These cells grew spheres in low adherence culture, glandular structures in

Matrigel and recapitulated the tumour histology in mice complete with basal, luminal and neuroendocrine cells (though these tumours were not passaged on). As the authors recognized, immortalization is not equivalent to cancer stem cell isolation, but it confirms the potential of such cells.

Finally Collins *et al* (2005) applied their experience from benign stem cells to prospectively isolate cancer stem cells from primary localised and metastatic prostate cancer tissue. All the tumours contained between 0.1 and 0.3% of $CD133^+$ cells. In colony forming assays, primary cultured $CD44^+\alpha2\beta1^{+/Hi}$ $CD133^+$ cells represented the most clonogenic fraction, and uniquely, these colonies also formed secondary colonies when replated. These cells from tumours also showed greater proliferation in culture than similar benign cells (managing 25 population doublings compared to $\approx$12). When in differentiation promoting culture, the $CD44^+\alpha2\beta1^{+/Hi}$ $CD133^+$ cells regenerated phenotypically mixed populations of nonclonogenic cells expressing AR and PAP.

Collins *et al* (2005) also attempted to confirm the malignant nature of their histologically selected cancer cells. Cancer cells and cell lines demonstrated invasion in an invasion assay, while benign cells and a benign cell line did not. The cancer cells also grew better in semisolid methylcellulose. Genotype comparisons did not demonstrate mutations in all tumours though detected some microsatellite instability in two of six compared to the patients' lymphocyte DNA (but not benign tissue from the same prostate). $CD133^+$ basal cells were nominated as the likely source of prostate cancer.

Though this work is singular in its use of primary cancer cells it has been criticized for its lack of *in vivo* assays, which as shown above can result in different cellular behaviours (Patrawala *et al*, 2007). Litvinov *et al* (2006) have also questioned the low calcium culture medium used for the cancer cells, which according to their work promotes benign cell growth. They suggested p63 negativity as a useful discriminator of benign or malignant cells.

The target cell for transformation is still unknown, and will likely have to await definitive isolation of the prostate cancer stem cell. A number of candidate

markers are under investigation, and though none have demonstrated transplantable tumourigenicity, considerable enrichment is being achieved. Current markers exclude >99% of terminally differentiated or TA cells which should allow a closer inspection of stem cell gene expression through microarray analysis to identify novel therapeutic targets. The identification of the prostate cancer stem cell is a priority. Current therapies eradicate the bulk of the tumour, but cannot prevent the emergence of incurable androgen-independent disease. To achieve cure, treatments must selectively target cancer stem cells, either to kill them, or drive them towards differentiation and senescence, as a form of 'differentiation therapy' (Cunha, 1994). Unlike many other cancers in stem cell tissues, any treatment targeted against the prostate would have to be organ specific, but need not be cancer specific. Complete obliteration of all prostate stem cells and thus the entire prostate is not life threatening, and would be preferable to death from metastatic disease.

1.11 The aims of this project

Study of the prostate epithelium should focus on the small population of proliferative and regenerative cells rather than the heterogeneous whole. Techniques of *in vitro* culture already select for androgen independent epithelial cells and against stromal cells by using a feeder layer and excluding androgens (Freshney, 2002a). Hudson *et al* (2000) reported that the cells that can grow generate two different colony types, demonstrating clearly that in culture, prostate epithelial cells still represent a heterogeneous population. The aim of this project was to study and compare the cells within these two colony types both from benign and malignant prostate tissues.

Stem cells and TA cells are both highly proliferative, but differ in their self-renewal abilities. While colony-forming assays are still used as a measure of the proliferative ability of a cell population, no studies have further refined on the heterogeneity of the colonies. Yet, the study of these two more homogeneous cell populations that self-segregate according to colony type represents an opportunity to better unravel the nature of stem cells and their immediate progeny (albeit retrospectively). Studying such segregation also promises to be

more biologically meaningful than sorting cells for a speculative marker, as colony morphology depends on the very characteristics in question – the proliferation and differentiation of the constituent cells.

Hudson *et al* (2000) postulated that type I colonies derived from the clonal expansion of a TA cell, while type II colonies were stem cell derived. Working from this hypothesis, each colony type was assessed for various stem cell attributes with the lack of them being TA cell attributes. Additionally, their gene expression profiles were compared using cDNA microarrays.

It was also hypothesized that the stem cell model of cancer applied in prostate tissue. Thus is was proposed that low-density culture of prostate cancer tissue would also demonstrate the proliferative heterogeneity of two colony types derived from putative stem and TA cells. Parallel cultures of benign and malignant tissue were compared, but further analysis of the differences between their colonies was confounded by difficulties in confirming the malignant nature of early prostate cancer cells in culture. The outcomes of these enquiries are reported below.

CHAPTER 2:
MATERIALS AND METHODS

2.1 Culture media

2.1.1 Prostate Epithelial Growth Medium (PrEGM)

PrEGM, a selective medium with appropriate growth factors was used to preferentially culture primary prostate epithelial cells. Serum was excluded to eliminate transforming and platelet-derived growth factors that favour stromal cells (Freshney, 2002a). Nine aliquots of additives of unknown concentration (PrEGM™ SingleQuots®) were added to 500ml flask of PrEBM (Cambrex Bio Science Ltd, Wokingham, UK). These were 2ml bovine pituitary extract, 0.5ml transferrin, 0.5ml insulin (bovine), 0.5ml tri-iodothyronine, 0.5ml human recombinant epidermal growth factor, 0.5ml retinoic acid, 0.5ml epinephrine, 0.5ml GA-1000 (gentamycin, amphotericin B) and 0.5ml hydrocortisone. This medium was thus serum and androgen free and low in calcium (i.e. <300μmol/L Ca^{2+}).

2.1.2 Dulbecco's Modified Eagle's medium (DMEM)

For culture of 3T6 mouse fibroblasts, DMEM (Gibco BRL, Paisley, U.K.) was supplemented with 8% foetal calf serum (FCS, Sigma-Aldrich Company Ltd, Gillingham, UK).

2.1.3 Tissue Collecting Medium

Human prostate tissue was transferred from the operating theatre to the laboratory at room temperature in sterile tissue collecting medium consisting of RPMI-1640 medium (Life Technologies, Paisley, UK) supplemented with 20mmol/l HEPES (Sigma Chemical Co., Poole, UK). 8% FCS, penicillin (100U/ml), streptomycin (100μg/ml), fungizone (Amphotericin B, 25μg/ml) and 2mmol/l L-glutamine (all from Life Technologies). 0.48g of HEPES per 100ml collecting medium was dissolved in 10ml RPMI, then filter sterilized and added to the complete medium.

2.1.4 Conditioned medium

Conditioned PrEGM culture medium was derived from flasks of irradiated or mitomycin C treated mouse 3T6 fibroblast feeder cells at intervals of 2, 3 and 4 days of culture. After defrosting (see section 2.3), feeder cells were plated out in DMEM with 8% FCS and incubated overnight at 37°C. The following day, the layer of adherent feeder cells was washed 3 times with PBS, then re-fed with PrEGM medium. This medium was pipetted off the feeder layer at intervals for up to 9 days after which the feeders were discarded. The conditioned PrEGM medium was centrifuged at 1000rpm for 5 minutes to remove cell debris then filter sterilized prior to use. Aliquots were frozen at -80°C. pH was measured with a Hanna pH meter from Sigma-Aldrich.

2.1.5 Collagenase solution

200IU/ml concentration of collagenase was obtained from desiccated type 1A collagenase powder, (Sigma-Aldrich, stored at -20°C) dissolved in collecting medium with low dose antibiotics penicillin (10U/ml), streptomycin (10µg/ml) and fungizone (Amphotericin B, 2.5µg/ml) or RPMI and 8% FCS, and filter sterilized. At least 7.5ml of solution was required for 1g of tissue.

2.2 Tissue Culture

All cells were cultured in a humidified incubator at 37°C in 5% CO_2. Media was changed aseptically three times a week. Cells were grown initially on 6cm diameter Nunclon™ surface treated polystyrene dishes, then subsequently on similarly treated polystyrene flasks (Nunc, A/S, Denmark). All flasks were collagen coated with sterile rat-tail collagen type 1 (Vitrogen 100; Imperial Laboratories, Andover, UK) diluted in PBS (Gibco, Invitrogen Ltd., Paisley, UK) to 10µg/ml. Tissue culture flasks containing sufficient collagen solution to cover the base were incubated at 37°C for at least 1 hour. The excess collagen solution was aspirated prior to use.

2.3 Preparation of mouse 3T6 fibroblast feeder cell layer.

Feeder cell stocks were stored in 10% dimethylsulphoxide (DMSO, Sigma) at -80°C for use within a month, or at -180°C in liquid nitrogen for longer storage. Defrosted cells were immediately resuspended in DMEM with 8% FCS, and centrifuged once at 1000rpm for 5 minutes and the supernatant aspirated to remove the DMSO. Feeder cells were plated in DMEM with 8% FCS at densities of 750,000–1 million cells per 25cm^2 and incubated overnight at 37°C. Prior to seeding with prostate epithelial cells, the feeder cell layer was washed 3 times with PBS, then re-fed with PrEGM medium.

3T6 feeder cells were treated with either 40 Gray of radiation or mitomycin C to obtain viable, metabolically active, non-dividing cells. For irradiated feeders, 12 175cm^2 confluent flasks of 3T6 cells were harvested into a 30ml 'universal' tube (Sterilin Polystyrene tube, Barloworld Scientific, Stone, UK) which was irradiated on ice (40 Gray at 2.5Gy/min) for 16 minutes. The cells were then centrifuged at 1000rpm for 5 minutes, resuspended in FCS with 10% DMSO and counted. Aliquots of 20x10^6 cells were stored in 1ml cryotubes (Nunc) in liquid nitrogen at -180°C after initial cooling at -20°C overnight.

Mitomycin treatment of 3T6 cells was performed on nine 80% confluent 175cm^2 culture flasks. Mitomycin C (Sigma) was dissolved in PBS to a concentration of 200µg/ml. 1.1ml of this solution in 21ml of DMEM with FCS was added to each 175cm^2 flask, which were then incubated at 37°C for 2-3 hours. For smaller 25cm^2 flasks, 150µl of Mitomycin C solution was added to 3ml of DMEM with FCS. After incubation, the flasks were washed 3 times with PBS and the cells were harvested and counted. Aliquots of 20x10^6 cells were stored in FCS with 10% DMSO in liquid nitrogen.

2.4 Acquisition of prostate tissue

2.4.1 Acquisition of benign hyperplastic prostate tissue

Full ethical approval for the project design and patient information and consent forms was obtained from the ethical committees of the institutions from where specimens were obtained (University College Hospital, Ref 01/0094, The London Clinic, Harley Street, London). Men due to undergo prostate tissue resection were approached preoperatively and asked for consent (see Appendix A for consent forms). Exclusion criteria were treatment with 5α-reductase inhibitors or a previous diagnosis of, treatment of or a high clinical suspicion of prostate cancer. If consent was given, 3-6 large, non-charred prostate chips comprising no more than 10% of resected tissue were selected and transported in sterile collecting medium for immediate processing.

2.4.2 Acquisition of paired malignant and benign prostate tissue samples.

Full ethical approval was obtained from the ethical committees of the institutions from where specimens were obtained (University College Hospital, Ref 01/0094, The London Clinic, Harley Street). Men with biopsy proven prostate cancer who had elected to undergo a radical prostatectomy were approached preoperatively and invited to participate in the research project. Those patients in whom pre-operative biopsies suggested involvement of a large number of cores on one side of the prostate were selected to maximise the likelihood of a large area of cancer to sample. Where consent was given, the freshly excised prostate was immediately transported whole in sterile collecting medium from the operating theatre to the Histopathologist. The prostate was cut into several saggital sections and for earlier patients inked on its external surface. These cut surfaces were then inspected for any abnormal areas using the information from the digital rectal examination, biopsy and any prostate imaging to guide the site of tissue sampling. Small samples of cancer and benign tissue were excised from the peripheral zone using a sterile scalpel. These samples were processed in parallel as soon as possible while the rest of the prostate was fixed in 10% formalin for routine histological processing. Fixed haematoxylin and eosin (H&E) stained wholemount slides from the level of the prostate where tissue was taken were assessed by the Histopathologist and areas of cancer demarcated. Usually a defect was visible, indicating the site of fresh tissue sampling. These slides gave an early indication of the degree of success with which areas of cancer and benign tissue had been selected in the fresh prostate.

2.5 Processing Prostate Tissue

All prostate tissue whether derived from trans-urethral resection of the prostate (TURP) or radical prostatectomy specimens was handled similarly. In a laminar flow hood, tissue was washed 3 times with PBS to remove adherent blood cells, any charred areas of BPH were trimmed and the remaining tissue was weighed. After addition of 0.5ml collagenase solution, the tissue was minced into <1mm diameter pieces using fine scissors on a sterile culture plate resting on ice. These pieces were transferred to a 30ml universal container, resuspended in PBS and allowed to sediment for 5 minutes. The cloudy supernatant was aspirated and the step repeated until the supernatant was clear. The tissue was then digested with collagenase solution (7.5mls of 200U/ml per gram of tissue) to separate stromal cells from the still intact epithelial acini over 16 hours on a moving platform at 37°C.

After digestion, the tissue 'broth' was passed 10 times through a wide bore needle to produce a single cell suspension. This represented a modification of the protocol described by Hudson *et al* (2001), which used two brief 20-second centrifugations of the broth then a 30-minute trypsin digestion step to separate acini into single cells. This modification was motivated by a wish to preserve cell membrane proteins for potential applications such as cell sorting. The digested tissue broth was centrifuged at 1500rpm for 20 minutes; the cells were washed once in PBS, then were centrifuged for a further 20 minutes. Finally the cell pellet was resuspended in PrEGM and a 100µl sample, diluted 1:1 with 0.1% trypan blue to identify viable cells (Cambrex Bio Science Ltd, Wokingham, UK) was counted using a haemocytometer. Red blood cells, distinguishable by their biconcave shape were disregarded. The cells were plated at 10^3 cells/25cm^2 onto collagen-coated flasks with a 3T6 fibroblast feeder layer in PrEGM. Colonies became visible from day 6, and cells were cultured for 2 weeks.

2.6 Sampling Type I or Type II prostate epithelial colonies.

At two weeks, flasks were scored for colony number and type. The plated epithelial cells show proliferative heterogeneity, such that clonal expansion of a single cell

results in two distinct colony morphologies, as described by Hudson *et al* (2001). The characteristics of these colonies are as shown in Table 2.1, and colonies were typed accordingly under direct vision or x10 low power magnification (though immunocytochemistry was not performed). On the few occasions where a colony was difficult to type or appeared to have merged with another, the colony was not harvested.

The colony cell density was measured by placing the flask on a clear acetate grid colony on the microscope stage. For cell number, the density of cells was squared, and multiplied by the number of grid squares under the colony. Using cell number, the number of doublings was calculated from its $\log^2$ and rounded up.

	Type 1 colony	Type 2 colony
Size	Small (max 4mm) up to 8500 cells (5 –12 doublings)	Larger (≥3mm) 8000 – 40,000 cells (12-14 doublings)
Density	Loosely packed (<30cells/mm)	Denser (30 – 50 cells/mm)
Frequency	90%	10%
Outline	Irregular	Regular
Immunocytochemistry	K8 or K8 & K14	K14 only

Table 2.1: Characteristics of BPH derived type I and type II prostate epithelial colonies after two weeks in culture.

Colonies were harvested either by ring cloning, scraping with a cell scraper (Nunc) and immediate aspiration off the plate (see below) or by trypsinization of flasks in which all colonies of one type were first scraped up and washed off with PBS three times leaving only the other type of colonies for collection.

2.6.1 Ring cloning of colonies.

The top surface of a culture flask containing colonies for harvesting was removed with a hot scalpel, and the flask washed three times with PBS leaving only a thin layer of PBS. Rings were cut with a hot scalpel from the sterile threaded top of a 7ml 'bijou' tube (Sterilin Polystyrene tube, Barloworld Scientific) or 30ml universal tube depending on the size of the colony to be cloned. Using forceps, one ring edge was

coated with sterilized silicon vacuum grease (Dow Corning®, GBR Technology Ltd, Reading, UK) and this was pressed to obtain a water-tight seal onto the surface of the culture flask, centred over the colony. Fifty to 100µl of 0.25% trypsin/versene in buffered saline (Invitrogen) was added into the ring and cells were incubated within the laminar flow hood at room temperature for 3-5 minutes until the cells had rounded up and aggregated in the centre of the ring. Cells were then repeatedly flushed off the flask with PBS and pipetted into a sterile 15ml centrifuge tube (CLP Ltd, Northampton, UK). The tube was centrifuged at 1000rpm for 5 minutes and the trypsin containing supernatant aspirated off. The pellet was resuspended in PrEGM and the cells counted then transferred to a new collagen coated culture flask or into Matrigel™.

2.6.2 Harvesting of passaged colonies for RNA extraction.

Individual ring cloned colonies were transferred into collagen coated 25cm^2 tissue culture flasks with a feeder layer. Cells were expanded in culture for 1 to 2 weeks prior to harvesting, counting and RNA extraction. Cells were harvested when approximately 75% confluent by eye, while they were actively dividing, rather than when confluent which would trigger a change in gene expression. At harvesting, any remaining adherent feeder cells were first rinsed off with a brief trypsin solution incubation followed by three PBS washes. The still adherent prostate epithelial cells were then incubated in 1ml of trypsin solution at 37°C until detached. The cells were transferred to a 15ml centrifuge tube, centrifuged at 1000rpm for 5 minutes and the pellet was then resuspended in PBS for counting prior to RNA extraction.

2.6.3 Harvesting of single or multiple colonies for RNA extraction.

Where DNA or RNA from a single type II colony was required, the top of the flask was removed using a hot scalpel and all other colonies were scraped off. The remaining colony was harvested using trypsin solution, and the cells suspended in PBS. The cells were counted and 90% were allocated for DNA extraction and 10% for RNA extraction. These latter cells were centrifuged at 1000rpm for 5 minutes and the cell pellet resuspended in 1ml RLT buffer (a highly denaturing guanidine

isothiocyanate containing lysis buffer, Qiagen Ltd, Crawley, UK) prior to RNA extraction.

Colonies were closely adherent to the plastic and colonies of different types often grew close together. Where multiple colonies of one type were to be harvested together, a vacuum device was used to allow harvesting of selected colonies under x4 magnification (figure 2.1).

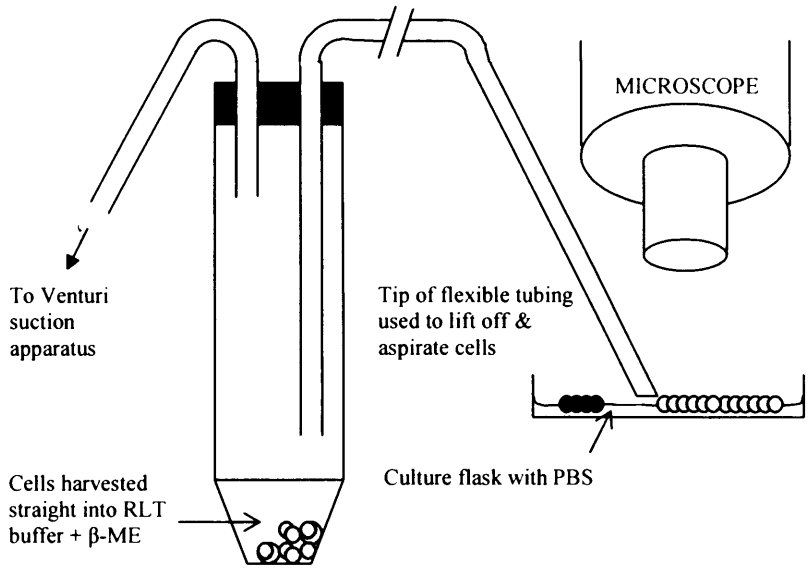

Figure 2.1: Apparatus for selective harvesting of type I or type II colonies for total RNA extraction.

The top surface of the flask to be harvested was removed, and the colonies washed three times with PBS leaving a thin layer of PBS. Colonies were selected and areas containing each type were segregated using a liquid repellent 'PAP' pen (Invitrogen) on the base of the flask. This prevented the thin layer of PBS flowing beyond the marked boundaries. Under x10 magnification, type I colonies were first elevated off the plastic surface using the sterile bevelled tip of some sterile flexible, 1mm diameter PTFE tubing (Extruded Plastics Ltd, Macclesfield, UK); and immediately aspirated with the PBS into an RNAse-free 15ml centrifuge tube (CLP Ltd). The amount of fluid aspirated with the cells was kept as low as possible to avoid

excessive dilution of RNA prior to extraction. Cells were aspirated straight into RLT buffer containing 1% 14.3M β-mercaptoethanol (Sigma Chemicals). The ratio of cell aspirate to RLT buffer was kept below 1:3.5 (personal communication, Qiagen helpdesk). After all type I colonies were harvested, the flask was washed a further three times with PBS, and type II colonies were similarly harvested into a new container. Not all colonies in a flask were harvested, as overlapping or inaccessible colonies were sacrificed.

2.7 Three dimensional culture in Matrigel™

Matrigel™ basement membrane matrix is a solubilized basement membrane preparation derived from mouse sarcoma. It contains laminin, collagen IV, heparan sulfate proteoglycan, entactin and fibroblast growth factor, TGF-beta, tissue plasminogen activator and other growth factors. 1ml of Matrigel™ (Promega, Southampton, UK.) was defrosted overnight at 4°C, mixed with 1ml of chilled PrEGM on ice, and then 200µl aliquots were pipetted into a 24 well plate. The solution solidified after 30 minutes at 37°C, and a further 1ml of PrEGM was carefully pipetted onto the Matrigel. 10,000 pooled type I or type II colony cells were added onto the Matrigel and cultured at 37°C for 14 days prior to harvesting, fixation and paraffin embedding for immunohistochemistry. Photographs of the structures obtained were taken at intervals using a microscope mounted Nikon Coolpix 995 digital camera.

2.8 Preparation of histological sections.

The tissue or cells for sectioning were wrapped in tissue paper inside a plastic fenestrated cassette and soaked overnight in 10% formaldehyde (VWR International Ltd, Poole, UK). It was next dehydrated over 24 hours in 70% ethanol, and then embedded in paraffin. The chilled paraffin block was sliced with a microtome into 4µm sections using a microtome which were mounted on glass microscope slides at 40°C and incubated at 60°C for 20 minutes to attach the specimen to the slide.

Flasks with colonies were fixed and permeabilized for staining. After aspiration of the culture medium and two PBS washes, 5ml of chilled 1:1 Methanol:Acetone (VWR International Ltd) were added to the flasks on ice for 10 minutes. Flasks were washed a further two times before staining. Colonies were stained with Rhodanile blue (Sigma-Aldrich Company Ltd, Gillingham, UK) by immersing them in the dye at room temperature for five minutes, then rinsing with tap water and leaving to air dry.

2.9 Immunohistochemistry

The primary antibodies used are given in table 2.2. Unlabelled primary antibodies were detected with an immunoperoxidase method using a standard avidin-biotin-complex kit (Vectorstain Elite ABC kit, Vector Laboratories, Peterborough, UK). Antibody binding was visualized using 3,3'-diaminobenzidine tetrahydrochloride (DAB; DAB substrate kit for peroxidase, Vector Laboratories).

Paraffin-embedded sections were de-waxed in xylene (VWR International Ltd, two times 3 minutes) then were rehydrated in 100%, 70% and 70% alcohol for 1 minute each and then rinsed in distilled water. Formalin fixation involves the formation of cross-links between molecules that alter the structure of proteins and affect their recognition by antibodies (Macintyre, 2001). Reversal of this process, so called antigen retrieval was performed by microwaving in 1600ml of boiling distilled water containing 15ml citrate-based antigen unmasking solution, (Vector Laboratories) for 30 minutes, then washing twice in PBS. Thereafter both fixed culture dishes and paraffin-embedded sections were treated similarly.

Endogenous peroxidase was quenched by incubating cells with 0.3% peroxide in 70% methanol for 30 minutes. After two 5 minute PBS washes non-specific protein binding was blocked using 1.5% normal horse serum in PBS for 20 minutes. The primary antibody diluted as required in 0.1% bovine serum albumin in PBS was then applied to the sections for 1 hour at room temperature. After three 5 minute PBS washes, 100µl of biotinylated secondary antibody (horse anti-mouse IgG diluted 1:100 in 1.5% normal horse serum in PBS) was added to the sections and incubated for 30 minutes. Following three further 5-minute PBS washes, the sections were

incubated in Vectastain ABC reagent (an avidin and biotinylated horseradish peroxidase macromolecular complex) for 30 minutes then washed twice more. Finally 100µl DAB peroxidase substrate solution was added to the slides for 10 minutes, which resulted in the release of oxygen, which then combines with DAB to form a brown end product.

The sections were counterstained in Mayer's haematoxylin for about 10 seconds, washed then dehydrated in 70%, 70% and 100% alcohol each for 1 minute, then twice in xylene. Coverslips mounted on DPX (Merck) were set, then allowed to dry.

Antigen	Clone	Species	Isotype	Dilution	Source
Androgen Receptor	MU256-UC	mouse	IgG1	1:250	Affinity Biogenex[1]
K14	LL002	mouse	IgG3	1:10	Gift from EB Lane
K8	35bH11	mouse	IgM	1:40	Dako[2]
AC133	AC133	mouse	IgG1	1:100	Miltenyi Biotec[3]
K5,K6 & K18	LP34	mouse	IgG1	1:10	Dako[2]

[1]Affinity Biogenex, Launch Diagnostics Ltd, Kent, UK; [2]Dako UK Ltd, Cambs, UK; [3]Miltenyi Biotec GmbH, 51429 Bergisch Gladbach, Germany.

Table 2.2: Antibody Reagents

2.10 Genomic DNA extraction from large and small tissue samples.

Genomic DNA was obtained from a number of tissue sources. Histologically confirmed malignant and benign areas of the paraffin-embedded radical prostatectomy specimen were sampled either by scraping cells with a sterile scalpel blade off sections using a drop of 100% alcohol on the slide, or by taking thin cores of the paraffin block from within the cancer / benign areas with a 5mm skin biopsy punch (Stiefel Laboratorium, Offenbach am Main, Germany). Often a defect was visible, indicating the site of fresh tissue sampling, so cells immediately adjacent were harvested as a source of corresponding DNA. Baseline normal benign DNA from the same patient was obtained from paraffin embedded negative lymph node samples as cores of the paraffin block (see figure 2.2).

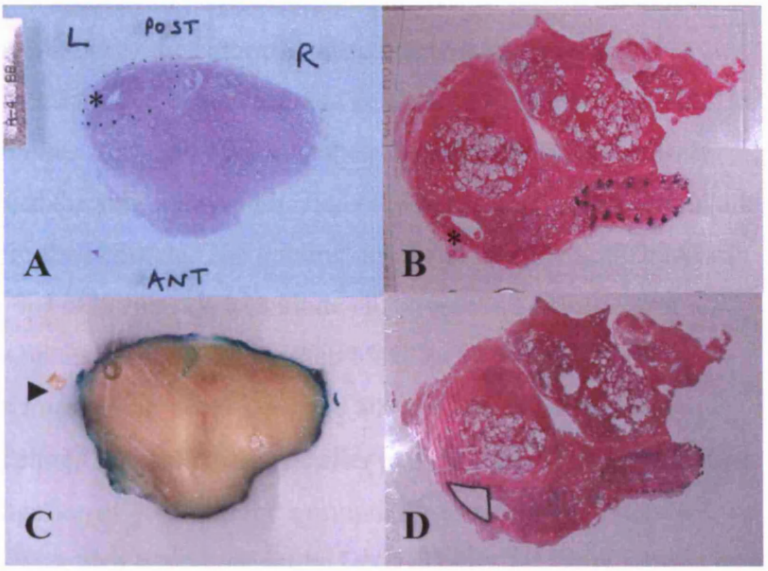

Figure 2.2: Sourcing DNA from the prostate blocks. **A** shows a haematoxylin and eosin stained section from the paraffin embedded prostate block shown in **C**. The histologically confirmed focus of cancer was marked on slide A with the defect due to fresh tissue sampling visible within it (*). A core of the cancer focus in the paraffin block was taken and DNA extracted (►). It was hypothesized that colonies derived from the fresh cancer tissue would show the same genotype as those from the original cancer focus. **B** shows a wholemount slide with a defect at the site of benign tissue sampling (*). In **D**, adjacent tissue has been scraped off to obtain representative 'benign' DNA.

DNA was obtained from colonies derived from fresh tissue by scraping the whole colony using a scalpel blade for fixed cells or a 200µl Gilson pipette tip for cells where the medium had just been removed. Larger, denser type II colonies were harvested preferentially when available. Cell line DNA was obtained from near confluent flasks of cells that were trypsinized, removed from the flask then centrifuged into a cell pellet for DNA extraction.

For paraffin embedded tissue samples the Qiagen DNeasy™ kit was used to lyse cells and bind DNA to a silicone membrane, from which proteins and divalent cations are washed before eluting DNA as 30-50kb fragments. Paraffin embedded samples were incubated overnight with 180µl of buffer ATL (an enzymatic buffer containing sodium dodecyl sulphate) and 20µl of proteinase K in eppendorfs at 55°C in a humidified chamber to chemically and enzymatically lyse connective tissue. Subsequently, 200µl of buffer AL, a chaotropic salt was added which dehydrated the DNA to optimise binding of the exposed negatively charged phosphate backbone to

the positive silicon membrane of the column. It also inactivated proteins and carbohydrates in the solution. The eppendorf was vortexed and incubated at 70°C in a water bath for 10 minutes. 200µl of 100% ethanol was then added, to further dehydrate the DNA, and the solution was pipetted onto the DNeasy spin column and centrifuged at 8000rpm for 1 minute. The column membrane with bound DNA was washed twice with 500µl of buffer AW1 (a dilute chaotropic salt solution that removed residual protein and carbohydrate), then 500µl of buffer AW2 (dilute ethanol solution) with intervening 1 and 3-minute 8000rpm centrifugation steps. Finally the DNA was eluted in 80µl buffer AE after one minute's room temperature incubation by centrifugation at 8000rpm for a minute. Buffer AE was a simple alkaline buffer (pH 8-9), which bound the acidic DNA. The 160µl DNA sample was stored at –20°C.

For small samples, where the column would dilute the DNA excessively an alternative method was used. Sterile DNA extraction buffer (50mM KCl, 10mM Tris-HCl pH 8.0, 2.5mM $MgCl_2$, 0.1mg/ml Gelatin, 0.45% NP40, 0.45% Tween 20 and water) and 10mg/ml of desiccated Proteinase K enzyme (Sigma) in deionised water was used to make a 1:20 Proteinase K: Buffer solution. 50µl was added to the cell sample in an eppendorf, which was incubated overnight at 55°C in a humidified chamber. The proteinase K was then inactivated by heating at 95°C for 10 minutes and the DNA was stored at –20°C.

DNA concentration and purity were measured using the Genequant Pro (Biochrom Ltd, Cambridge, UK) ultraviolet spectrophotometer with an absorbance of 1 at 260nm equating to 50µg/ml of genomic DNA and a ratio of absorbance at 260nm:280nm of 1.8 denoting pure DNA.

2.11 Polymerase Chain Reaction (PCR)

Amplification of specific regions of genomic DNA and cDNA was performed for loss of heterozygosity (LOH) and gene expression analysis following reverse transcription of mRNA. The PCR is an *in vitro* cyclical process of heating and cooling to denature, anneal and enzymatically amplify DNA. Specific DNA sequences can be multiplied exponentially using a system that combines a thermal

cycler with a heat stable enzyme (*Taq* polymerase). The reaction used two approximately twenty oligonucleotide long primers that were complementary to and hybridised with opposite DNA strands flanking the region of interest in the target DNA. The reaction consisted of the following steps with steps 2 to 4 repeated 35-45 times depending on the quality and length of the DNA used and the efficiency of primer annealing.

1 *Initial denaturing* at 94°C for 5 minutes.

2 *template denaturation* at 94°C for 45 seconds to separate the DNA strands.

3 *primer annealing* at 52-62°C for 45 seconds; the primers annealed to the template at an optimum temperature determined by the nucleotide composition of the primers.

4 *extension* at 72°C for 1 minute; the new DNA strands were synthesized from the primers, complementary to the single-stranded template DNA to which the primer had hybridised.

5 *final extension* at 72°C for 10 minutes.

The cycling meant that the newly synthesized DNA strands could themselves act as templates for further rounds of DNA synthesis in the subsequent cycles of the reaction. DNA amplification was theoretically 2^n times where n was the number of cycles, although in practice the efficiency is not 100%. The primers were incorporated into the new DNA strands, so were added to the reaction mixture at concentrations in excess of the final DNA concentration.

PCR was performed using the Qiagen Taq PCR Master Mix kit which provided a ready mixed solution of Taq DNA polymerize, Buffer, $MgCl_2$ and equal quantities of deoxyribonucleotides; dATP, dCTP, dGTP and dTTP. The final concentrations in the 20µl reaction mix were:

Taq PCR Master Mix	10µl	0.5 units of Taq Polymerase 1x Buffer 1.5mM $MgCl_2$ 0.2mM of each dNTP
Sense Primer	1.0µl	0.25 µM
Antisense Primer	1.0µl	0.25 µM
DNA	1.5-5.0µl	0.2-0.5µg total, 100-250ng/µl
Distilled water	3.0-6.5µl	
Total reaction mix	20µl	

All reagents were defrosted on ice and vortexed well before use. Each PCR contained a negative control lacking DNA to identify contamination and a positive control where possible depending on the parameter being optimised. All primers used are listed in Appendix B. Each primer was optimised before use to determine the best annealing temperature. The highest annealing temperature between 50-62°C that gave the best PCR product was used.

Primers for LOH analysis were those used by Bott *et al*, (2006) which were directed at the most commonly reported sites of LOH in prostate cancer. These loci are widespread throughout the genome on chromosome arms 1q, 2q, 3p, 5q, 6q, 7q, 8p, 9p, 10p, 10q, 11p, 11q, 12p, 13q, 16q, 17p, 17q, 18q and 21q. LOH primers were fluorescently labelled, 18-21 nucleotides long and had a Guanine-Cytosine (GC) content of 40-60%. The fluorochromes attached to the reverse primer of each pair were FAM, HEX or TET dye. All LOH analysis primers were 'blasted' using the 'Basic Local Alignment Search Tool' on the NCBI website (http://www.ncbi.nlm.nih.gov/BLAST/) to confirm that they would not amplify any contaminating mouse DNA, given the necessity of culturing prostate cells on a mouse fibroblast feeder layer.

Unlabeled primers for reverse transcription PCR were designed with similar properties as above at www.yeastgenome.org using published sequences of the genes of interest.

DNA quantities for LOH analysis were often limited. During primer optimisation when 100ng of DNA template was used in the reaction mix the PCR product was often only barely visible. Using 200ng yielded easily visible results and this amount

was used thereafter. Colony DNA was often in too limited a supply to allow estimation of DNA concentration. 2.5µl of colony DNA was amplified for GAPDH, and those that demonstrated a visible band on gel electrophoresis were used for LOH analysis.

2.12 Semi-quantitive reverse transcription PCR (RT-PCR)

The relative expression levels of different genes can be assessed by reverse transcription PCR. Using a known amount of total RNA, DNA copies of all mRNA transcripts are synthesized with highly expressed genes being represented in higher abundance than weakly expressed genes in the DNA sample. PCR of equal amounts of the DNA sample directed at specific genes produces quantities of PCR product in proportion to the abundance of the mRNA transcript in the initial total RNA. This does not reflect any post-translational modification or variations in protein transcription occurring downstream so may not accurately reflect the quantity of functional protein within the tissue.

Reverse transcription involves the synthesis of single stranded complementary DNA (cDNA) from mRNA by reverse transcriptase enzyme. The antisense cDNA strand is produced by RNA-dependent DNA polymerase activity following the annealing of oligo-dT primers to the mRNA poly-A tails. The bound RNA template is then digested by a hybrid dependent exoribonuclease activity also demonstrated by the enzyme. The resulting cDNA sample is then used for PCR of sequences of interest.

The Qiagen Omniscript Reverse Transcription kit which uses an *E coli* derived Reverse Transcriptase enzyme was used. RNase inhibitor (Qiagen Ltd) was added to minimise RNA degradation during the reaction. All reagents were defrosted on ice and vortexed well before use. The 20µl reaction mix was made up with the concentrations below and incubated at 37°C for 1 hour. The resultant cDNA was stored at –20°C.

10x Buffer RT	2µl	1x Buffer
dNTP mix	2µl	0.2mM of each dNTP
Oligo dT primer	2µl	1µM
RNAse inhibitor	1µl	10 units
Omniscript Reverse Transcriptase	1µl	4 units
Total RNA	1-3µl	0.5µg total, 0.17-0.5µg/µl
RNase-free water	9-11µl	
Total reaction mix	20µl	

2.13 Loss of Heterozygosity (LOH) Analysis.

LOH analysis is a well-established technique to identify areas of chromosomal deletion from 2 to hundreds of bases long within cells. Such loci may indicate the sites of tumour suppressor genes. By definition both alleles of these genes must be disabled for loss of function. Typically this occurs through a point mutation in one allele and DNA deletion at the other, so loci that consistently show LOH in cancer samples are likely to be near important tumour suppressor genes.

Within the 97% of the human genome that is non-coding, are areas of repeated DNA sequences known as tandem repeats. These areas vary in size from over 1Mb to less than 150 base pairs (bp), and are termed satellites, minisatellites or microsatellites in decreasing size order. Microsatellites (also called short tandem repeats (STRs) have repeated sequences of 1 to 6 base pairs, making up regions of DNA up to 150bp long and may be found both between and within genes. The number of these repeats is polymorphic, so that they usually differ between maternal and paternal alleles. Microsatellite DNA is likely to have arisen through strand misalignment or slippage during replication, recombination or repair. PCR amplification of a specific stretch of DNA that contains an area of microsatellite DNA, would be expected to yield a heterogeneous product containing two different lengths of amplified DNA, one derived from each parent. These may vary by only 2 base pairs in length but can be distinguished using high-resolution electrophoretic techniques. Where only one band is obtained, this is for one of three reasons.

1 DNA deletion of one allele has occurred at this locus. This is characteristic of cancer and implies truncation or loss of part of a chromosome within the tissue. Thus LOH or allelic imbalance has occurred.
2 The degree of polymorphism at different microsatellite DNA loci varies with an average heterozygosity rate of 70% (Dib *et al*, 1996). Thus, both parents will be homozygous at about 30% of loci, having the same number of microsatellite repeats within the amplified segment and yielding only one length of PCR product. This locus is therefore 'non-informative' for that particular individual. For this reason, LOH analysis in a malignant tissue requires a benign control sample from the same patient to distinguish between lost and non-informative loci.
3 The non-informative locus with one allele only present in both benign and malignant tissue may represent a germ line mutation, carried by all cells.

In some instances, subtler changes than complete deletion may be identified, where mutations have resulted in an increase or decrease in the number of repeats within the cancer tissue due to strand misalignment during replication, recombination or repair. When both benign and malignant specimens yield two PCR product each, but with different lengths this demonstrates 'microsatellite instability'. Microsatellite instability arises spontaneously, but more often reflects reduced function of certain DNA repair pathways (Figure 2.3).

LOH analysis was used in this project as a means of differentiating between benign and cancer colonies. The method of tissue acquisition and the multifocal nature of prostate cancer made it possible that within each sample were contaminating benign or malignant cells that might have produced colonies derived from a cancer cell amongst benign colonies and vice versa. Thus the nature of each colony had to be determined individually. In general it is not possible to reliably differentiate between primary cultures of benign and malignant prostate tissue at the microscopic level (Bright *et al*, 1997). LOH analysis therefore aimed to distinguish cells in terms of their chromosomal deletions.

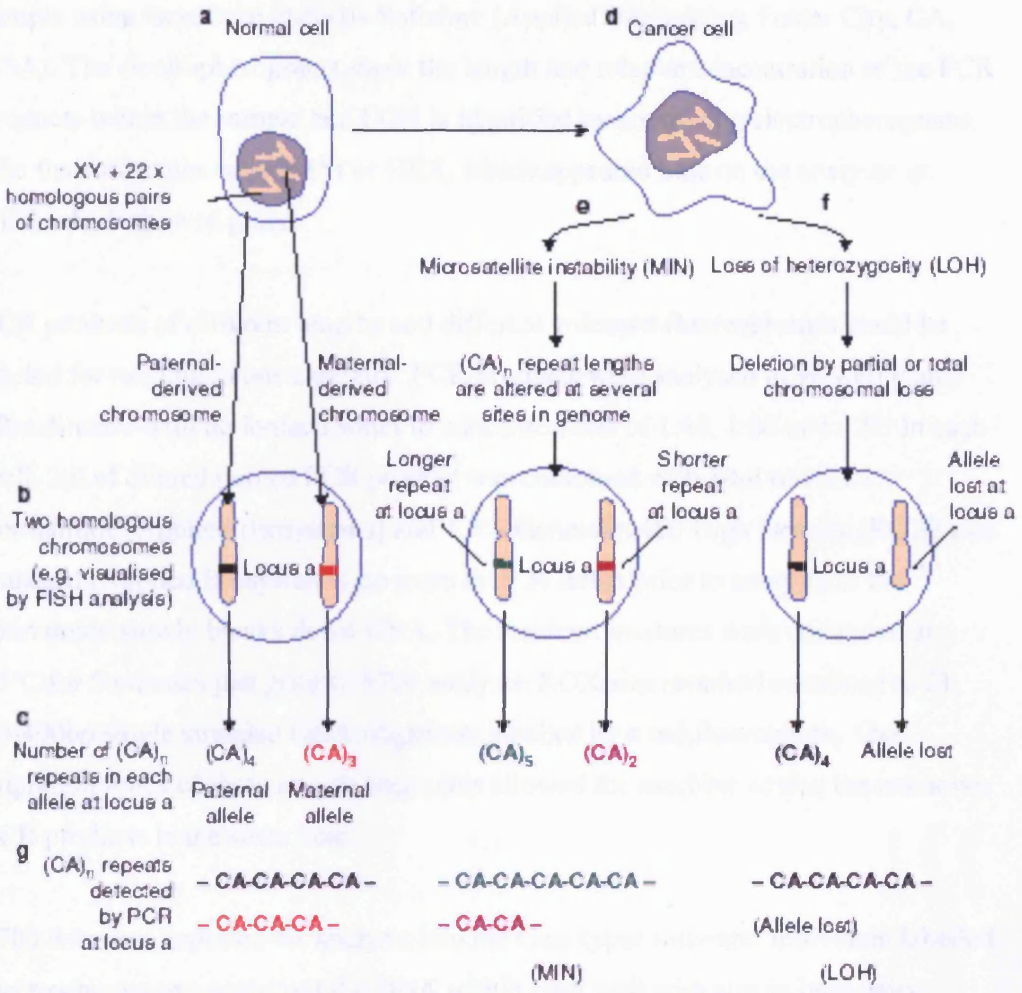

Figure 2.3: The underlying genetic differences in microsatellite instability and LOH. (from Pharoah & Caldas, 1999).

Up to 55 regions of polymorphic genomic DNA that had previously been reported as lost in prostate cancer were analysed in prostate block or colony genomic DNA using PCR. For each locus for each colony any differences in PCR product length were detected by the ABI Prism® 3700 DNA analyser, an automated, high-throughput, capillary electrophoresis system. This contains fine glass capillary tubes containing a stationary polymer. Each PCR product generated using fluorochrome labelled primers is drawn up into one of the capillary tubes and a 1000-volt charge applied across it. PCR products migrate along the capillary, with smaller and more negatively charged products moving faster. As the fluorochrome-containing DNA fragments leave the capillary, an argon laser excites them and their emitted

fluorescence is measured. An electropherogram is constructed for each capillary sample using GeneScan analysis Software (Applied Biosystems, Foster City, CA, USA). The electropherograms show the length and relative concentration of the PCR products within the sample and LOH is identified by comparing electropherograms. The fluorochromes were FAM or HEX, which appeared blue on the analyser or TET, which showed green.

PCR products of different lengths and different coloured fluorochromes could be pooled for running in one capillary. PCR products were analysed in 96 well plates after dilution with de-ionized water to concentrations of 1:40, 1:80 or 1:120. In each well, 2µl of diluted pooled PCR product was combined with 10µl of Hi-Di Formamide (Applied Biosystems) and 1.5% Genescan 400 High Density (ROX) size standard (Applied Biosystems) no more than 24 hours prior to analysis as the formamide slowly breaks down DNA. The resultant mixtures were denatured at 95°C for 5 minutes just prior to 3700 analysis. ROX size standard consisted of 21 50-400bp single stranded DNA fragments labelled by a red fluorophore. The migration times of these known fragments allowed the machine to size the unknown PCR products in the same lane.

3700 data was imported for analysis into the Genotyper software. Individual labelled electropherograms portrayed the DNA within each well with size in base pairs plotted against the amount of fluorescence (measured in arbitrary fluorescence units) and therefore product. Peaks relating to each DNA product were quantified by the software. The highest peak was chosen for each allele, though there were often a number of adjacent smaller peaks a few base pairs longer or shorter caused by slippage of the Taq polymerase enzyme during DNA amplification. The longer allele was always present in lower quantities than the shorter allele but this difference in peak heights was assumed to be constant. LOH was present where the change in peak height of the two alleles in the malignant specimen was significantly greater than that of the benign specimen. This standardized for PCR amplification differences and loading variability between the two and was calculated as:

$$\frac{\text{peak height of lower allele in malignant specimen}}{\text{peak height of higher allele in malignant specimen}}$$

$$\frac{\text{peak height of lower allele in benign specimen}}{\text{peak height of higher allele in benign specimen}}$$

The amount of DNA in each PCR product varied, so all samples were first analysed at the 1:80 concentration. When PCR products were too concentrated then the excessive fluorescence (levels over 10,000 arbitrary fluorescence units) saturated the detector and electropherogram peaks were blunted. If they were too dilute, peak heights less than 200 were indistinguishable from baseline noise and disregarded. Samples were re-run at 1:40 or 1:120 as necessary. The definition of a significant difference varies throughout the literature from 0.8 to 0.2 (Canzian *et al*, 1996; Barratt *et al*, 2002; Narla *et al*, 2001, Gray *et al*, 1995). The likelihood of true LOH being detected depends on the purity of the cancer sample, which is in turn dependent on the origin of the tissue and the means of obtaining the DNA. For heterozygous alleles where one allele has been lost in the cancer, there should in theory be only one allele present in the cancer sample compared to two in the benign sample. However in practice, few primary tissue samples are not contaminated with benign cells or perhaps different cancer clones. Thus the two alleles contained in these contaminants are detected and contribute to an albeit smaller peak in the cancer sample. In this project, loci were considered positive for LOH when the calculated difference was ≤ 0.5 (though a threshold of ≤ 0.3 was also considered) given the likely presence of contaminating non-epithelial tissue such as stroma and vessels in the prostatectomy block samples.

DNA obtained from the malignant or benign areas of the whole mount radical prostatectomy specimen was screened for LOH using 55 microsatellite markers. Lymph node DNA represented the benign control. DNA from colonies grown from the fresh malignant or benign tissue was then screened at loci showing LOH. This aimed to identify whether the colony matched the LOH pattern of the area of malignant prostate that it came from thus confirming that cancer colonies had been cultured. Cell line DNA from paired benign and malignant prostate cell lines as

described by Bright *et al* (1997) were similarly compared for 29 markers to act as control samples. Figure 2.4 shows typical electropherograms.

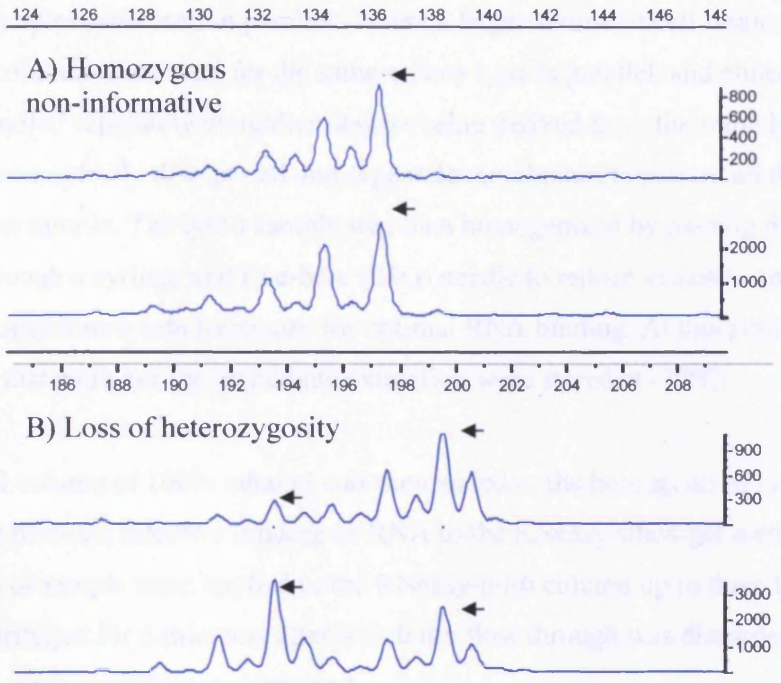

Figure 2.4: Electropherogram pairs demonstrating A) a homozygous, non-informative locus and B) LOH with 81% loss of the shorter allele in the upper specimen. The peaks that are compared are indicated (◄).

2.14 RNA extraction

Total RNA was extracted at room temperature using the Qiagen RNeasy™ midi kit. RNA isolation entails initial lysis and homogenisation of cells which are passed through a silica-gel membrane by centrifugations at 3000 x g. The membrane selectively binds total RNA, allowing other molecules to be washed through. An eluting step releases this RNA providing a sample for further applications. All RNA molecules longer than 200 nucleotides are isolated, thus the procedure enriches for mRNA since most RNAs <200 nucleotides (such as 5.8S rRNA, 5S rRNA, and tRNAs, which together comprise 15–20% of total RNA) are selectively excluded.

Cell pellets for RNA extraction were immediately resuspended in 1ml of RLT buffer to lyse cell membranes and inactivate RNases and ensure isolation of intact RNA. Type I and II BPH colony cells were harvested directly into RLT buffer and the paired samples processed in parallel. Where a large volume of cell lysate existed, several columns were used for the same colony type in parallel, and eluted total RNA handled separately thereafter despite being derived from the same lysate. Lysis aimed to completely disrupt cell and organelle membranes to release all the RNA within the sample. The lysed sample was then homogenized by passing the lysate ten times through a syringe and fine-bore (21G) needle to reduce viscosity and create the homogeneous lysate necessary for optimal RNA binding. At this point, any RNA samples that were not for immediate extraction were stored at -70°C.

An equal volume of 100% ethanol was then added to the homogenized lysate and mixed to promote selective binding of RNA to the RNeasy silica-gel membrane. Aliquots of sample were applied to the RNeasy-midi column up to three times and it was centrifuged for 5 minutes, after which the flow through was discarded. Further columns were used if lysate remained.

On-column DNase digestion was next performed to wash through any residual DNA (Qiagen RNase-Free DNase Set). The column was washed with 2ml buffer RW1 (a guanidinium thiocyanate containing buffer) spun through for 5 minutes. Then 160µl of buffered DNase I (0.34 Kunitz units/µl in RDD buffer) was applied to the RNA bound to the silica-gel membrane at room temperature for 15 minutes. After incubation in buffer RW1 for 5-minutes, centrifugation as above washed the DNase off the column.

Prior to RNA elution, the column was washed again with 2.5ml of ethanol-based buffer RPE with a 2 minute centrifugation and then 2.5ml of RPE buffer was spun through for 5 minutes. Finally the RNA was eluted into an RNase-free eppendorf (Ambion Europe Ltd, Huntingdon, UK) using 30-100µl of RNase-free water (depending on initial number of colonies harvested) with a 3-minute centrifugation after 1 minutes incubation. A second elute into the same eppendorf was performed similarly. RNA solutions were immediately frozen at -80°C.

2.15 Quantification and quality assessment of RNA samples

Two methods of RNA assessment were used. The Genequant Pro (Biochrom Ltd) ultraviolet spectrophotometer assessed the quality and quantity of RNase-free water diluted total RNA samples drawn into glass capillary tubes. Absorbance at 260nm wavelengths allowed calculation of concentration where an absorbance of 1 equates to 40μg/mL of RNA, and the ratio of absorbance at 260nm / 280nm gave a measure of purity with 2.0 implying pure RNA.

For total RNA for application onto gene chips, the RNA 6000 Nano LabChip Kit and the 2100 Bioanalyser from Agilent Technologies UK Ltd, West Lothian, UK was used. In this lab-on-chip procedure, the denatured RNA sample combined with a marker dye is drawn along a fine gel-filled capillary by electrophoresis. RNA molecules of different lengths travel at different speeds allowing the quantity and relative abundance of different sizes of RNA to be measured. A ladder allows standardization of the RNA run in each capillary. Each single use chip allows the analysis of 12 samples simultaneously in 30 minutes. Only 1μl of total RNA is required to quantitate concentrations of 25-500ng/μl to an accuracy of ± 50% (manufacturer's specifications). The LabChip was first primed with 9μl of a gel matrix and dye mix. 1μl of heat denatured (70°C for 2 minutes) sample RNA and 5μl of RNA 6000 Nano Marker (Ambion) was added to each well with denatured RNA 6000 ladder (Ambion) placed in a separate well. The chip was vortexed and placed in the Agilent 2100 Bioanalyser. Sample quality and quantity was demonstrated by a gel image, electropherogram, rRNA signal height ratio (28S/18S) and calculated RNA concentration.

In addition, the electropherogram plot data for each sample was run through the Degradometer program (from www.dnaarrays.org) devised by Auer *et al* (2003). This program sought to improve on the rRNA ratio calculation used by the Bioanalyser software as a measure of RNA integrity. The ratio is determined by the relative area under the 18S and 28S peaks, however the start and end of these are not easily defined. In addition, other assessments of quality such as the appearance of the gel or electropherogram are amenable only to subjective evaluation. The degradometer program provides a single figure – the 'degradation factor' - that

allows direct comparison and ranking of samples, and also bands them into five quality ranges from black (worst) through red, orange and yellow to no colour (best). The degradation factor figure increases as quality worsens. As degradation occurs, the rRNA peaks are seen to diminish and a greater number of shorter RNA molecules cause degradation peaks. The degradation factor is calculated using the ratio of the average RNA peak height to the 18S peak height to account for this. All these RNA measures were considered together to select the best quality RNA samples for further analysis.

2.16 Concentration of RNA samples

Given the difficulty selectively harvesting colonies, and the need to maximize harvested cell numbers, the resultant RNA solutions were often too dilute. Concentrations of 500ng/µl or at least 100ng/µl with an amplification step were required for downstream application onto Affymetrix® GeneChips® (Eberwine *et al,* 1992). When required, RNA samples were therefore concentrated within the eppendorf on ice at 4°C, by evaporation under a flow of nitrogen gas directed at the surface of the sample using a sterile glass pipette (figure 2.5). Concentration was stopped when the volume of liquid had reduced sufficiently depending on the known starting concentration, and the sample concentration and quality was rechecked using the Agilent RNA 6000 Nano LabChip Kit and 2100 Bioanalyser.

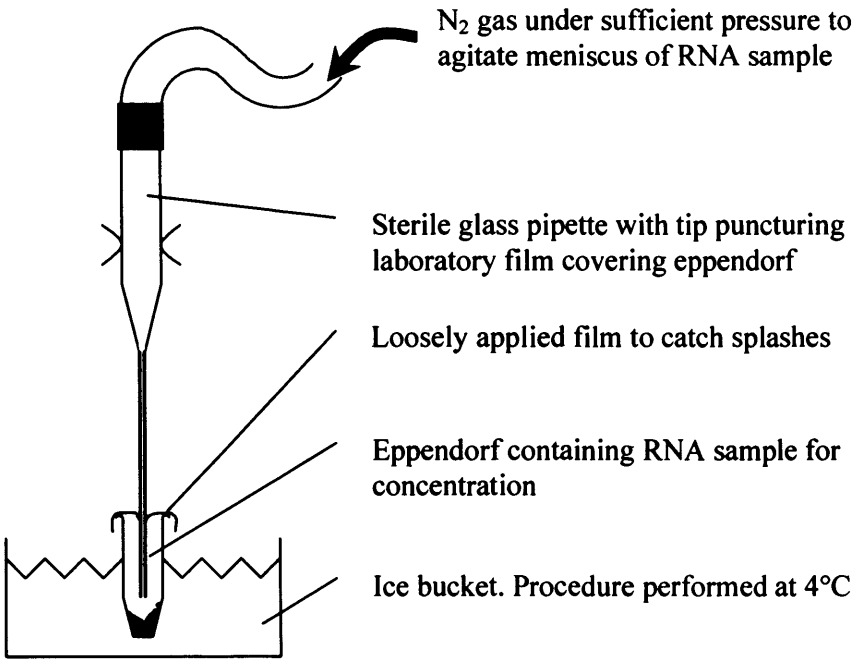

Figure 2.5: Concentration of RNA samples using N_2 gas.

2.17 Agarose gel electrophoresis

Total RNA samples and PCR products were assessed for integrity, size or concentration using agarose gel electrophoresis. Two percent agarose gels were used. These were made from powdered agarose (Invitrogen) added to Tris Acetate Electrophoresis buffer (TAE buffer: 4.84g Tris base, 1.142ml glacial acetic acid, 2ml 0.5M EDTA pH 8.0, made up to 1000ml with distilled water), covered and heated until it had dissolved. The agarose solution was allowed to cool, then mixed with 0.5µg/ml of ethidium bromide and left to set in a gel tray with combs *in situ*. Gels were loaded while immersed in TAE buffer in the gel tank with 5µl of total RNA or 6µl of PCR product with 2µl of loading dye per well. Where required 1µl of a 1kb DNA ladder (GeneRuler™, Fermentas Life Sciences, Germany) in 5µl of gel loading buffer was also loaded. A120-volt charge was applied and negatively charged DNA migrated through the gel. Gels were viewed on a GeneFlash UV imaging system at 254-300nm (Syngene Cambridge, UK). UV fluorescent images were captured using the GeneFlash system and GeneSnap image acquisition software (Syngene Cambridge, UK). For RT-PCR band intensity measurement,

images were analysed using GeneTools software (Syngene Cambridge, UK) and data exported to Excel (Microsoft, Berkshire, UK) for statistical analysis.

2.18 Total RNA processing, amplification and application onto oligoarrays to obtain raw gene expression data.

The expression of many thousands of genes can be studied simultaneously using DNA microarrays or oligoarrays. Thousands of DNA fragments or oligonucleotides, each known to correspond to a specific gene, expressed sequence tag or other DNA sequence are bound in a set pattern to a glass slide or silicon wafer. Processed mRNA is incubated as cDNA fragments with the array, and any mRNA fragment that hybridises to the complementary DNA probe is detected. From the position on the slide, semi quantitative and qualitative information regarding the expression of a specific gene is obtained. Developed in the 1990s, microarray technology has opened up a new era in high throughput expression analysis, and allowed an understanding of the global gene expression patterns underlying cell behaviour.

2.18.1 Transcription of total RNA and hybridisation onto the Affymetrix GeneChip® array

Affymetrix GeneChip Human Genome U133 Plus 2.0 (Affymetrix UK Ltd, High Wycombe, UK) oligoarrays were used. This high-density array allows genome-wide expression analysis of the known human transcriptome on a single microarray.

Each chip is a thin coated quartz wafer upon which millions of DNA fragments have been chemically bonded and extended using a photolithographic manufacturing process. Each chip is divided into over 1.3 million 11μm squares called features. Each feature contains millions of copies of a specific 25-nucleotide long DNA probe bound to it at one end to which cDNA target fragments will bind if complementary. Along with various control sequences, the expression level of >47,000 transcripts and variants, including approximately 38,500 well-characterised human genes are demonstrated by >54,000 sets of probes on the chip. Each gene, expressed sequence tag or other sequence (termed 'gene' hereon) is specifically represented at 11 different features by 11 different unique 25-mer probes.

These sequences were derived from the most appropriate sequences on a number of databases in the public domain (dbEST, NCBI, Feb. 2003; GenBank®, NCBI, Feb. 2003 Release 134; RefSeq, NCBI, March 2003 and a draft human genome assembly, NCBI, November 2002, Build 31), avoiding those that might fold in on themselves or cross hybridise. Sequences were also selected from within 600 bases of the 3′ end of each mRNA transcript as RNA degradation starts at the 5′ end.

For any probe there will be a degree of non-specific binding causing background noise. To control for this, each of the 11 probes representing each gene has a further 11 features dedicated to it which contain very similar 25-mer probes, but with one different base pair in the middle of the sequence. This is sufficient to destabilize specific binding, while non-specific binding is unchanged. This 'perfect match:mismatch' system allows the quantification of non-specific binding for each probe, and by subtraction, the quantification of true specific binding to the perfect probe. The use of probe sets containing 11 pairs of probes increases the sensitivity of a chip for detecting the expression of the gene to a resolution of 1 in 200,000 total transcripts in a sample. All probes have to be hybridised in the same conditions, and will differ in their affinities due to their different sequences. This means a scaling process is required to normalize all signals to a common base line, but increases sensitivity, as a low abundance transcript will be detected by a high affinity probe while plentiful transcripts which saturate high affinity probes can still have differential expression demonstrated by low affinity probes.

Variations in microarray expression data may be technical or biological. Throughout the process of patient selection, tissue culture, sample acquisition and microarray application standard protocols were followed to minimize technical variation. Affymetrix GeneChip Human Genome U133 Plus 2.0 arrays were used as in a comparison of six commonly used gene expression analysis platforms, these demonstrated low levels of technical variability (Yauk *et al*, 2004). Twelve arrays analysed the five selected sample pairs and the reserve pair which was required as high background in the prostate I Type II chip might have lead to reduced detection of low level expressed genes. All GeneChips were from the same batch and were run in succession. Sample amplification, labelling and gene chip hybridisation were all

performed by Dr N. Jina at the Institute of Child Health, University College London. Figure 2.6 shows the steps within this process, which are further elaborated below.

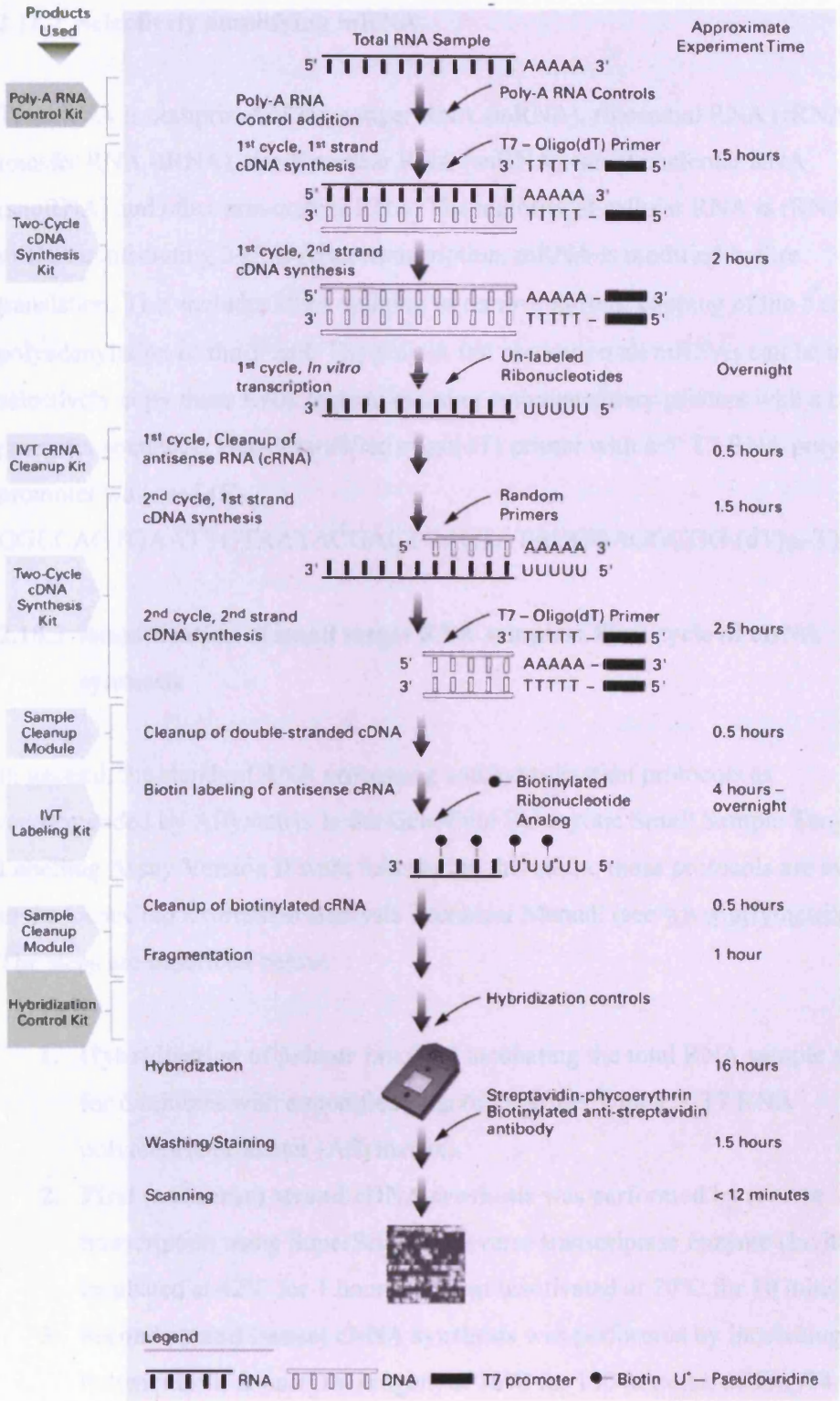

Figure 2.6: Human prostate epithelial target amplification and labelling for Affymetrix GeneChips from the GeneChip Expression Analysis Technical Manual. (www.affymetrix.com)

2.18.2 Selectively amplifying mRNA

Total RNA is comprised of messenger RNA (mRNA), ribosomal RNA (rRNA), transfer RNA (tRNA), small nuclear RNA (snRNA), small nucleolar RNA (snoRNA) and other non-coding RNA. The majority of cellular RNA is rRNA, with mRNA contributing 3–5%. After transcription, mRNA is modified before translation. This includes RNA splicing to remove introns, capping of the 5′ end and polyadenylation of the 3′ end. The poly-A tail present on all mRNAs can be used to selectively copy these RNA molecules using complementary primers with a built in promoter sequence. Here a modified oligo(dT) primer with a 5′ T7 RNA polymerase promoter was used (5′-GGCCAGTGAATTGTAATACGACTCACTATAGGGAGGCGG-$(dT)_{24}$-3′).

2.18.3 Amplification of small target RNA samples: First cycle of cDNA synthesis

In general, the standard RNA processing and hybridisation protocols as recommended by Affymetrix in the GeneChip Eukaryotic Small Sample Target Labelling Assay Version II were followed in this study; these protocols are available in the GeneChip Expression Analysis Technical Manual (see www.affymetrix.com). The steps are described below.

1. **Hybridisation of primer** involved incubating the total RNA sample at 70°C for 6 minutes with a modified oligo(dT) primer with a 5′ T7 RNA polymerase promoter (Affymetrix).
2. **First (antisense) strand cDNA synthesis** was performed by reverse transcription using SuperScript II Reverse transcriptase enzyme (Invitrogen) incubated at 42°C for 1 hour then heat inactivated at 70°C for 10 minutes.
3. **Second strand (sense) cDNA synthesis** was performed by incubating DNA Polymerase I, *E. coli* (Invitrogen) at 16°C for 130 minutes, adding T4 DNA polymerase (Invitrogen) for the last 10 minutes.
4. **Double-stranded cDNA clean up** used overnight ethanol precipitation.

5. **In-vitro transcription** of the second (sense) strand of cDNA produced antisense cRNA using the Ambion MEGAscript T7 Kit and unlabelled ribonucleotides.
6. **Antisense cRNA clean up** used Qiagen RNeasy mini columns.

2.18.4 Second cycle of cDNA synthesis to produce biotin-labeled cRNA

7. **First (sense) strand cDNA synthesis** from antisense cRNA used a 10 minute 70°C incubation to anneal random hexamer oligonucleotides (Invitrogen). These primed the cDNA strand from random 3′ binding locations on the cRNA and were extended from 5′ to 3′, ending in the synthesis of a 3′ poly-A tail. The first strand cDNA were therefore shorter than the template antisense cRNA.
8. **Second strand cDNA synthesis** was primed using the T7-$(dT)_{24}$ oligomer primer again.
9. **Clean up of double-stranded cDNA** used the GeneChip® Sample Cleanup Module (Qiagen Ltd).
10. **In-vitro transcription of first (sense) cDNA** strand used biotinylated UTP and CTP ribonucleotides to produce biotinylated antisense cRNA (ENZO Diagnostics, Farmingdale, NY, ENZO® Bioarray™ HighYield™ Transcript Labelling Kit).
11. **Labelled cRNA clean up** used the GeneChip® Sample Cleanup Module (Qiagen Ltd).
12. **cRNA quality assessment** by Agilent RNA 6000 Nano LabChip Kit and the 2100 Bioanalyser (results not shown).

2.18.5 Fragmentation, hybridisation, array processing and scanning

13. **Full length cRNA fragmentation** into 35-200bp fragments by metal induced hydrolysis using the GeneChip Sample Cleanup Module (Qiagen Ltd).
14. **GeneChip hybridisation** involved the preparation of a hybridisation cocktail including the fragmented target cRNA, probe array controls, bovine serum albumin and herring sperm DNA derived from the GeneChip

Hybridisation, Wash, and Stain Kit (Affymetrix). It was then hybridised to the Affymetrix GeneChip cassette during a 16-hour incubation. Premixed control cRNA molecules were added from the GeneChip Eukaryotic Hybridisation Control Kit (Affymetrix). These were a mixture of biotinylated and fragmented cRNA of *bioB*, *bioC* and *bioD* from *E. coli,* and *cre* from P1 bacteriophage in staggered concentrations with corresponding probes represented on Affymetrix Eukaryotic expression probe arrays.

15. **Processing of hybridized arrays** involved washing and staining with phycoerythrin-conjugated streptavidin in an Affymetrix Fluidics station.
16. **Raw Data gathering.** Images were scanned with a Hewlett-Packard GeneArray scanner / Affymetrix GeneChip Scanner 3000 7G. A YAG laser is directed onto the chip and the amount of light emitted at 570nm is proportional to the bound target at each location on the probe array. This process bleaches the fluorophore by 3-5% such that the data is best captured on the first scan.

2.19 Built in controls for GeneChip expression analysis.

Several quality control parameters are built into the Affymetrix GeneChip system to allow monitoring of assay data quality. Detailed information is available in the GeneChip Expression Analysis Data Analysis Fundamentals manual. These parameters were assessed across all GeneChips analysed.

2.19.1 Visual array inspection

At the most basic level, the probe array is inspected for any image artefacts such as high or low intensity spots, scratches and overall background levels.

2.19.2 B2 Oligo Performance

Just prior to hybridisation a number of labelled transcripts from the Affymetrix GeneChip® Eukaryotic Hybridisation Control Kit were added to the labelled target to serve as hybridisation, washing and staining controls. These included 50 pM of a

synthetic biotinylated control oligo B2 which is used by the software to align a grid on the probe array prior to image analysis.

2.19.3 Average Background and Noise Values

The average background level on the chip is recommended to fall between 20 and 100. A high background implies that sample impurities are binding non-specifically which can obscure genes at very low levels of expression leading to an overall loss of sensitivity. Noise is a measure of pixel-to-pixel variability within a probe cell and is a feature of the scanner and the sample. Replicates should ideally have comparable noise levels.

2.19.4 Poly-A Controls

The efficiency of the labelling of the cRNA target was assessed using the Poly-A RNA Control Kit (Affymetrix) which contains sense RNA strands synthesized from four *B. subtilis* genes (*dap, lys, phe* and *thr)* modified by the addition of poly-A tails and then amplified with T3 RNA polymerase. A mixture of these 4 exogenous cRNAs is added to the target cRNA sample at known concentrations (*lys* 1:100,000; *phe* 1:50:000; *thr* 1:25,000 and *dap* 1:7,500). For amplified samples efficient target labelling should result in all lys being called 'present' on the chip in >70% of arrays , with the other controls always being present at increasing intensities. An estimation of assay sensitivity is thus also possible.

2.19.5 Hybridisation Controls

The GeneChip Hybridisation Control Kit also contains staggered concentrations of biotinylated fragmented antisense cRNA of *bioB, bioC* and *bioD* from the biotin synthesis pathway of *E. coli*, and *cre* from the recombinase gene of bacteriophage P1. Their corresponding probes are included in Affymetrix Eukaryotic expression probe arrays. These controls are added to the target cRNA prior to hybridisation. The concentration of *bioB* is lowest at 1.5pM and should be detected in 50% of arrays, while the other controls at 5pM, 25pM and 100pM respectively should always be detected.

2.19.6 Internal Control Genes

By comparing the signal values of probes for the 3', middle and 5' ends of β-actin and GAPDH, RNA sample and assay quality can be assessed. In general the 3'/5' ratio is <3 for the standard protocol. When samples are amplified, the use of random primers during the second amplification cycle means that it is inevitable that the 5' end is not represented in all cDNA transcripts, so ratios tend to be >3 and the 3' to mid-transcript ratio (3'/M) is a better guide. A high ratio may indicate degraded RNA or inefficient first strand cDNA synthesis and/or cRNA transcription.

2.19.7 Percent Present calls

The number of probe sets called "Present" relative to the total number of probe sets on the array is dependent on multiple tissue, sample and chip factors and should be similar across samples.

2.19.8 Scaling Factors

For global scaling, the average overall array intensity was calculated and the deviation from this for each GeneChip was measured as a scaling factor. This variability in overall intensity was most likely due to assay factors, which were then controlled for by adjusting individual signal intensities by the scaling factor. Scaling factors should ideally not vary more than 3-fold.

2.20 Analysis of GeneChip expression data.

Data from the scanned array was stored as a *.dat file by the GeneChip scanner. A *.cel file was derived from this, which contained a single intensity value for each probe cell. The probe cells were then grouped into their perfect match:mismatch pairs and their relative intensities compared. The true intensity level was assigned a detection p value and called present, marginal or absent in relation to a predefined threshold intensity. The relative proportion of these three states for all 11 probe sets was combined into an overall p value for likelihood of expression for the gene along

with the mean intensity of expression. This data was expressed in a *.chp file and exported as *.txt file into the expression analysis software.

Using Genespring GX, Version 7.2 (Agilent technologies UK Ltd) the data was further transformed to focus on biological variation. First the data was normalised. All measurements less than 0.01 were set to 0.01 to remove all negative expression levels and other biologically irrelevant and unacceptable values. The intensity of each gene on one chip was then normalised to the 50^{th} percentile of all gene intensities on that chip to standardize for variations in hybridisation and array performance and allow comparison between arrays. Finally all genes across all chips were rescaled to the median value of all genes so that genes with similar expression patterns would now look similar. These normalization steps assumed that the overall gene expression profile was similar on all chips (which was reasonable as they contained >1000 genes covering a wide range of biological functions). Each gene now had an assigned value for raw signal, control signal and a normalized value along with its t-test p-value expressing the likelihood of expression.

The data was viewed and manipulated using the natural log of the normalized values. This made the data more symmetrical and reduced the influence of outliers allowing better estimates of variance. Thus equal emphasis could be given to up and down regulation of genes and the data more closely approached a normal distribution (Morrison and Ellis, 2003). The cross gene error model was also employed to compensate for the limited number of replicates (Rocke and Lorenzato, 1995). This used details of the overall variability of the data and applied this to individual genes. It assumed that the expression of a gene within type I or II colonies was normally distributed, that most genes were not differentially expressed and had a mean of 1 and that genes expressed at a similar level had similar variances. This made gene selection more stringent when activated.

This transformed data contained readings for all 54,675 genes on the Affymetrix Human Genome U133 Plus 2.0 array. Those genes showing significantly different expression between type I and type II colonies were obtained through a series of filtering and statistical steps.

First a step 'filtering by fraction Present' was performed as recommended by McClintick and Edenberg (2006) to exclude most non-expressed genes and reduce the false discovery rate associated with later statistical selections. Genes that are not detectably expressed nevertheless generate signal values and contribute disproportionately to the false discovery rate. These usually low, random fluctuations can still often produce apparently large fold-changes. By retaining only those genes which were called present in at least 3 out of the 12 chips (i.e. 50% of one experimental arm of 6) this excluded the majority of non-expressed genes while retaining highly significant genes and interesting transcripts that were turned on or off. McClintick and Edenberg found this filter to exclude 92% of absent probe sets while removing 4.2% present probe sets in their data. This filtering step was useful as the data did not tolerate later multiple testing corrections that also aimed to reduce the false discovery rate.

It is generally accepted that fold change alone is not a valid test for differential expression (Morrison and Ellis, 2003; Allison *et al*, 2006). Therefore a one-sided analysis of variance (ANOVA) with no multiple testing correction steps was used at a p-value of 0.05 to identify those remaining genes that were significantly differently expressed between the two colony types. This level of significance was chosen as a compromise between type 1 error (finding false positive genes) and type II error (excluding false negative genes). No post-hoc tests were necessary as only two groups were being compared and no multiple testing corrections were included as these were too stringent, excluding all remaining genes.

The ANOVA identified those genes that were significantly differentially expressed. Next those genes with a t-test p-value of >0.05 in one of the two experimental arms – type I or II were excluded. This retained genes whose expression was similar between replicates and therefore probably more meaningful.

A cluster diagram as first described by Eisen *et al* in 1998 was constructed. Using hierarchical clustering, genes and samples showing similar expression patterns were grouped closest together with the branch lengths on the dendrogram reflecting the degree of similarity between each one.

K-means clustering was also explored as an alternative to the two-dimensional gene tree, to further categorize the final gene list (Hartigan and Wong, 1979). This clustering algorithm aims to group genes with similar expression patterns together. The default number of starting clusters, 5, was used and genes were assigned in the order of the gene list to one of these 5 clusters which were plotted in 'expression space' with the centre of each representing the average location. Each gene was then reassigned to the cluster with the centre nearest its position and the centres' locations were recalculated. After 100 iterations the clusters were defined.

This is one of several available unsupervised clustering tools. However there is no clear consensus as to which clustering algorithms are most biologically useful or reproducible, and for K-means clustering, how many starting clusters are required (Allison *et al*, 2006). K-means clustering can produce different outcomes each time it is run on the same data if the starting cluster allocations are random (not the case in Genespring 7.2) which can be expressed as its stability. In a comparison study of several different clustering models, K-means was found to be more stable than some, though only with a 55% stability at best (Garge *et al*, 2006).

The genes listed in each cluster were then examined in context of their biological functions with the help of the Netaffx™ Analysis Center hosted by www.affymetrix.com and databases curated by or accessed via the National Centre for Biotechnology information at http://www.ncbi.nlm.nih.gov/.

2.21 Statistical analysis.

All statistical analysis was performed using Microcal Origin 4.0 (Microcal Software Inc., Northampton, MA, USA), Excel (Microsoft, Berkshire, UK) or the online statistical calculators available at http://www.physics.csbsju.edu/stats/. Expression array analysis was performed using Genespring GX.

CHAPTER 3:
ACQUISITION AND ANALYSIS OF EPITHELIAL COLONIES FROM BENIGN PROSTATIC HYPERPLASIA TISSUE.

3.1 Morphological characteristics of primary prostate epithelial colonies

Fresh primary prostate tissue from TUR specimens was collected and processed according to the protocol described above. After 14 days in monolayer culture type I and type II colonies were distinguishable. Such colonies had previously been characterised by Hudson *et al* (2000) in terms of their frequency, size, morphology, cell density and cytokeratin expression. The colonies obtained in this study were similarly assessed to confirm the reproducibility of the technique. The colony forming efficiency of the prostate cells is given for all dishes from ten experiments in table 3.1. Figure 3.1 shows the distribution of colony size and type derived from ten dishes from each of three experiments.

Experiment	No. of dishes scored	Mean total % CFE (≥32 cells)	Mean % type II CFE	% total colonies type II
1	20	0.45	0.06	13.3
2	20	0.48	0.17	35.4
3	17*	0.36	0.05	13.9
4	23*	0.20	0.04	20.0
5	24	0.27	0.02	7.4
6	15*	0.03	0.00	0.0
7	18*	0.15	0.05	33.3
8	20	0.13	0.03	23.1
9	23*	0.48	0.09	18.8
10	25	0.10	0.00	0.0
mean	20.5	0.27	0.05	16.5
s.e.m.	-	0.05	0.02	3.87

CFE = colony forming efficiency, s.e.m. = standard error of the mean, *excludes dishes lost to infection that were not scored.

Table 3.1: Colony forming efficiencies of primary prostate epithelial cell cultures.

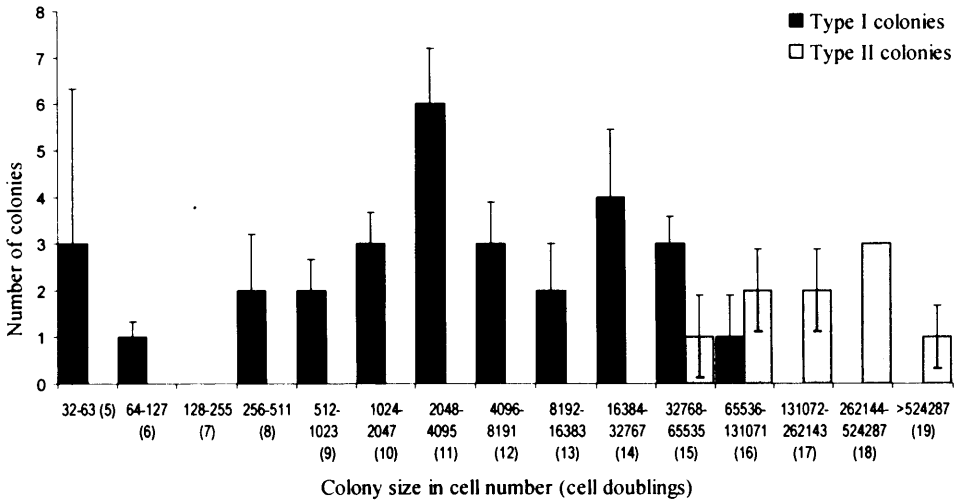

Figure 3.1: Distribution of prostate epithelial cell colony size by type. Error bars show the standard error of the mean over 10 dishes from 3 experiments.

Colonies were typed primarily on their morphology and overall appearance under direct vision. However four other criteria were also recorded: colony diameter, number of cells across 1mm (cell density), total colony cell number and the number of cell divisions this reflected. All these criteria were significantly different between the two colony types ($p<0.0001$, Students t-test, data shown above for colony cell number only) and were useful objective discriminators alongside the more subjective assessment of morphological appearance. A typical dish and magnified views of both colony types are shown in figure 3.2.

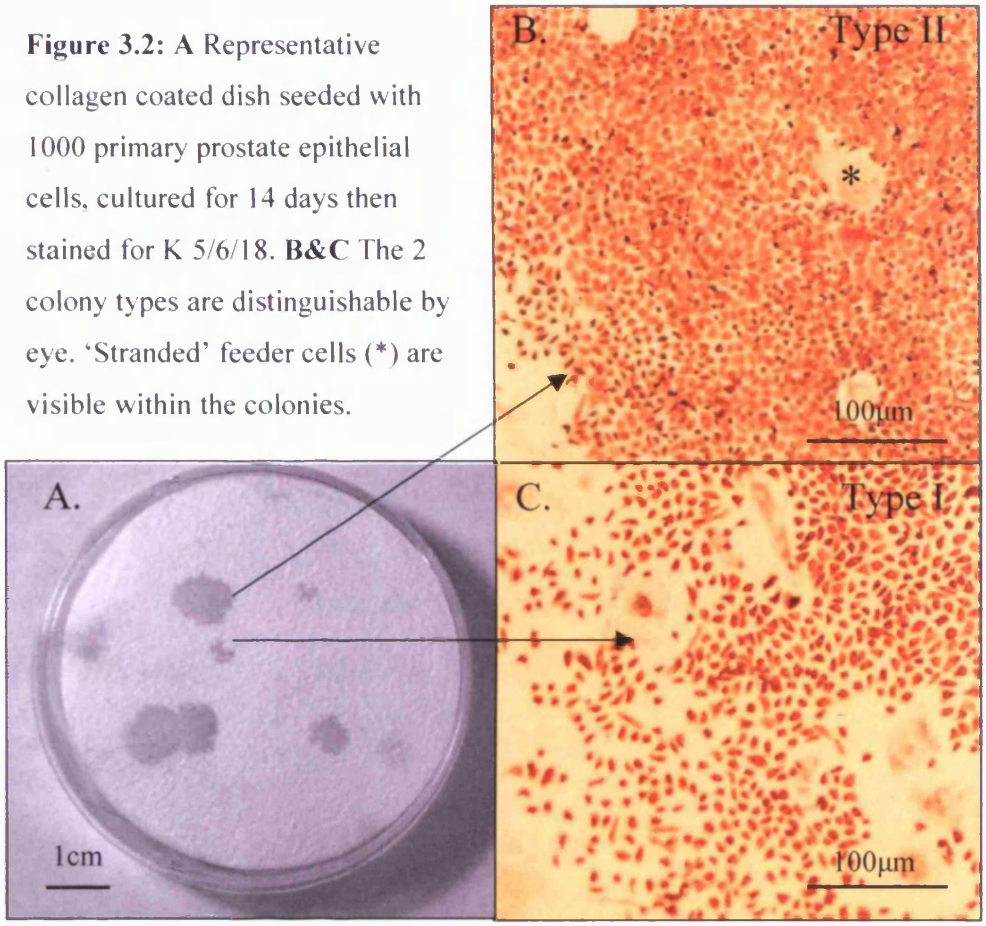

Figure 3.2: A Representative collagen coated dish seeded with 1000 primary prostate epithelial cells, cultured for 14 days then stained for K 5/6/18. **B&C** The 2 colony types are distinguishable by eye. 'Stranded' feeder cells (*) are visible within the colonies.

	Hudson *et al*, 2000		Present study	
Colony type	I	II	I	II
Diameter (mm, mean)	≤ 4	≥3	0.5 – 16 (4)	9 – 20 (11)
Cell number (mean)	≤ 8,500	8,000 – 40,000	40 – 48,000 (8300)	28,000 – 607,000 (169000)
Number of doublings (mean)	5 – 12	12 - 14	5 – 16 (11)	15 – 19 (17)
Density (cells/mm, mean)	<30	30 – 50	7 – 32 (19)	33 – 59 (40)
Outline	Irregular	Regular	Irregular	Regular
Frequency of colonies	90%	10%	83%	17%
Incidence of colony forming cells	1/17	1/185	1/377	1/1961
Immunocytochemistry	K8 or K8 & K14	K14 only	not assessed	not assessed

Table 3.2: Characteristics of the two colony types obtained from primary prostate epithelial cell culture by Hudson *et al*, (2000) and in the present study.

To summarise, the characteristics of the colonies as defined by Hudson *et al* (2000) are given in table 3.2 alongside those of the colonies obtained for this study. Both series describe colonies that are similar in appearance. Type I colonies tended to be smaller with fewer, more loosely arranged cells, while type II colonies were less common but larger and more dense. In both studies, type II colonies were grown in 8 of 10 experiments.

Unlike the previous report, in this study both colony types were far rarer, particularly type I colonies even though initial plating density was the same. Those colonies that were obtained were larger both in diameter and cell number, while density was more consistent. Colonies were derived from fresh prostate tissue using

a very similar protocol to that described by Hudson and tissue was sourced from the same London population. However, the modifications made to the protocol as described in section 2.5 account for the observed differences. The replacement of the trypsin and two brief 20 second centrifugation steps by mechanical tissue disruption and a longer spin would result fewer cells being lost with the discarded supernatant in this study. The resultant 'cell rich' single cell suspension was counted prior to plating at 1000 cells/25cm^2 dish. It appears most likely that a greater number of non-epithelial cells were included in the count. All viable cells were counted excluding recognisable red blood cells, which could include a greater proportion of leucocytes and stromal cells. Certainly the longer spin did not increase the yield of prostate epithelial cells. Thus fewer than 1000 true prostate epithelial cells could have been plated, with reduced colony yields.

The larger size of colonies may relate to more favourable growing conditions and less competition for resources given the lower colony numbers. The Hudson series used irradiated mouse fibroblasts whereas a mitomycin treated feeder layer was used in this series, purely because these feeders could be generated 'in house'. Both feeder layer treatments are well established, though neither is known to confer a growth advantage (Ponchio *et* al, 2000). The individual epithelial cells that form the largest colonies must divide at least daily, and even a slight variation in time on the day of scoring the colonies (that were not fixed for this study) would cause exponential increases in cell number.

3.2 Growth characteristics of type I and type II colonies

Hudson *et al* (2000) suggested that the two colony types formed by the clonogenic fraction of human prostate epithelial cells reflected different cell subpopulations. They suggested that the rarer type II colonies might be clones of stem cells, having indefinite proliferative capacity while being undifferentiated, while type I colonies might derive from transit amplifying cells as they were more differentiated and less proliferative. Thus type I colonies would be expected to reach replicative senescence sooner than type II cells. The proliferative potential of cells ring cloned from type I and type II colonies was assessed. Growth curves are shown in figure 3.3.

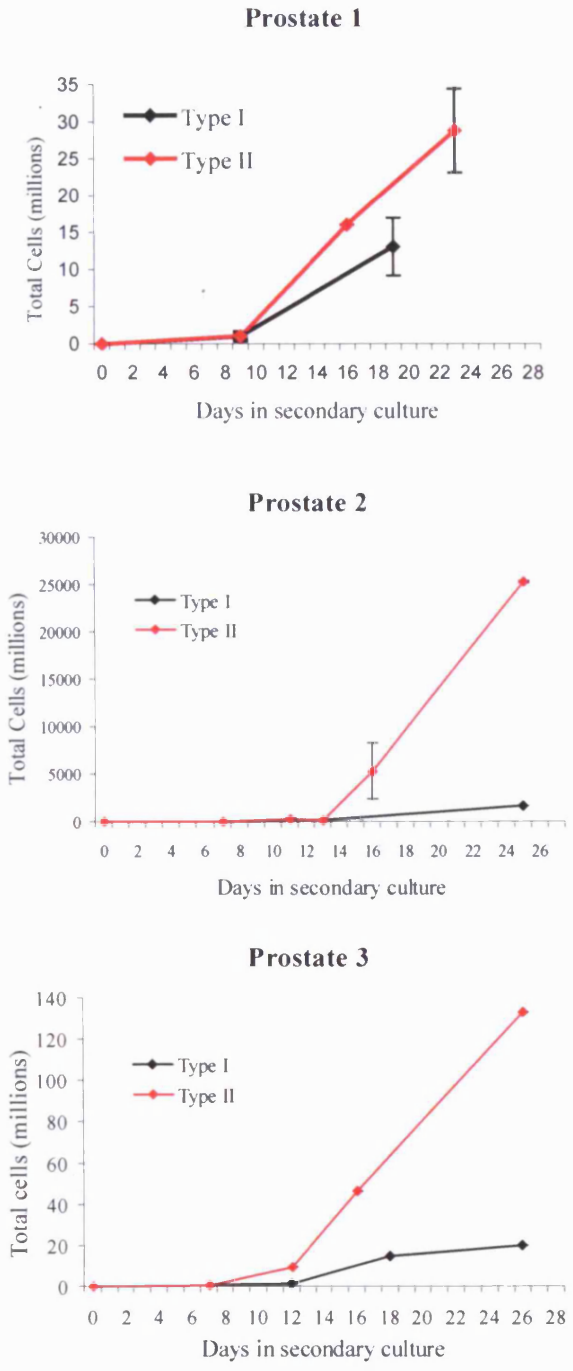

Figure 3.3: Proliferation of type I and II colonies. After 14 days in culture, 10,000 pooled type I or type II colony cells were cultured in 25cm^2 collagen coated flasks for 28 days. Flasks were counted when nearing confluency and 10,000 cells were passaged on. The mean total cumulative cell number for 2–5 flasks over days in secondary culture are shown for three separate patient prostate samples. Error bars show the standard error of the mean.

These growth experiments were terminated after 28 days due to attrition with infection. Three to four passages were necessary over this time. In some experiments the flasks were cultured for up to a further 2 weeks and none of these flasks approached confluency or required further passaging, though cell numbers were not counted in such dishes. Both colony types demonstrated significant proliferative ability, even though these cells were derived from primary colonies at 14 days that had already divided a mean of 11 times for type I colony cells and 17 times for type II colony cells. In secondary culture, each type I colony cell yielded between 1,300 and 168,000 cells (10 – 17 further doublings) and each type II colony cell between 2,900 and 253,000 cells (11 to 21 further doublings). Thus the most proliferative type I cells demonstrated 27 doublings in total from the time of initial plating to 42 days later, and type II cells demonstrated 38 total doublings. In each of the three samples, type II cells appeared more proliferative, though the few data points were not amenable to statistical comparisons so significance cannot be proven.

In 1961, Hayflick and Moorhead determined that human diploid cells underwent a total of 50 population doublings before undergoing growth arrest, termed cellular senescence (Hayflick and Moorhead, 1961). This Hayflick limit is thought not to apply to telomerase expressing cells such as stem cells and cancer (Rubin, 2002). Cells that are dividing have exponential growth curves, but as they senescence the curve plateaus, creating a sigmoid shape. Some of the cells in these experiments are approaching their Hayflick limit, and on the strength of the few data points here, there is a suggestion that the growth rates of type II cells in the first prostate and both types in the third are starting to slow down. It is not possible to comment on the other cells and a longer period in culture would have been desirable. The fact that the last passages failed to reach confluency suggests that a degree of senescence was occurring. In line with the hypothesis of Hudson *et al.* (2000), the TA cells in the type I colonies would be expected to senesce in contrast to self-renewing type II stem cells that should proliferate indefinitely. Given that these too appear to slow their growth, suggests either that these cells are in fact even earlier TA cells, or that the conditions of growth favour proliferation over self-renewal.

There is also extreme biological variation between these three patients with the cell yields differing by orders of magnitude. Such variation is already apparent in the colony forming abilities of different patients that differ 16-fold amongst ten patients. Formal quantification of these colonies proliferative abilities will require greater patient numbers and a longer duration in culture.

3.3 Three-dimensional culture of type I and type II colonies

Hudson *et al* (2000) demonstrated that ring cloned type II colonies produced three-dimensional structures in Matrigel culture, consistent with the differentiation that would be expected of possible stem cell derived colonies (though this assay does not conclusively demonstrate pluripotency). The ability of the type I colonies to form such structures was not explored.

In this study, ten thousand pooled type I or type II colony cells were cultured in Matrigel. After two weeks the resulting structures were harvested, paraffin embedded and stained for various cell markers. Figure 3.4 shows the microscopic appearance of the ducts and acini obtained and figure 3.5 the distribution of basal and luminal cell marker expression.

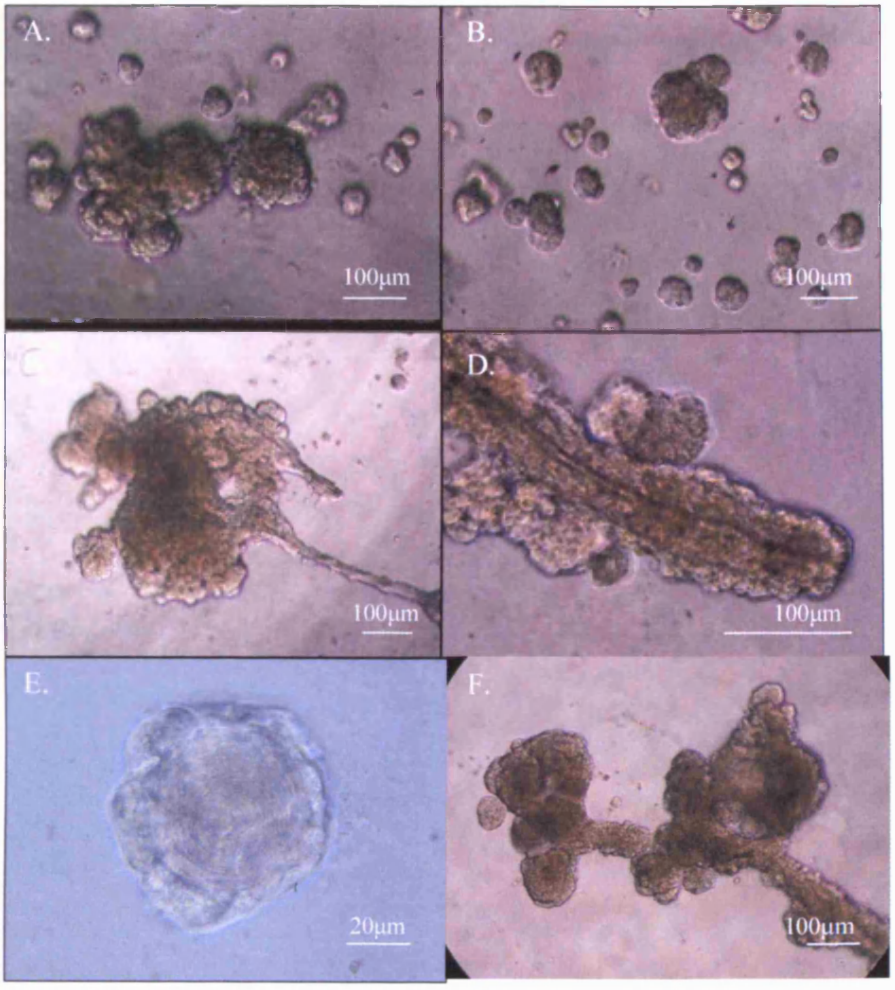

Figure 3.4: Appearances of acini and ducts obtained from pooled type I (A, C & E) or type II (B, D & F) colonies in Matrigel culture at 4 (A & B) and 14 days (C to F). Clumps of cells developed first with branches emerging after 6 days. These branches then formed an inner core structure, suggestive of a lumen after 10 days.

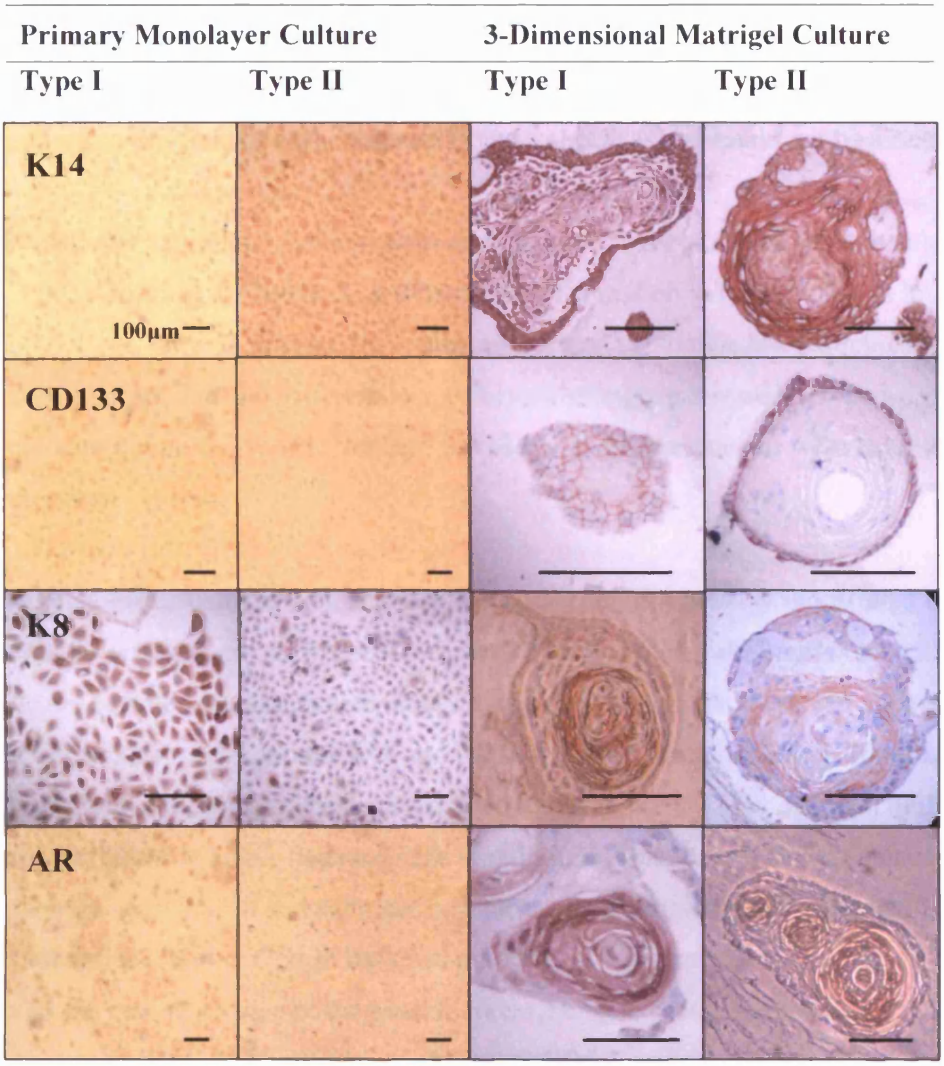

Figure 3.5: All scale bars are 100μm. Expression of prostate epithelial basal markers K14 and CD133, and luminal markers K8 and AR in monolayer primary and three-dimensional Matrigel secondary culture.

There was no difference in the number or appearance of structures formed by each colony type, with far more spherical acinar structures than ducts seen. Some cells added onto the Matrigel migrated to the base of the well and grew in monolayer culture so the yield of each structure from total cells added could not be assessed.

Monolayer expression patterns were as expected (Fry *et al*, 2000; Hudson *et al*, 2000; Hudson *et al*, 2001). K14 showed little expression in type I colonies in monolayer, but was moderately expressed in type II colonies. K8, expressed by transit amplifying and differentiated cells was strongly expressed in type I primary colonies but not in type II. Neither CD133 nor androgen receptor were expressed in monolayer culture.

Immunohistochemistry of the acinar and duct structures better demonstrated their cellular arrangement as different layers were picked out by different markers. Three layers could be discerned: a continuous single cell outermost layer that stained for basal and stem cell markers K14 and CD133, further similar layers within this that were similarly tightly packed and positive for basal marker K14 and then multiple further layers of larger flattened cells that defined a lumen that also contained cells. Luminal markers K8 and androgen receptor were expressed only in this last layer. Cell surface marker CD133 has been proposed as a prostate stem cell marker and was the most exclusive of the basal markers, being expressed in a subset of those expressing K14. The appearances of several CD133 positive layers in the type I structure shown in figure 3.5 may reflect an early 'acinus' in the process of forming a lumen, or a cross-section taken through the edge of an 'acinus'. K14 expression was seen to a lesser extent in the luminal layers, which may represent a high background given the strong basal staining seen, as this marker has been described as exclusively basal (Hudson *et al*, 2001).

Three dimensional secondary culture did produce heterogeneous structures with basal and luminal layers typical of prostate epithelium *in vivo* from a type I or II colony cell population, though there were no distinguishing features between them. This alone does not give sufficient evidence for self-renewal as both transit amplifying cells and stem cells would be expected to demonstrate such proliferative

abilities. Such proof would require a second generation Matrigel structure derived from selected cells of the first.

Matrigel also induced the expression of markers not seen in monolayer culture. These were early basal markers such as CD133 and markers of terminal differentiation such as androgen receptor (Richardson *et al*, 2004). The cells comprising each colony type were therefore sufficiently undifferentiated to express this marker of stem and early TA cells. It can only be assumed that the fact that they did not do so in monolayer culture (where they were surely no more differentiated) is due to the culture environment. The *in vitro* expression of CD133 in prostate epithelial populations has not been reported, as it is usually sought in freshly sorted cells or prostate tissue sections.

Less clear, is why apparently more differentiated type I colony TA cells that express K8, lose this in Matrigel culture and express CD133 instead. The process of prostate differentiation is assumed to be one-way and irreversible, so type I cells should only be able to generate later basal layers and luminal ones. An explanation may be that the type I colonies are not as homogeneous as thought, and contain less differentiated cell within them. Type II cells may have contaminated the 10,000 ring-clone selected, pooled type I cells from the same dish, though no fewer structures were seen. There may have been luminal cell only structures within the Matrigel culture that were not recognized against a noisy background of cell debris. Alternatively, Matrigel may have the ability to induce basal marker expression in such cells, which either implies that keratins are not as indicative of the level of differentiation as previously thought, or that dedifferentiation has occurred. Dedifferentiation does occur and is driven by external signals, the ultimate example being the successful cloning of "Dolly" the sheep by implanting the nucleus of an adult mammary gland cell into an enucleated sheep oocyte. Here the nucleus of a terminally differentiated cell regained complete embryonic stem cell abilities (Wilmut *et al*, 1997). Lang *et al* (2001) studied the ability of seven-day-old cultured prostate epithelial cells to form 'spheroids' in Matrigel. They reported that $CD44^+$ cells did form structures, but $CD44^-$ cells did not. If dedifferentiation did not occur in that case, then it may be that type I colony cells do not need to dedifferentiate as they are sufficiently undifferentiated in themselves and will express a range of

markers dependant on their position within the structure and interactions with surrounding cells.

3.4 Comparison of gene expression profiles of type I and type II prostate epithelial colonies.

3.4.1 Optimising samples for gene expression analysis.

To compare the gene expression profiles of type I and type II prostate epithelial colonies it was important to ensure that the cells harvested were as representative and uniform as possible, both within and between patient samples. Ultimately, a total of six patients were used providing six paired type I and type II cRNA samples that were used for microarray analysis. A number of issues were addressed before the final experimental design was established.

3.4.1.1 Use of a single representative colony per patient versus pooling of cells from several colonies.

For gene chip analysis, the initial RNA requirement for application onto an Affymetrix gene chip was 20µl of 500ng/µl total RNA, equivalent to 10µg of sample in total. Alternatively, the incorporation of a double linear amplification step into the protocol reduces the minimum sample size required to 2µl of 100ng/µl total RNA, or 200ng of sample. It was therefore necessary to ensure sufficient RNA was obtainable from both colony types for every patient. While type I colonies are more frequently obtained than type II, they are less dense in cell number so total RNA yield is correspondingly lower per colony. To obtain enough total RNA either a single selected colony had to be further cultured until it yielded sufficient cells, or a number of representative colonies of the same type from the same patient could be harvested and the cells pooled.

Both these options were studied for three prostate samples.

A number of type I and type II colonies were ring cloned after 2 weeks in primary monolayer culture and the morphologies of cells and colonies during secondary

culture on feeders (the first passage of these cells) was assessed over the following 1–2 weeks. For one prostate, flasks were harvested for total RNA extraction once approximately 75% confluent. The results are shown in table 3.3.

Patient	Colony type	No. of cells transferred	Colony morphology when 75% confluent in secondary culture.	No. cells on day 12 ($x10^3$)	Total RNA yield (μg)
#1	I	5200	Loose type I colonies and scattered cells	284	26.9
		3300	"	100	10.9
		1700	"	522	36.8
		2700	"	106	11.5
		8100	"	163	15.4
		900	"	122	8.9
	II	50000	Loose type I colonies and scattered cells, no type II	689	30.6
		58000	"	490	32.1
		2200	"	233	26.1
		2800	"	228	17.0
		3200	"	344	37.4
		2100	"	552	39.4
#2	I	42000	Loose type I colonies and scattered cells	-	-
		21000	"		
		25000	"		
		10000	"		
		2500	"		
		45000	"		
	II	1100	Loose type I colonies and scattered cells, no type II	-	-
		20000	"		
		91000	"		
		27700	"		
		7000	"		
		7700	"		
#3	I	1800	Loose type I colonies and scattered cells	-	-
		1900	"		
		6200	"		
		8200	"		
	II	15400	Loose type I colonies and scattered cells, no type II	-	-
		23200	"		

Table 3.3: Outcome of ring cloning and passaging of individual type I and type II colonies.

There was a wide variability in cells transferred by ring cloning (table 3.3). In some cases the ring did not form a watertight seal with the flask leading to a leak of trypsin or the silicon grease used spread inwards to cover some cells. Some cells did not survive this traumatic procedure so only viable cells as assessed by trypan blue exclusion were counted, though the proportion of dead cells in a ring cloned cell suspension was from 0 to 29% (data not shown). Type I colony cells took longer to reach 75% confluence at around 11-14 days while type II took 9-11 days (data not shown). However in secondary culture (1st passage) the morphology of the loose colonies and scattered cells derived from type I and II colonies were indistinguishable. The typical appearances of a type I and a type II colony immediately prior to ring cloning and in secondary culture on feeders over 11 days is shown in figure 3.6. No type two colonies were seen in any of these or subsequent passages of primary epithelial cell colonies.

Though this experiment was intended to assess RNA yields, it was also a colony self-renewal assay. It is significant that putative type II colony stem cells were unable to recreate themselves a second time. In some cases, all cells from a primary colony were transferred, so even if a small population of stem cells remained in the type II colony at 14 days culture these should have been present in the first passage (barring traumatic cell death).

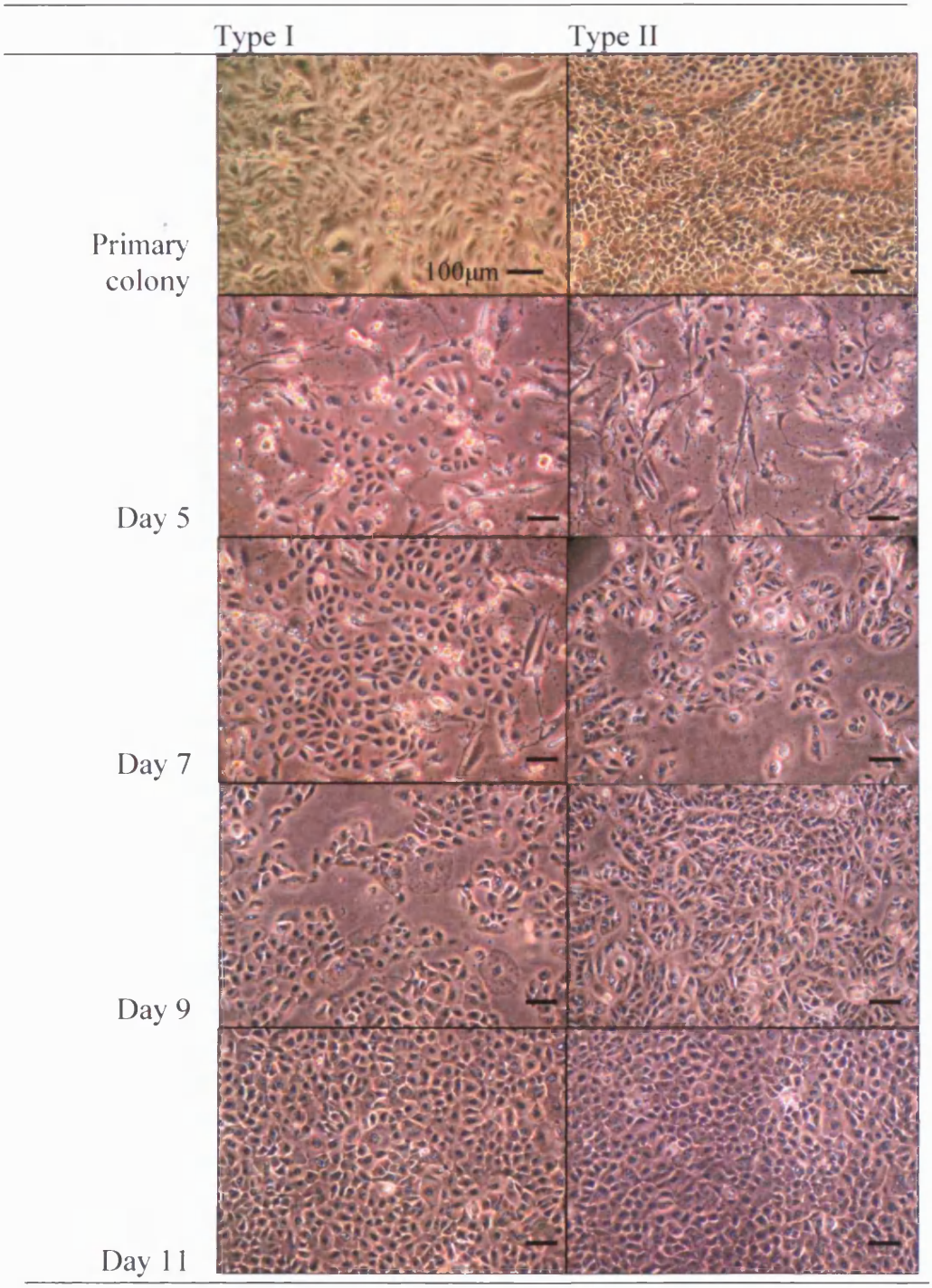

Figure 3.6: All scale bars are 100μm. The appearance of two colonies from prostate 2 in table 3.3 before ring cloning and at intervals during secondary culture on a feeder layer. The type I colony with a cell density of 27 cells/mm yielded 42,000 cells of which 10,000 were passaged. A type II colony with cell density 42 cells/mm yielded 7000 cells. At near confluence, the most compact areas of cells had a cell density of 20 cells/mm (see lowest panels) regardless of originating colony type.

Though the yield of total RNA from a single colony expanded by secondary culture was adequate for application onto a gene chip (average 24.4μg), the fact that no recognisable type II colonies were seen and that these passaged cells have not been previously characterised confirmed that this method could not be used to obtain total RNA for comparison of gene expression between these two morphologically defined primary colonies.

The alternative approach was to pool primary colonies of a similar type after two weeks in monolayer culture to obtain sufficient RNA. This would also allow an averaging out of morphologically similar colonies so that the characteristics of each type would be more likely to emerge from gene expression analysis. The RNA yields for three prostates are shown in table 3.4.

Patient	Colonies harvested		Mean harvested colony diameter in mm (s.d.)		No of cells harvested ($x10^3$)		Total RNA yield (μg)		RNA / colony (μg)	
	I	II	I	II	I	II	I	II	I	II
1	35	9	3.1 (4.0)	14.9 (4.3)	281	1990	2.6	27.6	0.07	3.07
2	32	4	4.8 (2.9)	10.8 (1.0)	571	249	8.6	3.78	0.27	0.95
3	18	9	5.4 (2.0)	14.1 (3.2)	-	-	10.5	74.5	0.58	8.28

s.d. = standard deviation

Table 3.4: Total RNA yield from pooled type I or type II primary colonies

Not all colonies were useable, depending on their location in the flask and relation to other colonies. The type I colonies obtained were not infrequently larger than those described by Hudson *et al* though they demonstrated typical type I morphology and cell density, and contrasted clearly with type II colonies within the same flask. The smallest colonies harvested contained 40 cells and had a diameter of 0.5mm. Pooling of like colonies provided sufficient total RNA for use on gene chips, though in all three patients the yields from one or both colony types were lower than the 10μg required to avoid an amplification step in the generation of cRNA for use on gene chips. Amplification has been shown to produce high fidelity microarray expression

data of comparable quality to non-amplified sample analysis (Jenson *et al*, 2003; King *et al*, 2005,).

3.4.1.2 Culture of prostate epithelial cells in the absence of a feeder layer.

The use of a feeder layer of mitotically arrested yet metabolically active cells has long been used in cell culture (Rheinwald and Green, 1975). Feeder cells promote proliferation of cells at low density through secreted conditioning factors; direct cell-surface contact and contributions to the basement membrane (Miller *et al*, 1982; Blacker *et al*, 1987). Irradiated or mitomycin C treated mouse 3T6 fibroblasts are used as standard in prostate epithelial cell culture. After two weeks of culture, the feeder cells were generally sparse, and it was possible that a few remained after rinsing off briefly with trypsin. It was felt preferable to grow cells without a feeder cell layer to avoid contamination of prostate colony RNA with feeder cell RNA and it was anticipated that conditioned PrEGM would at least contain the secreted molecules provided by the mouse fibroblasts. A number of different feeder-free culture conditions were tested (table 3.5).

CONDITIONS	Flasks with colonies / total flasks (total colony number)			
	1	2	3	4
Collagen + mouse 3T6 feeder layer	19/20 (107)	1/5 (1)	4/4 (17)	4/5 (22)
Collagen + PrEGM	-	0/5	0/4	0/4
Collagen + 2 day Conditioned PrEGM	-	0/4	0/5	0/5
Collagen + 2 day Conditioned PrEGM (frozen & defrosted)	-	0/5	-	0/4
Collagen + 3 day Conditioned PrEGM	3/5 (8)	0/4	-	0/4
Collagen + 4 day Conditioned PrEGM	-	0/5	0/5	0/4
Collagen + 4 day Conditioned PrEGM (frozen & defrosted)	-	0/4	-	0/4

Table 3.5: Colony yield in alternative feeder-layer free culture conditions.

The pH of these media remained within physiological levels ranging between 7.55 for PrEGM, and 7.22 for 2 day conditioned PrEGM (data not shown). All colonies obtained had typical appearances.

A feeder layer was essential for the primary culture of prostate epithelial cells. Colonies grown in such conditions had to be used as a source of RNA for use on gene chips, and type I cells due to the larger numbers harvested and their more sprawling morphology would be more likely to be contaminated. The sequences on the Affymetrix chip do have a degree of cross-reactivity with mouse sequences when the two genomes are compared.

3.4.2 Acquisition of total RNA from pooled type I and type II prostate epithelial colonies.

A series of patient prostate samples were cultured on collagen coated flasks with a feeder layer for two weeks. Colonies of each type were harvested separately and total RNA extracted as described. The patient characteristics, histological findings, colony yields and RNA extracted are given in table 3.6. In five out of nine patients, the RNA yield from one or both colony types was less than 10μg so a double linear amplification step was necessary, and used across all samples.

No.	Patient age	Clinical details	PSA (ng/dl)	Histology	Tissue weight	Acquired cells x 10^6 / g	Cells plated x10^3	Colonies grown		Colonies harvested		Total RNA yield (μg)	
								I	II	I	II	I	II
1	77	Moderate LUTS, on prazosin	2.1	BPH	0.2	0.72	24	35	10	34	9	2.6	27.6
2	73	Catheterized	unknown	BPH & chronic inflammation.	1.4	3.40	28	59	5	32	4	8.6	3.78
3	57	LUTS, failed medical management	4.5	BPH	0.6	1.55	24	57	12	18	9	10.5	74.5
4	80	Re-do TURP previous TURP 1992	2.0	BPH	0.5	4.90	28	111	13	14	7	2.9	24.0
5	68	Catheterized	unknown	BPH with foci of fibrosis	0.3	0.28	24	21	5	11	5	1.5	14.3
6	61	LUTS on tamsulosin	0.8	BPH	0.7	2.80	25	54	9	36	8	15.3	25.5
7	60	mild/moderate LUTS on tamsulosin	2.2	BPH	0.4	0.11	27	90	20	35	12	6.2	27.1
8	58	LUTS	1.6	BPH	0.3	0.33	25	62	10	22	10	13.5	82.7
9	71	Catheterized	7.4	BPH	0.6	6.10	27	86	14	30	14	38.3	31.0
Mean	67		2.9		0.6	2.20	26	63.9	10.9	25.9	8.8	11.0	34.5
s.d.	8.6		2.3		0.4	2.20	1.7	27.9	4.6	9.8	3.2	11.3	26.4

LUTS = lower urinary tract symptoms, TURP = transurethral resection of the prostate, BPH = benign prostatic hyperplasia, s.d. = standard deviation

Table 3.6: Culture of primary prostate epithelial cells: patient characteristics, histology, and colony and total RNA yields.

3.4.3 Concentration of dilute total RNA samples

For each sample, total RNA was extracted from type I and II colony cell lysates in parallel. The RNA quality was expressed as the 28S/18S rRNA signal ratio; the degradation factor and the colour of the quality range it fell into; and visually as an electropherogram and gel image. All samples contained sufficient total RNA, but nine were too dilute at <100ng/µl. These were concentrated by nitrogen gas evaporation and then reassessed. Table 3.7 shows the concentration steps and characteristics of the nine samples.

Patient	RNA sample		Volume (µl)	Concn (ng/µl)	Total RNA yield (µg)	28S/18S rRNA ratio	Degrad-ation factor	Quality range colour
1	I	eluted	150	17	2.6	2.0	12.79	yellow
		concentrated x1	10	76	0.8	1.5	8.61	yellow
		concentrated x2	5	169	0.8	2.0	6.07	none
3	I	eluted	500	21	10.5	1.5	9.78	yellow
		concentrated	47	641	30.1	1.6	14.99	yellow
	IIb*	eluted	500	72	36.0	1.6	11.22	yellow
		concentrated	45	1225	55.1	1.2	14.94	yellow
4	Ia*	eluted	90	26	2.3	1.5	17.24	orange
		concentrated	20	114	2.3	2.1	12.33	yellow
5	Ib	eluted	50	17	0.8	1.3	9.63	yellow
		concentrated	10	135	1.4	1.7	14.11	yellow
6	Ia	eluted	70	84	5.9	2.0	9.51	yellow
		concentrated	25	206	5.2	1.8	10.92	yellow
7	Ia	eluted	85	47	4.0	1.8	11.92	yellow
		concentrated	30	181	5.1	2.1	9.70	yellow
9	I	eluted	500	77	34.3	2.1	4.55	none
		concentrated	20	1831	36.6	2.0	2.33	none
	II	eluted	500	62	31.0	1.8	9.05	yellow
		concentrated	22	1476	29.5	1.8	9.76	yellow

* a and b denote first and second elution of RNA through the same extraction column collected as separate samples.

Table 3.7: Concentration of RNA samples by nitrogen evaporation. The degradation factor and the quality range (denoted by colours from none, through yellow, orange, red and black) are objective measures of RNA sample integrity as devised by Auer *et al* (2003, see section 2.15).

Concentrating the samples did alter 28S/18S rRNA ratios and degradation factors though not in a predictable way. The ratio is a less accurate measure of RNA integrity as equal degradation of both rRNAs would lead to a worsening in degradation factor while the ratio would remain unchanged. There can be no improvement in RNA integrity by this evaporation process but the improved signal to noise ratio of a more concentrated sample may lead to more accurate measurement by the bioanalyser. In general, no sample was ruined by the process and all remained suitable for use on a gene chip (see figure 3.7).

At times evaporation appeared to increase total RNA amounts in the sample. This enigma relates to the degree of error in measuring small volumes. In the Agilent process, accuracy when quantitating 25-500ng/µl RNA concentrations is of ± 50% (manufacturer's specifications).

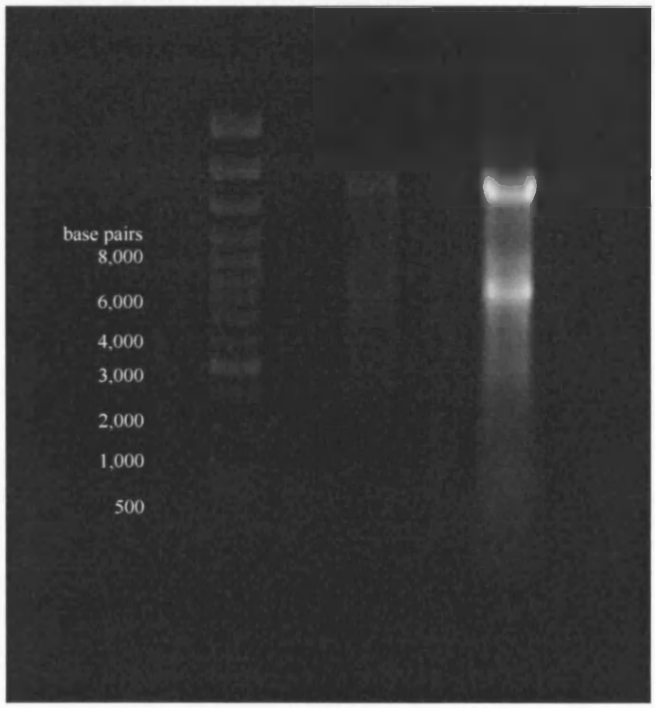

Figure 3.7: Agarose gel electrophoresis of total RNA samples before and after nitrogen gas concentration. 10µl of total RNA solution was run with 5µl gel dye buffer and a 1kb ladder on a 1% agarose gel. The more concentrated sample appeared to retain the desired relative 2:1 intensity of the two 18S and 28S rRNA bands suggesting little degradation occurred.

3.4.4 Choice of RNA samples for gene chip analysis

All RNA samples ultimately obtained from nine patients are shown in table 3.8. Five paired samples (patients 1,4,6,7 and 9) were chosen with a sixth reserve sample (patient 5). A degradation quality range of none or yellow was required, and where possible an rRNA ratio >1.6. Figure 3.8 shows the electropherograms and gel appearances of the 'worst' sample; patient 3 colony type II, and the 'best'; patient 9, colony type I.

Patient	Colony type	Volume (µl)	Conc^{n} (ng/µl)	Total RNA yield (µg)	28s/18s rRNA ratio	Degradometer factor	Colour of quality range	Usage of sample
1	**I**	**5**	**169§**	**0.8**	**2.0**	**6.07**	**none**	**used**
	II	**50**	**552**	**27.6**	**1.8**	**2.70**	**none**	**used**
2	I a•	600	9	5.5	1.1	25.24	red	discarded
	I b•	170	18	3.1	1.2	17.03	orange	discarded
	II	180	21	3.8	1.2	23.17	orange	discarded
3	I	47	641§	30.1	1.6	14.99	yellow	not used
	II a	500	77	38.5	1.5	9.63	yellow	not used
	II b	45	1225§	55.1	1.2	14.94	yellow	not used
4	**I a**	**20**	**114§**	**2.3**	**2.1**	**12.33**	**yellow**	**used**
	I b	50	12	0.6	1.3	unrecordable	black	discarded
	II a	50	182	9.1	2.1	6.66	none	not used
	II b	**90**	**166**	**14.9**	**2.1**	**6.48**	**none**	**used**
5	I a	80	9	0.7	0	unrecordable	black	discarded
	I b	**10**	**135§**	**1.4**	**1.7**	**14.11**	**yellow**	**used in reserve**
	II	**120**	**119**	**14.3**	**2.2**	**5.61**	**none**	**used in reserve**
6	**I a**	**25**	**206§**	**5.2**	**1.8**	**10.92**	**yellow**	**used**
	I b	100	94	9.4	1.0	24.48	red	discarded
	II a	**90**	**227**	**20.4**	**3.0**	**3.71**	**none**	**used**
	II b	60	85	5.1	2.3	4.96	none	not used
7	**I a**	**30**	**181§**	**5.1**	**2.1**	**9.70**	**yellow**	**used**
	I b	95	23	2.2	1.0	unrecordable	black	discarded
	II a	**75**	**253**	**19.0**	**2.3**	**9.27**	**yellow**	**used**
	II b	70	116	8.1	2.1	10.01	yellow	not used
8	I	155	87	13.5	1.9	25.35	red	discarded
	II a	90	766	68.9	2.2	2.07	none	not used
	II b	35	395	13.8	2.3	2.03	none	not used
9	**I**	**20**	**1831§**	**36.6**	**2.0**	**2.33**	**none**	**used**
	II	**22**	**1476§**	**29.5**	**1.8**	**9.76**	**yellow**	**used**

- a and b denote first and second elution of RNA through the same extraction column collected as separate samples, § = these samples were concentrated using nitrogen evaporation prior to being used, Conc^{n} = concentration

Table 3.8: Characteristics of paired colony total RNA samples (chosen 6 in bold)

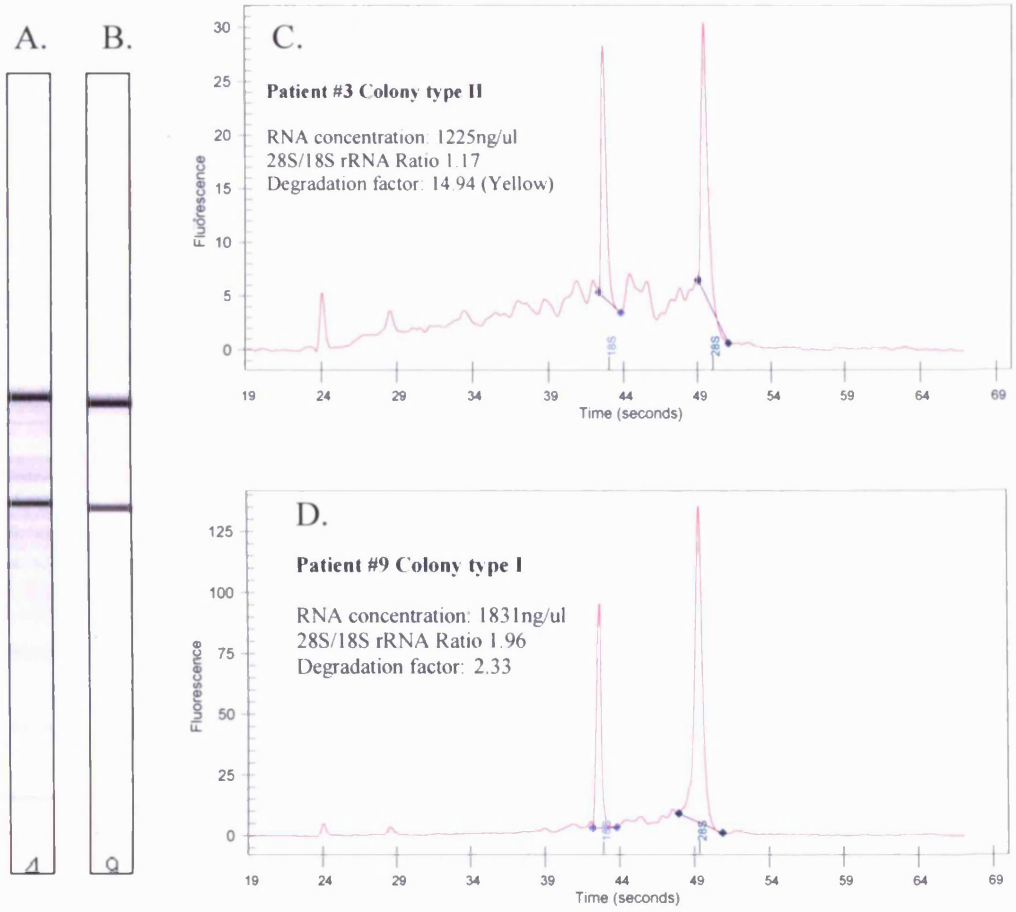

Figure 3.8: Agilent bioanalyser electropherograms and gel images for two total RNA samples for GeneChip analysis. A & B: gel image a from patient #3 sample showed some degradation in comparison to gel image B, from patient #9. C & D: corresponding electropherograms for these two samples. As total RNA degraded, strands were shortened. The ratio between the 28S and 18S rRNA peaks reduced and a higher baseline level of smaller RNAs was seen as shown by C in comparison to D.

3.5 GeneChip Quality control parameters

Quality control measurements are shown in table 3.9. There were high background (ideally 20-100) and noise (ideally <4) readings on the first type II chip which obscured low-level gene expression and lead to correspondingly fewer probe sets being detected (% present should have been similar for all chips). Hybridization was universally successful, however the desired >70% detection of the *B. subtilis lys* probe set was not achieved (58% present), suggesting reduced efficiency of the poly-

A primer binding and possibly reduced sensitivity. The 3'/M ratio of the GAPDH gene was well preserved though values for β-actin suggested some degradation, even allowing for the fact that it is a longer gene. In an investigation of the quality control criteria of Affymetrix gene chips, Dumur *et al* (2004) found that the recorded intensities of the 3' β-actin probe set were sensitive to experimental variations such as day to day variability and RNA source, while other probe sets were not. They suggested that these changes might be related to a rather less robust probe design than actual differences in the concentration of that particular transcript, so the GAPDH results here may be more accurate.

Overall, all chips were of acceptable quality and could be analyzed, though the potential reduced sensitivity of some chips was noted. In reality, the implications of variations in quality control parameters and therefore their usefulness in distinguishing between analytical and biological variability remains unsubstantiated (Allison *et al*, 2006; Dumur *et al*, 2004).

	Type I colonies						Type II colonies					
Prostate #	1	4	5	6	7	9	1	4	5	6	7	9
Mean background	56.3	44.9	56.2	42.2	45.0	44.3	101.9	43.7	55.8	34.3	35.8	45.3
Mean noise	1.9	1.5	1.9	1.4	1.6	1.5	4.9	1.4	1.9	1.1	1.2	1.5
B. subtilis lys present	No	Yes	No	Yes	Yes	No	No	Yes	Yes	Yes	Yes	No
E. coli bioB present	Yes	Yes	Yes	Yes	Yes	Yes	Yes	Yes	Yes	Yes	Yes	Yes
% probe sets present	35	41	40	41	38	33	28	40	39	38	37	35
GAPDH 3'/M ratio	1.2	1.2	1.2	1.2	1.5	1.5	1.2	1.4	1.1	1.3	1.3	1.5
β-actin 3'/M ratio	3.7	2.0	3.2	3.7	5.5	4.0	4.3	4.0	3.4	3.5	6.2	4.5
Scaling factor	1.1	1.3	0.8	1.3	1.7	1.7	1.2	1.5	1.0	2.5	2.3	1.4

Table 3.9: Quality control parameter outcomes for each GeneChip

The inherent variability between replicates was also assessed using logistic regression. When the raw data from two type I or type II samples was plotted against each other the line of best fit correlated with R values between 0.64 and 0.80 (see table 3.10. Both type I and II replicates were similarly variable. One such plot is

shown in figure 3.9. Such variability was expected in a small experiment based on 6 individual patients but will result in more subtle differences in gene expression being overlooked.

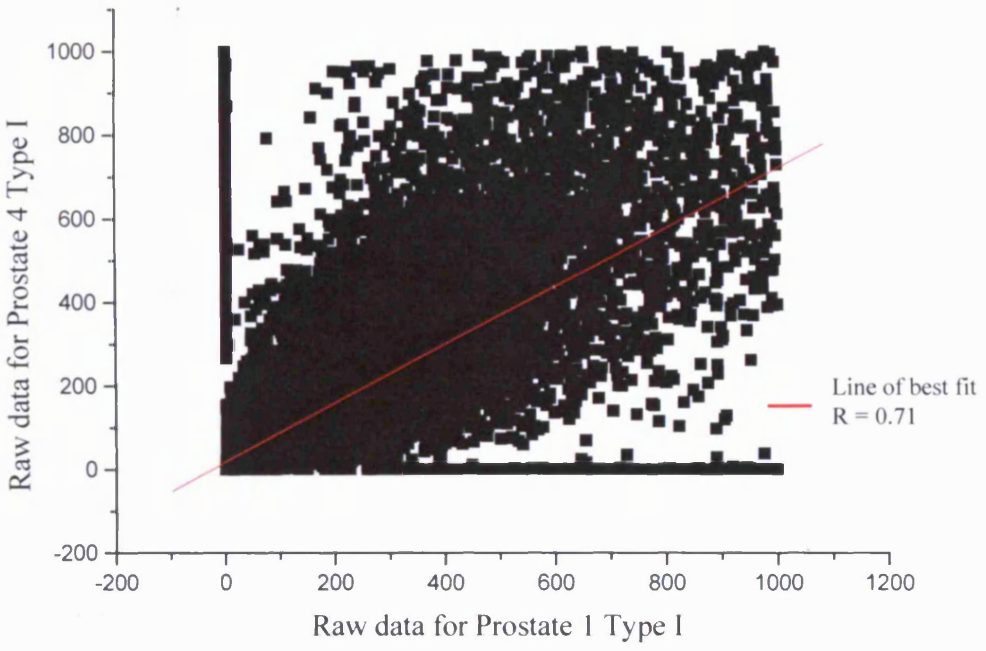

Figure 3.9: Graph of Prostate 1 type I colony raw signal intensity data plotted against Prostate 4 type I raw data.

Type I Colonies	1	4	5	6	7	9
1	1	0.71	0.80	0.72	0.77	0.70
4	0.71	1	0.73	0.80	0.75	
5	0.80	0.73	1	0.74	0.79	0.70
6	0.72	0.80	0.74	1	0.76	0.71
7	0.77	0.75	0.79	0.76	1	0.68
9	0.70	0.64	0.70	0.71	0.68	1
Type II colonies	1	4	5	6	7	9
1	1	0.70	0.71	0.72	0.70	0.72
4	0.70	1	0.76	0.77	0.77	0.71
5	0.71	0.76	1	0.74	0.80	0.72
6	0.72	0.77	0.74	1	0.72	0.67
7	0.70	0.77	0.80	0.72	1	0.79
9	0.72	0.71	0.72	0.67	0.79	1

Table 3.10. Logistic regression values of R when type I or type II sample raw signal intensity data is compared.

3.6 Validation of cDNA microarrays using RT-PCR

The expression array findings were validated using semi-quantitative RT-PCR of the same RNA samples and primer sequences equivalent to those on the GeneChip. There was insufficient remaining RNA from prostate #5 so this was omitted. Five genes were chosen that were present on all sample arrays and showed a large fold-change which was also statistically significant. The RT-PCR results are shown in figure 3.10.

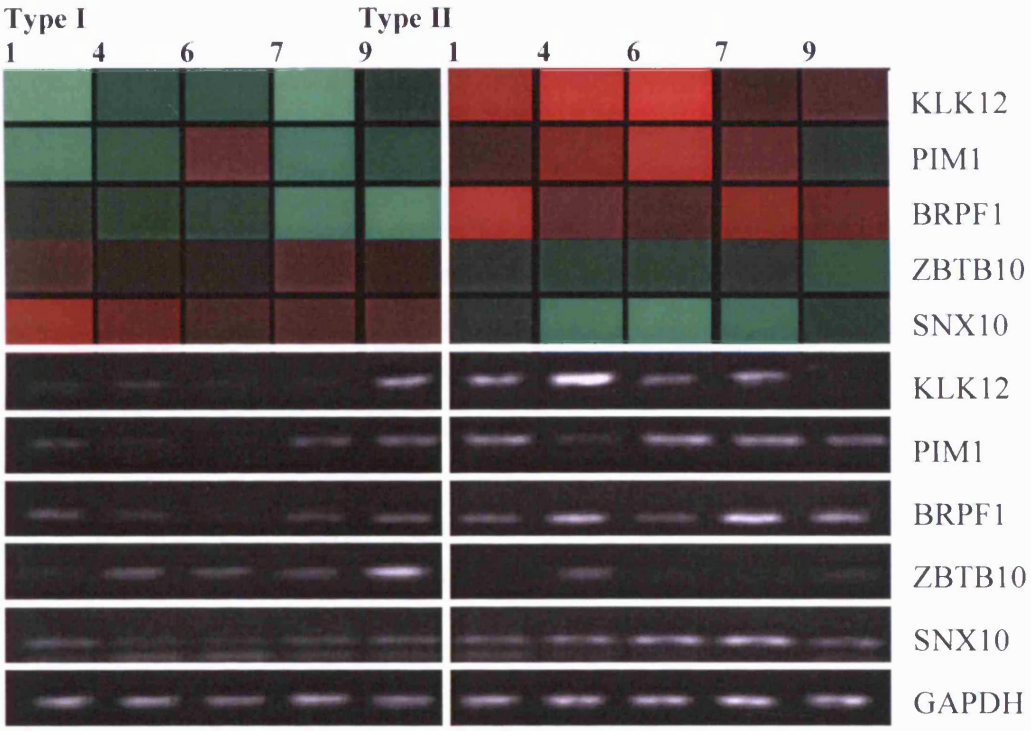

Figure 3.10: Validation of expression levels on GeneChip using RT-PCR for five genes with GAPDH control.

The heatmap squares were coloured red for those genes upregulated compared to the median value of all genes on all chips and green for those downregulated. The intensity of the colour was determined by the extent of upregulation and also the degree of 'trust' i.e. statistical significance that could be attributed to the result. The intensity of the RT-PCR product bands compared reasonably well to the expression levels suggested by the GeneChips for genes KLK12, PIM1, BRPF1 and ZBTB10. Even where gene products were seen in specimens in which they were

downregulated, the band was more intense in the opposite colony type confirming the correct differential gene expression. The RT-PCR results were poorly representative of the GeneChip results for SNX10, and the prostate sample 9 most often contradicted the array results.

The underlying variability of expression levels for individual genes between samples is clear both from the RT-PCR and the heatmap appearances, though not always appreciated when comparing the two colony types on the basis of their overall expression level and p-value. Some disagreement was to be expected. Due to the small number of specimens in the experiment, the identification of significant results could not incorporate a multiple testing correction step as these were too stringent. As such corrections aim to reduce the false discovery rate, without them some genes may be false positives. Finally, though genes showing the highest fold-change difference are often selected for validation, it has emerged more recently that this is not always optimum as 'regression toward the mean' by such outlying results tends to underestimate overall agreement levels between microarrays and validation samples (Dhanasekaran *et al*, 2001; Miron *et al*, 2006). On the basis of these results, further expression array analysis was undertaken but with the exclusion of sample 9.

3.7 Identification of differential gene expression between type I and type II colonies using cDNA microarrays.

This relatively simple experiment consisted of 2 conditions (RNA from type I or II colonies derived from the same patient) with 6 biological replicates. Initial filtering by fraction Present reduced 54,675 genes to 22,486. An ANOVA at $p \leq 0.05$ with cross gene error model applied further reduced this to 874 genes. The hierarchical cluster diagram of these is shown in figure 3.11.

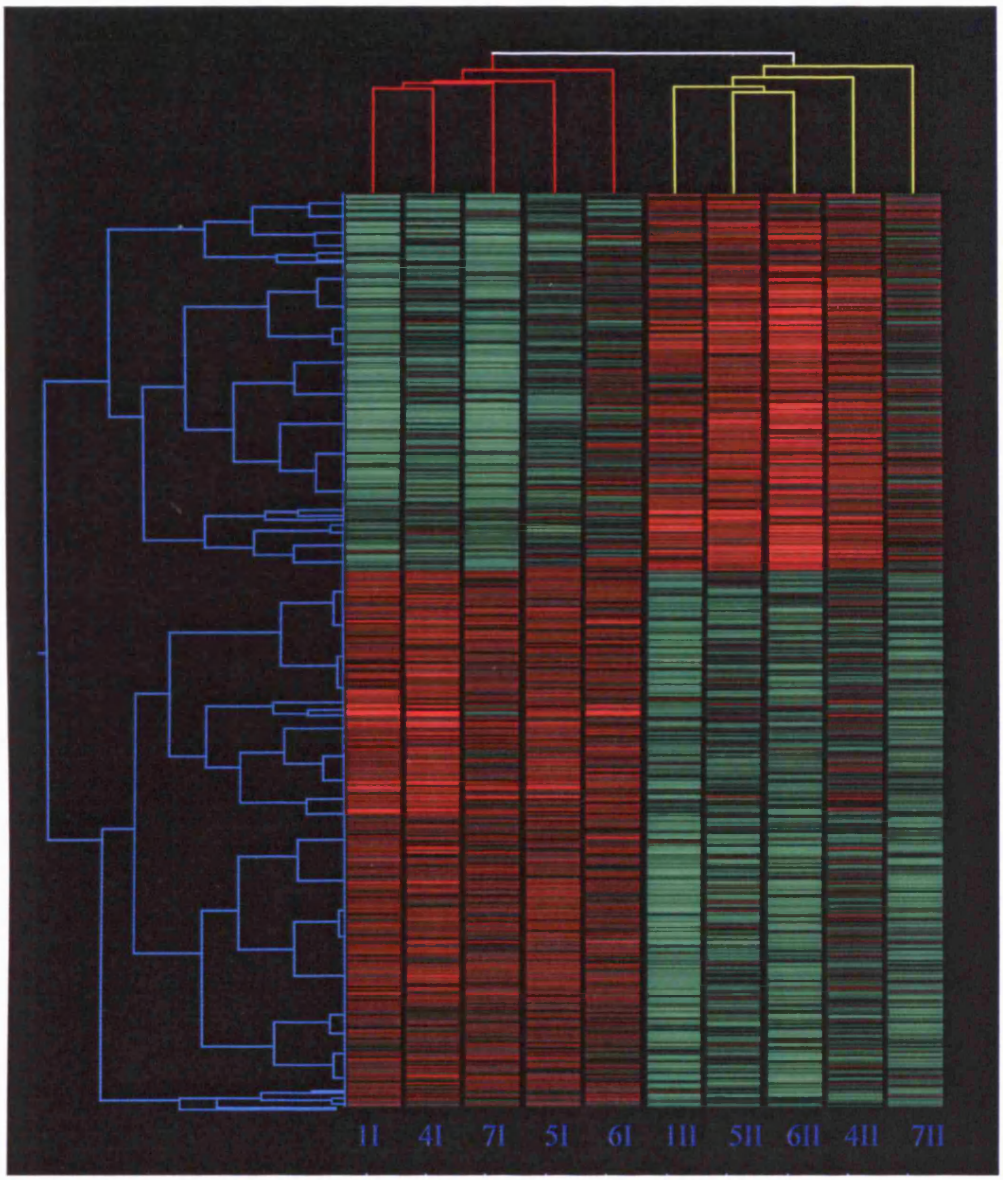

Figure 3.11: Normalised dye intensities for 874 genes significantly ($p \leq 0.05$) differentially expressed between type I and type II colonies. Red denotes up-regulation or increased expression relative to the global mean level of dye intensity, while green denotes down-regulation or reduced gene expression. A hierarchical clustering algorithm was used to group genes and samples on the basis of similarities of gene expression. The relationship between the genes or samples were demonstrated by the arrangement and length of the branches of the dendrograms.

From these 874 genes, a list of the 200 most significant genes (with a p value cut off of <0.0126) and a list of the 200 genes with the greatest difference in expression (with a fold-change of >2.88) was generated. Ninety-three genes common to both lists were chosen for further consideration. The distribution of these genes is demonstrated in a 'Volcano Plot' in figure 3.12. Thirty-six genes were upregulated in type I and 57 were upregulated in type II colonies. A hierarchical cluster diagram of these genes suggested six main clusters, so k-means clustering was performed using 6 starting nodes. The processing of the normalized expression data is shown in a flow diagram in figure 3.13. The clusters generated are shown as a scatter diagram in figure 3.14. The genes are listed in their clusters in table 3.11.

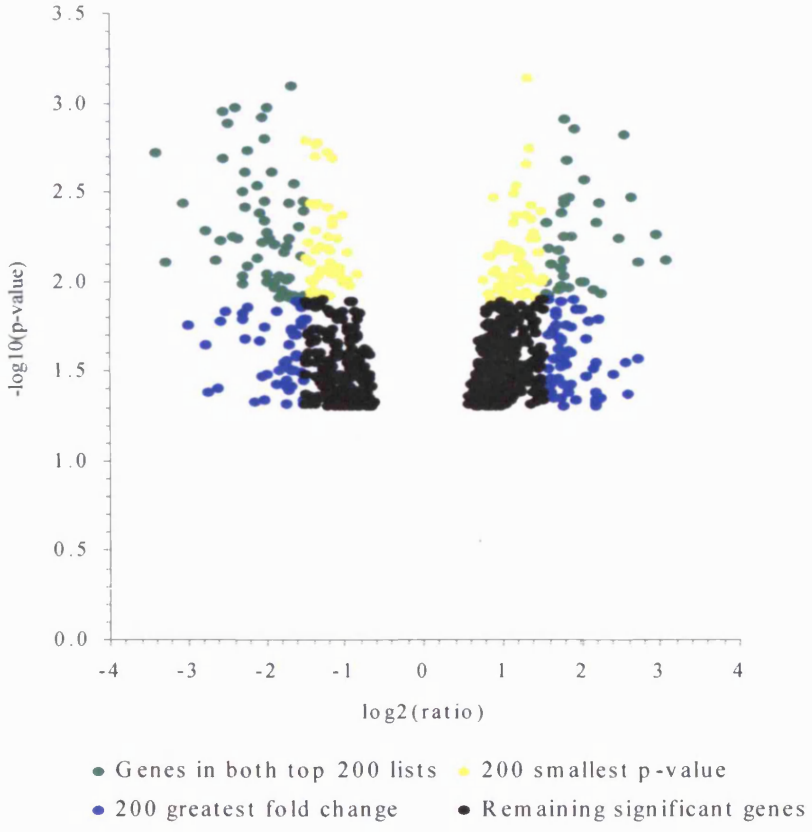

Figure 3.12: Volcano plot of all 874 selected genes showing their degree of differential expression (fold change or ratio of type I to type II) and their significance (as the p value derived from the ANOVA). A $\log^2$(ratio) of –1 is equivalent to a two-fold higher expression of the gene in type II colonies compared to type I. Blue and

green data points represent the 200 genes with the greatest fold change. Yellow and green points represent those 200 genes with the highest significance. Green data points demonstrate the 93 genes common to both groups.

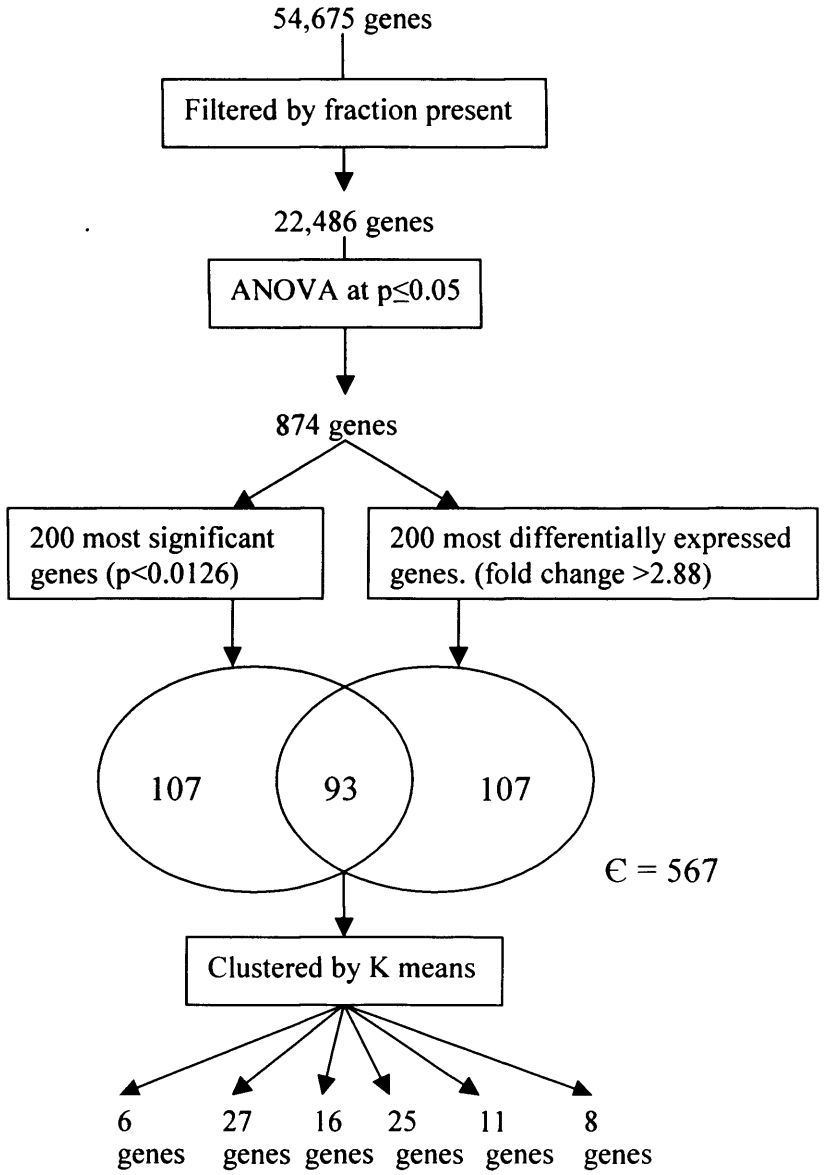

Figure 3.13: Flow diagram showing selection of the most significant and differentially expressed genes from the original normalised GeneChip data.

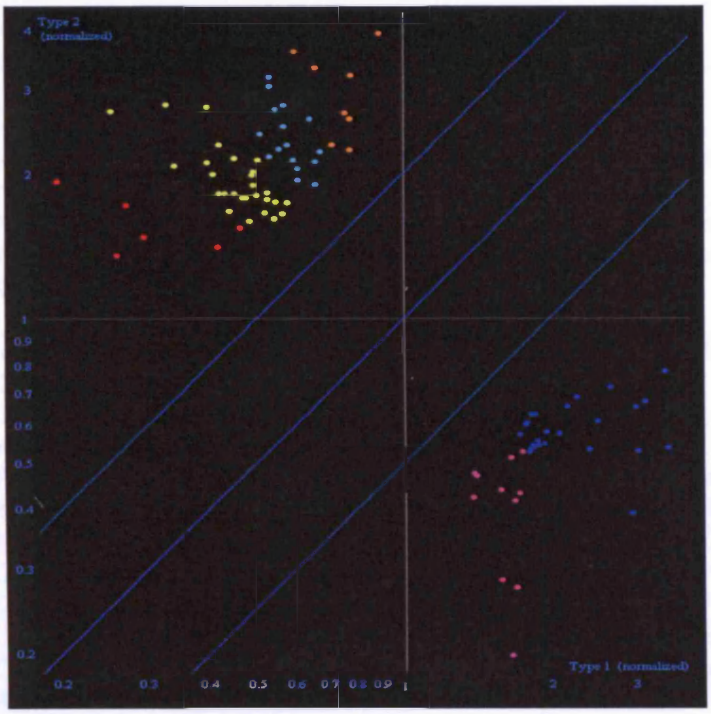

Figure 3.14: Scatter diagram showing the relationship of genes between clusters. Those 36 genes upregulated in type I colonies were divided into 2 clusters shown as blue (25 genes) and purple (11 genes) and those upregulated in type II were divided into 4 clusters: red (6 genes), yellow (27 genes), cyan (16 genes and orange (8 genes).

Cluster #	Common name	p value	Fold change	Description
		GENES UPREGULATED IN TYPE II COLONIES		
1	ZNF540	0.006	5.236	zinc finger protein 540
1	DKFZp686O1327	0.006	3.344	hypothetical gene supported by BC043549; BX648102
1	ATP6V1C2	0.008	6.369	ATPase H^+ transporting, 42kDa, V1 subunit C2
1	KRTDAP	0.008	9.901	keratinocyte differentiation-associated protein
1	UPK1A	0.010	5.025	uroplakin 1A
1		0.012	3.378	Transcribed locus.
	C10orf99	0.001	5.348	chromosome 10 open reading frame 99
	KLK12	0.001	4.255	kallikrein-related peptidase 12
	ALOX12B	0.002	10.753	arachidonate 12-lipoxygenase, 12R type
	ANKRD22	0.002	3.846	ankyrin repeat domain 22
	GDPD3	0.004	4.115	glycerophosphodiester phosphodiesterase 3
	SDR-O	0.004	8.547	orphan short-chain dehydrogenase / reductase
	IL1F5	0.004	2.933	interleukin 1 family, member 5δ
	HPGD	0.008	4.785	hydroxyprostaglandin dehydrogenase 15-NAD
	HPGD	0.004	4.926	hydroxyprostaglandin dehydrogenase 15-NAD
	HPGD	0.004	4.348	hydroxyprostaglandin dehydrogenase 15-NAD
	BBOX1	0.005	3.012	butyrobetaine γ, 2-oxoglutarate dioxygenase 1
	MUC15	0.005	6.944	mucin 15
	MUC15	0.006	5.464	mucin 15
	HAL	0.005	4.082	histidine ammonia-lyase
	OLAH	0.006	6.098	oleoyl-ACP hydrolase
	PIP5K1B	0.006	4.255	phosphatidylinositol-4-phosphate 5-kinase, type Iβ
	ICEBERG	0.006	3.802	ICEBERG caspase-1 inhibitor
	ATP13A4	0.007	3.497	ATPase type 13A4
	LOC196264	0.007	2.976	hypothetical protein LOC196264
	SPINK5	0.009	3.610	serine protease inhibitor, Kazal type, 5
	CYP4F3	0.010	3.367	cytochrome P450, family 4F, polypeptide 3
	RAPGEFL1	0.010	4.049	RAP guanine-nucleotide-exchange factor-like 1
	SLURP1	0.010	3.817	secreted LY6/PLAUR domain containing 1
	TREM1	0.011	3.745	triggering receptor expressed on myeloid cells 1
	KLK7	0.012	3.205	kallikrein-related peptidase 7
	GRHL1	0.012	3.311	grainyhead-like 1 (Drosophila)
	A2ML1	0.013	3.205	alpha-2-macroglobulin-like 1
3	KLK12	0.001	4.065	kallikrein-related peptidase 12
3	KLK12	0.002	4.098	kallikrein-related peptidase 12
3	RPTN	0.001	5.714	repetin
3	WFDC12	0.002	4.762	WAP four-disulfide core domain 12
3	ACPP	0.002	5.988	acid phosphatase, prostate
3	CLDN17	0.002	4.902	claudin 17
3	BNIPL	0.003	3.205	Bcl2/adenovirus E1B 19kD interacting protein like
3	BPIL2	0.003	4.405	bactericidal/permeability-increasing protein-like 2
3	LOC147645	0.003	4.975	hypothetical protein LOC147645
3	ATP6V1C2	0.004	3.289	ATPase, H+ transporting, 42kDa, V1 subunit C2
3	MARCH3	0.006	4.000	membrane-associated ring finger (C3HC4) 3
3	KRT78	0.006	3.378	keratin 78 / keratin 5b
3	LCE3D	0.009	4.065	late cornified envelope 3D
3	HOP	0.012	3.226	homeodomain-only protein
3	ELOVL4	0.012	2.882	elongation of very long chain fatty acids-like 4
3	RASGEF1B	0.012	3.597	RasGEF domain family, member 1B

4	OVOL1	0.001	3.226	ovo-like 1(Drosophila)
4	NDRG2	0.004	2.899	NDRG family member 2
4	SASP	0.005	4.115	skin aspartic protease
4	AZGP1	0.007	4.405	alpha-2-glycoprotein 1, zinc-binding
4	LCE1B	0.010	3.356	late cornified envelope 1B
4	SPRR2B	0.011	3.534	small proline-rich protein 2B
4	SPRR2G	0.001	6.061	small proline-rich protein 2G
4	SPRR3	0.009	5.025	small proline-rich protein 3
		GENES UPREGULATED IN TYPE I COLONIES		
5	PTGS2	0.006	3.414	prostaglandin-endoperoxide synthase 2
5	KRTAP2-1	0.008	6.502	similar to keratin associated protein 2-4
5	CCND2	0.007	2.953	cyclin D2
5	TGM2	0.013	2.929	transglutaminase 2 (C polypeptide)
5	VIM	0.001	3.374	vimentin
5	NNMT	0.008	3.292	nicotinamide N-methyltransferase
5	PLOD2	0.011	3.293	procollagen-lysine, 2-oxoglutarate 5-dioxygenase 2
5	FBN1	0.006	3.604	fibrillin 1 (Marfan syndrome)
5	IL8	0.005	4.508	interleukin 8
5	CXCL1	0.001	3.696	chemokine (C-X-C motif) ligand 1α
5	L1CAM	0.003	3.372	L1 cell adhesion molecule
5	SLC26A2	0.004	3.393	solute carrier family 26 member 2 -sulfate transport
5	FAP	0.004	4.572	fibroblast activation protein, alpha
5	FN1	0.011	4.425	fibronectin 1
5	COL5A1	0.009	3.369	collagen, type V, alpha 1
5	DCBLD2	0.002	5.722	endothelial and SM cell-derived neuropilin-like
5	COL3A1	0.012	4.663	collagen, type III, alpha 1
5	NEFL	0.006	7.547	neurofilament, light polypeptide 68kDa
5	RBM22	0.005	2.887	RNA binding motif protein 22
5	MAP1B	0.008	3.016	microtubule-associated protein 1B
5	REPS2	0.010	2.928	RALBP1 associated Eps domain containing 2
5	CTSB	0.003	4.085	cathepsin B
5	PGM2L1	0.002	3.456	phosphoglucomutase 2-like 1
5	PHLDB2	0.003	3.531	pleckstrin homology-like domain, family B, 2
5		0.008	3.427	
6	ZBTB10	0.003	6.146	zinc finger and BTB domain containing 10
6	GLIPR1	0.004	3.312	GLI pathogenesis-related 1 (glioma)
6	GLIPR1	0.007	3.221	GLI pathogenesis-related 1 (glioma)
6	IL6	0.006	5.507	interleukin 6 (interferon, beta 2)
6	PPBP	0.008	8.333	pro-platelet basic protein (chemokine) ligand 7
6		0.010	4.029	Full length insert cDNA clone ZM10C10
6	TGFB2	0.010	3.986	
6	LGALS1	0.011	3.582	lectin, galactoside-binding, soluble, 1 (galectin 1)
6	MSI2	0.011	3.261	musashi homolog 2 (Drosophila)
6	NRG1	0.012	2.899	neuregulin 1
6	FNDC3B	0.012	2.985	fibronectin type III domain containing 3B

Table 3.11: The most significant and differentially expressed genes between type I and II colonies. Those 57 genes upregulated in type II colonies are shown segregated into cluster numbers 1-4, those 36 upregulated in type I colonies in their clusters numbered 5 and 6.

3.8 Identifying the biological significance underlying statistically significantly differently expressed genes in type I and II colonies.

Oligoarrays are being used extensively in molecular biology. They generate a vast amount of data, which can be manipulated in numerous different ways. This analysis attempted to appropriately filter out statistically relevant genes that were correspondingly biologically significant. While technical variations were avoided wherever possible, biological variation can only be overcome by large numbers of replicates. With the small number of replicates here, many genes failed to reach statistical significance, and a relatively small final gene list was obtained. In addition, this will contain some falsely positive genes, as the data did not allow a multiple testing correction step. This also reflects the very similar origin of the colonies and the subtle difference under investigation. A further note of caution is required as three genes apparently upregulated in type I colonies (in cluster 5), vimentin, fibrillin 1 and fibroblast activation protein α are likely to be derive from contaminating murine fibroblasts. For instance, vimentin is used diagnostically as a stromal marker and its expression in epithelia is usually seen in the epithelial mesenchymal transition of increasingly malignant cancers (Fry *et al*, 2000; Ramaekers *et al*, 1989).

Whole genome oligoarrays are often used somewhat speculatively to identify activated genes or biological processes that merit further study. Clustering genes assists identification of these, as it is likely that genes that are over or underexpressed simultaneously are interacting. The clusters generated here, did not always segregate genes well. Some of the 93 genes, expressed sequence tags or other sequences identified had as yet no known function, while others had not been studied in epithelia or the prostate and it was impossible to draw biological meaning from them. Despite this, some surprising gene expression patterns did emerge.

3.8.1 Genes upregulated in type I colonies

Genes involved in extracellular matrix interactions, cell migration, inflammation and proliferation were upregulated in type I colonies, though seemed spread between both clusters.

Prostaglandin-endoperoxide synthase 2 (also known as COX2), galectin 1 and transglutaminase 2 are all important in extracellular matrix interactions contributing to cell migration. Increased expression of COX2 and galectin caused increased cell adhesion, with galectin binding laminin and fibronectin (Tsujii and DuBois, 1995; Ellerhorst *et al*, 1999). Transglutaminase 2 plays a central role in regulating ECM remodeling and controls dynamic adhesion formation in cell spreading and migration (Stephens *et al*, 2004). Extracellular matrix proteins fibronectin, type III collagen and type V collagen are also upregulated. Two microtubule genes (microtubule-associated protein 1B and pleckstrin homology-like domain B2) are upregulated, which may suggest further internal cytoskeletal rearrangements.

Cell motility is also promoted by the L1 cell adhesion molecule, which promotes the scattering of epithelial cells from compact colonies; pro-platelet basic protein, which allows neutrophil adhesion and transendothelial migration, and transforming growth factor β2 (isoform 2), which enhances prostate cancer cell motility and metastasis (Shtutman *et al*, 2006; Schenk *et al*, 2002; Aalinkeel *et al*, 2004). Also cathepsin B is found in basal cells of the prostate acinus, can degrade extracellular matrix and plays a key role in cancer cell migration and invasion (Sinha *et al*, 1989; Gondi *et al*, 2006).

Most notable in the list of upregulated type I colony genes was the number of pro-inflammatory cytokines. Interleukins 6 and 8 are both potent prostate epithelial and stromal growth factors and are upregulated in BPH (Giri and Ittmann, 2001; Kramer *et al*, 2007). Neuregulin 1 is also upregulated. This is the ligand of ERBB2, a transmembrane receptor tyrosine kinase which is a critical component of IL6 signaling through the MAP kinase pathway (Qiu *et al*, 1998). COX2 enzyme converts arachidonic acid to various pro-inflammatory prostaglandins while pro-platelet basic protein recruits neutrophils to sites of inflammation. Conversely transforming growth factor β2 is thought to be inhibitory to prostate growth, though its levels are high in BPH suggesting it is not entirely able to suppress hyperplastic growth (Kramer *et al*, 2007). An inflammatory process underlying the aetiology of BPH has long been postulated (Kramer *et al*, 2007). These colonies were derived

from BPH tissue, and the upregulation of inflammation related genes in these proliferative cells would support this theory.

3.8.2 Genes upregulated in type II colonies

Clustering was more effective though not perfect for those genes upregulated in type II colonies as genes with similar functions were grouped together. In cluster 4 were upregulated genes predominately responsible for keratinisation of stratified epithelia, while cluster 3 contained markers of differentiated prostate and epithelial cells. Concentrated in cluster 2 were genes involved in ensuring the impermeability of epithelia along with some differentiation markers. Cluster 1 contained two genes of known function, which again related to epithelial differentiation.

The epidermal differentiation complex on 1q21 contains a large number of genes that are of crucial importance for the maturation of the human epidermis (Marenholz *et al*, 2001). Six such genes upregulated in type II colonies are small proline-rich protein genes 2B, 2G and 3, late cornified envelope genes 1B and 3D, and repetin (Krieg *et al*, 1997). A further four upregulated genes: elongation of very long chain fatty acids-like 4, interleukin 1 family, member 5δ, arachidonate 12-lipoxygenase and Kazal type 5 serine protease inhibitor were involved in the generation of the epidermal permeability barrier which is critical for viable skin function (Li *et al*, 2007; Patel *et al*, 2006; Moran *et al*, 2007, Hachem *et al*, 2006).

Other genes expressed in keratinizing epithelium include keratinocyte differentiation-associated protein (KRTDAP), which is seen in suprabasal cell layers of the embryonic epidermis, and kallikrein-7 is known to be involved in desquamation of corneocytes (Oomizu *et al*, 2000; Shaw and Diamandis, 2007). SLURP1 and α2-macroglobulin-like 1 are late markers of epidermal differentiation (Favre *et al*, 2007; Galliano *et al*, 2006).

Type II colonies also overexpressed a number of recognised markers of prostate and bladder epithelial differentiation. These were prostate acid phosphatase, kallikrein 12 which has been localised to the luminal cells of the normal prostate, zinc-binding alpha-2-glycoprotein 1 which is produced by prostate epithelial cells and represents

30% of seminal plasma proteins and uroplakin 1A, a marker of urothelial differentiation (Memari *et al*, 2007; Lapointe *et al*, 2004; Southgate *et al*, 2007).

Some pro-apoptotic and anti-proliferative genes were also found, such as BCL2/adenovirus E1B 19kD interacting protein and NDRG family member 2, and another, skin aspartic protease helps trigger terminal differentiation (Xie *et al*, 2005; Kovacevic and Richardson, 2006; Rhiemeier *et al*, 2006).

3.8.3 Apparent biological differences in gene expression between type I and type II colonies

Even significant genes may have their expression levels altered within the cell by post-translational modifications, so confirmation at the protein expression level would be necessary to confirm the patterns identified here. For the purposes of further discussion similar gene and protein expressions were assumed.

The gene expression profile of type I colonies suggested that these cells are proliferating rather than differentiating, migratory and interacting with the extracellular matrix rather than other cells. In contrast, almost all the genes upregulated in type II colonies related to epithelial differentiation, and predominately keratinocyte differentiation raising the possibility that the epithelial cells are undergoing squamous differentiation. Given that the type I colonies were postulated to derive from TA cells and the type II from stem cells, the expectation had been that these phenotypes would have reversed.

3.9 Discussion

This project aimed to study the small population of prostate epithelial cells that grow in serum and androgen free culture and gain a better understanding of the differences between the two cell populations identified retrospectively by their differing colony morphologies.

It was hypothesized that type II colonies derived from stem cells, so in comparison with the TA derived colonies would be expected to be more proliferative,

demonstrate self-renewal, differentiate into all lineages of the prostate and demonstrate a gene expression profile consistent with this.

These investigations have demonstrated that type II cells tend to be more proliferative in culture than type I, though they proliferate far more in the first 14 days in culture. There appears to be no difference in the Matrigel-induced differentiation potential of both colony types, but type II colonies do not demonstrate any colony self-renewal when replated, and assume a type I phenotype. Monolayer immunohistochemistry of the two colony types (figure 3.5) confirms the K14 expression of the more undifferentiated type II colonies and the more differentiated luminal K8 staining of the type I colonies as reported by Hudson *et al* (2000). However, when the gene expression profiles of the two colonies are compared, the type I cells are more proliferative and undifferentiated and the type II cells are expressing late markers of (presumably androgen-independent) squamous differentiation.

A reason for this apparent switch in phenotypes may relate to the cell-cell interactions within the type II colony, which are lacking in the type I. The cell of origin of a type II colony may be a stem cell, which loses its self-renewal abilities in culture by commencing differentiation, or an early transit amplifying cell. At the time of plating, type II generating cells may be expressing genes that promote tight cell-cell adhesion to create an intact basal layer. These cells are highly proliferative over the first two weeks and generate a tightly packed colony. Eventually, cells in the center of the colony will be contact-inhibited which predisposes to differentiation, which in this case proceeds down an apparently squamous route (Ura *et al*, 2004). Squamous differentiation genes might be expected to stand out when colony gene expression is compared, as differences between the undifferentiated glandular epithelial type II basal cells and the type I cells may be of a much lower magnitude than differentiating type II cells that are switching to a different histological cell type entirely.

At the time of plating, the later TA cells that generate type I colonies may be expressing genes to help them migrate within the prostate epithelial layers. They form looser colonies and without contact inhibition remain proliferative and more

migratory as they form a colony. When a type II colony is replated, the cells assume a type I phenotype. This may be because their contact inhibition is lifted, or that differentiation in monolayer culture is only be possible on a foundation of basal cells, which is lost with replating, or alternatively that the type II cells have become more differentiated over two weeks so are now at the level in the epithelial hierarchy that the type I cells were when originally plated.

It is likely, if stem cells exist in primary cultures, that they are lost with serial passage or overgrown by non-stem cells. Gao *et al* (2001) found that prostatic epithelial cell organoids immediately placed in Matrigel and injected into mice, exhibited stem cell-like activity by forming acini with basal and luminal cells. However if cells were isolated and grown in primary culture prior to implantation, they remained as small basal cell nests. Unlike the organoids, the previously cultured cells did not induce infiltration and smooth muscle differentiation of mesenchymal cells, an event that may be critical for maintenance and function of stem cells.

This interpretation implies that the morphology of the prostate epithelial cells in primary culture may be determined by their gene expression patterns at the time, but the environmental cues and cell interactions that they experience in culture has an impact. The exact cells of origin of the type I and type II colonies remains unclear though their behaviour would suggest that they are differently aged transit amplifying cells. What is certain, is that their phenotype is unlikely to remain the same after two weeks in monolayer culture.

Squamous differentiation of prostate epithelial cells is rarely reported, though interestingly some of the Matrigel structures obtained in this project from both type I (figure 3.4, E) and type II (figure 3.5) colony cells are reminiscent of a stratified keratinising epithelium. Clinically, squamous differentiation is encountered sporadically in prostate cancers and oestrogen will induce squamous metaplasia in rodent prostates (Parwani *et al*, 2004; Cunha *et al*, 2001). Dalrymple *et al* (2005) observed prostate transit amplifying cells dividing using time-lapse video-microscopy. The two daughter cells migrated apart to fill the culture surface, ceasing proliferation at confluence. However if grown in high calcium concentration medium, cells gathered into small groups and ceased proliferation due to contact

inhibition. They then underwent squamous differentiation - developing cornified envelopes before dying.

Though no other authors have studied these colonies individually, more recently the phenotype of primary cultures of prostate epithelium in low calcium, serum free medium has been described as representing transit amplifying cells (Uzgare *et al*, 2004). These cells progressively mature over time in culture, with later passages showing an increasing proportion of slower cycling, $K8^+$/ $K18^+$ cells until they lose proliferative ability by the 7–10th passage. Liu and Peehl (2001) also concluded that such cells were TA cells on the basis of their cluster designation antigen expression. One other study has highlighted the heterogeneity of prostate cells in culture. Tokar *et al* (2005) plated out individual cells from a human papillomavirus–18 immortalised prostate epithelial cell line, and selected two clones on the basis of different morphology, calling them WPE-stem (as they were potentially stem cells) and WPE-int (potentially intermediate TA cells). The former were small cells, which expressed high levels of p63 and CK5/14 and grew in soft agar while the latter expressed K18, had larger polygonal cells and was less clonogenic. However no further investigation of stemness was undertaken, and as the WPE-stem cells were $p63^+$ again these two cell populations are both likely to be TA cells.

3.10 Future directions

When the proliferative heterogeneity of the prostate was first reported in 2000, it represented the first *in vitro* evidence for the existence of the then unknown prostate stem cell (Hudson *et al*, 2000). Without knowing the marker expression on the stem cell, this modified colony-forming assay was invaluable for demonstrating any degree of enrichment achieved by selecting for speculative markers (Collins *et al*, 2001). Colony forming assays are still used but the heterogeneity of the colonies has not been investigated further other than in this study. Most of the impressive progress towards identifying the prostate stem cell has used cell sorting of primary cells, a reflection of the change in phenotype that occurs with *in vitro* culture. However the assays required for identification and proof of stem cells such as mouse xenografts are laborious. With confirmation of the prostate stem cell phenotype, it will be interesting to see what colonies are grown when a pure stem cell population

is plated. If colonies are characteristic, then low-density culture could re-emerge as a more convenient way of confirming the presence of stem cells for the rapid, large scale screening of stem cell killing molecules. If type II colonies are derived initially from a stem cell, then a drug added to culture medium that consistently yields only type I colonies may be selectively destroying stem cells, and would represent a candidate for clinical studies.

CHAPTER 4
ACQUISITION AND ANALYSIS OF EPITHELIAL COLONIES FROM RADICAL PROSTATECTOMY TISSUE.

4.1 Introduction

It was hypothesized that the stem cell model of cancer would apply in prostate cancer. Thus cultures of malignant prostate tissue would, like BPH, demonstrate proliferative heterogeneity. As the most undifferentiated and rarest of the cell fractions in low-density culture, type II colonies were of particular interest. While many studies have compared benign and malignant tissue, few have compared such a small fraction of prostate epithelial cells. Identification of expression differences between these colonies had the potential to identify genes peculiar to stem cells, which could ultimately be manipulated for clinical benefits.

In this study colonies were obtained from parallel cultures of benign and malignant prostate tissue derived from early prostate cancers. In view of the risk of contaminating benign or malignant cells within each sample, the nature of each colony had to be determined individually. It was hypothesized that LOH analysis would be sufficiently discriminatory, allowing accurate comparison of the characteristics and differential gene expression of the benign and malignant colonies.

4.2 Acquisition of paired benign and malignant prostate tissue samples from radical prostatectomy specimens.

In total, 18 radical prostatectomy specimens were sampled for malignant and benign prostate tissue. Typical of the radical prostatectomy population, patients were relatively young with a median age of 64 (range 54-70 years old), and had a median biopsy and gland Gleason grade of 3+4 (range 3+3 to 4+5) and a mean prostate weight of 40g (standard deviation 9.7g). Patient characteristics, prostate biopsy results and corresponding radical prostatectomy histology are listed in table 4.1. Many potential patients undergoing surgery had unsuitable biopsy

results, as selection required a high percentage (by length) of core involvement. A biopsy core was between 10 and 16mm long so 70% involvement for example, equated to 7-11mm cancer diameter along the line of the biopsy.

Patient	Age	PSA (ng/ dL)	Biopsy Gleason Grade	Biopsy histology	RRP Gleason grade	Gland weight and cancer location
1	69	14.5	3+4	All 8 cores positive, but L 70-90%, R 10-20%. L sided nodule	4+3	58g, multifocal, bilateral tumour, largest 28mm on L
2	70	5.7	3+3	3/6 positive, all R 80-90% involved. L: Atypia & HGPIN	3+3	40g, bilateral foci R>L, largest 20mm on R
3	67	8.3	3+4	2/6 positive, R apex 55%, L <1mm	3+4	52g, 2 foci, R side, 8 & 11mm
4	64	5.2	3+3	3/6 cores positive, R 10%, L 40% apex & 90% base	3+4	48g, multifocal, largest tumour 36mm L & centre
5	59	7.4	3+3	2/6 positive: 70% L base, 15% L midzone. L nodule.	3+3	34g, 10mm focus on R side
6	58	5.9	4+4	3/6 positive. 60% of R mid & base cores, <10% L apex	3+4	46g, 3 foci & HGPIN. Largest 8mm
7	61	5.2	3+3	3/6 cores positive on R 40-60%	3+4	33g, 20mm focus R
8	68	8.3	3+4	2/6 cores, R central 35% 5mm, L <1mm	4+4	57g, 2 foci 13 & 20 mm on R / midline
9	70	9.7	3+4	2/10 cores positive. 30&70% on R	4+3	47g, 2 foci R&L, largest 10mm on L, HGPIN
10	66	6.2	3+4	3/8 cores positive, all L: 80-90%	3+4	51g, 32mm L focus HGPIN
11	54	3.4	3+3	3/6 cores positive, all L sided <10-90%	3+4	34g, L side 15mm focus
12	68	8.5	4+3	3/8 biopsies positive, all on L	4+3	28g, 2 foci merge 30mm anterior & L
13	63	10.0	4+5	All 6 cores positive, <20% R, >80% L	4+4	43g, 6 foci. Largest 16mm on L
14	66	8.0	3+4	80% of 1/4 R cores, <10% of 1/4 L cores	4+3	50g, bilateral, 2 foci, 16mm R, 8mm L
15	54	4.0	3+3	2/7 cores positive. R apex/midzone 70- 80%	3+4	61g, 2 foci on R, largest 22mm
16	55	7.2	4+3	2/10 cores positive. 60-80% L base. MRI: L capsular breach	4+3	38g, T3 on L. 18mm focus & HGPIN
17	62	4.9	3+4	3/6 cores positive. 40-50% L, <10% R	3+4	56g, bilateral, 5 foci largest L, 16mm.
18	63	4.9	3+4	2/6 cores positive L apex . 10%, L midzone 70%	4+3	40g, L sided 34mm tumour
Median	64	6.7	3+4		3+4	

HGPIN – High grade prostatic intra-epithelial neoplasia, MRI – Magnetic Resonance Imaging, RRP – radical retropubic prostatectomy.

Table 4.1: Patient characteristics and histopathology of prostates sampled for benign and malignant tissue.

4.3 Outcomes of culture of paired benign and malignant radical prostatectomy tissue samples.

From each fresh prostate, one benign tissue sample and one or two cancer tissue samples were cut by the histopathologist. It was usually easy to distinguish the hyperplastic transitional zone from the peripheral zone. Presumed benign tissue was taken from the peripheral zone on the side of the prostate most negative for cancer on biopsies.

To the naked eye, areas of prostate cancer were not as easily distinguishable, though high-grade (Gleason 4 or 5) cancer looked slightly more yellow in the unfixed gland (personal communication, Dr M Constance Parkinson). The sampling of cancer tissue specimens thus relied on tissue appearance and firmness using fingertip palpation, guided by the biopsy and preoperative magnetic resonance imaging results and the experience of a dedicated Consultant Urological Histopathologist.

Even in patients with appropriate biopsy findings, these did not always predict the Gleason grade or distribution of the prostate cancer in the whole gland, though tumours tended to be large (see table 4.1). This made the prospective identification of prostate cancer tissue in the fresh specimen more difficult, especially as histological fixing, embedding, staining and assessment of the whole gland was not complete until eight days after specimen acquisition. As part of the histological assessment of the whole gland, the sites of tissue sampling were assessed in terms of its location in relation to the cancer foci.

From each prostate, the presumed benign and malignant samples were immediately processed into a single cell suspension, plated out and colonies assessed at two weeks. The samples acquired and the outcome of culture are summarised in table 4.2.

The colonies were used for a number of purposes.

Given the difficulty in distinguishing between benign and malignant areas of fresh prostate tissue, the first requirement was to confirm the presumed origin of each colony individually, before further characterisation could be done. It was assumed that each colony represented the clonal expansion of a single prostate epithelial cell plated 14 days previously, and thus that all cells within the colony would be genetically identical. It was hypothesized that the genotype of a benign colony would match that of benign prostate tissue from the original specimen, and that of a cancer colony would match that of the focus of prostate cancer that had been sampled.

Loss of heterozygosity (LOH) analysis has been used by many authors to identify common sites of mutation and chromosomal loss in prostate cancer and was also used by Bright *et al* to successfully distinguish between three otherwise morphologically identical paired benign and malignant early prostate cancer cell lines (Bettendorf *et al*, 2005; Bostwick *et al*, 2002, Bott *et al*, 2006; Bright *et al*, 1997; Cheng *et al*, 1998; Fromont *et al*, 2003; Ruijter *et al*, 1999). LOH analysis was therefore applied to DNA extracted from lymph nodes (for a germ line control), histologically confirmed benign and malignant areas of the formalin fixed prostate (to identify loci of interest) and individual presumed benign / malignant colonies (to analyse at loci of interest).

Though some colonies were scraped up entirely for DNA extraction, others were individually ring cloned into a $25cm^2$ tissue culture flask and allowed to proliferate to semi-confluence. When successful, this provided far greater numbers of cells for extraction of DNA (10% of cells) and total RNA (90%). RNA was extracted from individual colonies with the intention that after confirmation/exclusion of malignancy their gene expression could be evaluated using DNA microarrays.

Patient	Sample	Tissue weight	Cell yield x 10^6 / g	Cells plated x10^3	% flasks remaining at 2 weeks	Outcome
1	Benign 1 R anterior	0.5	32	10	80%	Colony DNA
	Benign 2 R	0.3	6	10	80%	extracted
	Cancer L	0.4	16	40	75%	
2	Benign L	0.03	8.7	8	50%	Colony DNA
	Cancer 1 R posterior	0.07	2.7	24	56%	extracted
	Cancer 2 midline	0.05	6	16	38%	
3	Benign L	0.2	5.6	18	22%	74% flasks infected,
	Cancer 1 R	0.2	5.9	18	11%	no cancer colonies
	Cancer 2 R	0.2	8.1	18	44%	grown
4	Benign R	0.05	13	16	0%	76% infected,
	Cancer 1 R	0.15	8.9	17	6%	including all benign
	Cancer 2 L	0.2	4.7	17	6%	flasks
5	Benign R	0.5	4.6	25	96%	Cancer sample from
	Cancer L	0.3	6.4	25	88%	benign area of gland
6	Benign	0.34	1.7	25	4%	96% infected
	Cancer	0.30	1.9	25	0%	
7	Benign	0.08	3.2	20	85%	Poor colony yield
	Cancer	0.10	3.1	20	80%	throughout
8	Benign R	0.04	4.7	24	71%	No benign colonies
	Cancer 1 R	0.2	0.08	24	92%	
	Cancer 2 R	0.04	0.003	24	73%	
9	Benign R	0.33	5.3	20	100%	100% survived, but
	Cancer L	0.31	7.2	20	100%	few benign colonies. Lost at ring cloning
10	Benign R	0.24	10	20	100%	Colonies lost during
	Cancer L	0.08	6	20	95%	ring cloning
11	Benign	0.16	2.8	22	91%	Colony DNA
	Cancer	0.07	9.7	18	94%	extracted
12	Benign R	0.07	4.3	29	100%	Colony DNA & RNA
	Cancer L anterior	0.07	3	29	100%	extracted
13	Benign R anterior	0.6	0.1	18	94%	Atypical appearance
	Cancer L	0.4	0.07	18	78%	of cancer colonies
14	Benign L anterior	0.3	3.2	24	100%	Colony DNA & RNA
	Cancer R posterior	0.2	4.4	24	96%	extracted
15	Benign	0.2	0.9	18	94%	Colony DNA & RNA
	Cancer	0.2	1.9	18	100%	extracted
16	Benign R	0.21	1.3	21	100%	Colony DNA
	Cancer L lateral	0.3	1.1	21	100%	extracted – not used
17	Benign	0.18	0.52	21	86%	Cancer sample from
	Cancer	0.11	0.95	21	100%	benign area of gland
18	Benign	0.18	1.1	21	71%	Colonies lost to ring
	Cancer	0.12	0.7	21	29%	cloning
Mean	Benign	0.2 (0.2)	5.7 (7.2)	19 (5)	72 (34%)	
(s.d.)	Cancer	0.2 (0.1)	4.5 (4.0)	22 (5)	65 (34%)	

s.d. – standard deviation

Table 4.2: Outcome of culture of benign and malignant prostate tissue.

Of 18 prostates used, only seven prostates yielded colony RNA and DNA or DNA alone for further experimentation, of which six were used (see table 4.2). Of the eleven prostates lost, in three cases this was due to contamination with fungal spores, most likely introduced when the pathologist dissected out the samples. On two occasions, while colonies grew well, during the histological assessment of the whole gland (seven days into the tissue culture process), it was evident that the tissue sampled from the cancerous side of the prostate had not come from within the focus of cancer. The colonies from three prostates were dedicated to ring cloning to obtained paired DNA and expanded RNA colony samples, but became infected in secondary culture or failed to settle and proliferate. For two prostates, colony yield was insufficient; with globally low yields in one, and adequate cancer colony numbers, but no matching benign colonies in the other. Finally cancer colonies from one prostate were very atypical, with thin cells with irregular outlines, which were not used.

Early attempts at prostate tissue culture were remarkable for the extent of infection encountered. Culture flasks were largely contaminated with fungal growth, though yeast infection was encountered rarely. Though cultures of TURP tissue occasionally became contaminated, infection rates were far higher in the culture of radical prostatectomy tissue obtained from the pathologist. Fungal colonies were seen at any time during the two weeks in culture with progressive attrition of flask numbers.

A number of changes were introduced to reduce the infection rate. Antibiotic concentrations in the collecting medium were increased to 10%. PrEGM culture medium routinely contained 0.1% by volume of amphotericin B and gentamicin antibiotics, so further antibiotics were added to a concentration of 1% by volume. Careful review of tissue culture technique was undertaken and cell culture was switched from 5cm diameter Petri dishes, to 25cm^2 Nunc flasks, which were easier to handle. The number of flasks set up for each experiment was also increased in response to the high attrition rate. Replacing culture medium twice a week rather than three times did not appear to reduce contamination rates, despite the perception that infection was being introduced during tissue culture due to the sporadic timing of infections.

Requiring the pathologist to wear sterile gloves and use sterile instruments (a change from the usual laboratory protocol) greatly reduced infection rates and this coincided with a change in pathologist. The first pathologist inked the edges of the freshly sliced prostate before dissecting out the samples, to allow identification of the surgical margins. Though this ink did not come into contact with the tissue taken, it is almost always contaminated with fungal spores (personal communication, Dr C Corbishley). These changes were instituted between prostates number six and seven. Infections were reduced but not eradicated by these interventions, and continued vigilance was required at all stages, especially during sample acquisition.

4.4 Morphological characteristics of primary prostate epithelial colonies derived from presumed benign and malignant colonies.

Surviving flasks of presumed benign and malignant cells were scored after two weeks monolayer culture. Visually, and under low and high power microscopy there were no distinguishing morphological differences between the colonies (see figure 4.1).

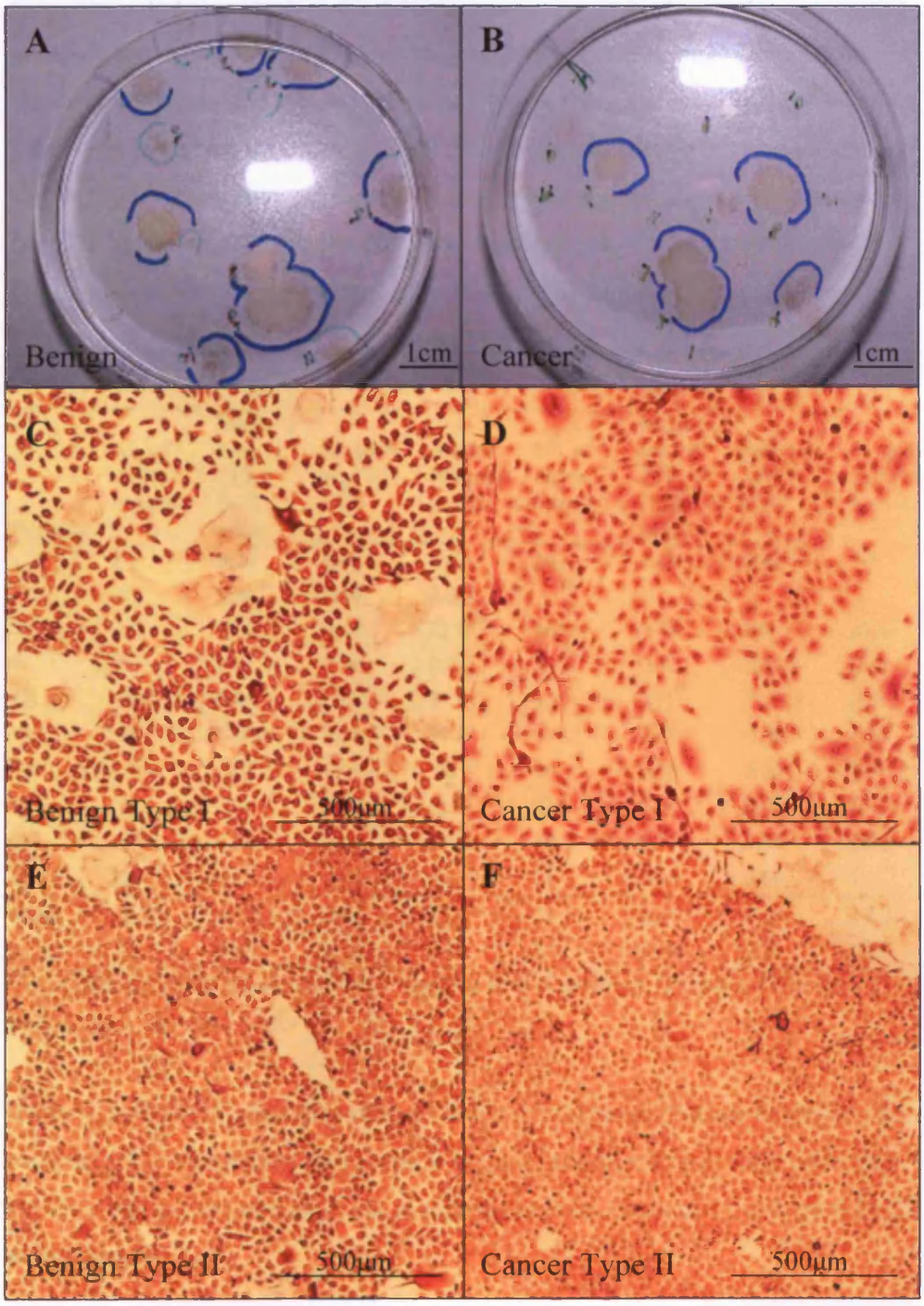

Figure 4.1: A&B Representative dishes after 14 days of low density culture of 1000 primary prostate epithelial cells from presumed benign or malignant radical prostatectomy tissue; stained for cytokeratins 5,6 and 18. Type I colonies from benign (**C**) and malignant (**D**) cells, and type II colonies from benign (**E**) and malignant (**F**) cells looked similar.

Both type I and II colonies were present based on their characteristic appearance under direct vision. Within and between patients there was great variation in flask colony yields and the ratio of colony types, though invariably there were more type I colonies than type II. Table 4.3 shows the colony forming efficiency for the 9 prostates out of 18, for which characteristic colonies were obtained from both the benign and cancer samples, and <25% of cells plated for each sample became infected.

	Presumed benign				Presumed malignant			
Prostate	No. of dishes scored	Mean total % CFE (≥32 cells)	Mean % type II CFE	% total colonies type II	No. of dishes scored	Mean total % CFE (≥32 cells)	Mean % type II CFE	% total colonies type II
1	8*	0.74	0.00	0.0	30*	0.48	0.02	3.5
	8*	0.56	0.00	0.0				
7	17*	0.02	0.01	25.0	16*	0.04	0.01	28.6
9	20	0.01	0.00	0.0	20	0.42	0.11	26.2
10	20	0.09	0.03	27.8	19*	0.79	0.19	23.8
11	20*	0.49	0.20	39.8	17*	0.17	0.08	44.8
12	29	0.53	0.05	9.8	29	0.36	0.02	5.8
14	24	0.34	0.09	25.6	23*	0.04	0.00	11.1
15	17*	0.26	0.04	13.6	18	0.36	0.07	18.5
16	21	0.12	0.00	4.0	21	0.38	0.00	1.3
Mean	18	0.32	0.04	15.0	21	0.34	0.56	18.0
s.e.m.	2.2	0.09	0.10	0.05	1.7	0.08	0.21	0.05

CFE = colony forming efficiency, s.e.m. = standard error of the mean, *excludes dishes lost to infection that were not scored.

Table 4.3: CFEs of presumed primary benign / malignant prostate epithelial cell cultures. CFE and proportion of type II colonies was not significantly different between the presumed benign and malignant samples (student's t-test, p= 0.84 & 0.59 respectively).

As with the TUR derived prostate tissue, colonies were typed on their morphology and overall appearance under direct vision and their diameter, cell density, number of cell doublings and total colony cell number. Proliferative heterogeneity was apparent for the two colony types in both presumed benign and presumed malignant tissue. The distribution of colony cell numbers for each

type is shown in figure 4.2. Though cell number, diameter and the cell density was significantly different between the populations of type I and type II cells (student's t-test, $p<0.0001$ for all) in practice the cell density across 1mm for each colony was the most useful objective discriminator. Though no one parameter demonstrated precise partitioning of the two colony types, this would be expected due to the normal biological variation present in two normally distributed cell populations whose extremes overlap. The distribution of cell densities across colony type for each tissue source is shown in figure 4.3.

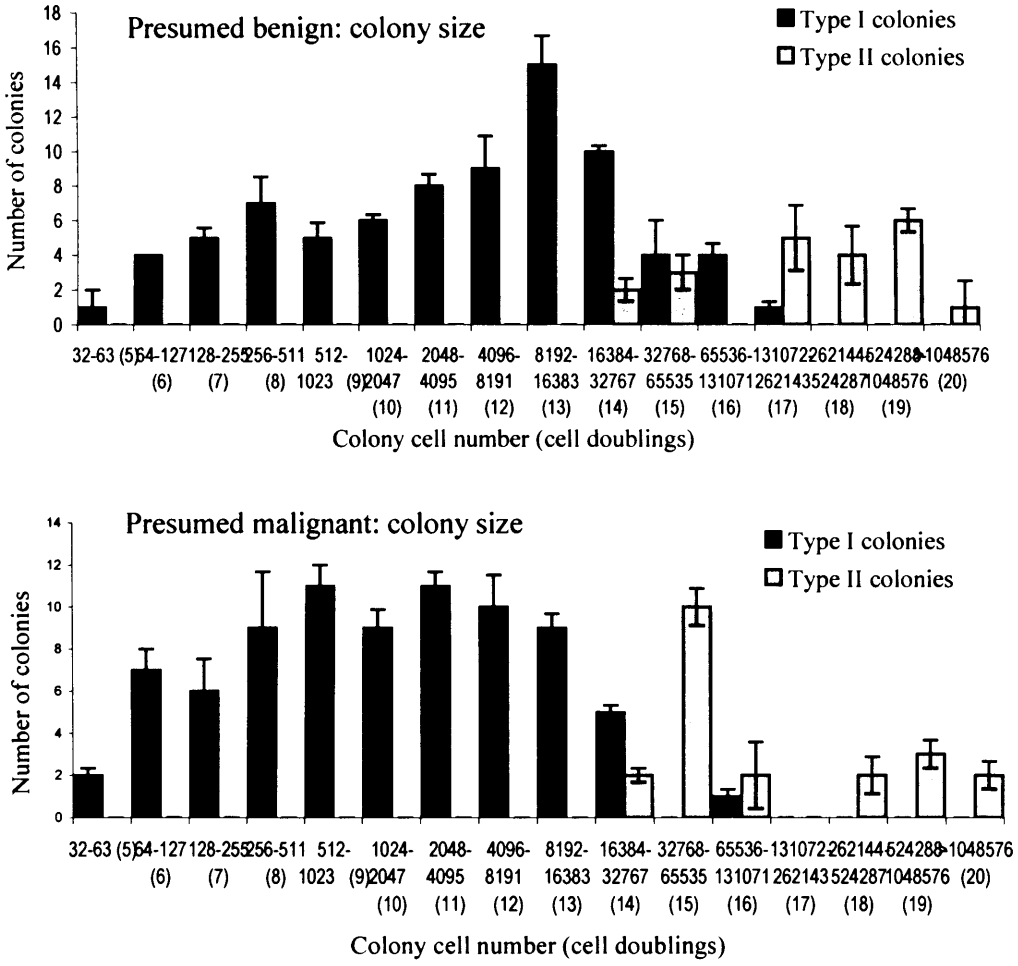

Figure 4.2: Distribution of presumed benign and malignant prostate epithelial cell colonies by total colony cell number (binned by potential cell doublings) and type. Error bars show the standard error of the mean for the first 10 dishes from 3 experiments (prostates 1, 7 and 11).

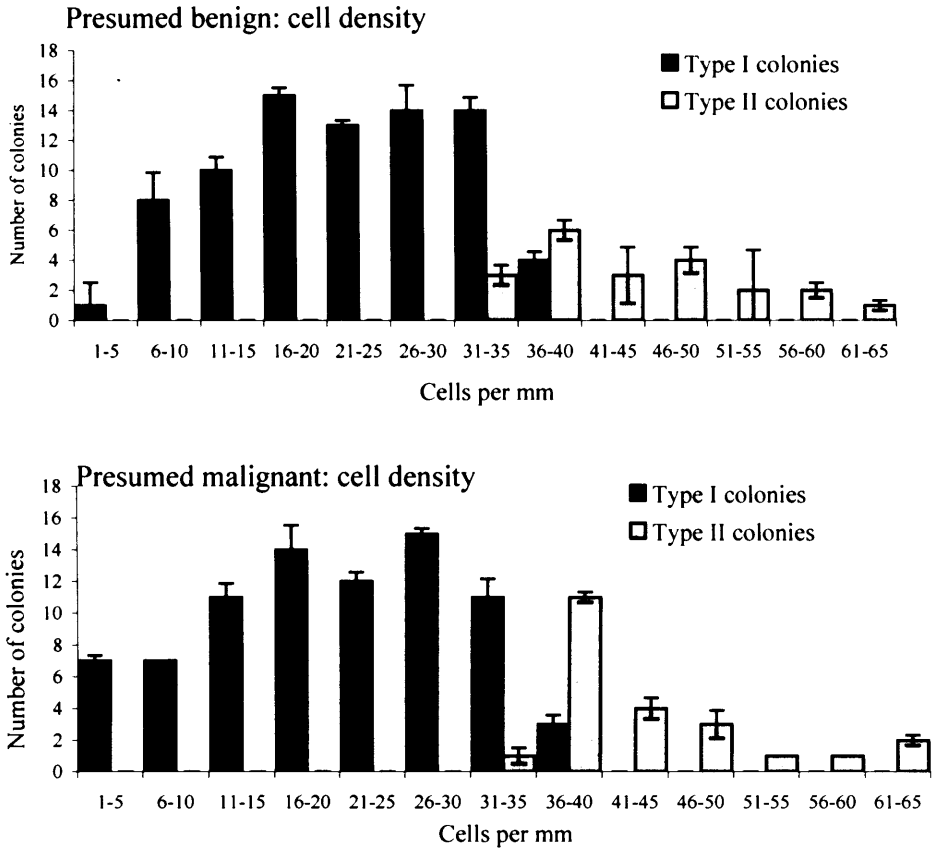

Figure 4.3: Distribution of presumed benign and malignant prostate epithelial cell colonies by cell density per millimetre. Error bars show the standard error of the mean for the first 10 dishes from 3 experiments (prostates 1, 7 and 11).

Table 4.4 (extended from table 3.2) shows how the colonies derived from presumed benign or malignant peripheral zone radical prostatectomy tissue compares to colonies derived from transitional zone prostate tissue harvested at TURP in this study and as reported by Hudson *et al*, (2000).

	Hudson *et al*, 2000		Present study					
Tissue source	TURP		TURP		Radical prostatectomy			
Tissue Type	Transitional zone BPH		Transitional zone BPH		Peripheral zone Presumed benign		Presumed cancer	
Colony type	I	II	I	II	I	II	I	II
Diameter (mm, mean)	≤4	≥3	0.5–17 (4)	9–20 (11)	0.5–18 (4)	5-27 (14)	0.5–10 (2)	5–32 (13)
Cell number x10^3 (mean)	≤ 8.5	8–40	0.04–48 (8.3)	28–607 (169)	0.03-176 (13)	22–1,456 (309)	0.07-80 (5.3)	26–1,736 (380)
Number of doublings (mean)	5–12	12-14	5–16 (11)	15–19 (17)	5–17 (11)	14–20 (17)	6–16 (10)	14–20 (17)
Density (cells/mm, mean)	<30	30–50	7–32 (19)	33–59 (40)	4–39 (21)	30–56 (40)	6–38 (22)	30–56 (40)
Outline	irreg	reg	irreg	reg	irreg	reg	irreg	reg
Frequency of colonies	90%	10%	83%	17%	85%	15%	82%	18%
Mean % CFE	5.26	0.54	0.22	0.05	0.28	0.04	0.28	0.06
Incidence of colony forming cells	1/17	1/185	1/377	1/1961	1/419	1/2091	1/335	1/1950

CFE – colony forming efficiency, reg – regular, irreg - irregular

Table 4.4: Characteristics of the two colony types obtained from primary prostate epithelial cell culture by Hudson *et al*, (2000) and in the present study from peripheral benign and malignant and transitional zone tissue.

The characteristics of the colonies grown from transitional zone BPH, and presumed malignant and benign peripheral zone tissue are remarkably similar (discussed below). Type I colonies are commoner than type II which were grown in seven out of nine of the scored experiments. As discussed in section 3.2,

overall colony yield is reduced compared to the findings of Hudson *et al* (2000) and the likely reasons behind this stand, as tissue was processed in the same way.

These colonies were derived from different zones of the prostate. The transitional zone is traditionally the site of benign prostatic hyperplasia, while cancers predominately arise within the peripheral zone (McNeal 1968; McNeal *et al*, 1988). No difference in clonogenicity was encountered between the two zones, which concurs with the findings of Laczko *et al* (2005) who reported no difference in Ki-67 staining between the transition zone and peripheral zone of cadaveric donor prostates.

The malignant and benign colonies demonstrated no distinguishing features between them. Confirmation of each colony's benign/ cancer status was required before any formal conclusions could be drawn about them, and prior to any comparisons of differential gene expression or *in vitro* / *in vivo* characteristics. .

4.5 Differentiating between benign and malignant colonies using LOH analysis.

The method of tissue acquisition and the multifocal nature of prostate cancer made it possible that within each sample were contaminating benign or malignant cells that might have resulted in colonies derived from a single cancer cell amongst benign colonies and vice versa. It is common to identify a number of different foci of prostate cancer within a radical prostatectomy specimen. These foci may be very small, may merge to create an apparently larger focus which in reality is derived from two different clones, and can have irregular borders so that benign tissue may interdigitate with malignant tissue (Ruijter *et al*, 1999). In addition, other histological entities such as proliferative inflammatory atrophy, atypical adenomatous hyperplasia and high grade prostatic intraepithelial neoplasia (HGPIN) may also be sampled within a macroscopically benign or malignant area of prostate, each of which may differ in its genetic changes, including LOH.

4.5.1 Establishing LOH control samples using early prostate cancer cell lines with LOH at known loci.

Bright and colleagues (1997) developed seven paired benign and malignant immortalised prostate epithelial cell lines from six successive patients. Using fresh prostate specimens, pure tumour or benign samples were microdissected out by an experienced pathologist. Despite this, even the smallest samples contained a diverse mixture of cell types including stroma, normal epithelium, PIN, and invasive tumour. Primary prostate cell cultures were established and then immortalized using the E6 and E7 transforming proteins of human papilloma virus serotype 16. Extensive cloning and passaging resulted in stably transfected cell lines.

Out of a number of techniques tried, all but LOH analysis failed to demonstrate a difference between the cell line pairs. Both cancer and benign cells had similar karyotypes (usually normal male in localised prostate cancer), similar phenotypes, similar growth rates in culture and in nude mice and similar PSA

expression. However, LOH analysis of 8p 12-21, a region especially implicated in prostate adenocarcinoma, demonstrated allele loss in the cancer cell lines which corresponded to one or more of the foci microdissected from the original cancer, which was absent in the corresponding benign cell lines. Not all cancers had LOH on 8p 12-21 and one patient showed LOH in multiple benign glands as well as his cancer.

To establish positive controls for the colony LOH analysis, the LOH analysis of three of these paired cell lines was repeated, for four of the eight loci reported by Bright *et al* (1997) and for 25 other microsatellite loci also reported as lost in prostate cancer on other chromosomes. The results and a comparison with those of Bright *et al* (1997) are shown in table 4.5.

Paired cell lines (benign / cancer)	1532NPT/ 1532CPT		1535NPT/ 1535CPT		1542NPT/ 1542CPT	
Micro-satellite marker	Bright *et al*	Present study	Bright *et al*	Present study	Bright *et al*	Present study
D1S158		hom		0.85		0.97
D1S414		0.93		0.99		0.97
D3S1263		0.84		Hom		0.97
D5S656				0.99		0.95
D6S314		0.88		0.97		0.96
D6S501		0.34		Hom		0.94
D7S523		0.98		0.98		0.75
SFTP2	hom	hom	LOH	0.93		0.93
D8S133	LOH		LOH		LOH	0.00
D8S136	LOH	0.05	LOH	0.99	LOH	0.11
NEFL	LOH	0.02	LOH	0.99		0.32
D8S137			hom		LOH	
D8S131	hom		LOH		LOH	
D8S339	het		het			
ANK			hom			
D8S1991		0.10		0.94		0.06
D8S255		0.08		0.97		0.14
D8S549		hom				hom
D9S1748		0.78		0.95		0.94
D9S1679		0.92		0.64		0.98
D10S541		0.82		0.98		0.98
D10S587		0.83		Hom		0.93
D11S902		hom		0.96		0.79
D11S990		1.00		0.95		hom
D12S89		0.98		1.00		0.95
D12S1697		hom		0.98		hom
D13S171		0.99		0.99		0.06
D13S284		0.97		0.99		0.97
D16S505		0.97		0.95		0.94
D16S422		hom				0.94
D16S413		0.90		1.00		1.00
D16S515		0.89		0.90		0.98
D18S363		0.92		0.91		0.98

LOH - LOH seen in cancer sample compared to benign sample.

Table 4.5: LOH analysis of three paired cell lines for the eight loci assessed by Bright *et al* and for 29 loci assessed in the present study. Absent data occurred where the locus was not examined or electropherograms were uninterpretable, usually because concentrations of PCR product were too high.

hom	Homozygous / uninformative
	Heterozygous = 0.71-1.00
	30-49% loss: 0.51-0.70
	50-74% loss: 0.25-0.50
	75-100% loss: <0.25
	blank = unknown

When performing their LOH analysis, Bright and colleagues used autoradiography of radiolabelled DNA bands on a high-density gel. LOH was called if there was at least 75% loss of one allele as visualised by three independent observers. The ABI Prism 3700 DNA analyser is more quantitative and requires the imposition of a somewhat arbitrary cut-off value to determine whether LOH is present, in the face of occasionally equivocal results. Extending the LOH analysis to 29 microsatellite markers with a cut-off of 75% identified two further loci with LOH in 1532CPT and three in 1542CPT. For the four loci published by Bright *et al* (1997) that were checked, there was complete agreement for 1542CPT and 1532CPT cell lines and complete disagreement for 1535CPT. The cell lines analysed as 1535NPT and 1535CPT were a match as their alleles reliably agreed in length and were often different lengths to the other two cell line pairs. However it seems most likely that the two flasks of cells harvested for DNA had been previously mislabelled and both contained the benign cells 1535NPT, and that 1535CPT was never analysed. This accounts for the heterogeneous product lengths found at the three loci used for comparison as if both samples had been 1535CPT then all three would have been homozygous.

When comparing two clonally expanded cell lines, one would expect either complete presence of two alleles or complete loss of one allele. However this does not occur, and it demonstrates the degree of noise associated with this analysis. The LOH detected here had percentage allele losses of 86-100% and interestingly, even when two identical cell lines were compared, as was inadvertently done with 1535NPT cells, allele losses of 0-15% were demonstrated with one outlying result of 36% allele loss. Noise will derive from perturbations in the PCR process and the resolution of the bioanalyser. The finding of 36% LOH at locus D9S1679 for this 'pair' of cell lines requires explanation as there should be no LOH or any approach to it. The presence of a subclone with a mutation at this locus in one of the cell lines, acquired in culture could account for this, though an artefact of the technique seems more likely.

Understanding the significance of equivocal results such as the 66% and 68% LOH found by the assay system at use in this project is difficult. In some cancers, duplication of chromosomes can occur, such that there are three or four

copies of a locus. If a cancer has two copies of one allele length and one of another, with each gene amplified equally, a 50% allele loss would be reported (even though no sequences have been lost). Because of this, some authors have adopted the term 'allelic imbalance' to better acknowledge such possibilities.

The variability inherent in this system can be accommodated if the cut-off point is relaxed, and 75-80% loss appears appropriate. However in the analysis of primary tissue, the presence of uncertain levels of contaminating normal cells will further obscure the true presence of LOH so thresholds must be lowered.

Bright *et al* (1997) repeated their LOH analysis twice if DNA allowed. Here LOH analysis was performed only once for these cell lines, though loci used as positive controls were confirmed many times in later analyses. Cell line pairs 1532NPT/1532CPT and 1542NPT/1542CPT were used as positive controls at loci D6S501, D8S133, D8S136, D8S255, D8S1991, NEFL and D13S171.

4.5.2 LOH analysis of original tumour / benign prostate tissue sampled for culture of colonies

In order to identify those loci of interest for each sampled prostate cancer, LOH analysis was performed on DNA derived from the paraffin embedded prostate at sampled sites that had been histologically confirmed as malignant or benign. Those loci demonstrating LOH were then analysed in DNA from corresponding benign and malignant colonies. Six patients' prostate tissue was assessed for up to 55 loci in total. Table 4.6 shows the LOH analysis findings.

As the prostate tissue was not a pure sample of prostate epithelial cells, but was contaminated with stromal cells, blood cells, nerves and vessels any LOH within the malignant epithelium would be diluted by the other cells' normal genotypes. Two threshold levels for assigning LOH were considered, and these were relaxed to 50% loss (calculated as ≤ 0.5 if loss of the shorter allele or ≥ 2.00 if loss of the longer allele) and 30% loss (calculated as ≤ 0.7 if loss of the shorter allele or ≥ 1.43 if loss of the longer allele). A wide variety of allele loss was encountered each side of this value.

Patient	#1			#2			#11		#12		#14		#15	
Marker	Be1	Be2	Ca	Be	Ca1	Ca2	Be	Ca	Be	Ca	Be	Ca	Be	Ca
D1S158	0.89	0.93	0.93	0.98	0.89	0.99	0.90	0.93	1.05	1.06	Hom	Hom	0.95	1.08
D1S305	0.54	0.93		0.99	1.05	1.03					Hom	Hom	Hom	Hom
D1S414	1.00	1.01	1.06	0.95	0.93	1.00	Hom	Hom			0.94	0.87	Hom	Hom
D1S422	1.05	1.06	1.05	0.96	0.98	1.00	Hom	Hom	1.15	0.98	0.95	1.06	1.15	1.08
D2S222	Hom	Hom	Hom	Hom	Hom	Hom	0.95	0.90	1.00	0.95	Hom	Hom	0.84	0.89
D3S1263				1.06	1.01	1.00	0.92	0.95	0.94	0.91	0.98	1.12	Hom	Hom
D5S500				1.02	1.04	0.95	0.99	1.09	1.04	1.00	0.97	0.95	0.93	0.93
D5S656	1.05	1.08	1.06	0.86	0.93	1.05	1.03	0.97	Hom	Hom	1.17	0.98	0.83	0.86
D6S251											0.89	0.93	0.97	1.03
D6S314	1.03	1.07	1.01	Hom	Hom	Hom	Hom	Hom	1.00	0.98	0.99	0.97	0.97	0.96
D6S501	0.97	1.08	0.99	1.01	1.01	0.97	1.08	1.00			1.06	1.07	0.97	1.00
D7S480	0.97	0.95	0.96	0.95	1.06	1.05	1.03	1.00	1.00	0.96	1.01	1.00	0.95	0.95
D7S523	1.07	0.99	1.04	1.02	0.95	1.17	1.06	1.06	Hom	Hom	Hom	Hom	0.98	0.97
D8S133	Hom	Hom	Hom				0.93	0.99	1.08	1.02	0.99	0.94	1.25	0.99
D8S136	0.93	0.89	0.49	0.98	1.01	0.99	0.97	1.48	1.07	0.97	0.92	1.18	0.95	1.03
D8S137	0.97	0.97	0.99	0.99	0.99	1.02	Hom	Hom	1.13	1.02	Hom	Hom	Hom	Hom
D8S255	0.96	1.04	1.03	0.99	0.95	0.95	1.02	1.14	Hom	Hom	0.99	0.95	0.94	1.12
D8S549	0.95	1.01	0.94	0.98	0.86	0.93	1.06	1.01	1.05	0.93	0.99	1.01	Hom	Hom
D8S1991	0.97	0.53	0.44	1.08	1.05	1.06	Hom	Hom	1.06	0.88	0.94	0.99	Hom	Hom
NEFL	0.99	1.04	0.51	0.92	0.59	0.58	0.89	0.88	1.06	1.01	0.96	1.04	Hom	Hom
SFTP2	1.01	0.98	0.86				1.01	1.14	0.99	0.96	0.90	1.05	0.93	1.13
D9S1679							0.94	0.92	1.02	0.99	Hom	Hom	0.98	1.01
D9S1748							1.01	1.03	1.06		0.99	1.11	0.97	1.00
D10S211	1.00	0.87	1.01	1.03	1.04	1.07	1.05	1.10			1.10	1.09		
D10S541				1.10	0.93	1.02	2.17	0.22	1.12	1.03	1.07	1.02	1.06	0.89
D10S587	1.05	1.04	0.18	0.95	0.99	1.00	1.00	1.12	0.99	1.10	0.96	1.03	0.94	0.94
D10S1246	1.08	1.10	0.55	0.91	0.88	1.00	0.97	1.01	Hom	Hom	Hom	Hom	1.02	0.98
D10S1765	0.99	1.04	1.00	0.95	0.95	1.00					0.81	1.13	1.00	0.95
D10S2491	0.98	1.11	0.99	1.01	0.94	0.97		1.08			0.90	1.06	0.97	0.90

Hom	Homozygous / uninformative
	Heterozygous = 0.71-1.42
	30-49% loss: 0.51-0.70 or 1.43-1.99
	50-100% loss: ≤0.50 or ≥2.00
	blank = unknown

Table 4.6: DNA derived from histologically confirmed benign / malignant areas of six paraffin embedded prostates that had been sampled for colonies was analysed at 55 loci for LOH. The proportion of LOH is given compared to lymph node DNA.

Patient (cont...)	#1			#2			#11		#12		#14		#15	
Marker	Be1	Be2	Ca	Be	Ca1	Ca2	Be	Ca	Be	Ca	Be	Ca	Be	Ca
D11S902	1.19	0.88	1.19	1.09	0.91	0.97					1.15	1.06	0.97	0.99
D11S903	Hom	Hom	Hom				0.98	0.87			Hom	Hom	1.07	0.92
D11S916	0.89	1.13	1.04	0.91	1.00	1.00	1.01	1.02	0.91	0.97	1.00	1.01	1.01	1.04
D11S990	0.99	1.06	0.96	Hom	Hom	Hom	0.99	1.03	1.29	1.05	Hom	Hom	0.93	0.98
D11S2000	1.09	0.57	1.02	1.06	1.04	1.02	0.82	0.98		1.03	Hom	Hom	Hom	Hom
D12S89	1.02	1.00	1.05	1.18	1.01	1.00	0.96	0.93	1.07	1.00	Hom	Hom	1.02	0.94
D12S1697	1.04	0.55	1.10	1.06	0.97	1.09					0.95	0.90	0.92	0.96
D13S165											1.00	0.95	Hom	Hom
D13S171	0.99	0.99	0.91				1.01	1.02					0.96	0.97
D13S263	0.99	1.03	1.00	1.00	1.12	1.07	1.05	0.66	0.95	0.98	0.99	0.99	0.99	1.01
D13S269	0.86	0.93	0.97				0.94	0.59					1.01	1.07
D13S284							1.42	0.99	1.07	0.99	Hom	Hom	Hom	Hom
D15S1232	Hom	Hom	Hom	1.02	1.01	0.54	1.00	0.88	1.02	1.02			1.35	1.22
D16S413	1.14	1.05	0.21	Hom	Hom	Hom			1.02	1.01	1.03	1.05	Hom	Hom
D16S422							0.95	1.11	0.85	0.95			1.00	0.85
D16S505	0.95	0.90	1.09	1.00	0.99	0.99	0.91	1.03					Hom	Hom
D17S515	Hom	Hom	Hom	0.92	0.57	0.95								
D17S786							1.04	0.99	0.95	0.97	0.98	0.70	0.92	0.95
D17S855											0.87	0.49	1.24	0.25
D17S938								1.01			0.99	0.85	0.61	0.67
D18S363	1.09	1.07	1.99	1.00	0.90	1.01	0.95	1.08	1.13	0.99	0.96	0.98	0.94	0.97
D18S364								1.12			0.93	0.95	0.96	0.90
D18S470													0.90	1.03
D18S541	1.01	1.21	0.54	0.91	0.92	0.91	Hom	Hom			Hom	Hom	1.00	1.07
D19S223	1.11	0.53	1.08	0.98	1.05	1.05					1.01		1.06	1.17
D21S156	0.98	1.03	0.99	0.94	0.94	0.93	1.01	2.84	0.96	0.93	1.00	0.67	0.96	0.45
FALI at 50%	0.00	0.00	0.11	0.00	0.00	0.00	0.03	0.05	0.00	0.00	0.00	0.03	0.00	0.05
FALI at 30%	0.03	0.11	0.23	0.00	0.06	0.06	0.03	0.14	0.00	0.00	0.00	0.09	0.02	0.07

FALI - fractional allelic-loss index (proportion of informative loci showing LOH)

Table 4.6: continued.

Hom	Homozygous / uninformative
	Heterozygous = 0.71-1.42
	30-49% loss: 0.51-0.70 or 1.43-1.99
	50-100% loss: ≤0.50 or ≥2.00
	blank = unknown

For the six prostates analysed, Seventeen percent of all loci were homozygous. Using a cut-off of 50%, seven loci demonstrated LOH for one or more prostates and four prostates (67%) demonstrated one or more foci of LOH. Using a cut-off of 30%, 21 loci demonstrated LOH for one or more prostates and five prostates (83%) demonstrated one or more foci of LOH. The incidence of LOH is often given in terms of the fractional allelic-loss index (FALI), which is the proportion of informative loci showing LOH. The FALI for each sample is given at the bottom of table 4.6 and ranges from 0.0-0.11 for 50% cut-off, and 0.0-0.23 for 30%.

The presence of LOH is entirely dependent on the cut-off selected. The most convincing LOH demonstrated here showed an 82% loss of one allele. This suggests that in this tissue sample at least contamination with normal tissue might be in the region of 20%, so a relaxing of the threshold to 50% is reasonable. A plot of the distribution of all 493 LOH analysis outcomes (data not shown) showed a large clustering of values centred around 1.0 as would be expected and a much smaller cluster centred around 55-60% which could represent the population of loci with LOH. A cut-off of 30% would include these. As the threshold for designating LOH is lowered, the chance of incorrectly calling LOH increases. It was therefore decided to analyse the colonies at the loci demonstrating >50% loss first, as a proof of principle that the colonies will share LOH at these loci, with the option of returning to further loci as required.

The incidence of LOH identified in these six prostates is low, which limited the choice of loci to analyse in the colonies, and rendered at least one prostate unevaluable. This was despite exhaustively screening at 55 microsatellite loci. Others have reported higher rates of LOH in larger series of radical prostatectomy specimens. Bott *et al* (2006) studied 30 microsatellite loci in 62 men and identified LOH in 92% of cases, while Fromont *et al* (2003) studied only 12 loci in 48 men and found 94% had at least one missing locus. LOH rates may be lower in this study for a number of reasons. Firstly numbers are very small, so had more prostates been assessed the yield might have approached that experienced by others. The prostates harvested contain early prostate cancer that will not have accrued a great number of mutations yet though losses of DNA are five times more common than gains in primary prostate cancer (Visakorpi *et al*,

1995). Yield can also be increased by using several overlapping or adjacent markers for candidate loci, which was not done here for most chromosomes (Leube *et al*, 2002). Finally contamination of the tumour sample with normal cells or a mix of different cancer foci may be too great (Müller *et al*, 2004). There is also the possibility that early PCR cycles randomly favour benign alleles leading to over-representation of them in the final PCR product (Seiben *et al*, 2000).

4.5.3 LOH analysis of presumed benign and malignant colonies at loci demonstrating LOH in the primary tumour

Altogether seven loci demonstrated allele loss of >50% in four of the original cancer samples. For these seven loci, DNA derived from between 14 and 17 presumed benign and between 12 and 20 presumed malignant colonies was analysed. Figure 4.4 shows the electropherograms obtained from benign and malignant tissue from the original fixed tissue for prostate #1 and corresponding electropherograms for some colonies derived from tissue from the same area for locus D10S587. The LOH analysis for all such colonies from all four prostates are given in table 4.7. A threshold of 70% was used as a cut-off for LOH in these tissues, as the colonally derived colonies would be expected to contain a pure population of genotypically identical cells.

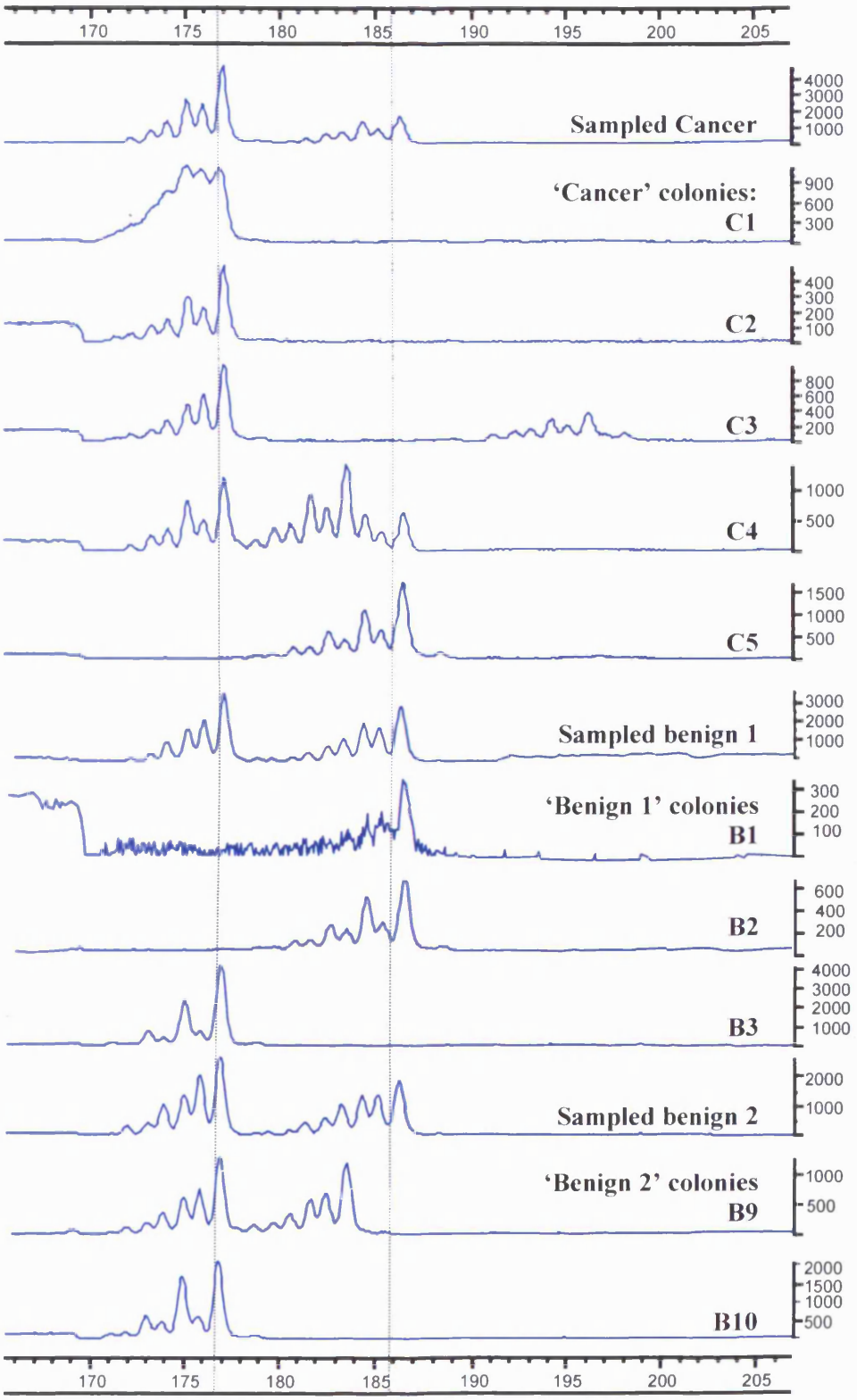

Figure 4.4: LOH analysis of original benign/malignant tissue from prostate #1 and corresponding colonies. The vertical dotted lines denote the lengths of the two alleles of microsatellite marker D10S587 in this patient (177 and 187 bp). Colonies showed various LOH patterns and allele lengths suggesting MSI.

Prostate	#1		#11		#14	#15	
Locus	D10 S587	D16 S413	D10 S541	D21 S156	D17 S855	D17 S855	D21 S156
Original Benign	1.05	1.14	2.17	1.01	0.87	1.24	0.96
	1.04	1.05					
B1	7.52	9.89	2.69	0.98	0.79	0.94	0.89
B2	16.0	MSI	0.90	1.05	0.99	0.99	1.23
B3	0.02	0.78	13.3	1.12	1.00	1.08	-
B4	0.98	0.99	-	0.89	MSI	-	1.10
B5	-	-	0.96	1.07	1.01	1.32	1.12
B6	1.10	-	-	-	0.90	0.62	0.96
B7	0.94	0.91	0.01	1.12	1.20	0.05	1.10
B8	MSI	1.48	0.87	0.88	0.99	1.04	1.22
B9	0.01	12.2	16.8	1.44	-	0.96	0.93
B10	0.02	1.24	-	-	0.03	1.02	0.81
B11	0.87	0.94	0.99	1.02	0.89	0.90	1.14
B12	15.6	1.37	-	1.13	-	1.01	1.28
B13	1.08	1.00	-	-	-	0.99	1.00
B14	-	0.99	1.01	0.83	0.53	0.06	2.29
B15	1.01	26.43	0.83	15.2	0.91		
B16	0.93	1.12			0.90		
B17					1.11		
Original Cancer	0.18	0.21	0.22	2.84	0.49	0.25	0.45
C1	0.02	MSI	0.78	1.13	1.00	1.09	1.27
C2	0.08	0.01	1.00	1.08	0.98	20.7	0.70
C3	MSI	0.01	0.04	0.90	0.78	-	1.03
C4	MSI	0.01	0.02	0.99	-	-	1.55
C5	12.1	1.11	-	-	0.98	1.00	0.61
C6	0.97	1.03	1.23	0.64	MSI	0.02	1.08
C7	-	-	-	2.50	1.02	0.88	1.33
C8	0.01	0.03	-	0.84	1.01	0.96	0.95
C9	-	-	0.76	1.01	0.96	-	1.27
C10	0.02	0.94	-	-	1.25	0.03	1.38
C11	1.00	1.07	0.03	1.11	-	0.79	1.44
C12	-	-	0.01	12.1	1.04	MSI	4.83
C13	-	-			-	0.95	1.13
C14	MSI	0.65			0.90	-	-
C15	0.02	0.01			-	1.03	1.01
C16	1.10	0.80			-		
C17					-		
C18					0.10		
C19					1.11		
C20					1.06		

Table 4.7: Outcome of LOH analysis of presumed benign and malignant colony DNA at loci identified as missing in the original prostate.

Heterozygous:	0.71-1.42	
30-49% loss:	Lower allele 0.51-0.70	
	Upper allele 1.43-1.99	
50-69% loss:	Lower allele 0.31-0.50	
	Upper allele 2.00-3.32	
70–100% loss:	Lower allele <0.30	
	Upper allele >3.33	
Microsatellite instability		MSI
Uninterpretable		-

Prostate	#1		#11		#14	#15	
Locus	D10 S587	D16 S413	D10 S541	D21 S156	D17 S855	D17 S855	D21 S156
			'BENIGN' COLONIES				
Number assessed	14	14	10	12	14	13	13
% (no.) with expected normal alleles	50(7)	71(10)	70(7)	92(11)	86(12)	85(11)	100(13)
% (no.) colonies with LOH	43(6)	21(3)	30(3)	8(1)	7(1)	15(2)	0
% (no.) with MSI	7(1)	7(1)	0	0	7(1)	0	0
			'CANCER' COLONIES				
Number assessed	12	12	8	10	14	11	14
% (no.) normal germ line alleles	25(3)	42(5)	50(4)	70(7)	86(12)	64(7)	64(9)
% (no.) colonies with expected LOH	42(5)	42(5)	50(4)	20(2)	7(1)	18(2)	0
% (no.) with other LOH	8(1)	8(1)	0	10(1)	0	9(1)	36(5)
% (no.) with MSI	25(3)	8(1)	0	0	7(1)	9(1)	0

MSI – Microsatellite instability

Table 4.8: Summary of findings of colony LOH analysis, using a cut off of 70%.

The hypothesis was that the LOH identified in DNA from the original benign and malignant tissue from each prostate would be present in the colonies grown from adjacent tissue, thus distinguishing those benign colonies contaminating the population of cancer colonies. Figure 4.4 and table 4.7 demonstrate that this is not the case. A far greater variety of allele lengths and loss was seen in both the presumed benign and presumed cancer colonies than seen in the original prostate tissue.

LOH was present frequently in the colonies. As expected, because the source of the DNA was from a purer, clonally derived population of cells, the signal from the lost allele was very weak if not absent compared to the signal from the retained allele, giving definitive LOH appearances and very high percentage losses. However, LOH was seen not only in the presumed malignant colonies,

but also in the benign ones. Furthermore, even where a colony demonstrated LOH, this was sometimes due to loss of the other allele than the one lost by the original cancer. A summary of the frequency of each of these outcomes is given in table 4.8. For individual benign colonies, between 50 and 100% of them had a normal genotype to match the original sample, but from 0 - 43% had LOH. For the cancer colonies, 0-50% had the same LOH pattern as the wholemount tumour, but 25-86% had a normal genotype and 0-36% showed another LOH pattern again. There was a higher number of cancer colonies with a normal phenotype at those loci where LOH in the original block was close to the cut off e.g. D17S855 had 51% allele loss and 86% 'normal' cancer colonies. Thus these loci may not in fact have been mutated in the original cancer, and benign colonies would be expected.

MSI was also seen in the colony DNA. Here both alleles were present, but one differed in length by up to 14 extra base pairs or by a loss of up to 4 base pairs compared to the original DNA. There was also evidence of duplication of some alleles with a third allele with a different length being present alongside both expected alleles. The electropherogram for the cancer colony C4 in figure 4.4 demonstrates this phenomenon with three peaks suggesting three alleles 177, 183 and 187 base pairs in length.

There was little internal consistency for colonies analysed at even only two loci, with a presumed benign or cancer colony demonstrating a normal genotype at one locus and LOH at the other. Only a minority of colonies matched the genotype of the original tissue for the two loci screened making them candidate confirmed benign and malignant colonies. Nor did the incidence of abnormality seem greater in the cancer colonies than the benign as might have been expected given that the real concern was that benign cells would contaminate cancer tissue, while truly benign tissue is easier to select. Given the large numbers of benign colonies that apparently harbour genetic alterations, and of cancer colonies that lack them, it would be necessary to screen these candidate colonies at a number of other loci before being confident of their pedigree. Of course, with the low rate of LOH in the original cancer, there are limited numbers of loci to use.

Such extreme apparent variation in the genotype of these colonies compared to the original prostate tissue sample rendered LOH analysis unusable as a means of classifying colonies. This may be the result of a number of factors. Inevitably, the tissue used to grow colonies, cannot be submitted for LOH analysis and vice versa. Though both were adjacent in the original prostate, the cultured tissue may have differed from the analysed tissue. Thus a different cancer with a different genotype could have been grown to that analysed for LOH. Equally two colonies with different genotypes could have grown on top of each other, appearing macroscopically as one colony, while its DNA was a mixture. This might account for the presence of two alleles in a cancer colony, but not for some of the other genotypes encountered.

Obtaining these results due to culture artefacts also seems unlikely. This extent of genetic variation might imply a high degree of genetic instability and acquisition of mutations as each cell rapidly clonally expanded during the weeks in culture before and after ring cloning. The development of LOH and MSI in the benign colonies would alter their two allele appearance, while development of MSI in cancer colonies, would cause the remaining allele to show heterogeneous allele lengths again. In reality, even if these cells were this unstable, the likelihood of so many colonies mutating at these specific loci is minimal. Indeed, the entire basis of tissue culture and the use of cell lines relies on their genetic stability in long term culture. Despite multiple passages, the cell lines established by Bright *et al* have retained their distinctive LOH pattern. One study evaluated changes in the restriction fragment length polymorphism patterns of four leukemic cell lines in culture at monthly intervals for a year (Parson *et al*, 2005). Two developed changes between the second and third month due to the emergence of heterogeneous subclones. However this is still far longer in culture than the few weeks spent by the colonies, and these cancer cell lines, with known mutations in mismatch repair genes would be expected to be more unstable than some benign prostate epithelium.

Although it is probable that the colony DNA is minutely contaminated with mouse DNA from their necessary growth on a feeder layer, the surviving feeder

cells were rinsed off prior to colony harvesting and all LOH analysis primers were blasted to confirm their specificity for human DNA. Also the mouse alleles for any locus would have to correlate closely in length.

Two plausible explanations remain to account for these findings: DNA artefact, and the selection by culture of individual mutation bearing cells not identified when the tissue as a whole is analysed for LOH or histologically.

The impact of experimental artefact on these results cannot be quantified, but could potentially be significant. Throughout these experiments the total amount of DNA available for analysis amounted to a few micrograms only. Original prostate DNA was paraffin embedded and stained, and some colonies were scraped off the culture flask so DNA quality might have been affected. Longer nucleotide products were harder to obtain results from and required a number of repeated reactions. The majority of experiments were performed once if a result was obtained first time. However, often an electropherogram was too weak to be interpreted so the concentration of PCR product was increased and the sample run again. If this did not yield a meaningful result, the PCR was repeated. For both the original and colony DNA confirmatory repeat LOH analysis would have been desirable, though DNA quantities would limit the number of loci re-screened.

Work by Seiben *et al* (2000) suggests that the amount of DNA used in the initial PCR reaction is critically related to the incidence of artefactual LOH or MSI. Mispriming during the PCR reaction especially in an early amplification cycle can result in incomplete, additional or entire non-amplification of alleles. Fixation and staining causes DNA fragmentation, which reduces the efficiency of the PCR. In addition, microsatellite DNA regions are already prone to erroneous transcription due to polymerase slippage on the repeat regions and misannealing and hairpin formation especially in CG rich sequences (Diaz-Cano, 2001). Plentiful DNA minimises the impact of these errors on the final outcome.

Seiben *et al* (2000) found that the incidence of artefactual LOH in 12µl PCR reactions containing 0.05ng of template DNA was 17.5% while this dropped to

3.2% for 5ng and 0.7% for 10ng. Artefactual MSI was seen in 16.5% of 0.05ng DNA reactions, but was absent when 5ng or 10ng was used. They found that LOH artefact rates were higher in fixed tissue, and MSI rates higher when longer fragments were being amplified (3.2% if <120 base pairs, 7.7% if >190 base pairs). A specific artefact was never reproduced in a second PCR reaction, though on occasion a different LOH artefact was seen. The authors recommended a minimum amount of 5ng of fresh tissue DNA or 10ng of archival tissue DNA be used in PCR reactions when investigating LOH. They commented that as quantification of DNA prior to LOH analysis is not routinely performed, so PCR artefact may be responsible for a proportion of the LOH and MSI reported in the literature, and may explain conflicting studies.

In this project, the colonies from the first two prostates were fixed and stained before being scraped off the plastic dish with a scalpel for DNA. Subsequent colonies were harvested fresh and also ring cloned with DNA obtained at first passage. The DNA from the first two prostates was extracted using the small cell sample method (see Methods, section 2.9), which yielded 50µl of template DNA solution. Subsequent samples were processed through a column with a final volume of 160µl. Because of limited DNA samples, early PCRs used 1.5µl of template, and later ones 2.5µl. DNA concentrations were not measured at the time of analysis, as their dilution meant that an optical density could not be obtained without committing large volumes of DNA solution to the analysis. Retrospective analysis of DNA quantities showed that colony DNA extracted from a single fresh type II colony had a mean concentration of 226ng/µl (standard deviation 39ng/µl) while ring cloned colony DNA had a mean DNA concentration of 223ng/µl (standard deviation 51ng/µl), which would have resulted in template quantities in the PCR well above the 10ng recommended by Seiben *et al.* However for prostates #1 and #2, insufficient volumes of DNA solution remained to permit analysis. It may be relevant that greater variations in results were seen in these early prostates than later ones.

DNA artefact may then underlie some of the results, but perhaps not all. An alternative explanation, assuming they withstood confirmatory repeat analyses is that the genetic make up of the individual cells that emerged in culture is far

more varied than that demonstrated by the tissue as a whole. The histological classification of the formalin fixed prostate specimen is based on its low power architecture (Gleason and Mellinger, 1974). Thus the histological diagnosis of an area of prostate tissue is based on its overall appearance, just as its genotype (as established by LOH analysis) is based on the overall LOH patterns within the cells contributing DNA. A small area of cancer though present, would be obscured by more predominant benign tissue. In contrast, the colony DNA submitted to LOH analysis reflects the genotype of a single cell within the prostate. A single malignant cell will not be recognised histologically, but might grow into a colony. This also applies to cells with proliferative inflammatory atrophy, atypical adenomatous hyperplasia or HGPIN. It is possible that the variety of colony genotypes encountered in this prostate tissue from a man in his sixties reflects the variety of cell genotypes within it.

It would be expected that as these genotypes should be present in the same proportions as in the original tissue, the majority of colonies from a grossly benign looking area of prostate tissue should have predominately matching benign genotypes. The fact that they seem not to may suggest that the culture conditions are selecting for this population of more genetically variable cells, which perhaps possess growth advantages conferred by these very mutations. That a mutation at this particular microsatellite locus carries with it a growth advantage is not implausible as the loci screened for were initially identified as lost in prostate cancer. These type II colonies arise once in approximately every 2000 cells plated (see table 4.4) so while the genetic instability they apparently possess may be rare in a largely benign area of prostate tissue, so are they.

In fact, the genotype of primary colonies derived from both benign and malignant prostate epithelium has not been previously reported. A similar study in breast tissue, another hormonally responsive, glandular tissue prone to malignancy has though. Lakhani *et al* studied colonies of 1000-5000 cells derived from 'normal' breast tissue adjacent to breast cancers and from non-cancerous breasts, performing LOH analysis at seven microsatellite markers (Lakhani *et al*, 1999). Normal cells showed allelic imbalance in five out of ten breast cancer cases and one of three breast reduction specimens free of cancer.

They argued against a culture artefact, as the LOH patterns seen were plausible, as they were also present in the cancers and concluded that the extent of genetic alteration in 'normal' tissue was likely to be underestimated.

Cancer arises through a series of mutations, and losses of DNA are five times more common than gains in primary prostate cancer, so microscopically benign areas may harbour LOH, especially in cancer prone peripheral zone tissue (Hanahan and Weinberg, 2000; Visakorpi *et al*, 1995). Bright *et al* (1997) also identified LOH in the benign cell lines from one patient. Numerous studies attest to the presence of a far greater degree of genetic variation in the prostate than currently envisaged. Though none have focused on the progeny of a single cell, the majority of investigators used laser capture microdissection to study small areas of HGPIN, other histological prostate entities and cancer. Regrettably few have similarly analysed adjacent benign tissue or BPH and indeed this tissue is sometimes used as a control.

A group under Schalken assessed allelic imbalance at 33 loci in laser microdissected HGPIN, and paraffin sections of different cancers and different areas within the same cancer of 17 radical prostatectomy specimens (Ruijter *et al*, 1999). Using a benign area of tissue as a control, they identified common patterns of allele loss in some distinct tumours, but also as much disagreement between different loci and within different areas of ostensibly the same tumour. Also small or low grade tumours and HGPIN showed considerable allelic imbalance. The overall picture was complex with evidence for clonal tumour spread in some areas that was lacking in other areas within even the same cancer. Their conclusion that further study of numerous samples at numerous loci was required appears correct. Had they assessed benign tissue against a germ line control such as peripheral blood lymphocytes, they might have identified an even more complex picture.

Other authors have studied the relative allelic imbalance in cancer, HGPIN, atypical adenomatous hyperplasia and occasionally benign tissue. Bostwick and colleagues (1998) found similar incidences of allelic imbalance in microdissected samples of HGPIN and cancer (65% and 82% respectively) at six microsatellite

loci, with evidence of clonal progression from one to the other. The same group studied atypical adenomatous hyperplasia and found allelic imbalance in 47% of 15 lesions, at five loci implicated in prostate carcinogenesis (Cheng *et al*, 1998). Another study also included this in their panel of samples, and notably evaluated adjacent benign prostate tissue as well (Bettendorf *et al*, 2005). Allelic imbalance at ten loci was identified in 64% of 14 cancer samples, and 55% of nine HGPIN samples. Only two of ten atypical adenomatous hyperplasia samples showed allelic imbalance, but interestingly 50% of 14 samples of non-neoplastic tissue adjacent to cancer foci showed allelic imbalance.

So at the individual cellular level, there may be more genotypic variation than previously thought, especially in a prostate that already contains some cancer. Though the extreme variations seen in the colonies are surprising, if all the different traces were taken together, both alleles would be well represented and the overall appearance would be one of heterozygosity as was encountered in the original prostate tissue.

There is no doubt that the possibilities raised by this small sample of colonies and prostates needs confirmation by a similar study repeated in duplicate at least, and on a larger scale. Parallel analysis of cancerous, benign and hyperplastic tissue derived prostate epithelial cell colonies alongside laser capture microdissected areas of the source prostate would allow mapping of the genotype of the prostate, and possibly matching of colony genotype to histologically defined lesions. It would be interesting to know whether the variety of genotypes in colonies derived from BPH or from younger men (usually cadaveric donors) conformed better to the 'normal'.

Such wholesale LOH analysis of so many samples was extremely laborious. However, high-throughput automated techniques have recently emerged in this arena. The Affymetrix Chromosome Copy Number Analysis software can analyse high-density single nuclear polymorphism oligonucleotide arrays to identify loss of heterozygosity and chromosomal gains and losses at loci across the whole genome in a matter of hours (Affymetrix UK Ltd, High Wycombe, UK; Zhao *et al*, 2004; Torring *et al*, 2007). Such techniques would provide an

unequalled view of the genotypes of these colonies and where they stand against the genotypes found in the prostate itself.

4.6 Differentiating between benign and malignant colonies using expression levels of genes upregulated in prostate cancer.

Colonies were also assessed for phenotypic differences. The mRNA levels of four genes that have been reported as being over-expressed in prostate cancer were assessed using semi-quantitative RT-PCR of colony total RNA. The four genes used were hepsin, AMACR, EZH2 and PIM1 with GAPDH as a control (see appendix 2 for PCR primer sequences).

Hepsin is a cell-surface serine protease that was found to be upregulated 4.3-fold in prostate cancer by microarray, 11.3-fold by northern analysis, and which was predominately expressed in HGPIN and hormone sensitive prostate cancer on tissue microarrays (Dhanasekaran *et al*, 2001). Pim-1 is a proto-oncogene which expresses a serine/threonine kinase. On tissue microarrays, it is absent or weakly staining in 97% of benign prostate samples, while being moderately or strongly present in about half of the prostate cancer samples (Dhanasekaran *et al*, 2001). The polycomb group protein enhancer of zeste homolog 2 (EZH2) appears to have a role in mediating cell proliferation and transcriptional repression in prostate cells (Varambally *et al*, 2002). It is significantly over-expressed in prostate cancer compared to benign prostate both on DNA microarrays, RT-PCR and tissue microarrays, where respective median staining intensity is 1.5 (95% confidence interval (CI) 1.4-1.6) for benign tissue, and 2.6 (CI 2.5-2.7) for localised cancer. AMACR has also been shown to be significantly upregulated in prostate cancer on DNA microarrays, RT-PCR, western blotting and tissue microarrays, where mean protein staining in benign tissue was 1.31 (CI 1.23-1.40) and in malignant samples was 3.20 (CI 3.10-3.28) (Rubin *et al*, 2002). Used diagnostically in prostate biopsy needle samples, it is 97% sensitive and 100% specific for detecting prostate cancer (Rubin *et al*, 2002).

Three prostates yielded colonies from which RNA was isolated: three colonies were analysed from prostate 12, 37 colonies from prostate 14 and 29 from

prostate 15. The RT-PCR products were visualised using gel electrophoresis and the relative measured intensities (in terms of highest intensity and total amount of fluorescence normalised for GAPDH intensity) of the benign colony bands were compared to the malignant colony bands using the Student's t test (see figure 4.5). Hepsin PCR yielded minimal product across all samples so was not analysed further.

Prostate (available colonies)	Gene	Colony source	Mean peak intensity, (significance)
#12 (1 benign, 2 cancer)	AMACR	Benign	
		Cancer	
	EZH2	Benign	
		Cancer	
	PIM1	Benign	
		Cancer	
	GAPDH	Benign	
		Cancer	
#14 (17 benign, 20 cancer)	AMACR	Benign	95.2
		Cancer	94.0 (p=0.96)
	EZH2	Benign	44.4
		Cancer	76.2 (p=0.01)
	PIM1	Benign	10.0
		Cancer	12.6 (p=0.57)
	GAPDH	Benign	45.5
		Cancer	47.9 (p=0.27)
#15 (14 benign, 15 cancer)	AMACR	Benign	57.0
		Cancer	50.7 (p=0.49)
	EZH2	Benign	61.5
		Cancer	43.1 (p=0.12)
	PIM1	Benign	18.1
		Cancer	14.5 (p=0.45)
	GAPDH	Benign	58.9
		Cancer	52.0 (p=0.94)

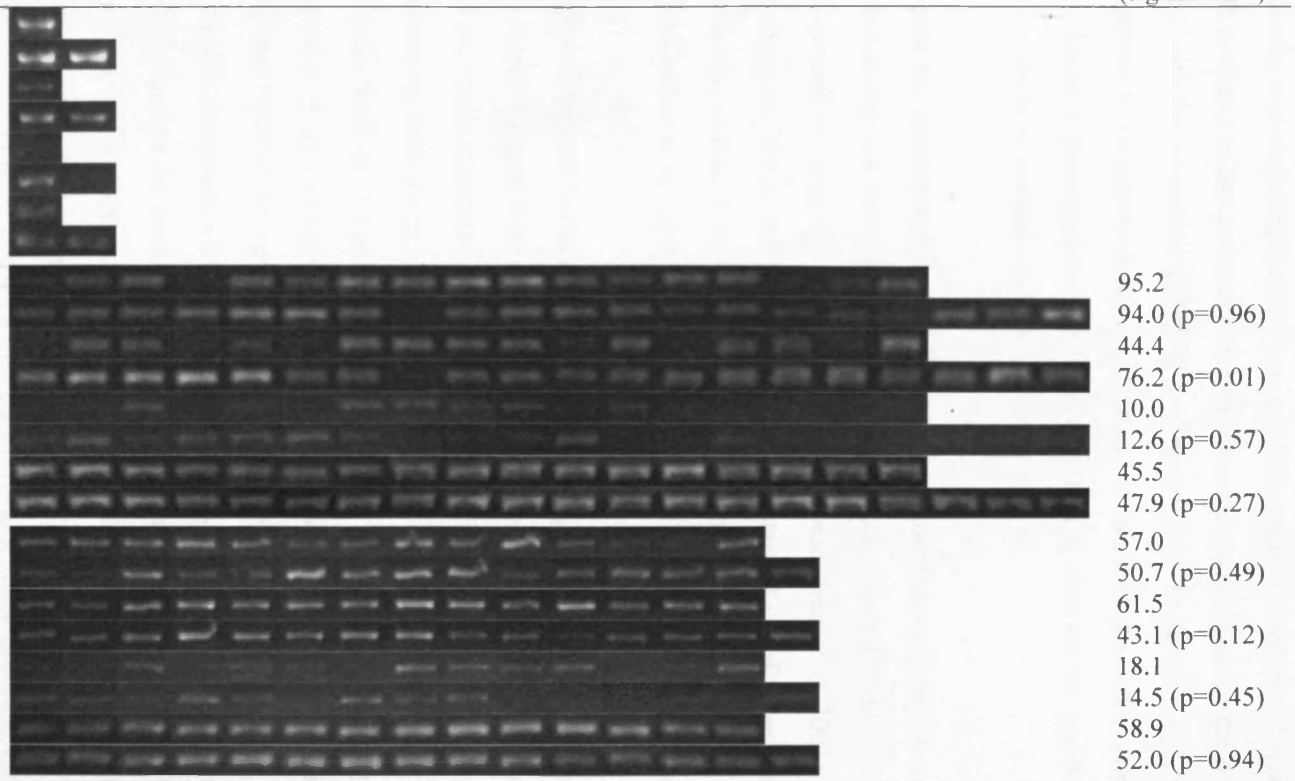

Figure 4.5: RT-PCR of total RNA from presumed benign and malignant colonies from three prostates was performed for 3 genes AMACR, EZH2 and PIM1 reported as being upregulated in prostate cancer, and for GAPDH. Significance assessed by student's t-test.

Both visually and statistically there was no difference in intensities between the RT-PCR products of the presumed benign/cancer colony types for the three prostates, with the exception of EZH2 for prostate #14. In prostate #15, while EZH2 appears to be approaching significance, in fact average expression in the benign colonies is greater than in the cancer colonies, thus the change in expression levels is contrary to that expected.

The studies that highlighted these genes as molecular discriminators between benign and malignant tissue used prostate cancer cell lines DU-145, LN-CAP and PC3 as well as fresh and archival tissue (Dhanasekaran *et al*, 2001; Varambally *et al*, 2002). All three markers are expressed in cell lines, and there is evidence that AMACR is expressed in primary prostate epithelial cell cultures (Maria McCrohan *et al*, 2006; Varambally *et al*, 2002; Kim O *et al*, 2004).

The lack of difference between the presumed benign and presumed cancer colonies would suggest that both 'benign' and 'cancer' tissue samples that were cultured may have contained a mixture of colonies. Alternatively, these markers were defined by their upregulation in 'whole' cancers, and their normal expression in these early epithelial cells in culture is unreported and may be heterogeneous in its own right. RT-PCR and immunohistochemistry of TURP tissue derived colonies as a representative source of benign DNA would be interesting. For instances where signal is similar between colonies, it may be that the RTPCR reaction for one sample reached its plateau phase and amplification ceased sooner that in another less abundant sample, which then 'caught up' with it. Real-time RTPCR allows quantification of PCR product during the exponential amplification phase of the reaction and is more accurate, though still may not have altered the conclusion here (Gilliland *et al*, 1990).

While care was taken to select those markers well established as differentially expressed in prostate cancer compared to benign tissue, no marker exists that demonstrates a true on/off expression in the benign/malignant state. Accordingly, it is possible that the cancers grown here were of the 50% that do not express PIM-1. However this would apply to all the cancer colonies grown from the same cancer, so homogeneity of expression (be it absent or present) would be

expected. Such a debate could be answered by immunohistochemistry of the paraffin embedded prostate for this marker, but would not assist in the interpretation of the RT-PCR here. Other markers also exist. p63 has been described as being absent in prostate cancer by immunohistochemistry, and *in vitro* it is not expressed by the prostate cancer cell lines LNCaP, DU145 and PC3 but is present in 80% of cells from the normal basal prostate epithelial cell line PrEC (Signoretti *et al*, 2000). Claudin-1, a tight junction protein, and annexin II, a calcium and phospholipid binding protein also predominately stain benign but not malignant glands in immunohistochemistry studies (Krajewska *et al*, 2007; Stewart *et al*, 2007).

4.7 Discussion

This study has demonstrated that when benign and malignant areas of peripheral zone prostate tissue are sampled, processed into a single cell suspension and cultured for two weeks, both yield distinguishable type I and type II colonies. Comparisons of colony incidence and morphology identified no differences between colonies from benign and malignant tissue, nor between these and those derived from BPH tissue.

It proved impossible in this project to confidently identify benign and malignant colonies using differences in genotype detected using LOH analysis, or in phenotype using semi-quantitative RT-PCR. Therefore, the characteristics of malignant and benign peripheral zone type I and type II colonies remain unknown. Indeed, while it is likely that benign colonies were grown, it is not proven that any malignant colonies were grown.

Culture of primary prostate epithelial cells is difficult; both due to the inherent risk of contamination during tissue selection, and in this project the need for reasonable quantities of corresponding benign and malignant colonies for downstream applications. Even for those prostates that were successfully cultured, there was a low incidence of LOH identified, despite extensive screening of relevant loci. Small DNA amounts and an unexpected variability in the genotypes of those colonies grown further confounded matters. The

hypothesis that LOH analysis would cleanly segregate cancer colonies from benign ones by matching the genotype of the parent cancer was disproved.

Semi-quantitative RT-PCR of early prostate cancer markers also failed to discriminate benign from malignant prostates, possibly due to baseline variability of expression, mixed benign/malignant colonies or insufficiently discriminatory markers.

The inherent difficulty of distinguishing benign from malignant prostate tissue both in the freshly cut specimen and in culture has been noted by others. Rose *et al* (2005) compared primary cultures (in serum free, low calcium medium) of six benign and six >90% malignant prostate samples using DNA microarray, real-time RTPCR and immunoblot techniques and found no gene or protein that was consistently over-expressed in all the cancer versus BPH cell cultures. In the absence of a specific biochemical or cell surface marker, *in vitro* behavioral properties have traditionally been evaluated. Cultured tumour cells may differ from their benign counterparts in a number of ways. These are listed by R Ian Freshney (2002b):

1. Aneuploidy revealed by conventional karyotyping or specific molecular probes.
2. Heteroploidy with different karyotypes found within the cell population.
3. Loss of contact inhibition at confluence with disorderly cell migration.
4. Loss of density limitation at confluence with continued proliferation.
5. Anchorage independence with greater colony formation in soft agar suspension.
6. Higher proteolytic activity.
7. Promotion of angiogenesis.
8. Invasiveness
9. Tumourigenesis in experimental hosts.

He does however note that freshly explanted tumour cells at early-passage need not express all these characteristics, and that as few are diagnostic alone several must be demonstrated before declaring malignancy. In fact, transplantation of

primary prostate cancer tissue into nude mice results in very infrequent tumour formation and prostate cancer does not differ from benign tissue in its response to stimulatory and inhibitory factors (Schroeder *et al*, 1976; Peehl *et al*, 1989). For prostate cell culture in general, and this study in particular, many of these characteristics are untestable. In this study, the difficulties encountered in primary cell culture and the number of individual colonies requiring assessment also precluded comparison of some of the above characteristics.

Cytology is often used to diagnose cancer, however microscopy of the colony cells after ring cloning did not demonstrate sufficient differences in cell size or nuclear-cytoplasmic ratio to allow distinction. Indeed, the 'virtually normal appearance of the individual cells' in cytological preparations of cancers derived from prostatectomy samples has long been noted (Mason, 1964).

In practice, a number of assays have emerged as useful discriminators. In a recent study with far reaching implications, Dalyrymple *et al* (2005) demonstrated that culturing primary malignant prostate tissue in low-calcium medium (defined as <260 μmol/L) selected for benign cells. Serum-free culture media are favoured for prostate tissue as serum contains undefined factors that are difficult to standardize for, and promotes the growth of stromal cells. Both PrEGM and keratinocyte serum-free medium (K-SFM) complete medium (Invitrogen, Carlsbad, CA, USA) are commonly used in studies on benign and malignant tissue, and contain low total calcium levels of 260 ± 14 μmol/L and 75 ± 2 μmol/L respectively. In contrast, all currently available prostate cancer cell lines, whether established from early cancers or bone metastases require 10% foetal calf serum supplemented media with calcium levels between 650 and 1,860 μmol/L. These cell lines demonstrate karyotypic abnormalities, are spontaneously immortal and able to undergo numerous serial passages, and form tumours when inoculated into mice. Tumours are also expected to demonstrate similar marker expression and LOH patterns to the cancer of origin.

Dalyrymple *et al* (2005) examined these attributes in cell cultures derived from prostate cancer specimens in PrEGM and compared them to cancer cell lines and commercially available PrEC benign cells (see section 1.6). Their markers

matched those of the benign cells, for instance, they were $AMACR^-$ like PrEC cells while all cancer cell lines are $AMACR^+$. Nor did these cultures progress in culture past 8 – 10 passages, or form tumours in mice over 6 months. Interestingly, when stromal cells and all the cancer cell lines are grown in supplemented but low-calcium medium they die within 3 passages. Conversely, PrEC cells undergo growth arrest when the calcium concentration in their medium is increased to 650 μmol/L.

This raises uncertainty about studies performed on putative cancer cells maintained in low-calcium medium. The comparison study by Rose *et al* (2005) described above used this, and could detect no reliable differences. A study of karyotype analysis in two to seven day cultures of 102 primary prostate cancers was performed by König and colleagues (1998). They assayed three different culture conditions for their cells, concluding that the one that excluded serum generated the most cultures. However analysis of the metaphase spreads showed that most cells had normal karyotypes and it was concluded that the culture conditions favoured diploid cells. The authors felt that karyotype analyses such as comparative genomic hybridisation that did not require a period in cell culture would have more relevance to the study of cancer genotypes.

In most studies, the malignant nature of the cells obtained is assumed, or at best compared to established prostate cancer cell lines (Hall *et al*, 2002; Bright RK *et al*, 1997; Maria McCrohan *et al*, 2006; Peehl DM *et al*, 1989; Rose *et al*, 2005; Collins *et al*, 2005). In most studies, pathologists dissect out fresh prostate cancer tissue as described by Wheeler and Lebovitz (1994), with histology of adjacent tissue on all sides confirming 70-90% cancer tissue and by definition 10-30% other types of cells. Improved accuracy has been reported using an operating microscope and staining the cut prostate surface with 0.5% aqueous toluidine blue (Fischer *et al*, 2001).

Collins *et al* (2005) did attempt to confirm the malignant pedigree of cells derived from radical prostatectomy specimens using growth in semisolid media, and invasion assay and LOH analysis. Demonstration of anchorage independent growth has long been used to discriminate between benign and malignant cells

(Sanders and Burford, 1964). Whereas most freshly isolated normal cells grow poorly in semisolid agar gel suspension, malignant cells are able to proliferate. Benign prostate cells do not form colonies in soft agar (Sinisi *et al*, 2002). Similarly, differences in growth and invasion were identified between primary benign and malignant prostate cells co-cultured with primary benign prostate stromal cells in a three-dimensional collagen gel (Hall *et al*, 2002). Collins and colleagues' (2005) cancer derived cells migrated through Matrigel coated filters towards a chemoattractant medium, and grew in semisolid methylcellulose and while prostate cancer cell lines were used as a positive control, but there were no benign negative controls. These cells achieved longevity in culture, which was on-going at the time of publication. Their LOH analysis was unable to unequivocally confirm the tumor cell origin of the cultured cells. Thus using the criteria of Dalyrymple *et al* (2005) only the increased proliferative ability of the 'cancer' cells (greater than a benign control) would concur with a malignant phenotype. Collins *et al* (2005) stopped short of *in vivo* tumourigenic assays, and might also have screened for cancer markers such as AMACR or p63. Litvinov *et al*, (2006) described their findings as 'intriguing' but demanded these assays to exclude selection of benign cells.

Finally at least one report exists of the development of a pair of hTERT-immortalized primary non-malignant and malignant human prostate epithelial cell lines from primary cultures that demonstrate appropriate malignant characteristics, despite being raised in low-calcium medium (Gu *et al*, 2006). Transformed cell lines may therefore differ from cancers that arise spontaneously. Certainly it is now mandatory that researchers confirm the malignant behaviour of the cells that emerge from cancer tissue culture.

The colonies in this project were cultured in low-calcium medium. While it is likely that cancer cells were present in the epithelial cell suspension plated, the malignant nature of the colonies obtained was not demonstrated using criteria suggested by Dalyrymple *et al* (2005). It was assumed that cancerous cells would grow well in the same culture conditions established for benign epithelial cells by Peehl and Stamey (1986) and demonstrated to successfully yield benign epithelial colonies by Hudson *et al* (2000). It was also assumed that these

colonies would look similar, and recognisable as prostate epithelium. Neither assumption is unreasonable as Bright *et al* (1997) reported no difference in morphology of their paired cell lines confirmed using LOH analysis and Peehl (2002) reports that 'no special techniques are required to culture tumor cells. Normal, BPH, and malignant tissues all yield finite cell lines with similar efficiencies (approaching 90% in our laboratory with tissues derived from radical prostatectomies)'. However these cells have a finite lifespan *in vitro* and she does acknowledge that as chromosomal abnormalities in primary cancer cultures are difficult to detect it is quite possible that current culture conditions do not support the survival of the most genetically aberrant cancer cells *in vitro* (Peehl, 2005).

It is notable that in this study there was no difference in the colony characteristics derived from benign and cancer tissues (see table 4.4), which could be interpreted as implying that all the colonies were benign. When Liu and Peehl (2001) compared the expression profiles of over 110 cluster designation cell markers between primary and malignant cells cultured in low-calcium medium they also found that these were 'notably similar'.

4.8 Future directions

The effect of calcium on the selective culture of benign or malignant prostate cells opens up some intriguing possibilities. Comparing cells in different culture media becomes difficult, as too many variables are present. However, the outcomes of benign and cancer tissue culture in terms of colony morphology and yield in the presence of high calcium medium would be of great interest. However, it would be important to exclude as many stromal cells as possible during processing to prevent overgrowth in culture. Any colonies obtained would have to be assessed for malignant features, and alongside LOH and real-time PCR, some colony cells could be dedicated to invasion, soft agar and *in vivo* tumourigenesis assays. With confirmed malignant and benign colonies, their interrogation for clinically relevant genes could commence.

CHAPTER 5: CONCLUSIONS

Though recent advances in the detection and management of prostate cancer have brought about a downward stage migration in the incidence of the disease, prostate cancer remains the fourth commonest cancer in the UK, representing 12% of cancer diagnoses and 7% of cancer deaths in 2004 (Tarone *et al*, 2000; http://info.cancerresearchuk.org/cancerstats). Despite advances in systemic therapies, once prostate cancer has spread beyond the prostate it is incurable (Kipp and McNeel, 2007; Arianayagam *et al*, 2007).

Research into effective therapies continues apace, and the study of prostate stem cells is still in its infancy. The theoretical basis behind the stem cell theory of cancer is robust and represents a novel approach to treating cancer, which might succeed where others have failed. Stem cell biology is a major focus of research in many fields and a remarkable similarity in stem cell markers is emerging across different tissues. Other recurring themes include the stem cell niche, common signal transduction pathways and the inherent drug resistance conferred by drug efflux transporter pumps and anti-apoptotic proteins (Pan *et al*, 2006; Massard *et al*, 2006). Thus a treatment that proves its effectiveness in one cancer may have a broader applicability to many others. Though no anti-stem cell treatment exists as yet, the full potential of stem cell targeted therapies remains unrealised.

PUBLISHED WORK: 2001 – 2007

Papers

Bott SR, Foley CL, Bull MD, Reddy CC, Freeman A, Montgomery BS, Langley SE. Are prostatic biopsies necessary in men aged > or =80 years? BJU Int. 2007; 99:335-8.

Foley CL, Bott SR, Shergill IS, Kirby RS. An update on the use of 5 alpha-reductase inhibitors. Drugs Today (Barc). 2004; 40:213-23.

Foley CL, Taylor C, Kirby RS. Counting the cost of treating benign prostatic hyperplasia. BJU Int. 2004; 93:250-2.

Foley CL, Kirby RS. Re: Bilateral laparoscopic inguinal hernia repair can complicate subsequent radical retropubic prostatectomy. J Urol. 2003; 169(4):1475.

Masters JR, Foley CL, Bisson I, Ahmed A. Cancer stem cells. BJU Int. 2003; 92:661-2.

Foley CL, Bott SR, Thomas K, Parkinson MC, Kirby RS. A large prostate at radical retropubic prostatectomy does not adversely affect cancer control, continence or potency rates. BJU Int. 2003; 92:370-4.

Foley CL, Kirby RS. 5 alpha-reductase inhibitors: what's new? Curr Opin Urol. 2003; 13(1):31-7.

CL Foley, SRJ Bott, M Arya, RS Kirby. Benign Prostatic Hyperplasia – new solutions to an ageing problem. Hosp Med 2002; 63:460-4.

Symes A, Foley C. Book Review: Living and loving after prostate surgery. BJUI 2005; 96:688.

Foley CL, Constantinou J, Kirby RS. Undertaking shared care of prostate cancer management. Prescriber 2005; 16(9):14-21.

Taylor C, Foley C, Kirby RS. Safe and effective management of BPH in primary care. Prescriber 2004; 15: 30-37.

Foley CL, Taylor CJ, Kirby RS. Cost-effectiveness of treatment options in BPH. Men's Health Journal 2003; 2:46-9.

Book Chapters

Prostate Cancer: Principles and Practice. Eds RS Kirby, AW Partin, M Feneley, JK Parsons. Taylor & Francis 2006. Stem cell concepts underlying prostate cancer. JRW Masters, I Bisson, CL Foley, A Ahmed.

Drug Treatment in Urology. Eds I Eardley, P Whelan, R Kirby, Schaeffer A. Blackwell 2005. Chapter 2: Medical Therapy for Benign Prostatic Hyperplasia. RJ Bott, CL Foley, RS Kirby.

Hot topics in Urology. Eds RS Kirby and M O'Leary. Saunders 2002. What's hot and what's not: the medical management of BPH. SRJ Bott, CL Foley, RS Kirby.

MIMS Handbook of Urology, Chapter 4: Investigations and diagnosis. Foley CL, Taylor C, Fitzpatrick J. Edited by Prof J Fitzpatrick 2002 - 2006

MIMS Handbook of Urology, Chapter 5: Drug Treatments. Foley CL, Kirby RS. Edited by Prof J Fitzpatrick 2002 - 2006

Prostate and renal cancer, benign prostatic hyperplasia, erectile dysfunction and basic research - An update. Progress and Controversies in Oncologic Urology VII (PACIOU VII). 7th Congress of the Dutch Urological Association. Eds Bangma CH, Newling DWW. The Parthenon Publishing Group, London 2003. Stem cells and differentiation in human prostate cancer. JRW Masters, TN Alam, CL Foley, I Laczko, DL Hudson.

MIMS Guide to Prostate Health. CL Foley, SRJ Bott, RS Kirby, J Fitzpatrick. Sept 2002

Presentations

A Forecast of the Future for Biomaterials - Professor Larry L. Hench Retirement Symposium, Imperial College London 2005. Isolation, characterisation and differentiation of epithelial stem cells/ progenitors from human prostate. I Bisson, CL Foley, A Ahmed, JRW Masters.

BAUS Annual Meeting 2005. Drug treatments for BPH – bringing cost-effectiveness into the equation. CL Foley, J Constantinou, RS Kirby.

British Prostate Group Autumn meeting 2004. Prostate biopsies in the over 80s – crucial or cruel? SRJ Bott, CL Foley, MD Bull, CJ Reddy, A Freeman, SEM Langley

AUA Annual Meeting 2003. Large prostate size at radical retropubic prostatectomy does not adversely affect cancer control, continence or potency rates. CL Foley, SRJ Bott, K Thomas, MC Parkinson, RS Kirby.

EAU XVIIIth Congress, 2003. Do prostate cancers in younger men have worse pathological characteristics in the PSA era? CL Foley, SRJ Bott, MC Parkinson, and contributors to the UCL prostate database.

EAU XVIIIth Congress, 2003. Significance of positive urethral margins at radical prostatectomy. SRJ Bott, CL Foley, D Besarani, RS Kirby. (awarded best poster in session).

BAUS Annual Meeting, 2003. Gleason Grade at biopsy and radical prostatectomy: does it correlate? SRJ Bott, CL Foley, S Stenning, MC Parkinson.

Urological Research Society 2003. Differentiation of clonogenic cells derived from peripheral zone prostate tissue. CL Foley, MC Parkinson, RS Kirby, JRW Masters, DL Hudson.

BAUS Annual Meeting, 2002. The value of anastomotic biopsies in patients with a rising prostate specific antigen after radical prostatectomy. CL Foley, SRJ Bott, MC Parkinson, RS Kirby.

BAUS Annual Meeting, 2002. Cancer control, continence and potency after radical retropubic prostatectomy - a UK series. SRJ Bott, K Thomas, D Besarani, CL Foley, RS Kirby.

Royal Society of Medicine, Section of Urology, Clinicopathological Meeting 2002. Big Prostate, small problem: Outcomes for radical retropubic prostatectomy with large prostates are equally as good. C Foley, S Bott, K Thomas, D Besarani, M Parkinson, R Kirby.

British Prostate Group Spring meeting, 2002. The management of vesico-urethral anastomotic stricture after radical retropubic prostatectomy. D Besarani, SRJ Bott, CL Foley, RS Kirby.

British Prostate Group Spring Meeting 2002. The value of anastomotic biopsies in patients with a rising PSA after radical prostatectomy. CL Foley, SRJ Bott, MC Parkinson, RS Kirby.

REFERENCES

Aalinkeel R, Nair MP, Sufrin G *et al.* Gene expression of angiogenic factors correlates with metastatic potential of prostate cancer cells. Cancer Res. 2004; 64:5311-21.

Al-Hajj M, Wicha MS, Benito-Hernandez A *et al.* Prospective identification of tumorigenic breast cancer cells. Proc Nat Acad Sci USA. 2003; 100:3983-8.

Allison DB, Cui X, Page GP, Sabripour M. Microarray data analysis: from disarray to consolidation and consensus. Nat Rev Genet 2006; 7:55-65.

Allsbrook WC Jr, Mangold KA, Johnson MH *et al.* Interobserver reproducibility of Gleason grading of prostatic carcinoma: urologic pathologists. Hum Pathol. 2001; 32:74-80.

Allsbrook WC, Pfeifer EA. Chapter 15, Histochemistry of the prostate. In: CS Foster and DG Bostwick (eds.) Pathology of the Prostate. WB Saunders Co.1998, pp 2294-296.

Arianayagam M, Chang J, Rashid P. Chemotherapy in the treatment of prostate cancer - Is there a role? Aust Fam Physician 2007; 36:737-9.

Auer H, Lyianarachchi S, Newsom D *et al.* Chipping away at the chip bias: RNA degradation in microarray analysis. Nat Genet 2003; 35:292-3.

Aumüller G. Morphologic and endocrine aspects of prostatic function. Prostate 1983; 4:195-214.

Aumüller G, Seitz J: Protein secretion and secretory processes in male sex accessory glands. Int Rev Cytol 1990; 121:127–231.

Aumüller G, Groos S, Renneberg H *et al.* Chapter 1, Embryology and postnatal development of the prostate. In: CS Foster and DG Bostwick (eds.) Pathology of the Prostate. WB Saunders Co. 1998, page 2.

Aumüller G, Leonhardt M, Janssen M *et al.* Neurogenic origin of human prostate endocrine cells. Urology 1999; 53:1041-8.

Aumüller G, Leonhardt M, Renneberg H *et al.* Semiquantitative morphology of human prostatic development and regional distribution of prostatic neuroendocrine cells. Prostate 2001; 46:108-15.

Barrack E, Berry S: DNA synthesis in the canine prostate: Effects of androgen induction and estrogen treatment. Prostate 1987; 10:45–56.

Barratt PL, Seymour MT, Stenning SP *et al*; UKCCCR AXIS trial collaborators. Adjuvant X-ray and Fluorouracil Infusion Study. DNA markers predicting benefit from adjuvant fluorouracil in patients with colon cancer: a molecular study. Lancet 2002; 360:1381-91.

Barry MJ, Fowler FJ Jr, Bin L *et al.* The natural history of patients with benign prostatic hyperplasia as diagnosed by North American urologists. J Urol. 1997; 157:10-4.

Berry SJ, Coffey DS, Walsh PC *et al.* The development of human benign prostatic hyperplasia with age. J Urol 1984; 132:474-9.

Bettendorf O, Schmidt H, Eltze E *et al.* Cytogenetic changes and loss of heterozygosity in atypical adenomatous hyperplasia, in carcinoma of the prostate and in non-neoplastic prostate tissue using comparative genomic hybridization and multiplex-PCR. Int J Oncol. 2005; 26:267-74.

Bhatt RI, Brown MD, Hart CA *et al.* Novel method for the isolation and characterisation of the putative prostate stem cell. Cytometry Part A 2003; 54A:89-99.

Blacker KL, Williams ML, Goldyne M. Mitomycin C-treated 3T3 fibroblasts used as feeder layers for human keratinocyte culture retain the capacity to generate eicosanoids. J Invest Dermatol. 1987; 89:536-9.

Bonkhoff H. Analytical molecular pathology of epithelial-stromal interactions in the normal and neoplastic prostate. Anal Quant Cytol Histol 1998; 20:437–42.

Bonkhoff H, Remberger K. Differentiation pathways and histogenetic aspects of normal and abnormal prostatic growth: a stem cell model. Prostate 1996; 28:98-106.

Bonkhoff H, Stein U, Remberger K. Multidirectional differentiation in the normal, hyperplastic and neoplastic human prostate. Hum Pathol 1994a; 25:42-6.

Bonkhoff H, Stein U, Remberger K. The proliferative function of basal cells in the normal and hyperplastic human prostate. Prostate 1994b; 24:114-8.

Bonkhoff H, Stein U, Remberger K. Endocrine-paracrine cell types in the prostate and prostatic adenocarcinoma are postmitotic cells. Hum Pathol. 1995; 26:167-70.

Bonnet D, Dick JE. Human acute myeloid leukaemia is organized as a hierarchy that originates from a primitive hematopoietic cell. Nature Med 1997; 3:730-737.

Bostwick DG, Brawer MK. Prostatic intra-epithelial neoplasia and early invasion in prostate cancer. Cancer 1987; 59:788-94.

Bostwick DG, Qian J, Frankel K. The incidence of high grade prostatic intraepithelial neoplasia in needle biopsies. J Urol 1995; 154:1791-1794.

Bostwick DG, Shan A, Qian J *et al.* Independent origin of multiple foci of prostatic intraepithelial neoplasia: comparison with matched foci of prostate carcinoma. Cancer 1998; 83:1995-2002.

Bott SR, Masters JR, Parkinson MC *et al.* Allelic imbalance and biochemical outcome after radical prostatectomy. Prostate Cancer Prostatic Dis. 2006; 9:160-8.

Bright RK, Vocke CD, Emmert-Buck MR *et al.* Generation and genetic characterization of immortal human prostate epithelial cell lines derived from primary cancer specimens. Cancer Res. 1997; 57:995-1002.

Brooks JD. Chapter 2, Anatomy of the lower urinary tract and male genitalia. In: Walsh PC, Vaughan ED, Retik AB *et al* (eds.) Campbell's Urology. 8th Edition, volume 1. WB Saunders Co. 2002.

Bui M, Reiter RE. Stem cell genes in androgen independent prostate cancer. Cancer Metastasis Review 1999; 17:391-399.

Buick RN, Pollack MN. Perspectives on clonogenic tumor cells, stem cells and oncogenes. Cancer Res. 1984; 44:4909-18.

Bunting KD. ABC transporters as phenotypic markers and functional regulators of stem cells. Stem Cells 2002; 20:11–20.

Burger PE, Xiong X, Coetzee S *et al.* Sca-1 expression identifies stem cells in the proximal region of prostatic ducts with high capacity to reconstitute prostatic tissue. Proc Natl Acad Sci USA 2005; 102:7180–5.

Cairns J. Somatic stem cells and the kinetics of mutagenesis and carcinogenesis. Proc Natl Acad Sci U S A 2002; 99:10567-70.

Campisi J. Senescent cells, tumuor suppression and organismal aging: good citizens, bad neighbours. Cell 2005; 120:513-22.

Canzian F, Salovaara R, Hemminki A *et al.* Semiautomated assessment of loss of heterozygosity and replication error in tumors. Cancer Res. 1996; 56:3331-7.

Cheng L, Shan A, Cheville JC *et al.* Atypical adenomatous hyperplasia of the prostate: a premalignant lesion? Cancer Res. 1998; 58:389-91.

Collins AT, Berry PA, Hyde C *et al.* Prospective identification of tumorigenic prostate cancer stem cells. Cancer Res. 2005; 65:10946-51.

Collins AT, Habib FK, Maitland NJ *et al.* Identification and isolation of human prostate epithelial stem cells based on $\alpha_2\beta_1$-integrin expression. J Cell Sci 2001; 114:3865-72.

Corbeil D, Roper K, Hellwig A *et al.* The human AC133 hematopoietic stem cell antigen is also expressed in epithelial cells and targeted to plasma membrane protrusions. J Biol Chem 2000; 275:5512-20.

Cunha GR. Role of mesenchymal-epithelial interactions in normal and abnormal development of the mammary gland and prostate. Cancer 1994; 74:1030-1044.

Cunha GR, Battle E, Young P *et al.* Role of epithelial–mesenchymal interactions in the differentiation and spatial organization of visceral smooth muscle. Epithelial Cell Biol 1992; 1:76–83.

Cunha GR, Hayward SW, Wang YZ. Role of stroma in carcinogenesis of the prostate. Differentiation 2002; 70:473–85.

Cunha GR, Ricke W, Thomson A *et al.* Hormonal, cellular, and molecular regulation of normal and neoplastic prostatic development. J Steroid Biochem Mol Biol. 2004; 92:221–36.

Cunha GR, Sekkingstad M, Meloy BA. Heterospecific induction of prostatic development in tissue recombinants prepared with mouse, rat, rabbit, and human tissues. Differentiation 1983; 24:174–80.

Cunha GR, Wang YZ, Hayward SW *et al.* Estrogenic effects on prostatic differentiation and carcinogenesis. Reprod Fertil Dev. 2001; 13:285-96.

Cunha GR, Young P. Inability of Tfm (testicular feminization) epithelial cells to express androgen-dependent seminal vesicle secretory proteins in chimeric tissue recombinants. Endocrinology 1991; 128:3293-8.

Dalerba P, Dylla SJ, Park IK *et al.* Phenotypic characterization of human colorectal cancer stem cells. Proc Natl Acad Sci U S A. 2007; 104:10158-63.

Dalrymple S, Antony L, Xu Y *et al.* Role of Notch-1 and E-Cadherin in the differential response to calcium in culturing normal versus malignant prostate cells. Cancer Res. 2005; 65: 9269-79.

Desgrandchamps F, de la Taille A, Azzouzi AR *et al.* Management of non-complicated BPH: proposition of a renewed decision tree. World J Urol. 2006; 24:367-70.

De Klerk DP, Heston WDW, Coffey DS: Studies on the role of macromolecular synthesis in the growth of the prostate. In Grayhack JT, Wilson JD, Scherbenske MJ (eds): Benign Prostatic Hyperplasia. Proceedings of a workshop sponsored by the Kidney Disease and Urology Program of the NIAMDD. Washington, DC, U.S. Government Printing Office, 1976, pp 43–51.

De Marzo AM, Meeker AK, Epstein JI *et al.*. Prostate stem cell compartments: Expression of the cell cycle inhibitor p27-Kip1 in normal, hyperplastic, and neoplastic cells. Am J Pathol 1998a; 153:911–9.

De Marzo AM, Nelson WG, Isaacs WB *et al.* Pathological and molecular aspects of prostate cancer. Lancet 2003; 361:955-964.

De Marzo AM, Nelson WH, Meeker AK *et al.* Stem cell features of benign and malignant prostate epithelial cells. J Urol 1998b; 160;2381-92.

Dermer GB. Basal cell proliferation in benign prostatic hyperplasia. Cancer 1978; 41:1857-62.

Dexter TM. Stem cells in normal growth and disease. BMJ 1987; 1192-4.

Dhanasekaran SM, Barrette TR, Ghosh D *et al.* Delineation of prognostic biomarkers in prostate cancer. Nature 2001; 412:822–6

Diaz-Cano SJ. Are PCR artifacts in microdissected samples preventable? Hum Pathol. 2001; 32:1415-6.

Dib C, Faure S, Fizames C *et al.* A comprehensive genetic map of the human genome base on 5,264 microsatellites. Nature 1996; 380:152-4.

Dick JE. Normal and leukemic human stem cells assayed in SCID mice. Semin Immunol 1996; 8:197–206.

di Sant'Agnese PA. Neuroendocrine differentiation in carcinoma of the prostate. Diagnostic, prognostic, and therapeutic implications. Cancer 1992; 70:254-268.

di Sant'Agnese PA, deMesy-Jensen KL. Endocrine-paracrine cells of the prostate and prostatic urethra: An ultrastructural study. Hum Pathol 1984; 15:1034–41.

di Sant'Agnese PA, deMesy-Jensen KL, Churukien CJ, Agarwall MM. Human prostatic endocrine-paracrine (APUD) cells: Distribution analysis for the comparison of serotonin and neuron-specific amylase immunoreactivity in silver stains. Arch Pathol Lab Med 1985; 109:607–12.

Dontu G, Al Hajj M, Abdallah WM *et al.* Stem cells in normal breast development and breast cancer. Cell Prolif 2003; 36 S1:59-72.

Dumur CI, Nasim S, Best AM *et al.* Evaluation of Quality-Control Criteria for Microarray Gene Expression Analysis. Clin Chem 2004; 50:1994–2002.

Eberwine J, Yeh H, Miyashiro K *et al.* Analysis of gene expression in single live neurons. Proc Natl Acad Sci U S A. 1992; 89:3010-4.

Eisen MB, Spellman PT, Brown PO *et al.* Cluster analysis and display of genome-wide expression patterns. Proc Nat Acad Sci USA. 1998; 95:14863-8.

Ellerhorst J, Nguyen T, Cooper DN *et al.* Differential expression of endogenous galectin-1 and galectin-3 in human prostate cancer cell lines and effects of overexpressing galectin-1 on cell phenotype. Int J Oncol. 1999; 14:217-24.

English HF, Kyprianou N, Isaacs JT. Relationship between DNA fragmentation and apoptosis in the programmed cell death in the rat prostate following castration. Prostate 1989; 15:233-51.

English HF, Santen RJ, Isaacs JT. Response of glandular versus basal rat ventral prostatic epithelial cells to androgen withdrawal and replacement. Prostate 1987; 11:229-42.

Evans GS and Chandler JA. Cell proliferation studies in rat prostate I. The proliferative role of basal and secretory epithelial cells during normal growth. Prostate 1987; 10:163-78.

Favre B, Plantard L, Aeschbach L *et al.* SLURP1 is a late marker of epidermal differentiation and is absent in Mal de Meleda.J Invest Dermatol. 2007; 127:301-8.

Fearon ER, Vogelstein B. A genetic model for colorectal tumorigenesis. Cell 1990; 61:759-67.

Fischer AH, Philips A, Taysavang P *et al.* Method for procuring specific populations of viable human prostate cells for research. Lab Invest 2001; 81:501–7.

Freshney RI (2002a): Culture of Epithelial cells. 2nd Edition. Freshney RI and Freshney MG (eds.). New York: Wiley-Liss Inc. Chapter 1, pp 7-9.

Freshney RI (2002b): Culture of Epithelial cells. 2nd Edition. Edited by Freshney RI and Freshney MG. New York: Wiley-Liss Inc. Chapter 1, pp 20-22.

Fromont G, Joulin V, Chantrel-Groussard K *et al.* Allelic losses in localized prostate cancer: association with prognostic factors. J Urol. 2003; 170:1394-7.

Fry PM, Hudson DL, O'Hare MJ *et al.* Comparison of marker protein expression in benign prostatic hyperplasia *in vivo* and *in vitro*. BJU Int. 2000; 85:504-13.

Galliano MF, Toulza E, Gallinaro H *et al.* A novel protease inhibitor of the alpha2-macroglobulin family expressed in the human epidermis. J Biol Chem. 2006; 281:5780-9.

Gao J, Arnold JT, Isaacs JT. Conversion from a paracrine to an autocrine mechanism of androgen-stimulated growth during malignant transformation of prostatic epithelial cells. Cancer Res 2001; 61:5038–44.

Garge NR, Page GP, Sprague AP *et al.* Reproducible clusters from microarray research: whither? BMC Bioinformatics 2005; 15:6(S2):10.

Gilbert SF. Chromosomal sex determination in mammals. In Developmental Biology, 6th Edition, Chapter 17. Edited by Gilbert SF. Sinauer Associates Inc. 2000.

Gil-Diez de Medina S, Salomon L, Colombel M *et al.* Modulation of cytokeratin subtype. EGF receptor, and androgen receptor expression during progression of prostate cancer. Human Pathology 1998; 29:1005-12.

Gilliland G, Perrin S, Blanchard K *et al.* Analysis of cytokine mRNA and DNA: detection and quantitation by competitive polymerase chain reaction. Proc Natl Sci Acad USA 1990; 87:2725-9.

Giri D, Ittmann M. Interleukin-8 is a paracrine inducer of fibroblast growth factor 2, a stromal and epithelial growth factor in benign prostatic hyperplasia. Am J Pathol. 2001; 159:139-47.

Gondi CS, Kandhukuri N, Kondraganti S *et al.* Down-regulation of uPAR and cathepsin B retards cofilin dephosphorylation. Int J Oncol. 2006; 28:633-9.

Gray IC, Phillips SM, Lee SJ *et al.* Loss of the chromosomal region 10q23-25 in prostate cancer. Cancer Res. 1995; 55:4800-3.

Gritti A, Parati EA, Cova L *et al.* Multipotential stem cells from the adult mouse brain proliferate and self-renew in response to basic fibroblast growth factor. J Neurosci. 1996; 1;16:1091-100.

Grönberg H. Prostate cancer epidemiology. Lancet 2003; 361:859-64.

Gleason DF, Mellinger GT. Prediction of prognosis for prostatic adenocarcinoma by combined histologic grading and clinical staging. J Urol 1974; 111:58-64.

Gu Y, Li H, Miki J *et al.* Phenotypic characterization of telomerase-immortalized primary non-malignant and malignant tumor-derived human prostate epithelial cell lines. Exp Cell Res. 2006; 312:831-43.

Gu G, Yuan J, Wills M *et al.* Prostate cancer cells with stem cell characteristics reconstitute the original human tumor in vivo. Cancer Res. 2007; 67:4807-15.

Hachem JP, Wagberg F, Schmuth M *et al.* Serine protease activity and residual LEKTI expression determine phenotype in Netherton syndrome. J Invest Dermatol. 2006; 126:1609-21.

Hall JA, Maitland NJ, Stower M *et al.* Primary prostate stromal cells modulate the morphology and migration of primary prostate epithelial cells in type 1 collagen gels. Cancer Res. 2002; 1:62:58-62.

Hanahan D, Weinberg RA. The hallmarks of cancer. Cell 2000; 100:57-70.

Hartigan JA, Wong MA. A K-means clustering algorithm. Appl Stat 1979; 28:100-8.

Hayflick L, Moorhead PS. The serial cultivation of human diploid cell strains. Exp. Cell Res. 1961; 25:585-621.

Hayward SW and Cunha GR. The prostate: development and physiology. Radiol Clin North Am 2000; 38:1–14.

Houghton J, Morozov A, Smirnova I *et al.* Stem cells and cancer. Semin Cancer Biol. 2007; 17:191-203.

Huang J, Wu C, di Sant'Agnese PA *et al.* Function and molecular mechanisms of neuroendocrine cells in prostate cancer. Anal Quant Cytol Histol. 2007; 29:128-38.

Hudson DL, Guy AT, Fry P *et al.* Epithelial cell differentiation pathways in the human prostate: identification of intermediate phenotypes by keratin expression. J Histochem Cytochem 2001; 49:271-8.

Hudson DL, O'Hare M, Watt FM *et al.* Proliferative heterogeneity in the human prostate: evidence for epithelial stem cells. Lab Invest 2000; 80:1243-50.

Huss WJ, Gray DR, Greenberg NM *et al.* Breast cancer resistance protein-mediated efflux of androgen in putative benign and malignant prostate stem cells. Cancer Res. 2005; 65:6640–50.

Huss WJ, Gray DR, Werdin ES *et al.* Evidence of pluripotent human prostate stem cells in a human prostate primary xenograft model. Prostate 2004; 60:77–90.

Isaacs JT. Antagonistic effect of androgen on prostatic cell death. Prostate 1984; 5:545–57.

Isaacs JT. Control of cell proliferation and cell death in the normal and neoplastic prostate: a stem cell model. In Rodgers CH, Coffey DS, Cunha JG, Greyhack JT, Hinman F and Horton R (eds). Benign prostatic hyperplasia Volume II. NIH Publication No. 87-2881, Bethseda, MD, 1987 pp 85-94.

Isaacs JT, Coffey DS: Etiology and disease process of benign prostatic hyperplasia. Prostate 1989; S2:33–50.

Jamieson CH, Ailles LE, Dylla SJ *et al.* Granulocyte-macrophage progenitors as candidate leukemic stem cells in blast-crisis CML. N Engl J Med. 2004; 351:657-67.

Jenson SD, Robetorye RS, Bohling SD *et al.* Validation of cDNA microarray gene expression data obtained from linearly amplified RNA. Mol Pathol. 2003; 56:307-12.

Kadkol SS, Brody JR, Epstein JI *et al.* Novel nuclear phosphoprotein pp32 is highly expressed in intermediate- and high-grade prostate cancer. Prostate 1998; 34:231-7.

Kellogg Parsons J, Gage WR, Nelson WG *et al.* p.63 protein expression is rare in prostate adenocarcinoma: implications for cancer diagnosis and carcinogenesis. Urology 2001; 58:619-24.

Kim O, Jiang T, Xie Y *et al.* Synergism of cytoplasmic kinases in IL6-induced ligand-independent activation of androgen receptor in prostate cancer cells. Oncogene 2004; 23:1838-44.

Kim NW, Piatyszek MA, Prowse KR *et al.* Specific association of human telomerase activity with immortal cells and cancer. Science 1994; 266:2011-5.

King C, Guo N, Frampton GM *et al.* Reliability and reproducibility of gene expression measurements using amplified RNA from laser-microdissected primary breast tissue with oligonucleotide arrays. J Mol Diagn. 2005; 7:57-64.

Kipp RT, McNeel DG. Immunotherapy for prostate cancer - recent progress in clinical trials. Clin Adv Hematol Oncol. 2007;m 5:465-74,477-9.

Kirby RS. The natural history of prostate cancer. Chapter 1, pp5-14 In Prostate Cancer by Kirby RS, Christmas T, Brawer M. 2nd Edition 2000. Mosby.

Klein KA, Reiter RE, Redula J *et al.* Progression of metastatic human prostate cancer to androgen independence in immunodeficient SCID mice. Nat Med. 1997; 3:402-8.

Kobayashi S, Demura T, Nonomura K *et al.* Auto-radiographic localization of alpha 1-adrenoceptors in human prostate: special reference to zonal difference. J Urol 1991; 146:887-90.

Kondo M, Wagers AJ, Manz MG *et al.* Biology of hematopoietic stem cells and progenitors: implications for clinical application. Annu Rev Immunol 2003; 21:759-806.

Kovacevic Z, Richardson DR. The metastasis suppressor, Ndrg-1: a new ally in the fight against cancer. Carcinogenesis. 2006; 27:2355-66.

Krajewska M, Olson AH, Mercola D *et al.* Claudin-1 immunohistochemistry for distinguishing malignant from benign epithelial lesions of prostate. Prostate 2007; 67:907-10.

Krajewska M, Wang HG, Krajewski S *et al.* Immunohistochemical analysis of in vivo patterns of expression of CPP32 (Caspase-3), a cell death protease. Cancer Res. 1997; 57:1605-13.

Kramer G, Mitteregger D, Marberger M. Is Benign Prostatic Hyperplasia (BPH) an Immune Inflammatory Disease? European Urology 2007; 51:1202–16.

Krieg P, Schuppler M, Koesters R *et al.* Repetin (Rptn), a new member of the 'fused gene' subgroup within the S100 gene family encoding a murine epidermal differentiation protein. Genomic. 1997; **43**:339–48.

Kurita T, Medina RT, Mills AA *et al.* Role of p63 and basal cells in the prostate. Development 2004; 131:4955–64.

Laczko I, Hudson DL, Freeman A *et al.* Comparison of the zones of the human prostate with the seminal vesicle: morphology, immunohistochemistry, and cell kinetics. Prostate 2005; 62:260-6.

Lakhani SR, Chaggar R, Davies S *et al.* Genetic alterations in 'normal' luminal and myoepithelial cells of the breast. J Pathol 1999; 189:496-503.

Lang SH, Stark M, Collins A *et al.* Experimental prostate epithelial morphogenesis in response to stroma and three-dimensional matrigel culture. Cell Growth Differ. 2001; 12:631-40.

Lapointe J, Li C, Higgins JP *et al.* Gene expression profiling identifies clinically relevant subtypes of prostate cancer. Proc Natl Acad Sci U S A. 2004; 101:811-6.

Larochelle A, Vormoor J, Hanenberg H *et al.* Identification of primitive human haematopoietic cells capable of repopulating NOD/SCID mouse bone marrow: implications for gene therapy. Nature Medicine 1996; 2:1329-37.

Lawson DA, Xin L, Lukacs RU *et al.* Isolation and functional characterization of murine prostate stem cells. Proc Natl Acad Sci U S A. 2007; 104:181-6.

Lee KL, Peehl DM. Molecular and cellular pathogenesis of benign prostatic hyperplasia. J Urol. 2004; 172:1784-91.

Lepor H. Pathophysiology, epidemiology, and natural history of benign prostatic hyperplasia. Rev Urol. 2004; 6(Suppl 9):S3-S10.

Lessard J, Sauvageau G. Bmi-1 determines the proliferative capacity of normal and leukaemic stem cells. Nature 2003; 423:255-60.

Leube B, Drechsler M, Muhlmann K *et al.* Refined mapping of allele loss at chromosome 10q23-26 in prostate cancer. Prostate 2002; 50:135-144.

Lexander H, Franzén B, Hirschberg D *et al.* Differential protein expression in anatomical zones of the prostate. Proteomics 2005; 5:2570-6.

Li A, Simmons PJ, Kaur P. Identification and isolation of candidate human keratinocyte stem cells based on cell surface phenotype. Proc Natl Acad Sci USA. 1998; 95:3902-7.

Li C, Heidt DG, Dalerba P *et al.* Identification of pancreatic cancer stem cells. Cancer Res. 2007; 67:1030-7.

Li W, Sandhoff R, Kono M *et al.* Depletion of ceramides with very long chain fatty acids causes defective skin permeability barrier function, and neonatal lethality in ELOVL4 deficient mice. Int J Biol Sci. 2007; 3:120-8.

Lilja H, Oldbring J, Rannevik G *et al.* Seminal-secreted proteins and their reactions during gelation and liquefaction of human semen. J Clin Invest 1987; 80:281–5.

Litvinov IV, Griend DJV, Xu Y *et al.* Low-calcium serum-free defined medium selects for growth of normal prostatic epithelial stem cells. Cancer Res 2006; 66:8598-607.

Liu AY, Peehl DM. Characterization of cultured human prostatic epithelial cells by cluster designation antigen expression. Cell Tissue Res. 2001; 305:389–97.

Lui AY, True LD, LaTray L *et al.* Analysis and sorting of prostate cancer cell types by flow cytometry. The Prostate 1999; 40:192-9.

Lui AY, True LD, LaTray L *et al.* Cell-cell interaction in prostate gene regulation and cytodifferentiation. Proc Nat Acad Sci 1997; 94:10705-10.

Lui AY, True LD, LaTray L *et al.* Cell-cell interaction in prostate gene regulation and cytodifferentiation. Proc Natl Acad Sci U S A. 1997; 94:10705-10.

Marenholz I, Zirra M, Fischer DF, Backendorf C *et al.* Identification of Human Epidermal Differentiation Complex (EDC)-Encoded Genes by Subtractive Hybridization of Entire YACs to a Gridded Keratinocyte cDNA Library. Genome Res. 2001; 11:341-55.

Maria McCrohan A, Morrissey C, O'Keane C *et al.* Effects of the dual 5 alpha-reductase inhibitor dutasteride on apoptosis in primary cultures of prostate cancer epithelial cells and cell lines. Cancer 2006; 106:2743-52.

Marshak DR, Gottlieb FD, Gardner RL. Chapter 1: Introduction: stem cell biology. In Stem cell biology. Pp1-16. Cold Spring Harbor Laboratory Press 2001.

Mason MK. Cytology of the prostate. J Clin Pathol. 1964; 17:581–90.

Massard C, Deutsch E, Soria JC. Tumour stem cell-targeted treatment: elimination or differentiation. Ann Oncol. 2006; 17:1620-4.

McClintick JN, Edenberg HJ. Effects of filtering by Present call on analysis of microarray experiments. BMC Bioinformatics 2006; 7:49-64.

McCulloch EA, Till JE. Proliferation of hemopoietic colony-forming cells transplanted into irradiated mice. Radiat Res. 1964; 22:383–97.

MacIntyre N. Unmasking antigens for immunohistochemistry. Br J Biomed Sci. 2001; 58:190-6.

Mackenzie IC. Stem cell properties and epithelial malignancies. Eur J Cancer 2006; 42:1204–12.

Mackillop WJ, Ciampi A, Till JE *et al.* A stem cell model of human tumor growth: implications for tumour cell clonogenic assays. J Natl Cancer Inst 1983; 70:9-16.

Mackillop WJ, Bizarri JP, Ward GK. Cellular heterogeneity in normal and neoplastic human urothelium. Cancer Res. 1985: 45:4260-365.

McConnell JD, Roehrborn CG, Bautista OM *et al*; Medical Therapy of Prostatic Symptoms (MTOPS) Research Group. The long-term effect of doxazosin,

finasteride, and combination therapy on the clinical progression of benign prostatic hyperplasia. N Engl J Med. 2003; 349:2387-98.

McDonnell TJ, Troncoso P, Brisbay SM *et al.* Expression of the protooncogene bcl-2 in the prostate and its association with emergence of androgen-independent prostate cancer. Cancer Res 1992; 52:6940-4.

McNeal JE, Regional morphology and pathology of the prostate. Am J Clin Path 1968; 49:347-57.

McNeal JE: Origin and evolution of benign prostatic enlargement. Invest Urol 1978;15:340–5.

McNeal JE. Anatomy of the prostate: an historical survey of divergent views. Prostate 1980; 1:3-13.

McNeal JE. Normal histology of the prostate. Am J Surg Pathol 1988; 1:619-33.

McNeal J. Pathology of benign prostatic hyperplasia: Insight into etiology. Urol Clin North Am 1990; 17:477-486.

McNeal JE, Redwine EA, Freiha FS *et al.* Zonal distribution of prostatic adenocarcinoma. Correlation with histologic pattern and direction of spread. Am J Surg Path 1988; 12:897-906.

McNeal JE. Anatomy and normal histology of the human prostate. In Pathology of the Prostate, Chapter 2, page 22. Edited by CS Foster and DG Bostwick. WB Saunders Co.1998.

Memari N, Diamandis EP, Earle T *et al.* Human kallikrein-related peptidase 12: Antibody generation and immunohistochemical localization in prostatic tissues. Prostate 2007; 67:1465-74.

Merchant DJ, Clarke SM, Ives K *et al.* Primary explant culture: an in vitro model of the human prostate. Prostate 1987; 4:523-42.

Miki J, Furusato B, Li H *et al.* Identification of putative stem cell markers, CD133 and CXCR4, in hTERT-immortalized primary nonmalignant and malignant tumor-derived human prostate epithelial cell lines and in prostate cancer specimens. Cancer Res. 2007; 1:67:3153-61.

Miller DR, Hamby KM, Slaga TJ. Contact-stimulated proliferation of cultured mouse epidermal cells by 3T3 feeder layers: inhibition of proliferation by 12-O-tetradecanoylphorbol-13-acetate (TPA). J Cell Physiol. 1982; 112:76-82.

Miron M, Woody OZ, Marcil A *et al.* A methodology for global validation of microarray experiments. BMC Bioinformatics 2006; 7:333.

Moll R. Cytokeratins in the histological diagnosis of malignant tumors. Int J Biol Markers 1994; 9:63-9.

Molofsky AV, Pardal R, Iwashita T *et al.* Bmi-1 dependence distinguishes neural stem cell self-renewal from progenitor proliferation. Nature 2003; 425:962-7.

Moran JL, Qiu H, Turbe-Doan A, Yun Y, Boeglin WE, Brash AR, Beier DR.A mouse mutation in the 12R-lipoxygenase, Alox12b, disrupts formation of the epidermal permeability barrier. J Invest Dermatol. 2007; 127:1893-7.

Morrison SJ, Shah NM, Anderson DJ. Regulatory mechanisms in stem cell biology. Cell 1997; 88:287-98.

Müller A, Giuffre G, Edmonston TB *et al*; German HNPCC Consortium German Cancer Aid. Challenges and pitfalls in HNPCC screening by microsatellite analysis and immunohistochemistry. J Mol Diagn. 2004; 6:308-15.

Nagle RB, Ahmann FR, McDaniel KM *et al.* Cytokeratin characterisation of human prostatic carcinoma and its derived cell lines. Cancer Res 1987; 47:281–6.

Nagle RB, Brawer MK, Kittelson J *et al.* Phenotypic relationships of prostatic intraepithelial neoplasia to invasive prostatic carcinoma. Am J Pathol 1991; 138:119-28.

Narla G, Heath KE, Reeves HL *et al.* KLF6, a Candidate Tumor Suppressor Gene Mutated in Prostate Cancer. Science 2001; 294:2563-2566.

Olumi AF, Grossfeld GD, Hayward SW *et al.* Carcinoma-associated fibroblasts direct tumor progression of initiated human prostatic epithelium. Cancer Res. 1999; 59:5002–11.

Oomizu S, Sahuc F, Asahina K *et al.* Kdap, a novel gene associated with the stratification of the epithelium. Gene. 2000; 256:19-27.

Pan CX, Zhu W, Cheng L. Implications of cancer stem cells in the treatment of cancer. Future Oncol. 2006; 2:723-31.

Paradis V, Dargère D, Laurendeau I *et al.* Expression of the RBA component of human telomerase (hTR) in prostate cancer, prostatic intraepithelial neoplasia, and normal prostate tissue. J Pathol 1999; 189:213-8.

Parson W, Kirchebner R, Mühlmann R *et al.* Cancer cell line identification by short tandem repeat profiling: power and limitations. The FASEB Journal 2005; 19:434-6.

Partin AW, Rogriguez R. The molecular biology, endocrinology and physiology of the prostate and seminal vesicles. In Campbell's Urology. 8th Edition,

Chapter 37, Volume 2. Edited by Walsh PC, Vaughan ED, Retik AB, Wein AW. WB Saunders Co. 2002.

Parwani AV, Kronz JD, Genega EM *et al.* Prostate carcinoma with squamous differentiation: an analysis of 33 cases. Am J Surg Pathol. 2004; 28:651-7.

Patel S, Xi ZF, Seo EY *et al.* Klf4 and corticosteroids activate an overlapping set of transcriptional targets to accelerate *in utero* epidermal barrier acquisition Proc Natl Acad Sci U S A. 2006; 103:18668–73.

Patrawala L, Calhoun T, Schneider-Broussard R *et al.* Highly purified CD44+ prostate cancer cells from xenograft human tumors are enriched in tumorigenic and metastatic progenitor cells. Oncogene 2006; 25:1696-708.

Patrawala L, Calhoun-Davis T, Schneider-Broussard R *et al.* Hierarchical organization of prostate cancer cells in xenograft tumors: the CD44+alpha2beta1+ cell population is enriched in tumor-initiating cells. Cancer Res. 2007; 67:6796-805.

Patrawala L, Calhoun T, Schneider-Broussard R *et al.* Side population is enriched in tumorigenic, stem-like cancer cells, whereas ABCG2+ and ABCG2- cancer cells are similarly tumorigenic. Cancer Res. 2005; 65:6207-19.

Peehl DM. Primary cell cultures as models of prostate cancer development. Endocr Relat Cancer 2005; 12:19-47.

Peehl DM, Stamey TA. Serum-free growth of adult human prostatic epithelial cells. In Vitro Cell Dev Biol. 1986; 22:82-90.

Peehl DM, Wong ST, Stamey TA. Clonal growth characteristics of adult human prostatic epithelial cells. In Vitro Cell Dev Biol. 1988; 24:530-6.

Peehl DM, Wong ST, Bazinet M *et al.* In vitro studies of human prostatic epithelial cells: Attempts to identify distinguishing features of malignant cells. Growth Factors 1989; 1:237–50.

Peehl DM (2002): Culture of Epithelial cells. 2nd Edition. Edited by Freshney RI and Freshney MG. New York: Wiley-Liss Inc. Chapter 6: Human Prostatic Epithelial cells, p 182.

Peichev M, Naiyer AJ, Pereira D *et al.* Expression of VEGFR-2 and AC133 by circulating human CD34(+) cells identifies a population of functional endothelial precursors. Blood 2000; 95:952-8.

Peschel RE, Colberg JW. Surgery, brachytherapy, and external-beam radiotherapy for early prostate cancer. Lancet 2003; 4: 233-241.

Pharoah PDP, Caldas C. Molecular genetics and the assessment of human cancers. Exp Rev Mol Med 1999: http://www.expertreviews.org/99000526h.htm

Ponchio L, Duma L, Oliviero B *et al.* Mitomycin C as an alternative to irradiation to inhibit the feeder layer growth in long-term culture assays. Cytotherapy 2000; 2:281-6.

Potten CS, Loeffler M. Stem cells: attributes, cycles, spirals, pitfalls and uncertainties: lessons for and from the crypt. Development 1990; 110:1001-20.

Potten CS, Owen G, Booth C. Intestinal stem cells protect their genome by selective segregation of template DNA strands. J Cell Sci. 2002; 115:2381-8.

Prince ME, Sivanandan R, Kaczorowski A *et al.* Identification of a subpopulation of cells with cancer stem cell properties in head and neck squamous cell carcinoma. Proc Natl Acad Sci U S A. 2007; 104:973-8.

Prins G, Birch L, Greene G. Androgen receptor localization in different cell types of the adult rat prostate. Endocrinology 1991; 129:3187–99.

Qiu Y, Ravi L, Kung HJ. Requirement of ErbB2 for signalling by interleukin-6 in prostate carcinoma cells. Nature. 1998; 393:83-5.

Quinn M, Babb P. Patterns and trends in prostate cancer incidence, survival, prevalence and mortality. Part I: International comparisons. BJU Int. 2002; 90:162-73.

Ramaekers FC, Verhagen AP, Isaacs JT *et al.* Intermediate filament expression and the progression of prostatic cancer as studied in the Dunning R-3327 rat prostatic carcinoma system. Prostate 1989; 14:323-39.

Rambhatla L, Bohn SA, Stadler PB *et al.* Cellular senescence: ex vivo p53-dependent asymmetric cell kinetics. J Biomed Biotech 2001; 1:27-36.

Reya T, Morrison SJ, Clarke MF *et al.* Stem cells, cancer, and cancer stem cells. Nature 2001; 414:105–11.

Rheinwald JG, Green H. Serial cultivation of strains of human epidermal keratinocytes: the formation of keratinizing colonies from single cells. Cell 1975; 6:331–44

Rhiemeier V, Breitenbach U, Richter KH *et al.* A Novel Aspartic Proteinase-Like Gene Expressed in Stratified Epithelia and Squamous Cell Carcinoma of the Skin. Am J Pathol. 2006; 168:1354-64.

Richardson GD, Robson CN, Lang SH *et al.* CD133, a novel marker for human prostatic epithelial stem cells. J Cell Sci. 2004; 117:3539-45.

Rietze RL, Valcanis H, Brooker GF *et al.* Purification of a pluripotent neural stem cell from the adult mouse brain. Nature 2001; 412:736-9.

Rizzo S, Attard G, Hudson DL. Prostate epithelial stem cells. Cell Prolif 2005; 38:363-74.

Robinson EJ, Neal DE, Collins AT. Basal cells are progenitors of luminal cells in primary cultures of differentiating human prostatic epithelium. Prostate 1998; 37:149-60.

Robinson MR, Smith PH, Richards B *et al.* The final analysis of the EORTC Genito-Urinary Tract Cancer Co-Operative Group phase III clinical trial (protocol 30805) comparing orchidectomy, orchidectomy plus cyproterone acetate and low dose stilboestrol in the management of metastatic carcinoma of the prostate. Eur Urol. 1995; 28:273-83.

Rocke DM, Lorenzato S. A two-component model for measurement error in analytical chemistry. Technometrics 1995; 37:176-84.

Rose A, Xu Y, Chen Z *et al.* Comparative gene and protein expression in primary cultures of epithelial cells from benign prostatic hyperplasia and prostate cancer. Cancer Lett. 2005; 227:213-22.

Rubin MA, Zhou M, Dhanaskaran SM *et al.* α-Methylacyl coenzyme A racemase as a tissue biomarker for prostate cancer. JAMA 2002; 287:1662-70.

Ruijter E, Miller GJ, Van de Kaa CA, Van Bokhoven A *et al.* Molecular analysis of multifocal prostate cancer lesions. J Pathol. 1999; 188:271-7.

Ruizeweld de Winter JA, Trapman J, Vermey M, Mulder E *et al.* Androgen receptor expression in human tissues: an immunohistochemical study. J Histochem Cytochem 1991; 39:927-36.

Rumpold H, Heinrich E, Untergasser G Hermann M *et al.* Neuroendocrine differentiation of human prostatic primary epithelial cells in vitro. Prostate 2002; 53:101–8.

Sanders FK, Burford BO. Ascites tumours from BHK 21 cells transformed in vitro by polyoma virus. Nature 1964; 201:786-9.

Scher HI, Issac JT, Zelefsky MJ. Prostate cancer. pp 1823-84. In Abeloff MD, Armitage JO, Licher AS (Eds), Clinical Oncology 2nd edition (2004). New York, Churchill Livingstone.

Schmelz M, Moll R, Hesse U *et al.* Identification of a stem cell candidate in the normal human prostate gland. Eur J Cell Biol. 2005; 84:341–54.

Schroeder FH, Okada K, Jellinghaus W *et al.* Human prostatic adenoma and carcinoma. Transplantation of cultured cells and primary tissue fragments in 'nude' mice. Invest Urol. 1976; 13:395–403.

Schalken JA, van Leenders GJIH. Cellular and molecular biology of the prostate: stem cell biology. Urology 2003; 62(Suppl 5a):11-20.

Schenk BI, Petersen F, Flad HD *et al.* Platelet-derived chemokines CXC chemokine ligand (CXCL)7, connective tissue-activating peptide III, and CXCL4 differentially affect and cross-regulate neutrophil adhesion and transendothelial migration. J Immunol. 2002; 169:2602-10.

Shaw JL, Diamandis EP. Distribution of 15 human kallikreins in tissues and biological fluids. Clin Chem. 2007 Aug;53(8):1423-32.

Sherley JL. Asymmetric cell kinetics genes: the key to expansion of adult stem cells in culture. Stem cells 2002; 20:561-72.

Sherwood ER, Theyer G, Steiner G *et al.* Differential expression of specific cytokeratin polypeptides in the basal and luminal epithelia of the human prostate. Prostate 1991; 18:303-14.

Shtutman M, Levina E, Ohouo P *et al.* Cell adhesion molecule L1 disrupts E-cadherin-containing adherens junctions and increases scattering and motility of MCF7 breast carcinoma cells. Cancer Res. 2006; 66:11370-80.

Sieben NL, ter Haar NT, Cornelisse CJ *et al.* PCR artifacts in LOH and MSI analysis of microdissected tumor cells. Hum Pathol. 2000; 31:1414-9.

Signoretti S, Loda M. Prostate stem cells: From development to cancer. Semin Cancer Biol. 2007; 17:219–24.

Signoretti S, Waltregny D, Dilks J *et al.* p63 is a prostate basal cell marker and is required for prostate development. Am J Pathol. 2000; 157:1769–75.

Sinha AA, Gleason DF, Limas C, Reddy PK *et al.* Localization of cathepsin B in normal and hyperplastic human prostate by immunoperoxidase and protein A-gold techniques. Anat Rec. 1989; 223:266-75.

Singh SK, Hawkins C, Clarke ID *et al.* Identification of human brain tumour initiating cells. Nature. 2004; 432:396-401.

Sinisi AA, Chieffi P, Pasquali D *et al.* EPN: a novel epithelial cell line derived from human prostate tissue. In Vitro Cell Dev Biol Anim. 2002; 38:165-72.

Southgate J, Varley CL, Garthwaite MA *et al.* Differentiation potential of urothelium from patients with benign bladder dysfunction. BJU Int. 2007; 99:1506-16.

Staack A, Kassis AP, Olshen A *et al.* Quantitation of apoptotic activity following castration in human prostatic tissue in vivo. Prostate 2003; 54:212-9.

Stephens P, Grenard P, Aeschlimann P *et al.* Crosslinking and G-protein functions of transglutaminase 2 contribute differentially to fibroblast wound healing responses. J Cell Sci. 2004; 117:3389-403.

Stewart J, Fleshner N, Cole H *et al.* Comparison of annexin II, p63 and α-methylacyl-CoA racemase immunoreactivity in prostatic tissue: a tissue microarray study. J Clin Pathol. 2007; 60:773-80.

Sufrin G, Coffey DS: A new model for studying the effects of drugs on prostatic growth: I. Antiandrogens in DNA synthesis. Invest Urol 1973; 11:45–54.

Takeda H, Chang C. Immunohistochemical and in situ hybridization analysis of androgen receptor expression during the development of the mouse prostate gland. J Endocrinol 1991; 129:83–9.

Tarone RE, Chu KC, Brawley OW. Implications of stage-specific survival rates in assessing recent declines in prostate cancer mortality rates. Epidemiology 2000; 11:167-70.

Thomas DFM Embryology Chapter 1, 1-11 in Essentials of Paediactric Urology by Thomas DFM, Rickwood AMK, Duffy PG. Martin Dunitz Ltd 2002

Tisell LE, Salander H: The lobes of the human prostate. Scand J Urol Nephrol 1975; 9:185-91.

Tokar EJ, Ancrile BB, Cunha GR *et al.* Stem/progenitor and intermediate cell types and the origin of human prostate cancer. Differentiation. 2005; 73:463-73.

Torring N, Borre M, Sorensen KD *et al.* Genome-wide analysis of allelic imbalance in prostate cancer using the Affymetrix 50K SNP mapping array. Br J Cancer 2007; 96:499-506.

Tran CP, Lin C, Yamashiro J *et al.* Prostate stem cell antigen is a marker of late intermediate prostate epithelial cells. Mol. Cancer Res. 2002; 1:113-21.

Tsujii M, DuBois RN. Alterations in cellular adhesion and apoptosis in epithelial cells overexpressing prostaglandin endoperoxide synthase 2. Cell. 1995; 83:493-501.

Tsujimura A, Fujita K, Komori K *et al.* Prostatic stem cell marker identified by cDNA microarray in mouse. J Urol. 2007; 178:686-91.

Tsujimura A, Koikawa Y, Salm S *et al.* Proximal location of mouse prostate epithelial stem cells: a model of prostatic homeostasis. J Cell Biol. 2002; 157:1257-65.

Tsurusaki T, Aoki D Kanetake H, Inoue S, Muramatsu M *et al.* Zone-dependent expression of estrogen receptors alpha and beta in human benign prostate hyperplasia. J Clin Endocrinol Metab. 2003; 88:1333-40.

Uchida N, Buck DW, He D *et al.* Direct isolation of human central nervous system stem cells. Proc Natl Acad Sci USA 2000; 97:14720-5.

Ura H, Takeda F, Okochi H. An in vitro outgrowth culture system for normal human keratinocytes. J Dermatol Sci. 2004 Jun;35(1):19-28.

Uzgare AR, Xu Y, Isaacs JT. *In vitro* culturing and characteristics of transit amplifying eithelial cells from human prostate tissue. J. Cell. Biochem. 2004; 91:196–205.

van der Heul-Nieuwenhuijsen L, Hendriksen PJM, van der Kwast TH *et al.* Gene expression profiling of the human prostate zones. BJU Int. 2006; 98:886–97.

van Leenders GJLH, Aalders TW, Hulsbergan-van de Kaa CA *et al.* Expression of basal cell keratins in human prostate cancer metastases and cell lines. J Pathol 2001; 195:563-70.

van Leenders G, Dijkman H, Hulsbergen-van de Kaa C *et al.* Demonstration of intermediate cells during human prostate epithelial differentiation in situ and in vitro using triple-staining confocal scanning microscopy. Lab Invest 2000; 80:1251-8.

van Leenders GJIH, Schalken JA. Stem cell differentiation within the human prostate epithelium: implications for prostate carcinogenesis. BJU Int 2001; 21:35–42.

van Leenders GJLH, Schalken JA. Epithelial cell differentiation in the human prostate epithelium: implications for the pathogenesis and therapy of prostate cancer. Critical Reviews in Oncology Haematology 2003; 46:S3-10.

Varambally S, Dhanasekaran SM, Zhou M *et al.* The polycomb group protein EZH2 is involved in progression of prostate cancer. Nature 2002; 419:624-9.

Vashchenko N, Abrahamsson PA. Neuroendocrine differentiation in prostate cancer: implications for new treatment modalities. Eur Urol. 2005; 47:147-55.

Veltri R, Rodriguez R. Chapter 85, Molecular biology, endocrinology, and physiology of the prostate and seminal vesicles. In: Wein AJ, Kavoussi LR, Novick AC *et al* (eds.) Campbell-Walsh Urology 9th Edition,. Saunders Elsevier, Philadelphia, USA 2007a, pp2684-2689.

Veltri R, Rodriguez R. Chapter 85, Molecular biology, endocrinology, and physiology of the prostate and seminal vesicles. In: Wein AJ, Kavoussi LR, Novick AC *et al* (eds.) Campbell-Walsh Urology 9th Edition. Saunders Elsevier, Philadelphia, USA 2007b, pp2690-2691.

Verhagan APM, Ramaekers FCS, Aalders TW *et al.* Colocalisation of basal and luminal cell-type cytokeratins in human prostate cancer. Cancer Res. 1992; 52:6182-7.

Visakorpi T, Kallioniemi AH, Syvanen AC *et al.* Genetic changes in primary and recurrent prostate cancer by comparative genomic hybridisation. Cancer Res. 1995; 55:342-7.

Wang S, Garcia AJ, Wu M *et al.* Pten deletion leads to the expansion of a prostatic stem/progenitor cell subpopulation and tumor initiation. Proc Natl Acad Sci U S A. 2006; 103:1480-5.

Wang Y, Hayward SW, Cao M *et al.* Cell differentiation lineages in the prostate. Differentiation 2001; 68:270-9.

Wheeler TM, Lebovitz RM. Fresh tissue harvest for research from prostatectomy specimens. Prostate 1994; 25:274-9.

Wilmut I, Schnieke AE, McWhir J *et al.* Viable offspring derived form fetal and adult mammalian cells. Nature 1997; 385:810-813.

Wojno KJ, Epstein JI. The utility of basal cell-specific anti-cytokeratin antibody (34β E12) in the diagnosis of prostate cancer: A review of 228 cases. Am J Surg Pathol 1995; 19:251–60.

Xie L, Qin WX, Li JJ *et al.* cDNA expression array analysis of gene expression in human hepatocarcinoma Hep3B cells induced by BNIPL-1. Acta Biochim Biophys Sin. 2005; 37:618-24.

Xin L, Lawson DA, Witte ON. The Sca-1 cell surface marker enriches for a prostate-regenerating cell subpopulation that can initiate prostate tumorigenesis. Proc Natl Acad Sci USA 2005; 102:6942–7.

Yang Y, Hao J, Liu X *et al.* Differential expression of cytokeratin mRNA and protein in normal prostate, prostatic intraepithelial neoplasia, and invasive carcinoma. Am J Pathol 1997; 150:693-704.

Yauk CL, Berndt ML, Williams A *et al.* Comprehensive comparison of six microarray technologies. Nucleic Acids Research 2004; 32:e124.

Yen TH, Wright NA. The gastrointestinal tract stem cell niche. Stem Cell Rev. 2006; 2:203-12.

Yin AH, Miraglia S, Zanjani ED *et al.* AC133, a novel marker for human hematopoietic stem and progenitor cells. Blood 1997; 90:5002-12.

Zhao X, Li C, Paez JG *et al.* An integrated view of copy number and allelic alterations in the cancer genome using single nucleotide polymorphism arrays. Cancer Res. 2004; 64:3060–71.

APPENDICES

Appendix A: Patient consent forms and information sheets

Appendix B: Sequences of primers for PCR for LOH and RT-PCR.

CONFIDENTIAL

Patient Information Sheet

Prostate Cancer Stem Cell Project

Prostate Cancer Research Unit,

Institute of Urology & Nephrology,
University College London,

Investigators:

Prof J R W Masters BSc PhD FRCPath
Professor of Experimental Pathology

Miss C L Foley BM BCh MA MRCS
Clinical Research Fellow

Dear Sir

Please could you help us with a research project. It will not affect your treatment in any way and we do not need you to do anything other than give us permission. We would like to have some of the prostate tissue that is taken at your operation.

We are studying the cells we think are responsible for prostate cancer. We call them cancer stem cells and we believe that they are derived from normal prostate stem cells. We want to select a small amount of the prostate tissue taken at your operation and grow the cells in the laboratory. Growing and investigating stem cells will help us understand how and why prostate cancer develops. We hope that eventually this will lead to new and better treatments for prostate cancer.

If you are willing, after your operation we will take the tissue that has been removed from your body and select a small amount to take to the laboratory. This will not affect your operation in any way, or your treatment. In order to protect confidentiality, no record will be kept of your name or other clinical details.

It is possible that some of your cells will be stored for future research beyond the confines of this project (if you agree to this). This future research may be carried out by different scientists or involve genetic analysis. This will have no repercussions to yourself.

You do not have to take part in this study if you do not want to. If you decide to take part you may withdraw at any time without having to give a reason. Your decision whether to take part or not will not affect your care and management in any way.

All proposals for research using human subjects are reviewed by an ethics committee before they can proceed. This proposal was reviewed by the Joint UCL/UCLH Committees on the Ethics of Human Research and the London Clinic Ethical Committee.

Please keep this information sheet. A consent form is attached for you to sign if you are willing to help us in this research. I (Charlotte Foley or John Masters) will be coming to see you and you can ask us any questions you want.

Charlotte L Foley , John R Masters .....

CONFIDENTIAL
Patient Consent Form
Prostate Cancer Stem Cell Project

Prostate Cancer Research Unit,

Institute of Urology & Nephrology, University College London,

Investigators:

Prof J.R W Masters BSc PhD FRCPath
Professor of Experimental Pathology

Miss C L Foley BM BCh MA MRCS
Clinical Research Fellow

Dear Sir

Thank you for reading the information about our research project. If you would like to take part, please read, place your initials in the boxes and sign this form.

☐ 1. I have read the attached information sheet on this project (dated 5th February 2002, version 3) and have been given a copy to keep. I have been able to ask questions about the project and I understand why this research is being done and any risks involved.

☐ 2. I agree to give a sample of prostate tissue for research in this project. I understand that giving a sample for this research is voluntary and that I am free to withdraw my approval for use of the sample at any time without giving a reason and without my medical treatment or legal rights being affected.

☐ 3. I give permission for someone from the research team to look at my medical records to get information on the histopathological findings following examination of the whole prostate specimen. I understand that this information will be kept confidential.

☐ 4. I understand that I will not benefit financially if this research leads to the development of a new treatment or medical test.

☐ 5. I know how to contact the research team if I need to.

☐ 6. I agree that the sample I have given and the information gathered about me can be stored by the Prostate Cancer Research Unit at the Institute of Urology & Nephrology, University College London, for possible use in future projects. I understand that some of these projects may be carried out by researches other than those who ran the first project.

☐ 7. I understand that the project using the sample that I give may include genetic research aimed at understanding the genetic influences on prostate cancer, but that the results of these investigations are unlikely to have any implications for me personally.

Name (Block capitals) Date Signature

....

Date of Birth Hospital number

....

Name of researcher Date Signature

....

Thank you for agreeing to take part in this research 5thFeb2002: Version 3

CONFIDENTIAL
Patient Information Sheet
Prostate Stem Cell Project

Prostate Research Unit,

Institute of Urology & Nephrology,
University College London,

Investigators:

Prof J R W Masters BSc PhD FRCPath
Professor of Experimental Pathology

Miss C L Foley BM BCh MA MRCS
Clinical Research Fellow

Dr. I. N. Bisson PhD
Post-doctoral Researcher

Dear Sir

Please could you help us with a research project? It will not affect your treatment in any way and we do not need you to do anything other than give us permission. We would like to have some of the prostate tissue that is taken at your operation.

We are studying the cells we think are responsible for growth within the prostate which we call prostate stem cells. We want to select a small amount of the prostate tissue taken at your operation and grow the cells in the laboratory. Growing and investigating stem cells will help us understand how and why the prostate grows. We hope that eventually this will lead to new and better treatments for diseases of the prostate.

If you are willing, after your operation we will take the tissue that has been removed from your body and select a small amount to take to the laboratory. This will not affect your operation in any way, or your treatment. In order to protect confidentiality, no record will be kept of your name or other clinical details.

It is possible that some of your cells will be stored for future research beyond the confines of this project (if you agree to this). This future research may be carried out by different scientists or involve genetic analysis. This will have no repercussions to yourself.

You do not have to take part in this study if you do not want to. If you decide to take part you may withdraw at any time without having to give a reason. Your decision whether to take part or not will not affect your care and management in any way.

All proposals for research using human subjects are reviewed by an ethics committee before they can proceed. This proposal was reviewed by the Joint UCL/UCLH Committees on the Ethics of Human Research.

Please keep this information sheet. A consent form is attached for you to sign if you are willing to help us in this research. I (Charlotte Foley or John Masters) will be coming to see you and you can ask us any questions you want.

Charlotte L Foley, Isabelle Bisson, John R Masters.....

CONFIDENTIAL

Patient Consent Form
Prostate Stem Cell Project

Prostate Research Unit,

Institute of Urology & Nephrology, University College London,

Investigators:
Prof J.R W Masters BSc PhD FRCPath
Professor of Experimental Pathology
Miss C L Foley BMBCh MA MRCS
Clinical Research Fellow
Dr. I. N. Bisson PhD
Post-doctoral Researcher

Dear Sir

Thank you for reading the information about our research project. If you would like to take part, please read, place your initials in the boxes and sign this form.

☐ I have read the attached information sheet on this project (dated 20th October 2001, version 2) and have been given a copy to keep. I have been able to ask questions about the project and I understand why this research is being done and any risks involved.

☐ I agree to give a sample of prostate tissue for research in this project. I understand that giving a sample for this research is voluntary and that I am free to withdraw my approval for use of the sample at any time without giving a reason and without my medical treatment or legal rights being affected.

☐ I give permission for someone from the research team to look at my medical records to get information on the histopathological findings following examination of the rest of the prostate specimen. I understand that this information will be kept confidential.

☐ I understand that I will not benefit financially if this research leads to the development of an new treatment or medical test.

☐ I know how to contact the research team if I need to.

☐ I agree that the sample I have given and the related histopathological information can be stored by the Prostate Research Unit at the Institute of Urology & Nephrology, University College London, for possible use in future projects. I understand that some of these projects may be carried out by researchers other than those who ran the first project.

☐ I understand that the project using the sample that I give may include genetic research aimed at understanding the genetic influences on the prostate, but that the results of these investigations are unlikely to have any implications for me personally.

Name (Block capitals)	**Date**	**Signature**
.....	.....	.....
Date of Birth	**Hospital number**	
.....	.....	
Name of researcher	**Date**	**Signature**
.....	.....	.....

Thank you for agreeing to take part in this research 20thOct2001: Version 2

Appendix B: Sequences of primers for PCR for LOH and reverse-transcription PCR.

Locus / Gene	Sequence	Chromophore marker	Size of product*
Primers used for LOH analysis			
D1S422	CATGGGGTATAGCAACAGAC TGATTTCCTGCAAACATTTT	TET	160
D1S158	GGGCCTTCTTATATTGCTTC GGAAAGACTGGACCAAAGAG	TET	137-163
D1S305	CCAGNCTCGGTATGTTTTTACTA CTGAAACCTCTGTCCAAGCC	HEX	156-176
D1S414	GCACAGTTCAACATCCATT TCTCTGTCATTTTAGGTCTATTTCT	FAM	185-205
D2S222	ACAAATGCAGAAAAAGCATATG CTGTCAGGCTGAGGAAATTT	HEX	118-138
D3S1263	CTGTTGACCCATTGATACCC TAAAATCACAGCAGGGGTTC	FAM	231-249
D5S500	ACCTATTCGACCTAATGACTAAAGA ATCGGTGAAATGCAACTACTT	HEX	188-214
D5S656	GCTAAGAAAATACGACAACTAAATG CATAATAAACTGATGTTGACACAC	TET	185-203
D6S251	TTCCTAACCAGGTTTCAATG ATATTTTTAAAGTAAGTTGCAC	FAM	150
D6S501	GCTGGAAACTGATAAGGGCT GCCACCCTGGCTAAGTTACT	TET	166-182
D6S314	AAAATGACTTCTTTGGGTGGGC GTGGGTAGCAACACTGTGGC	TET	243-259
D7S523	CTGATTCATAGCAGCACTTG AAAACATTTCCATTACCACTG	FAM	224-240
D7S480	CTTGGGGACTGAACCATCTT AGCTACCATAGGGCTGGAGG	HEX	189-206
D8S549	AAATGAATCTCTGATTAGCCAAC TGAGAGCCAACCTATTTCTACC	FAM	166-172
D8S1991	GTGAAGGAGGGCAGTCAT CAGGGTTGAAGCAATCTG	FAM	215
D8S136	GCCCAAAGAGGAGAATAAA CTGTTTCCACACCGAAGC	FAM	71-89
NEFL	GCAGTAGTGCCGCAGTTTCA TGCAATTCATCTTCCTTTCT	FAM	137-147
D8S255	TTTTGGAATTTCTAGCCTCC TGAAACCCACAGATATTGGG	FAM	107-129
D8S133	CAGGTGGGAAAACTGAGGGA GTTTAGCAACTGTCAACATATTGCTC	HEX	94-112
D8S137	AAATACCGAGACTCACACTATA GTTTGCTAATCAGGGAATCACCCAA	FAM	152-162
SFTP2	CAGCCCAGACAGGCTGGAA GTTTACTTTTCTGGCCAAACTCCTG	FAM	111-157

D9S1748	CACCTCAGAAGTCAGTGAGT GTGCTTGAAATACACCTTTCC	TET	130-150
D9S1679	CACCTCTGCCTGCCAA TGCTGTGGACCTAACAAAAA	FAM	135-145
D10S2491	GTTAGATAGAGTACCTGCACTC TTATAAGGACTGAGTGAGGGA	HEX	130-150
D10S541	AAGCAAGTGAAGTCTTAGAACCACC CCACAAGTAACAGAAAGCCTGTCTC	FAM	272
D10S1246	CTACGGACTCATTGAAGACTAGG AGCGTTTTCTATAGCTCTGACG	TET	210-234
D10S587	CCCAGATTCATGGCTTTC TTCTGCTGACACGGGC	FAM	172-186
D10S211	CTCCTGGTCTCATGCG CAGGCTCCTACTACCGTC	FAM	195-211
D10S1765	ACACTTACATAGTGCTTTCTGCG CAGCCTCCCAAAGTTGC	FAM	166
D11S903	AACACTTCGATGTTCCTTCC AGCTGAGAGCGCATGTATAA	TET	99-109
D11S902	CCCGGCTGTGAATATACTTAATGC CCCAACAGCAATGGGAAGTT	FAM	145-163
D11S916	CAGACTATTCTCATTGCTGC GGACTTCTAAGCCTCCATAA	FAM	135-153
D11S990	CCTCTTATTCAGTCACAGCA GAAATACTGTGGTGTACATC	TET	73-79
D11S2000	AGTAGAGAACAAAACACTGTGGC TTTGAAGATCTGTGAAATGTGC	TET	213
D12S89	ATTTGAGAGCAGCGTGTTTT CCATTATGGGGAGTAGGGGT	HEX	254-288
D12S1697	CATCTTGGCCCAGTCAAT CCTTCTGTTTATAGCAATGGGA	HEX	218-234
D13S165	GTTTCGCCAAGCCTGTT GTTGACAATAAAATACGCCACA	TET	183-195
D13S284	AAAATCAGGTGGAAACAGAAT AAAGGCTAACATCGAAGGGA	FAM	197-227
D13S171	CCTACCATTGACACTCTCAG TAGGGCCATCCATTCT	TET	227-241
D13S269	TGTCTTCCAGCAGGGC CAAAGTGGTTCATCTTGGTCT	FAM	116-134
D13S263	CCTGGCCTGTTAGTTTTTATTGTTA CCCAGTCTTGGGTATGTTTTTA	TET	144-160
D15S1232	CCAGAGAGATCTTTCCCCAT TTGCTCCACTGTTTTCTCAC	TET	255-295
D16S505	GACTGTGTCTGCCCAA TCTGCCTCCATACGTG	FAM	239-261
D16S422	CAGTGTAACCTGGGGGC CTTTCGATTAGTTTAGCAGAATGAG	HEX	188-212
D16S413	ACTCCAGCCCGAGTAA GGTCACAGGTGGGTTC	HEX	131-149
D17S938	CCGGATTGCTACACCTAAAT	HEX	164-182

	AACAGTCTCTNCTGGAGCAG		
D17S786	TACAGGGATAGGTAGCCGAG	FAM	135-157
	GGATTTGGGCTCTTTTGTAA		
D17S855	GGATGGCCTTTTAGAAAGTGG	HEX	143-155
	ACACAGACTTGTCCTACTGCC		
D17S515	TTAGGCCCAGCTTCCTGGGAGA	HEX	107-127
	ACCTGGTTTGAGTTAGCAGCGAG		
D18S364	AAATTGTGGGAAGTTCCTGG	TET	112-136
	CCCCTGGTCTCAGATATGTC		
D18S363	TTGGGAACTGCTCTACATTC	HEX	177-247
	GCTTCATTCTCTCACTGGAT		
D18S541	CTCCCAAATATGGAATGGAA	FAM	272-283
	TGAGCTGAGATCATATCAATGC		
D18S470	AGCTTACCACAAGGCATAACT	HEX	275
	AGGGTAGACTGTTAACTGCNTTAGA		
D19S223	CAAAATCGAGGTGCATAGAA	TET	228-246
	ACCATGACTGGCTAATTGTG		
D21S156	GTCAACATAGTGAGACCCCA	HEX	77-107
	ATCCAGCCTGTAACACATTC		
Genomic	CTTCATTGACCTCAACTACATG	-	391
GAPDH	TGTCATGGATGACCTTGGCCAG		

Primers used for Reverse Transcription PCR

SNX10F	TGTTGCTTTGTTACCCAGCCT	-	440
	TGTGTTTTTCAAAACTGCTGT		
KLK12	TGTTTGAGGGCACCAGCCT	-	509
	TGGCAGGAGTTAAAGTTCCA		
BRPF1	TGACTCATTTCTGGTCTTGGG	-	429
	CAAATGACTCTGGCGCGA		
PHLDB2	TGTGCTCTTTTGGATGGAGAA	-	435
	GGCTGGAGTATTTCTTTTCCA		
ZBTB10	CATGGTTAGATGCATCTTTTG	-	264
	AAGGAAGGGGATAAATGGGA		
PIM1	TCTACTCAGGCATCCGCGT	-	610
	AAGAAAACCTGGCCCCTGAT		
AMACR	TCGCTAGTGCTGGACCTGAA	-	546
	AACAGCCATGAATTCCCCAT		
EZH2	AAAAGCAGAAAGATCTGGAGG	-	688
	GGAGGTTCAATATTTGGCTTC		
cDNA GAPDH	TTTCCCATTCAAGACCTGTGG	-	204
	TGGCACAGATTTCAGCTCCTA		
Hepsin	AGAACAGCAACGATATTGCCC		756
	TTTATGGCCTGGAAGATCCA		

* Product size information for LOH loci obtained from the GDB Human Genome Database (www.gdb.org) when given.